ORIGINS AND SOURCES OF ATMOSPHERIC PRECIPITATION FROM AUSTRALIA: CHLORINE-36 AND MAJOR-ELEMENT CHEMISTRY

By

Melita Keywood

A thesis submitted for the

degree of Doctor of Philosophy

of the

Australian National University

October 1995

The work described in this thesis was carried out while I was a full-time post-graduate research student in the Research School of Earth Sciences at the Australian National University. Except where noted in the text, the research described here is my own and to my knowledge original. This thesis, or any part thereof, has not been submitted to any other university or place of higher learning for the purpose of accreditation.

Melita Keywood
October 1995

ACKNOWLEDGMENTS

There are many people to thank for the completion of this thesis. Firstly I wish to thank my supervisor Allan Chivas for initiating the rainfall collection program and for giving me the opportunity to work on this project. It's been a lot of fun and it goes without saying that I've learnt a great deal. I'd also like to thank my adviser Greg Ayers from the CSIRO who knows so much about atmospheric chemistry and has always been very encouraging. Keith Fifield from RSPhySE has given me excellent supervision and advice with respect to the ^{36}Cl section of the work, and has provided me with an insight into how differently geologists and nuclear physicists think.

Richard Cresswell was a great support, and has given me a lot of advice about all parts of several versions of the thesis. The overall structure of the thesis is in part thanks to Richard. Michael Bird, Mike Gagan, John Cram, Edward Linacre and Adam Kent also read various sections. I have also had many useful conversations with John Stone and Geoff Monighan, and correspondence with Mike Manton. I'd like to thank Paul Johnston, Dan Zwartz and Tony Purcell who wrote several programs for me.

I'd like to acknowledge the financial support of RSES to attend ICOG-8 in Berkeley, California and the Fifth Conference on Isotopes in the Australian Environment in Brisbane.

Collecting rainfall over two years each three months from 18 sites almost as far away from Canberra as you can get without using a passport, required the help of many people. Thanks to Dieter Burman, Joe Cali, Mike Gagan, Micnael Bird, Marcella, Lisa Hill, Elmer Kiss, Dusan Dammer, Joan Cowley and especially Leesa Carson, who managed to remain calm even under the most trying circumstances (40° temperatures and bogged above the axel and she was still cool calm and collected). I'd also like to thank all the owners of the properties on which the rain collectors were located. Bob Egan from the CSIRO Kapalga Research Station was especially helpful.

I thank Elmer Kiss, Audrey Chapman, Mike Shelley, Joe Cali and Les Kingsley for their help with analytical work at RSES, John Stone for showing me the Cl

precipitation technique, and the members of the AMS group in Nuclear Physics (Keith Fifield, Richard Cresswell, Jodi Evans and Gary Allan, and all the people that keep the accelerator running) for ^{36}Cl measurements. I also thank Penelope Fenley for all her help with library matters.

None of this would have been any fun without the people I have known in the last four years. Friends I'd like to thank are Paul, Richard, Monica, Sue, Jurgen, Deb, Geoff Batt (I'll get you back), Warwick, Gabrielle, Travis, Jennifer Delhaize, (Dirty) Phil, Sammy, Jeppo, Linda, Karen, Alusha, George, Mark, Darryl, Corine and Kevin. I'd also like to thank Paula, Sandra and Gary for staying in touch. Thank you Claudine for being so 'supportive', Geoff Fraser for often having a refreshingly alternative outlook, Dave John Brown (PhD almost) for being so talkative and such a stayer, Tony and Alfredo for stopping me from getting the Pink Slippers, and Stephen Pell for being an inspiration. Thanks to all the people I've shared houses with, in particular Steve Hill whom I wish good luck in his search (for the ultimate snow dome that is, I'll never be able to walk past a souvenir shop again). I'd also like to thank Adam Kent for always knowing the right thing to say. And thanks to Dan Zwartz for never being anything but himself. Thanks to Leah for giving me the mountain-biking bug, and Gill, Pete, Amanda, Dan and Dylan for the subsequent epics. And thanks to Steve Barry for the climbing. I had a great trip around the southwest of the USA with Leesa and Adam, who were just the right company in such a strange place.

Dylan Harrison deserves a medal for suffering not one, but three of his close friends writing up at the same time. We have yet to see if this experience has left any deep-rooted physcological scars. Thanks Dylan. Finally, I'd like to thank my family. They have always been very encouraging and will be very proud.

ABSTRACT

Temporal and spatial variations of major-element and ^{36}Cl chemistry in rainfall across Australia have been assessed. Bulk precipitation samples were collected from two arrays over two years at three-monthly intervals: the WE array (10 sites) extended in a west to east direction from the coast of Western Australia south of Geraldton, inland to Warburton in Central Australia, and the SN array (8 sites), extended in a south to north direction from Port Lincoln in South Australia to Kakadu in the Northern Territory.

The major-element chemistry shows that the main influence on the composition of precipitation in remote areas of Australia is mixing between seawater and continental sources. At most sites along the two arrays it is difficult to distinguish between the separate end-members of this source, except at coastal localities where seawater dominates the chemistry of precipitation. However, the influence of seawater is also evident at non-coastal sites in association with favourable synoptic conditions, such as cold frontal activity in south and western Australia during winter, and monsoonal activity in northern Australia during summer. The continentally-derived end-member is most likely composed of resuspended soil/dust material, including salt-lake and calcareous dune components. In the south of the SN array where agriculture is intense this continental source variably includes a fertiliser component. The chemistry of precipitation across Australia is also affected by an acid-base balance factor, the components of which are derived from natural sources such as biogenic emissions, biomass burning and lightning flash production. The nature of the collection program (i.e. samples are exposed to the atmosphere from the time of deposition to the time of sample retrieval) means biodegradation is also evident in the collected sample chemistry.

Chlorine-36 is a cosmogenic isotope with a half-life of 301,000 years. This time frame, combined with the hydrophilic nature of Cl, makes ^{36}Cl useful as a hydrological tracer. The use of ^{36}Cl as a hydrological tracer however, relies on predicted models of ^{36}Cl and stable Cl fallout to calculate $^{36}Cl/Cl$ ratios for recharge to hydrological systems. The results from this investigation agree with the general shape of the latitude-dependent theoretical ^{36}Cl fallout curve of Lal and Peters (1967), but suggests that the curve underestimates the rate of fallout. A revised mean fallout for the southern hemisphere of 15.4 ^{36}Cl atoms/m^2/s is suggested, and long-term average predictions of ^{36}Cl fallout rates used to predict the input ratios of

$^{36}Cl/Cl$ in hydrological investigations should be increased by a factor of 1.4 for the southern hemisphere. Further, while stable Cl concentrations in precipitation display a general exponential decrease with distance from the coast, the nature of this relationship is geographically variable, and Cl concentrations in precipitation should be investigated for each study by local direct measurements, a process that is simple and inexpensive.

The mean ^{36}Cl fallout for the southern hemisphere, calculated from this work is three times lower than has been measured for precipitation in the northern hemisphere. The lower southern hemisphere fallout rates reflect the lower rates of transfer of stratospheric air to the troposphere in the southern hemisphere, which results from the less dynamic nature of the lower stratosphere in the southern hemisphere. The mean global ^{36}Cl fallout that incorporates measurements from the northern hemisphere with the results of this work is calculated to be 25-35 atoms/m^2/s, 2-3 times greater than predicted by Lal and Peters (1967). This suggests that the cross-section for the cosmic-ray production of ^{36}Cl may be underestimated in their paper.

This work supports the use of ^{36}Cl as a tracer of atmospheric processes. Its production primarily in the stratosphere suggests that it may trace stratospheric-tropospheric exchange. Seasonal variations in ^{36}Cl fallouts and $^{36}Cl/Cl$ show high ratios and fallouts during spring, and at some localities, during summer (i.e. the north of the SN array). The increased spring ^{36}Cl fallouts are attributed to increased transfer of stratospheric ^{36}Cl to the troposphere that occurs as the tropopause height increases during the warmer months. High fallouts during summer in the north of the SN array may be attributed to the direct entrainment of stratospheric air into cumulus clouds during the monsoonal convection.

Chlorine-36 exists in the stratosphere predominantly as HCl gas (Wahlen et al 1991). The correlation between ^{36}Cl and NO_3 and the lack of any relationship between ^{36}Cl, stable Cl and Na concentrations (the latter being entrained as aerosols), suggest that ^{36}Cl is scavenged from the atmosphere as a gas rather than an aerosol phase.

CONTENTS

CHAPTER 1 INTRODUCTION

The Australian continent provides a unique laboratory in which the natural chemistry of the atmosphere may be investigated. The main reason for this is its relatively unpolluted nature. By northern hemisphere standards, the atmosphere of the southern hemisphere is very clean. As an example, the long-term average concentrations of SO_4, NO_3 and Ca in precipitation at Hubbard Brook in North America are elevated by more than 5.5 times relative to Katherine, Australia (Likens et al 1987), despite both sites experiencing similar rainfall. The cleanliness of the atmosphere over Australia may be attributed to its relatively small number of human inhabitants and the relatively short period of time that Australia has been industrialised. In addition, because of the concentration of the majority of Australia's population in the eastern coastal regions, vast areas of the interior of the continent remain little affected by human activity.

In addition to the unpolluted nature of the atmosphere, Australia is an ideal place to investigate precipitation because of the wide range of climatic conditions. These range from tropical to subtropical in the north, to arid in the centre, to temperate along the southeastern coastal areas. This means that rainfall chemistry can be compared with a variety of climate types on a single land mass. Further, the lack of significant topography across the Australian continent minimises orographic effects, thus simplifying the interpretative base. From a practical point of view, there are few places in the world where a comparable investigation sampling over such a vast area would be logistically possible. The inconvenience of crossing international borders was avoided and throughout this investigation, field equipment remained undisturbed by human activity.

This investigation concerns the assessment of the chemistry of precipitation collected across the Australian continent. Samples were collected from 18 sites over two arrays extending in an west to east direction through Western Australia (WE array), and in a south-north direction through South Australia and the Northern Territory (SN array) as shown in Figure 1.1. Precipitation was collected in bulk depositional collectors. The analytical work can be divided into two related sections; an investigation of the major-element chemistry and an investigation of ^{36}Cl composition. Interpretation of the ^{36}Cl data is reliant on an understanding of the

major-element chemistry, while ^{36}Cl can be used to highlight processes affecting the major-element chemistry.

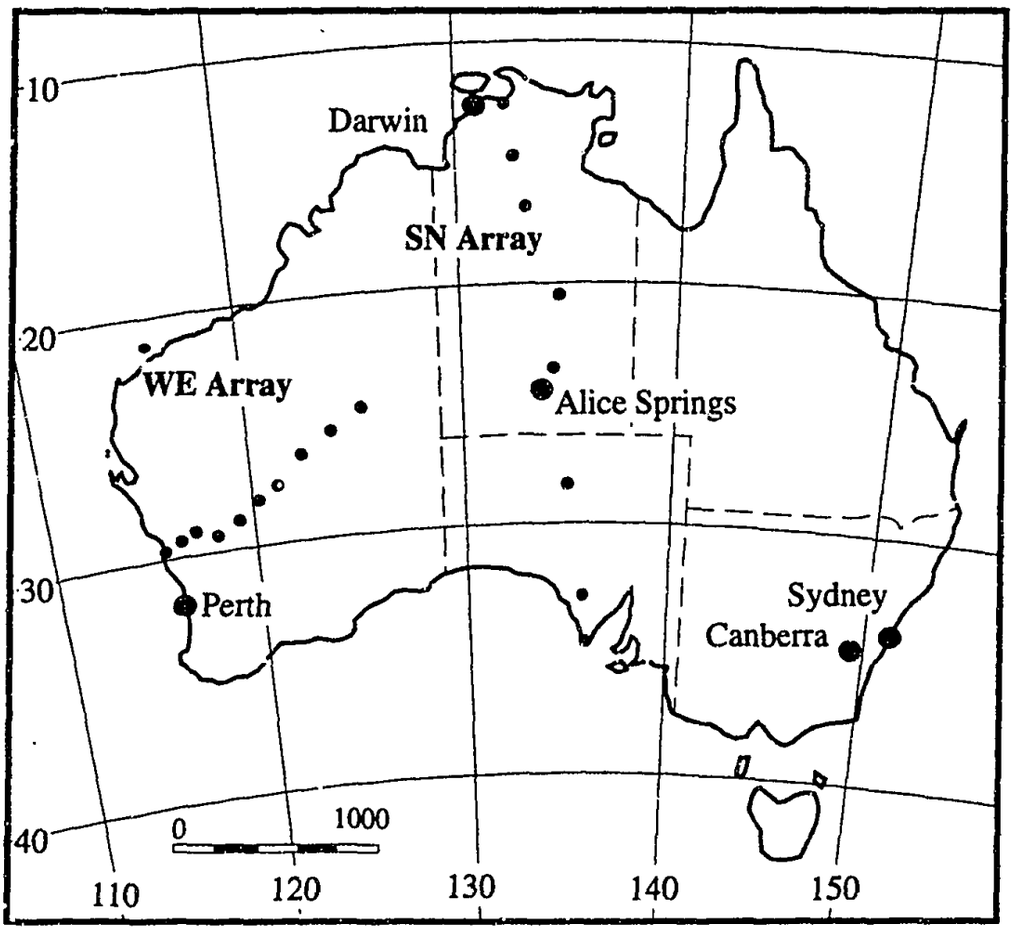

FIGURE 1.1 Location of the WE and SN rain collecting arrays. Small dots are sample sites. Large dots are major cities.

1.1 MAJOR ELEMENTS

It is important to understand the chemistry of precipitation from unpolluted areas for two reasons: 1) to understand the processes that control precipitation in the atmosphere of remote areas; 2) to use this understanding as a basis for establishing the effects of industrial, urban and agricultural emissions on precipitation chemistry in populated areas. In particular, the results from this project will expand the sparse data base of precipitation chemistry across Australia both by adding further data to sites that have been measured previously, and by providing the first analysis of precipitation for new sites, in particular in central and northern Australia. This provides fundamental information for other areas of research in the natural environment. For example, information concerning the rates of accession of salts to the Australian landscape is necessary for the understanding of salinisation issues. In

particular, studies using a mass balance approach to the problems of salinisation require data such as the amount of Cl deposited in rainfall.

1.2 CHLORINE-36

Chlorine-36 is a naturally occurring radioactive isotope with a half-life of 301,000 (±200) years (Browne and Firestone 1986). Its production in the atmosphere occurs primarily in the stratosphere (60%) by the cosmic ray spallation of ^{40}Ar. The production of ^{36}Cl in the stratosphere is dependent on latitude due to the influence of the Earth's geomagnetic field on the flux of cosmic rays to the Earth. However, the distribution of ^{36}Cl through the troposphere is dependent on geographically controlled atmospheric conditions and processes. [illegible]. Lal and Peters (1967) estimated the fallout curve of ^{36}Cl to the Earth's surface by utilising the latitude-dependence and fallout pattern displayed by ^{90}Sr produced during stratospheric bomb tests in the late 1950s.

Chlorine-36 activity in natural samples ranges from 10^{-10} to 10^{-16} atoms $^{36}Cl/Cl$, far below the detection limits of conventional (low energy) mass spectrometers. The development of accelerator mass spectrometry (AMS) as an analytical tool means most natural samples are within the range of analysis. Accelerator mass spectrometry allows great sensitivity (down to 5×10^{-16} atoms $^{36}Cl/Cl$) with small sample size (down to < 200µg Cl as AgCl).

Chlorine-36 has been used in a range of geological applications, eg. exposure-age dating of impact structures and measurements of weathering rates, and the half-life of ^{36}Cl coupled with the hydrophilic nature of Cl also makes ^{36}Cl an effective hydrological tracer, particularly for dating groundwater and estimating recharge rates. Many such investigations approximate the input rates of ^{36}Cl to groundwater systems by measuring the $^{36}Cl/Cl$ ratios of recharge to the system, requiring additional $^{36}Cl/Cl$ ratio measurements. An inexpensive and fast method of approximating input values involves estimations from theoretical calculations of the fallout of ^{36}Cl and stable Cl to the Earth's surface. Hence, this investigation will assess how well the predicted ^{36}Cl fallout values correspond to measured values in precipitation, and its relation to recharge values.

Chlorine-36 also has a number of applications in atmospheric investigations. With the growing interest in the behaviour of Cl in the atmosphere, ^{36}Cl has been used as

a tracer for stratospheric Cl chemistry (Wahlen et al 1991). The use of ^{36}Cl as a tracer of stratosphere-troposphere exchange has been investigated, and it is suggested that enhanced mixing during seasonal shifts in the height of the tropopause is portrayed by increases in the fallout of ^{36}Cl (Hainsworth et al 1994, Knies et al 1994).

Many of the applications mentioned above rely upon an understanding of the processes involved in ^{36}Cl deposition. However there are very few data concerning ^{36}Cl in modern deposition, and the existing measurements are all from the northern hemisphere. This thesis provides data for ^{36}Cl deposition in Australia and hence the southern hemisphere and can be used to address a number of uncertainties existing in our understanding of ^{36}Cl deposition. The SN array spans latitudes 12°S to 35°S, and allows an assessment of the latitude-dependent predictions of ^{36}Cl fallout used in many hydrological investigations. The WE array approximates a narrow range of latitudes, and lies equidistant between the northern and southern coasts of Western Australia. It allows an assessment of the change of $^{36}Cl/Cl$ ratios with increasing distance from the coast without the added complication of latitude variation. The 2-year seasonal sampling program allows an investigation of the seasonal variations in fallout of ^{36}Cl, thus further investigating the use of ^{36}Cl as a tracer of stratosphere-troposphere mixing. The relationship between ^{36}Cl fallout and rainfall amount can be investigated, and correlations between ^{36}Cl concentration and major-element concentrations provide information about the phase of ^{36}Cl in the atmosphere. The data, being the first from the southern hemisphere, allows comparison with northern hemisphere fallout rates.

1.3 OBJECTIVES AND THESIS OUTLINE

This thesis is directed towards an understanding of major-element and ^{36}Cl chemistry in precipitation from remote areas of Australia. This is achieved through the following objectives:

1) The characterisation of the meteorological features that produced rainfall during each season at each site for the sampling program.

2) The characterisation of the major-element chemistry of rainfall from remote areas of Australia and assessment of the flux of ions to the Australian continent.

3) The assessment of the source of material to the continent, and the isolation of the influences of different meteorological patterns on the rainfall chemistry (i.e. seasonal variations).

4) The characterisation of the fallout of ^{36}Cl to the Australian continent.

5) The assessment of the relationship between $^{36}Cl/Cl$ ratio with changing distance from the coast.
6) The assessment of the applicability of the latitude-dependent ^{36}Cl fallout model of Lal and Peters (1967).
7) The assessment of processes that perturb ^{36}Cl fallout over time (i.e. seasonal variations).
8) The assessment of the form of ^{36}Cl in the atmosphere before deposition.
9) The comparison of southern hemisphere and northern hemisphere fallout levels.

Point 1 will be the emphasis of Chapter 2 which describes the general features of the atmospheric processes and weather patterns that affect Australia. Chapter 2 also describes a simple classification system of rainfall-producing synoptic processes. This classification is devised to assign the production of rainfall at meteorological stations in the proximity of the sample locations to a particular synoptic process (or combination of processes). From this, the predominant synoptic process that produced rain for each sampling period at each site is determined. Thus, the predominant origin of moisture and movement of airmasses before deposition of precipitation is determined. This is a simple method of tracking the movement of airmasses when back-trajectory information is not available.

Chapter 3 describes the methods used in this investigation, including sampling and analytical procedures, methods of data analysis and checks of quality control. Chapter 4 provides an introduction to the formation and chemistry of precipitation and a summary of previous precipitation investigations in Australia. Points 2 and 3 are the emphasis of Chapter 5, which uses multivariate analysis to determine the sources of chemical constituents to the precipitation collectors. Simple analysis of different element ratios allows the determination of seasonal variations in the supply by the sources of material, and these variations are tied into the results from Chapter 2. Points 4 to 9 are covered in Chapter 6 whose emphasis is on ^{36}Cl. The conclusions of this thesis are summarised in Chapter 7.

CHAPTER 2 WEATHER PATTERNS OF AUSTRALIA

An understanding of the sources and movement of airmasses and moisture that produce rainfall is necessary to aid the successful interpretation of the chemical and isotopic composition of precipitation collected in the sampling vessels. It was impractical to make detailed meteorological observations at each site given their remoteness. This chapter combines the availabie meteorological observations with information on average weather patterns, to create a system of assigning rainfall during each sampling period to a particular synoptic process or combination of processes. Note that this system of classifying synoptic processes only includes rainfall-forming events and therefore does not take into account the effects of dry deposition. This system will be used subsequently in the interpretation of major-element and ^{36}Cl data.

2.1 CONTROLS ON AUSTRALIA'S CLIMATE PATTERNS

An assessment of the accession of material to the Australian continent by rainfall requires knowledge of the sources and movement of air before deposition occurs. This requires an understanding of air circulation over Australia, the airmasses that influence the Australian continent and rainfall distribution over Australia.

Air Circulation

General Circulation

A simplified picture of general global atmospheric circulation is shown in Figure 2.1. The interior of the circle in Figure 2.1 represents circulation at the Earth's surface. In the tropical regions (30°N to 30°S) the trade winds are present flowing from southeast to northwest in the southern hemisphere. The interaction of the northern and southern hemisphere trade winds creates an area of low surface pressure known as the intertropical convergence zone (ITCZ). In the middle latitudes, the westerlies are present. Between the westerlies and trade winds are the zone of high pressure known as the Subtropical High Pressure Belt. In the polar regions, the winds are on average easterly.

The exterior of the circle in Figure 2.1 represents circulation in the upper troposphere. Hadley cells involve air rising in tropical regions and subsiding at middle latitudes. This circulation gives rise to the trade winds and the subtropical

high-pressure belt. Hadley circulation makes up the main component of meridional circulation at low latitudes which maintains the heat flux required to balance the global energy budget. The ITCZ forms a barrier of exchange between the Hadley cells, dividing the troposphere into northern and southern hemispheres. The ITCZ oscillates northwards and southwards about an average position near the equator. Thus the exchange of airmasses between the two hemispheres is due to the seasonal relocation of the ITCZ (Figure 2.2). Other circulation cells shown in Figure 2.1 include Ferrel cells (or indirect circulation), which govern meridional circulation in the opposite direction to that required for thermally driven motion. The polar cells are weak systems that produce the polar easterlies.

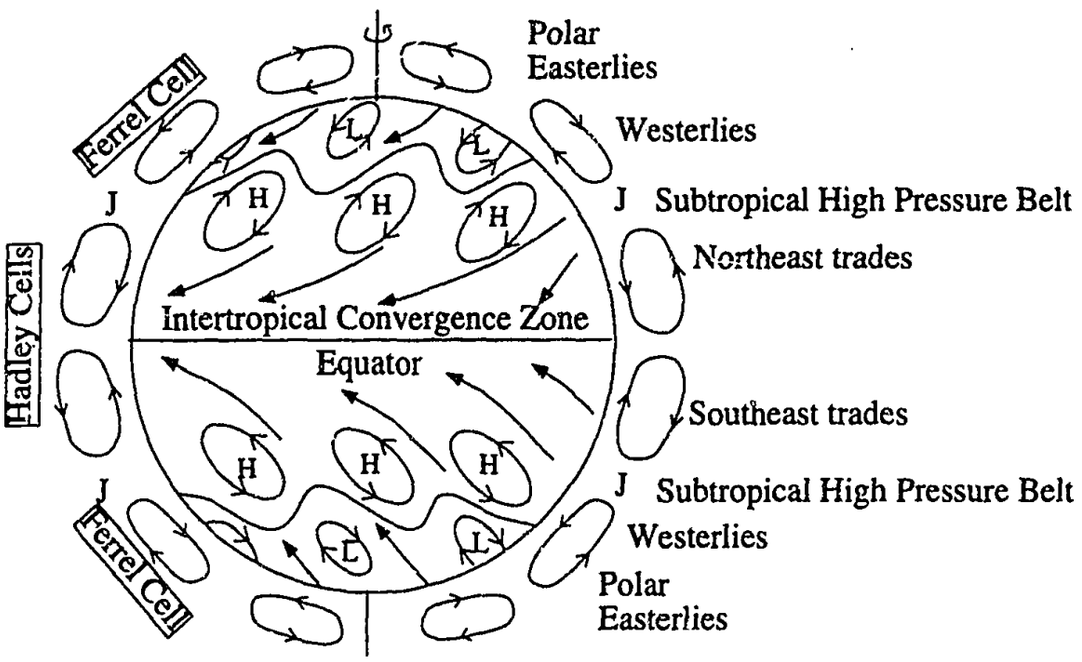

FIGURE 2.1 Simplified schematic diagram of the features of atmospheric circulation. The interior circle represents the lower troposphere, the exterior of the circle represents the upper troposphere. J = Jet streams, H=highs, L=lows. After Neiburger, Edinger and Bonner 1982.

Large-scale eddies (cyclones, anticyclones, waves in zonal currents) act to reduce instability in the global circulation that would result if Hadley circulation was the only method of meridional transport of energy and momentum. Large-scale eddies are in fact responsible for most of the transport of energy and momentum, except at low latitudes where Hadley cell circulation plays an equally important role. The transfer of momentum by eddy motions gives rise to the westerlies in the middle latitudes and upper troposphere, and surface friction in the westerlies gives rise to the weak reverse meridional circulations, forming the Ferrel cells.

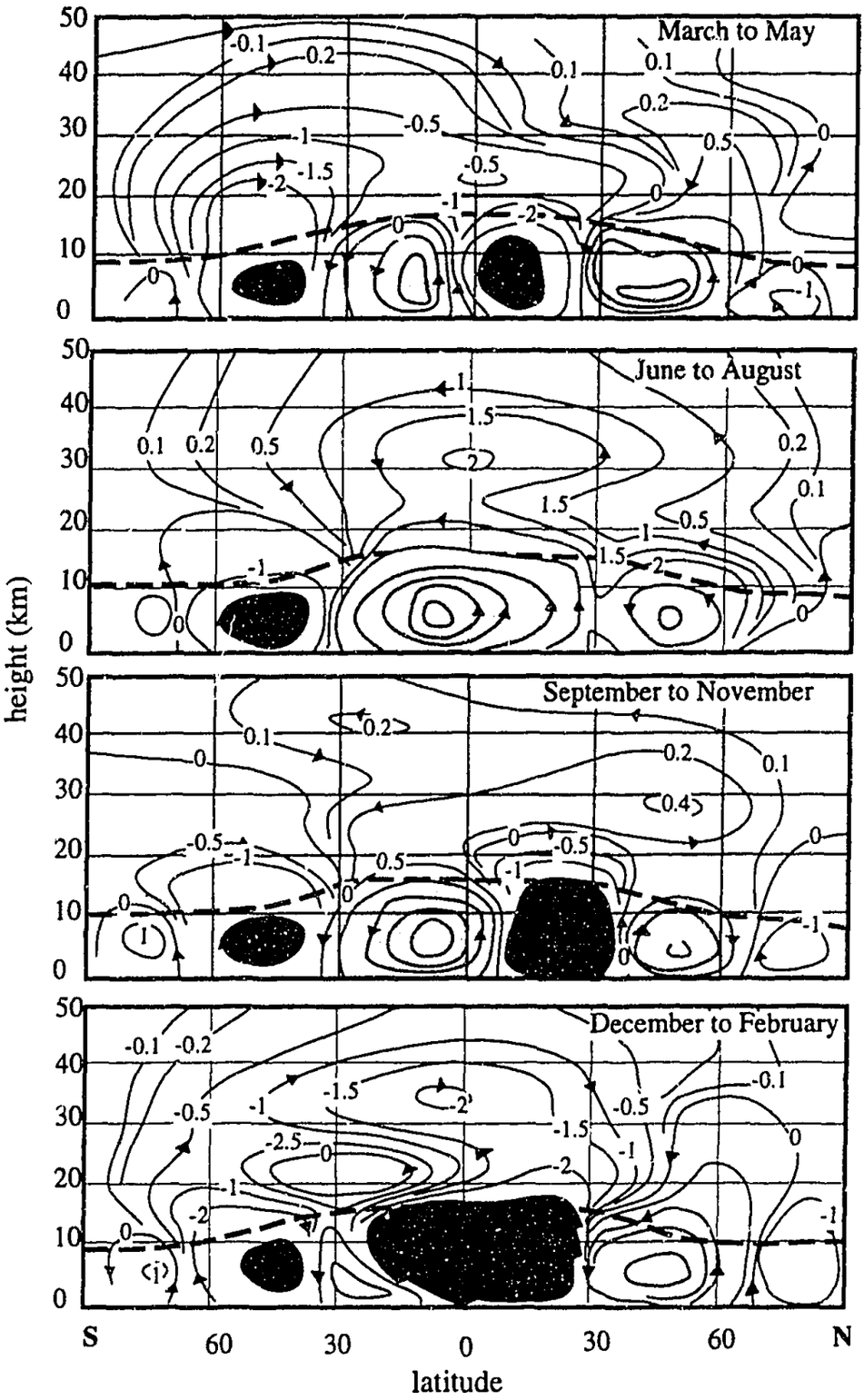

FIGURE 2.2 Mean meridional circulation. Mass streamlines in units of 10^{12} g/s. Dashed line is the mean tropopause height. The dark shaded area represents streamlines < -5 x10^{12} g/s. Light shaded areas represent streamlines > 5 x 10^{12} g/s. In spring (September to November) and autumn (March to May), there are 3 meridional circulation cells in each hemisphere. In summer (December to February) and winter (June to August) this pattern is distorted. After Warneck 1988.

Winds in the upper troposphere are westerly in all latitudes except at the equator. The westerlies encircle the globe in a wave like pattern (Rossby waves). The west wind maxima mark the jet streams (represented by J in Figure 2.1). The dimensions of the jet streams are of the order of 1000 km long, 100 km wide and 1 km deep. Australia is affected by two jet streams, the polar front jet stream being less significant than the subtropical jet stream. The polar jet stream occurs between 50-60° and lies above the boundary between warm air of the tropics and cold air of the pole. The subtropical jet stream is situated above the Subtropical High Pressure Belt at 32°S in February and 26°S between May and November (Figure 2.3) Its speed is greatest in July. A gap in the tropopause at 35-40°S occurs in association with the jet stream allowing maximum transfer of material from the stratosphere to the troposphere at this latitude (Reiter 1975). This is particularly important for the ^{36}Cl discussions of Chapter 6.

Circulation over Australia

Figure 2.3 displays a simplified picture of air circulation over Australia during summer and winter. Australia is influenced by the ITCZ during summer and during winter the ITCZ lies north of Australia. The Subtropical High Pressure Belt influences Australia throughout the year, during summer lying over the southern part of the continent, and during winter moving northwards to lie over the centre of Australia. Trade winds affect Australia northwards of the high-pressure belt.

During summer, when the high-pressure belt lies to the south of Australia, much of the continent is influenced by the steady easterly trade winds. During winter, the north of Australia becomes increasingly influenced by the easterly trade winds, as the high-pressure belt moves northwards. Areas south of the high-pressure belt become influenced by westerly winds, which often have low-pressure cells embedded in them. In the north of Australia, during summer, northwesterly winds associated with the monsoon dominate.

Airmasses

The atmosphere consists of a large number of regions in which conditions of temperature, humidity and stability are relatively uniform. These regions, or airmasses may have a diameter of 500-5000 km and an internal temperature gradient of less than 1°C per 100 km (Linacre and Hobbs 1982). Airmasses attain certain characteristics after prolonged contact with regions of the Earth's surface (source area) having a particular temperature and humidity (Gentilli 1971). Therefore, the

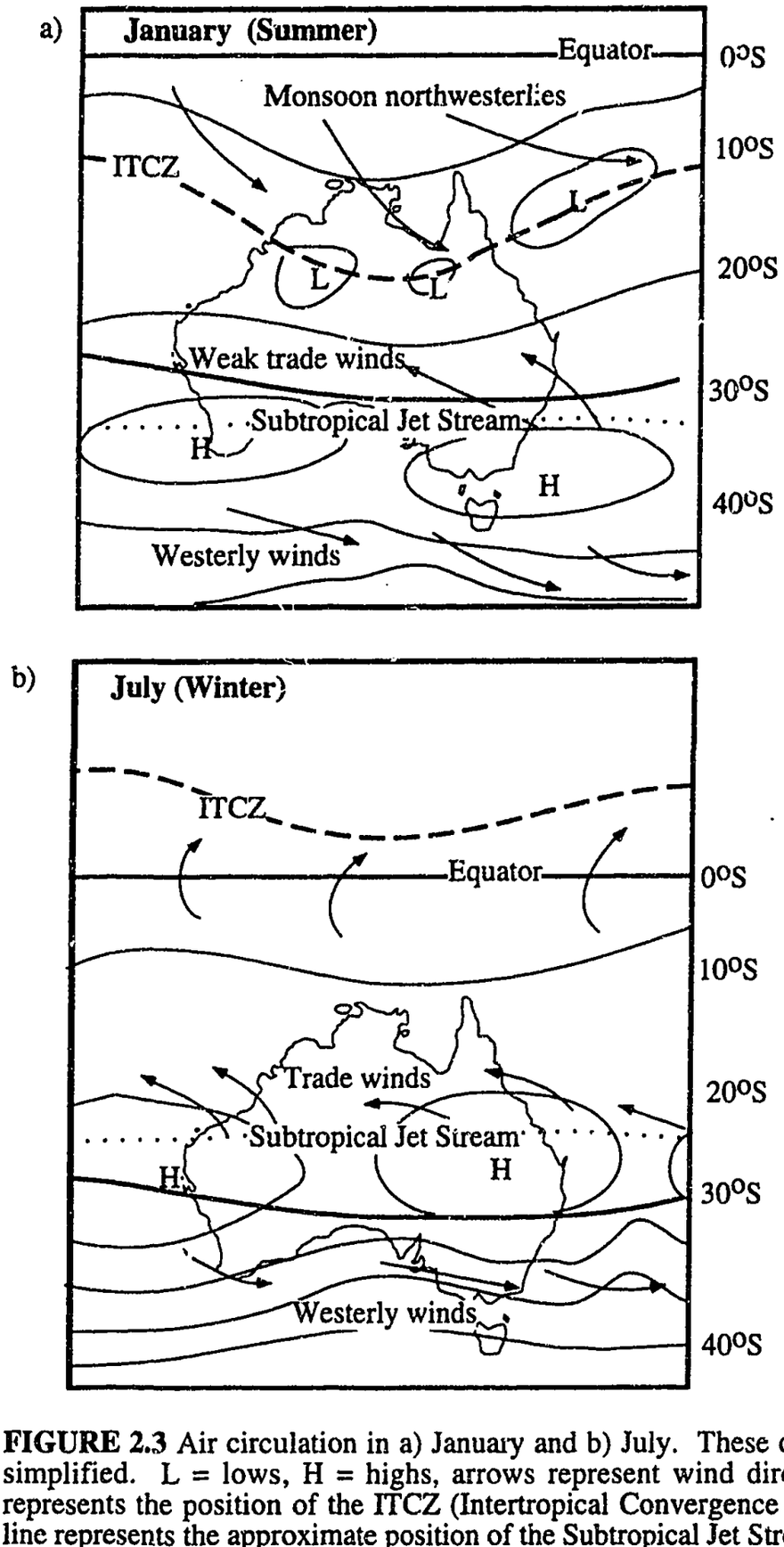

FIGURE 2.3 Air circulation in a) January and b) July. These diagrams are highly simplified. L = lows, H = highs, arrows represent wind direction, dashed line represents the position of the ITCZ (Intertropical Convergence Zone). The dotted line represents the approximate position of the Subtropical Jet Stream position. After Tapper and Hurry 1994.

characteristics of the airmass reflect the area from which it is sourced. Thus, understanding the movement of airmasses may lead to an identification of the source of the airmass, and ultimately the sources of material measured in precipitation.

The airmasses that affect Australia have a limited range of characteristics so their classification is simpler than for complex systems elsewhere in the world (Gentilli 1971). The source areas of airmasses that affect Australia are shown in Figure 2.4. The characteristics of these airmasses are shown in Table 2.1.

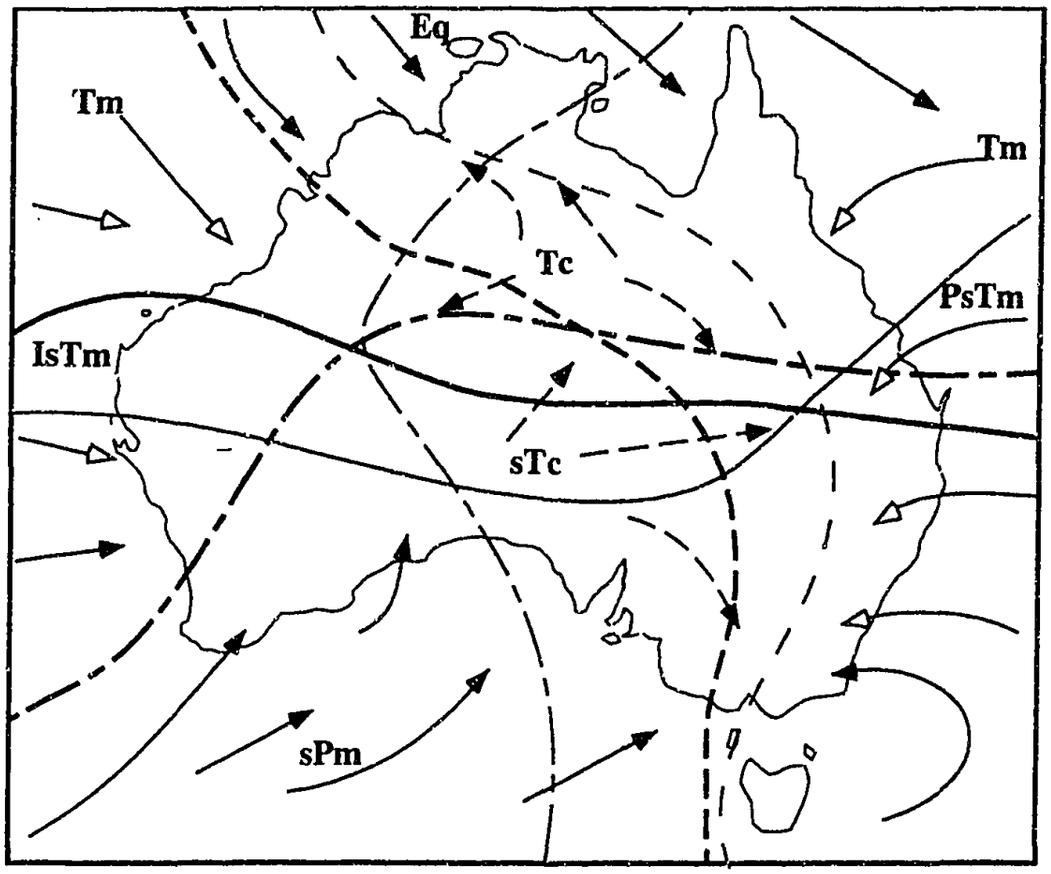

FIGURE 2.4 Source areas and limits of airmasses that affect Australia. Thick lines represent limits for January, thin lines represent limits for July. Solid lines represent limits of sPm, dashed lines represent limits of PsTm and dash-dot lines represent limits of IsPm. Tc = tropical continental, sTc = subtropical continental, Tm = topical marine, PsTm = Pacific subtropical marine, IsTm = Indian subtropical marine, Eq = equatorial and sPm = subpolar marine. Characteristics of these airmasses are given in Table 2.1. The limits of the airmasses are based on weather charts of 5 years and are indicative only. After Gentilli 1971.

The tropical airmasses (Tc and Tm) dominate over Australia. They originate equatorwards from a ridge of high pressure where sinking and convergence occur in a belt (Gentilli 1971). Subtropical airmasses (sTc and sTm) originate polewards of this ridge. Subtropical maritime airmasses (sTm) originate from the west Indian

TABLE 2.1 Characteristics of the airmasses that affect Australia (after Gentilli 1971 and Tapper and Hurry 1993).

Mass	Source Area	Area Affected	Features
tropical continental (Tc)	central Australia	anywhere in Australia	summer, hot dry and unstable (cooler in winter); dew point -4 to +2°C; heat waves
subtropical continental (sTc)	southern central Australia	inland southern Australia	year round, stable and dry; dew point 2-7°C;
tropical marine (Tm)	Timor and Coral Seas	northern and western Australia	warm and humid; winter T=22-24°C.; summer T=26-28°C; RH close to saturation; Northwest Cloud Band in winter, tropical cyclones in summer, torrential rains to northeast slopes in summer.
Indian subtropical marine (IsTm)	Indian Ocean	western and southern coastal areas	winter T=10-12°C, RH= 80-85%, air in the westerly stream; summer T=20-22°C, RH= 70-75%, air in the cool change between two anticyclones
Pacific subtropical marine (PsTm)	Pacific Ocean	southeast and central coast, Tasmania	winter T=14-16°C, RH near saturation, cyclogenic belt near Tasmania summer T=22-24°C, RH saturated, thunderstorms and torrential rains in the presence of orographic barriers
Equatorial (Eq)	Transequatorial	northwestern Australia in summer	summer only, dew point =21-24°C; monsoon
subpolar maritime (sPm)	Southern Ocean	southern coast	cool and moist; dew point = 7-13°C; cloudy drizzle that may develop into rain in the presence of orographic barriers

Ocean (IsTm) and the east Pacific Ocean (PsTm). Tropical maritime airmasses (Tm) have two major reservoirs, the Timor and Coral Seas. The Gulf of Carpenteria is a minor reservoir of tropical maritime air. The trapezoidal shape of Australia north of the Tropic of Capricorn means that there is very little difference between the influence of Indian Ocean and Pacific Ocean air to the Tm. Tropical continental airmasses (Tc) form over the continent further than 500 km from the coast (Linacre and Hobbs 1982). Equatorial airmasses (Eq) are sourced over the equator. Subpolar

maritime air (sPm) is sourced in the Southern Ocean and only influences southern areas of Australia.

An alternative way of considering the source of material in precipitation is by considering air streams (Figure 2.5). An air stream is the mean airflow averaged over some specific time whose temperature and moisture characteristics are continually changed by the surface over which they pass as well as in response to changes in vertical motion and stability fields (Wedland and McDonald 1985). Airmasses and air streams are not synonymous. However an air stream may become an airmass if it travels over a large homogeneous surface and acquires the temperature and humidity of that surface.

The airstreams that affect Australia have been investigated by Wedland and McDonald (1985), with streamline analysis identifying monthly air stream dominance regions from monthly mean surface winds from more than 30 stations around Australia over 18 years. Two major patterns were observed, a winter pattern of continental airstream dominance and a summer pattern of oceanic airstream dominance: streamlines are less constant in spring and summer than in autumn and winter, which may be due to the presence of confluences that only occur during summer and spring (Figure 2.5). These confluences are caused by the interaction of the northern limit of Southern Ocean maritime air and the south western limit of Pacific maritime air, and the interaction of the Indian Ocean maritime air from the northwest with the easterly trades from the Pacific. Migrating cyclones and fronts are concentrated along these confluences in spring and summer.

Rainfall Patterns of Australia

Figure 2.6 shows the distribution of rainfall across Australia. The highest rainfalls occur in coastal and mountainous terrains (eg. tropical coast of Queensland, western Tasmania. Tn contrast, much of the centre of Australia receives very little rainfall, because of the region's isolation from moist oceanic airmasses. The rainfall that the interior of Australia does receive is highly variable.

The rainfall pattern of Australia is seasonal, with a winter regime in the south and summer rainfall in the north (Figure 2.7). Of interest for this investigation, the wet summer in the tropical north occurs under the influence of the monsoon. The southward movement of the ITCZ brings moist equatorial air to the northern part of

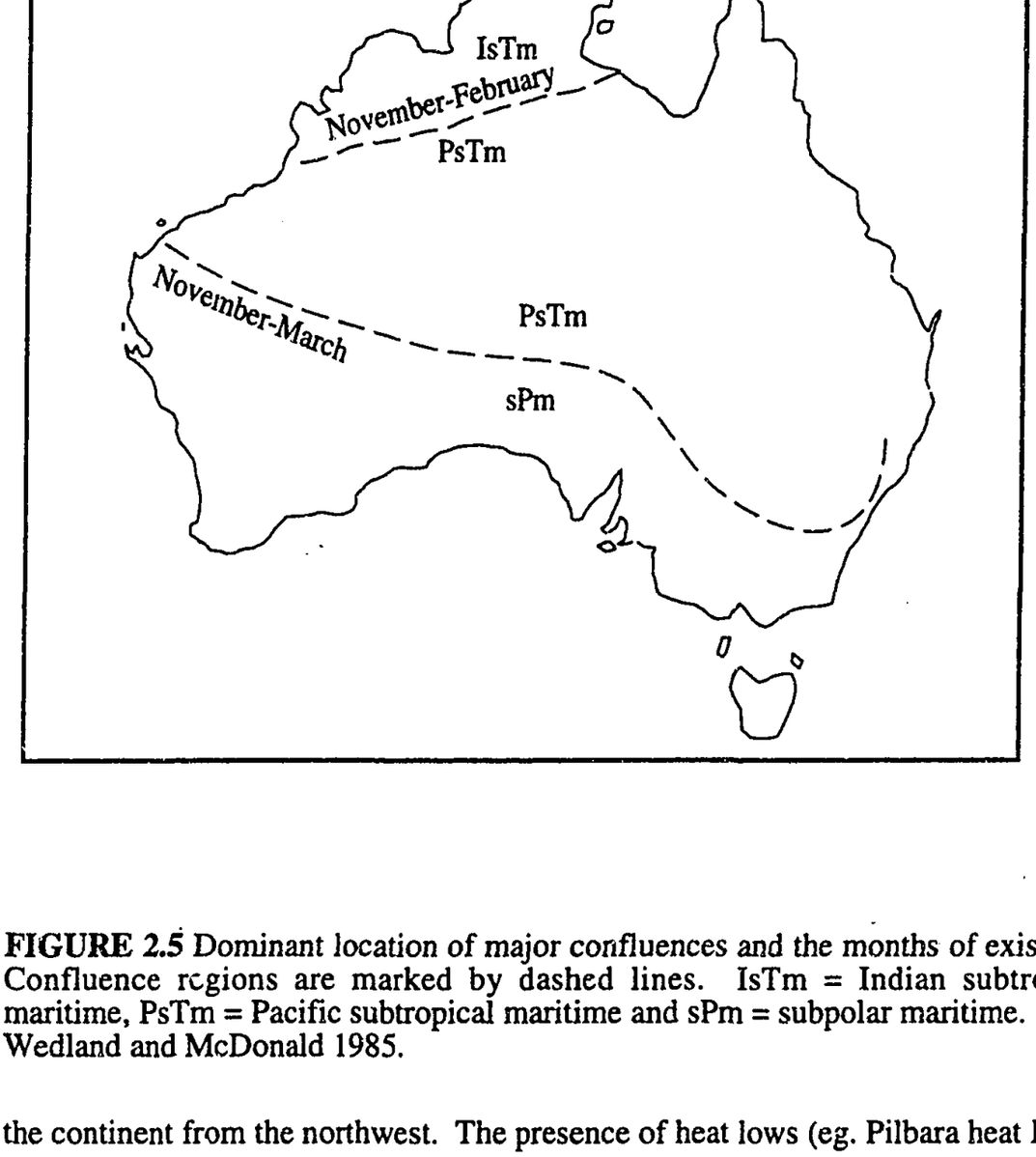

FIGURE 2.5 Dominant location of major confluences and the months of existence. Confluence regions are marked by dashed lines. IsTm = Indian subtropical maritime, PsTm = Pacific subtropical maritime and sPm = subpolar maritime. From Wedland and McDonald 1985.

the continent from the northwest. The presence of heat lows (eg. Pilbara heat low in WA) also allows the influx of moist air from the humid tropics. The presence of the subtropical high over the south of the continent during summer suppresses rainfall. During the dry season the north is under the influence of the southeasterly trade winds which blow off the continent. The south of Australia experiences winter rainfall with the passage of cold fronts and associated systems. During the winter months the major pressure systems (ITCZ and Subtropical High Pressure Belt) are further north than during summer, increasing the probability of cold fronts reaching southern Australia and bringing rain. Cold fronts may be responsible for generating high winter rainfall in the south of the arid zone (Figure 2.7). The arid zone has a distinct summer rainfall regime in the tropics and subtropics, and uniform seasonal rain to winter rainfall in the south.

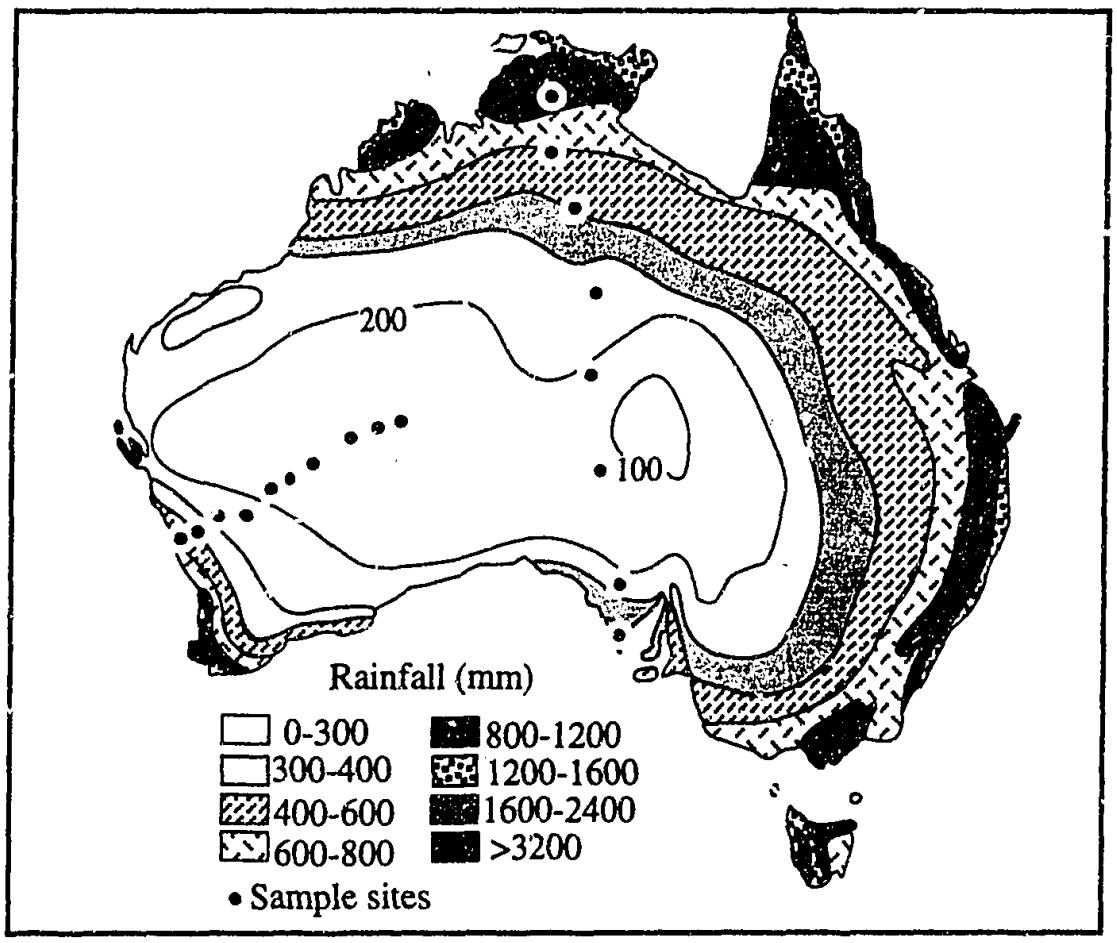

FIGURE 2.6 Median annual rainfall across Australia, and sampling localities from the present investigation. After Tapper and Hurry 1994.

2.2 GENERAL WEATHER PATTERNS

Atmospheric pressure, wind and precipitation are changing constantly over Australia. However there are basic patterns of pressure and wind that underlie these changes. Continuous observations of Australia's meteorological conditions over a long period of time allows the generalisation of seasonal weather patterns. These are discussed below for the areas in which the rain collecting arrays are located (i.e. Western Australia, Northern Territory and South Australia). The general weather patterns of each area are described in terms of seasonal changes to coincide with the seasonal sampling program detailed in Chapter 3. The descriptions of the seasonal weather patterns for Western Australia, South Australia and the Northern Territory are summarised from the Monthly Weather Review for each area (Bureau of Meteorology 1992a, Bureau of Meteorology 1993a, Bureau of Meteorology 1993b). Figure 2.8 gives the location of geographical place-names mentioned in this section.

Western Australia (Bureau of Meteorology 1992a) (Figure 2.8a)

Summer (December to February)

In a typical year, the weather in Western Australia during December is controlled by the presence of an anticyclone in the Great Australian Bight and an extensive heat low in the north. The heat low that affects Western Australia (the Pilbara heat low) is an area of low pressure resulting from the anticyclonic transportation of heat from the heart of the continent to the northwest. It remains stationary over the Pilbara area because of the hot land that creates a permanent centre of convection. The southern portion of Western Australia is influenced by dry easterly winds and the north of Western Australia by moist westerlies. As summer progresses, the high-pressure belt becomes centred over the south of Western Australia. In the north the airflow is strongly influenced by the presence of a deepening low pressure over land. Thus a gradient between the tropical and subtropical areas results in the flow of warm to hot continental air over much of Western Australia. January rainfall is therefore usually the result of thunderstorm activity over most of Western Australia. In the tropics, rainfall increases sharply, especially in the Kimberley and is commonly caused by cyclonic activity that originates near the northwest coast. The high-pressure belt remains to the south of the continent during February and West Coast troughs develop. As these troughs deepen northeasterly winds develop and temperatures increase in coastal districts.

The cyclone season in Western Australia spans November to March. Cyclones often develop in the Timor Sea and cyclones that cross the coast tend to decay into tropical depressions that may cause extensive flooding. The probability of Western Australia being affected by a tropical cyclone is highest in February.

Autumn (March to May)

The beginning of Autumn (March) represents the late part of the monsoon in the north of Western Australia so the monsoonal low-pressure area in the tropics is generally weaker. Tropical cyclones tend to develop further westwards and move west or south before decaying. With the impending end of the wet season in the north, there is a decrease in rainfall during March. With the end of the monsoon, the high-pressure belt begins its northwards movement and pressures rise over the state. Westerly winds become more frequent in the southwest, though the incidence of gales and heavy rainfall events remains low. The high-pressure belt continues its northward migration during May and establishes itself over the southern part of the continent. Thus easterly winds are able to move over the northern cooling land

mass, bringing a shift to winter conditions. Over southern parts of the continent westerly winds prevail although periods of calm are common. Incursions of moist middle-level tropical air over the northwest (Northwest Cloud Bands) can sometimes result in heavy rainfall extending from the northwest coast to the Goldfields, and as far east as the eastern states of Australia. Westerly winds in the southern half of Western Australia bring increasing rain over the southwest.

Winter (June to October)

The high-pressure ridge has completed its northward migration by the beginning of winter (June). Winter conditions are characterised by fine clear weather and drops in temperature over much of the state, and intense rainfall in the southwest. In the tropics, fine weather prevails, except when a strong southern front penetrates to the north coast. The sub-tropical ridge intensifies slightly during July so that skies are

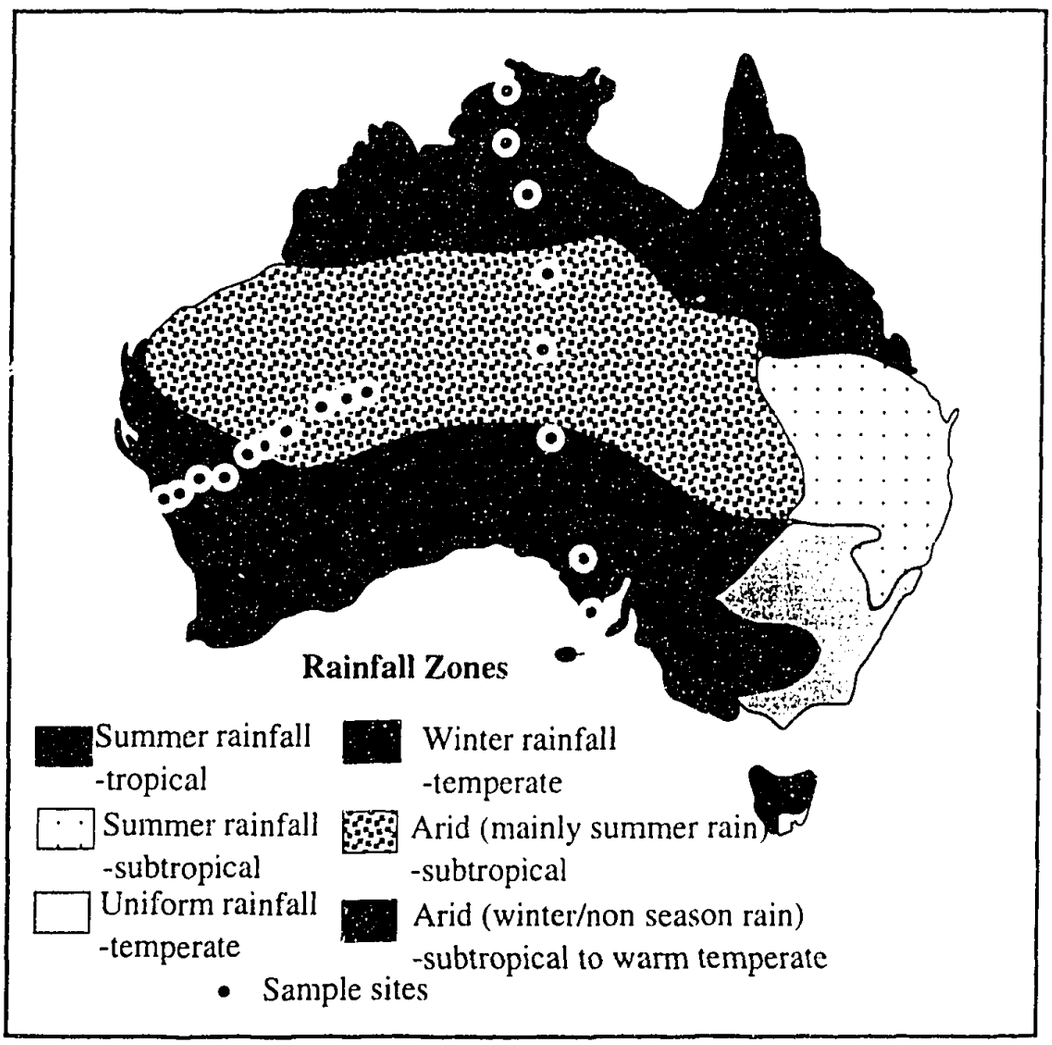

FIGURE 2.7 Rainfall zones of Australia and sample localities from the present investigation. After Tapper and Hurry 1994.

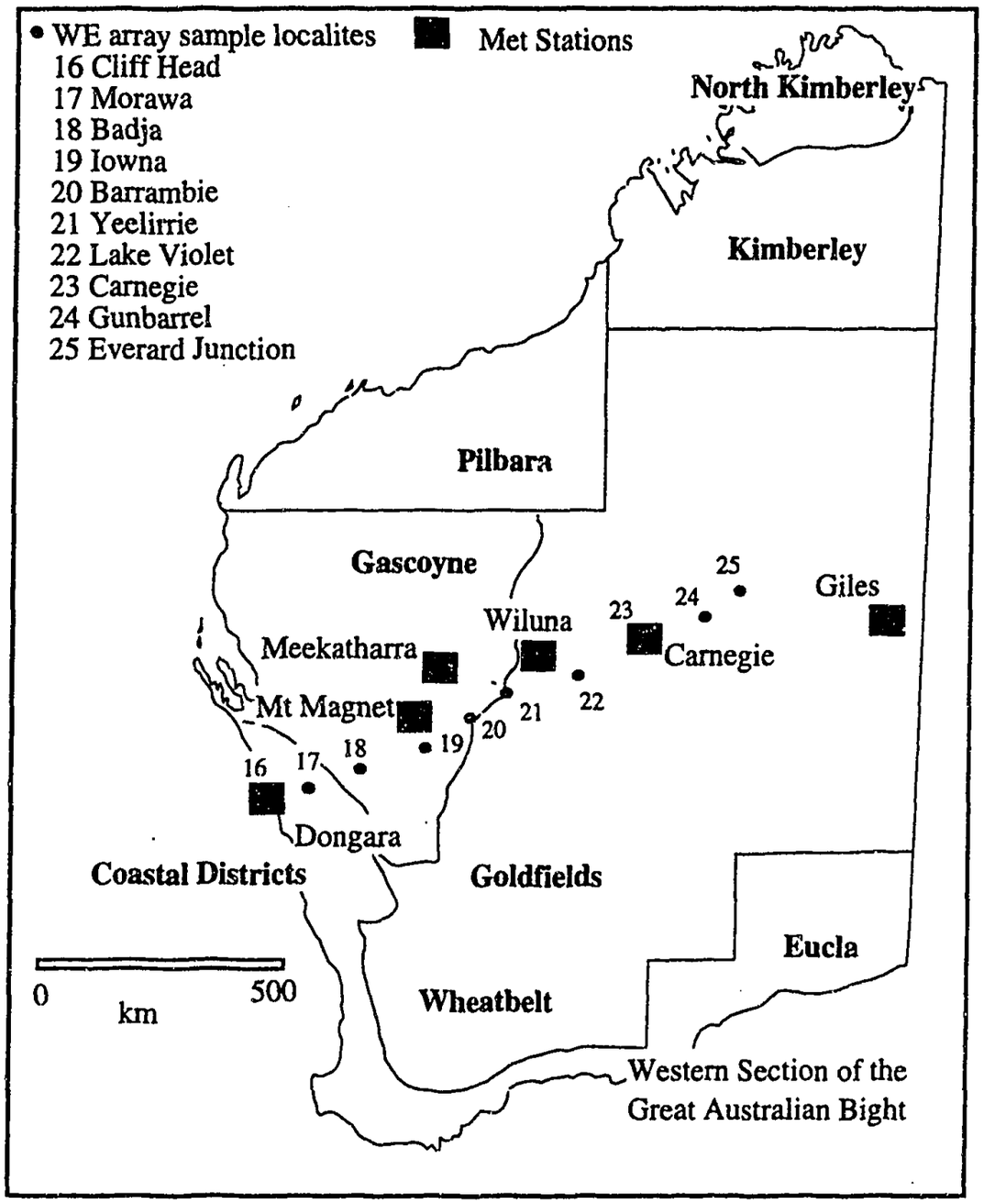

FIGURE 2.8A Sample localities along the WE array, Met Stations used for meteorological observations, and location of geographical place names discussed in the text.

more frequently clear, and the large net loss of radiation makes July the coolest month in the state. The tropical regions rarely receive rain in July. Again incursions of moist middle-level tropical air may result in widespread rain in the Pilbara, Gascoyne and Eucla. Cold fronts from the southwest Indian Ocean can interact with these disturbances to produce widespread heavy rain over most of the southern half of the state. The high-pressure system begins its southward movement by August, signaling the beginning of a gradual return to summer conditions. The wind patterns remain easterly to the north of the ridge and westerly to the south. In the north, August is the driest month.

Spring (September to November)

The first isolated thunderstorms of the spring season occur during September and may produce rain in the Kimberley. Westerly winds occur more frequently in the Northern Kimberley as the month progresses. Easterlies still prevail over the rest of the north while on the south coast, winds remain westerly. The remainder of the south of Western Australia is dominated by easterly winds as the high-pressure ridge moves southwards. Westerly gales occur with less frequency in the southern areas of the Western Australia. The high-pressure belt continues to move southward during October, so that the south of Western Australia experiences more days with easterly winds. The southward movement of the ridge allows an influx of moist tropical air into the Kimberley from nearby seas, contributing to the increased thunderstorms as the season progresses.

The high-pressure belt is mainly confined to the south of the continent by the end of spring and easterly winds are produced to the south of the belt. The southern areas experience westerly winds and scattered showers when the high-pressure belt is centred over the continent. There is usually no rain further north except over the Kimberley where rain becomes more frequent as the month progresses. Cyclones may cause very high rainfalls along the tropical coast although cyclones are rare during November.

Northern Territory (Bureau of Meteorology 1993a) (Figure 2.8b)

Summer (December to February)

The Northern Territory experiences the third month of the wet season during December. This is characterised by active monsoon bursts (broad areas of rain with sustained northwesterly winds) and break periods (light winds, isolated showers and storms, occasional gusty thunderstorms and squall lines) between the active

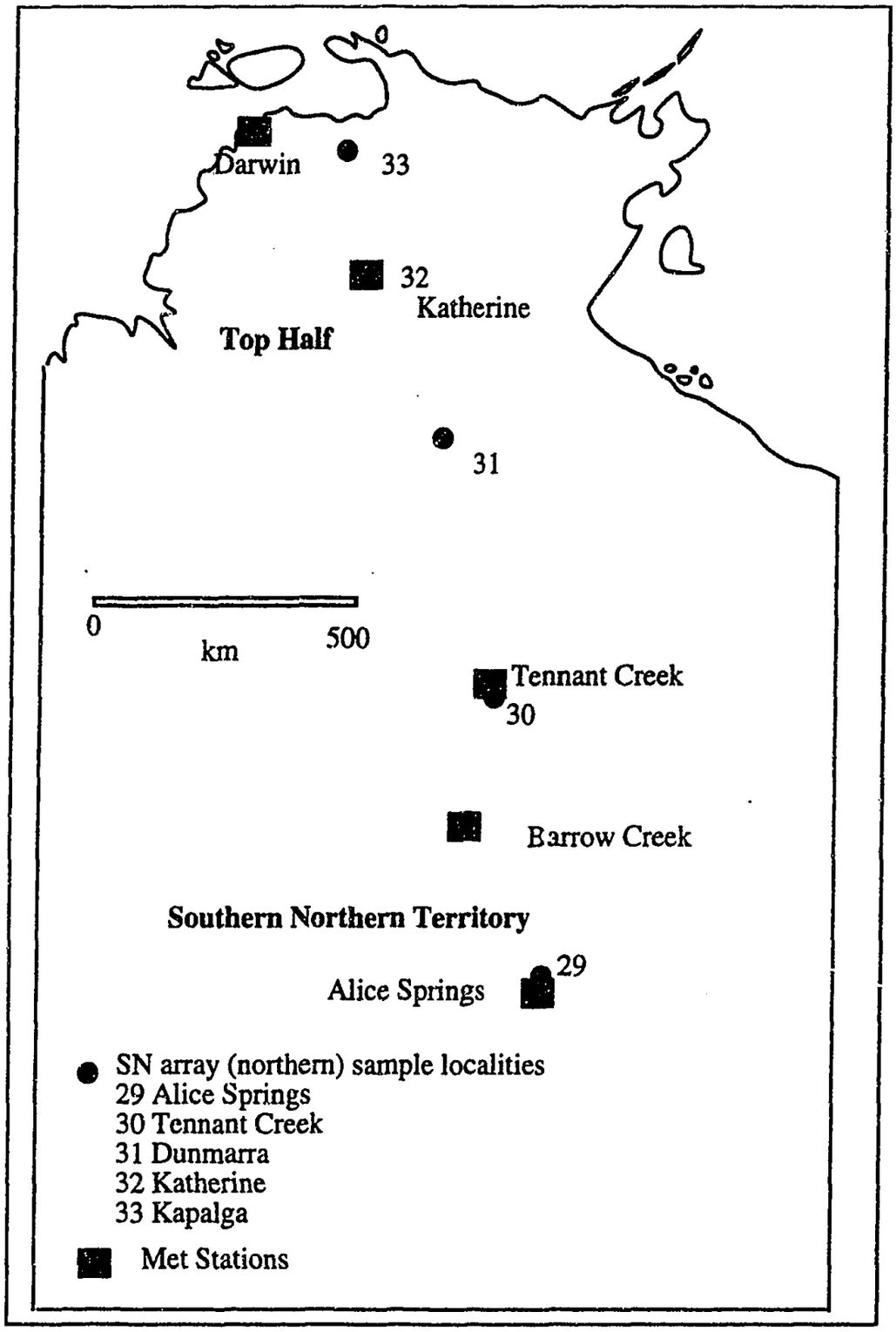

FIGURE 2.8B Sample sites along the northern section of the SN array in the Northern Territory, and Met stations used for meteorological observations.

monsoon bursts. Active monsoon bursts occur late in December. January and February represent the height of the wet season, with monsoonal bursts occurring for periods of up to seven days at a time. Active monsoonal bursts favour the development of tropical cyclones. December has a tropical cyclone once in every two years, January twice in every three years and February once in every two years.

East to southeasterly trade winds produce fine conditions over the southern half of the Northern Territory. Thunderstorms may develop during December when tropical moist air extends southwards. January and February rainfall in the southern half of the Territory may also be produced by the inland movement of the monsoonal trough.

Autumn (March to May)

Autumn sees the weakening of the wet season during March and the beginning of the dry season in May in the north of the Northern Territory. Active monsoon bursts persist for shorter periods during March, become less common and confined to the north during April, and are absent during May. March is the most likely month for the development of tropical cyclones, with the Territory being affected by tropical cyclones at the rate of one per year.

East to southeasterly winds predominate in the south of the Northern Territory during March and April, bringing fine conditions. These conditions extend over the entire Territory during May, except along the northeast coastal fringes which may experience brief morning thunderstorms Thunderstorms are uncommon during May and there is a marked decrease in the amount of rainfall from April to May.

Winter (June to August)

The dry season is firmly established in the north of the Northern Territory during winter. Fine conditions prevail with the establishment of east to southeasterly winds over the Territory except on the northeast coastal fringes. Occasionally troughs can bring rain and thunderstorms to the south. Northwest Cloud Bands may also become active over the Territory during winter.

Spring (September to November)

Wet-season type weather in the north of the Northern Territory occurs occasionally in September, but generally dry conditions prevail. October is the transitional month linking the wet and dry seasons over northern Australia. Light northerly air flow becomes predominant as the high-pressure ridge moves south. By November, the

wet season has begun and showers and thunderstorm activity occur with increasing frequency. Occasional active monsoon bursts with rain and sustained northwesterly winds occur in the north. Tropical cyclones are rare.
In the south, east to southeasterly winds dominate early in spring but northerlies become more frequent as the heat low establishes over northern Western Australia. As spring progresses, southeasterly winds persist but are lighter than in previous months. As the wet season develops in the north, thunderstorms may develop if tropical moisture extends to the south.

South Australia (Bureau of Meteorology 1993b) (Figure 2.8c)

Summer (December to February)
The weather in South Australia throughout the entire year is strongly controlled by the position of the subtropical high-pressure ridge. During summer the subtropical high-pressure ridge is established to the south of the continent and low-pressure systems cover the interior. The low-pressure systems enable moist tropical air from the north to reach the state, promoting the development of thunderstorms and showers in the north. The southerly position of the high-pressure ridge means that cold fronts that approach South Australia remain to the south of the state, and those that cross are generally weak.

Autumn (March to May)
During March the high-pressure ridge remains to the south of the continent and summer conditions persist. By May, the high-pressure ridge begins its northwards movement and oscillates between its summer position in the south and its winter position over the continent. The northern position of the ridge allows the northern movement of temperate cyclones and their associated cold fronts and brings rain to most parts of South Australia.

Winter (June to August)
During winter the subtropical high-pressure ridge generally remains in its favoured northern position over the continent at about the latitude of Brisbane. This allows the continued movement of lows and their associated cold fronts onto the south of the state. Northwest Cloud Bands interacting with cold fronts may produce large quantities of rain. The occasional southward movement of the high-pressure ridge to the latitude of Adelaide, may result in the suppression of cold front activity across South Australia by steering lows to the south of the South Australia.

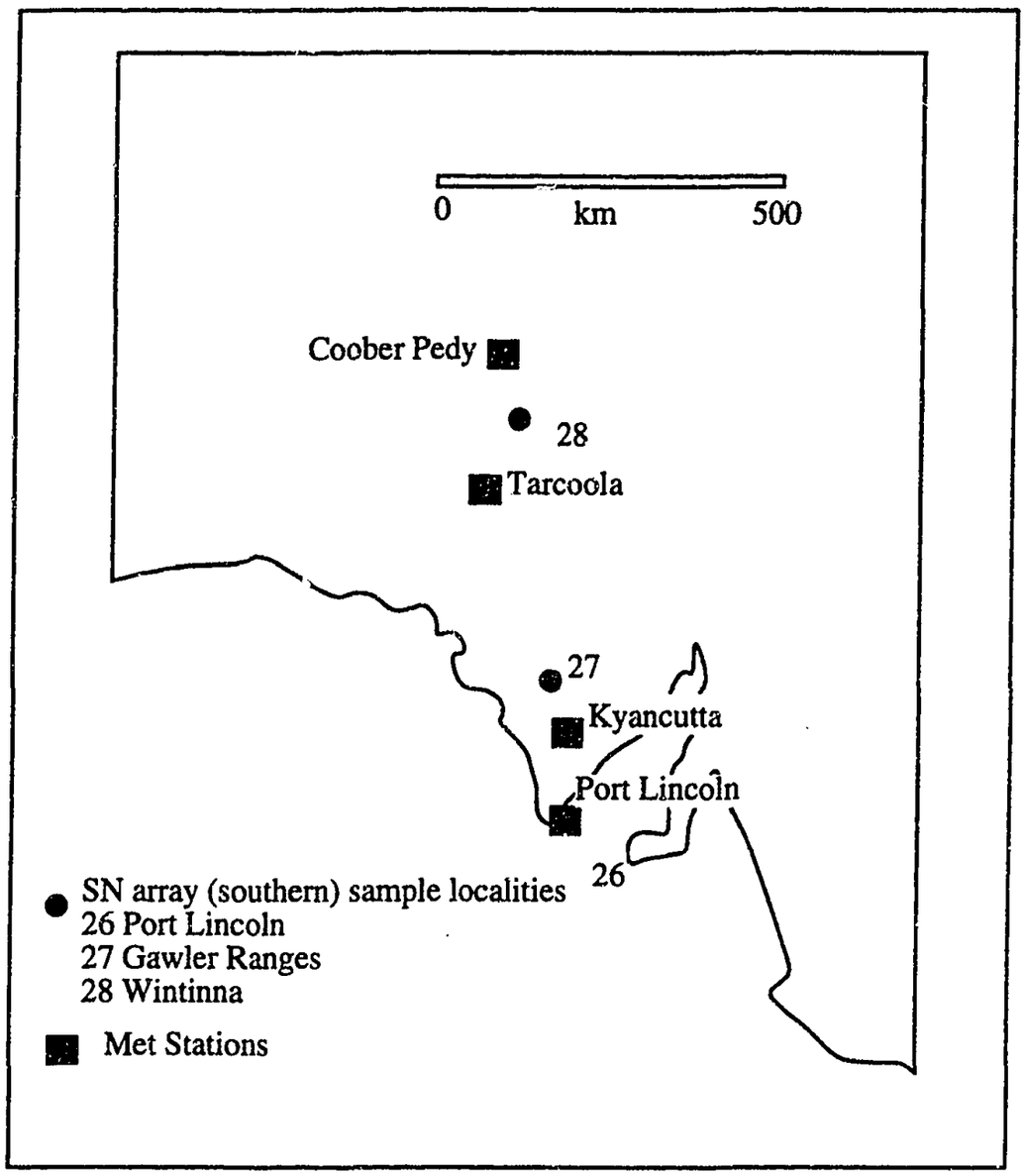

FIGURE 2.8C Sample sites along the southern section of the SN array in South Australia, and Met stations used for meteorological observations.

Spring (September to November)

Variable weather is typically experienced across South Australia during spring, because of the mobility of the subtropical high-pressure ridge between the Brisbane and Adelaide latitudes. This is common during September and October when the state experiences mixtures of summer and winter conditions. During November, the high-pressure system becomes established to the south of the state and low-pressure systems form over northern Australia, signaling the return to summer conditions in South Australia.

2.3 WEATHER PATTERNS 1991-1994

Data Description

Meteorological data were purchased from the Bureau of Meteorology. The observation stations (termed Met Stations) were chosen to lie as closely as possible to the sampling localities. Both three-hourly surface wind direction and daily rainfall data were used where available. The Met Stations used, their equivalent sample locality and the data available are listed in Table 2.2. Figure 2.8 shows the location of the Met stations and the sampling sites along the WE array, which extends in a west-east direction from the west coast of Western Australia, and the SN array, which extends in a north-south direction through the Northern Territory and South Australia. Details of these arrays are given in Chapter 3.

In general, except at the formal Met Stations (i.e. Giles), most observation stations are run by local residents who are not professional meteorologists. Thus wind direction data is approximate, and rainfall amounts are measured at 9 am each day, so may have fallen anytime between 9 am on the day of the measurement and 9 am of the previous day. This is taken into account when assigning rainfall to synoptic conditions.

Other data used are the daily surface synoptic charts published in the Monthly Weather Review for each state for each month, and the accompanying synoptic descriptions (Bureau of Meteorology 1992a, Bureau of Meteorology 1993a, Bureau of Meteorology 1993b). The synoptic charts published in the Monthly Weather Review are generalised to apply to the whole of Australia for each month, so that much of the detail described in the synoptic descriptions for each state is not always obvious from the synoptic maps.

Rain-producing Synoptic Classification System

Interpretation of daily surface synoptic charts and their accompanying descriptions has led to the development of a system by which the rainfall at each Met Station during the sampling program can be assigned to a particular synoptic process or a combination of processes. The range of synoptic processes used in the categorising system are described below. It should be noted however, that weather events are complex, and often do not fit into defined categories. In particular, in the development of rainfall, moisture and uplifting may come from a number of sources, and a rain event may be the result of a number of different mechanisms, some working to enhance the rainfall and some working to suppress rainfall. This is recognised in the following categorisation system, which is not designed to be a

TABLE 2.2 Summary of the Met Stations, the closest sample localities, and meteorological data.

Met Station	Sample locality[1]	data type	record period
Dongara	Cliff Head (16)	rainfall	March 91 to March 93
Mt Magnet	Morawa (17) Badja (18) Iowna (19)	rainfall,wind rainfall,wind rainfall,wind	March 91 to March 93
Meekatharra	Barrambie (20)	rainfall,wind	March 91 to March 93
Yeelirrie	Yeelirrie (21)	rainfall,wind	March 91 to March 93
Wiluna	Lake Violet (22)	rainfall,wind	March 91 to March 93
Carnegie	Carnegie (23)	rainfall,wind	March 91 to March 93
Giles	Gunbarrel (24) Everard Junction (25)	rainfall,wind rainfall,wind	March 91 to March 93
Port Lincoln	Port Lincoln (26)	rainfall	May 92 to June 94
Kyancutta	Gawler Ranges (27)	rainfall	May 92 to June 94
Tarcoola	Gawler Ranges (27)	rainfall	May 92 to June 94
Oodnadatta	Wintinna (28)	rainfall	May 92 to June 94
Coober Pedy	Wintinna (28)	rainfall	May 92 to June 94
Alice Springs	Alice Springs (29)	rainfall	May 92 to June 94
Barrow Creek	Alice Springs (29) Tennant Creek (30)	rainfall	May 92 to June 93
Tennant Creek	Tennant Creek (30)	rainfall	May 92 to June 94
Elliott	Dunmarra (31)	rainfall	May 92 to June 94
Katherine	Katherine (32)	rainfall	May 92 to June 94
Darwin	Kapalga (33)	rainfall	May 92 to June 94

[1] sample locality number in brackets (see Figure 2.8).

definitive work on the synoptic features that produced rainfall across Australia. Instead, this system is a means of assessing the likely sources of moisture and constituents to rainfall during the sampling period in a general sense, as shown in Table 2.3.

Tropical events

The northern half of Western Australia is affected by tropical events during summer. Tropical events along the WE array include tropical cyclones, tropical depressions, monsoonal depressions and the heat low, i.e. a synoptic process that involves airmasses with moisture sourced from the tropics to the north of Australia. Most of the rainfall that falls in the Northern Territory can be attributed to tropical events. For this reason, the categorisation system for the Northern Territory involves a break down of the tropical events group into the components that are applicable (i.e. tropical cyclones and gulf lines). Northern areas of South Australia may also experience tropical events. In particular, incursions of tropical air or the southern limits of monsoonal activity may occur during the wet season.

Tropical Cyclones

While several tropical cyclones formed north of Australia during the sampling program, only three were involved in producing rain over northern Australia. These were tropical cyclone Nina sourced in the Gulf of Carpentaria in December 1992, tropical cyclone Naomi sourced off the Western Australian coast in December 1993 (and downgraded to a tropical depression), and tropical cyclone Sadie that formed along the east coast of the Northern Territory in January 1994.

Gulf Lines and Tropical Flow

Gulf lines are peculiar to the Northern Territory and only affect the north of the Northern Territory. They are defined as north-south oriented lines of showers or storms that develop over the Cape York Peninsula and move westwards over the Gulf of Carpenteria and the Top End (Bureau of Meteorology 1993a). Tropical flow is the term given to moist northwesterly winds that produce showers and storms mainly in the north of the Northern Territory.

Troughs

A trough is an area of low pressure that extends over a wide region, and separates high-pressure ridges. Troughs are commonly oriented in a north-south direction (Tapper and Hurry 1994). Unlike the low, the trough does not have closed isobars. In the northern areas of Australia, lows and troughs act in a similar fashion as areas

of convergence. Thus for the purpose of this classification, lows and troughs are grouped together for northern Australia.

TABLE 2.3 Summary of rain-producing synoptic classification scheme.

Classification	Air mass and source of moisture
Tropical Events (TE)	Tm, moisture from north and northwest
Tropical Cyclones (TC)	Tc, dependent on origin of cyclone
Gulf Lines (GL)	Tm, moisture from northwest
Tropical Flow (TF)	Tm, moisture from the northwest
Troughs	
West Coast Trough (WCT)	Generally Tc
Inland Trough (T)	IsTm or ITm, moisture from Indian Ocean
Non-monsoonal Trough (T)	Tm, moisture from the north
Monsoonal Trough (MT)	Tm, moisture from northwest (Timor and Coral Seas)
Frontal Activity	
Cold Fronts (CF)	sTm, sPm, moisture from the south
Cut-off Low (CoL)	various
Cloudbands	
Middle-level Cloudband (MLCB)	Tm, sTm moisture from the north and northwest
Middle-level Disturbance (MLD)	various

West Coast Trough (Figure 2.9)

The West Coast Trough affects Western Australia in the summer and is especially important along coastal regions. It forms because of the alignment of isobars in an east-west direction over the state which is a consequence of the ridging of subtropical high-pressure cells through the Bight to the south of Western Australia. When the trough lies offshore, winds near the west coast are from an east to northeasterly direction, bringing hot, dry continental air (Tc) from inland areas. This situation usually involves very high temperatures if the offshore winds are strong enough to delay coastal sea breezes. If the West Coast trough deepens or moves inland, cool moist marine air is brought onshore from the west. Occasionally, this moisture may contribute to shower and thunderstorm activity in the unstable airmass to the east of the trough. However, on the majority of occasions, the development of thunderstorm activity near a West Coast Trough is dependent upon

moisture in the low-level continental airmass and in the middle-levels of the atmosphere.

Inland Troughs

Inland troughs affect all regions of the study, sourcing differing airmasses.

Western Australia (Figure 2.10)

The inland troughs that affect Western Australia are troughs in the easterlies that develop anywhere between the Kimberley and the southern coast in Western Australia. Convective thunderstorms develop usually to the east of the trough line where vertical uplift is enhanced (Tapper and Hurry 1994), and result in large isolated rainfall. Thunderstorms generally involve moisture from lower levels in the atmosphere. The source of moisture is most likely from IsTm. Intense heating of the continent during summer leads to an area of reduced pressure, which helps to draw in moist air from the Indian Ocean.

Northern Territory (Non-monsoonal Troughs)

Non-monsoonal troughs in the Northern Territory can form anywhere over the Territory. These troughs involve convergence of air to the trough, usually from the north, and generally move from west to east and or north or south.

South Australia

Troughs that produce rainfall in South Australia generally move into the state from the north or west. They involve the convergence of moist tropical air from the north, and are less common than those in the Northern Territory and Western Australia.

Monsoonal Trough (or active monsoonal bursts).

The monsoonal season operates in the Northern Territory between November and March, with maximum activity occurring in January and February. Active monsoonal bursts are represented by broad areas of rain with sustained northwesterly winds. During the monsoon season, the monsoonal trough oscillates between onshore and offshore of northern Australia. During an active burst, the trough is usually located at the base of the Top End (Figure 2.8b). The source of moisture during active monsoonal bursts is from the northwest, in the Timor and Coral Seas (i.e. Tm airmass).

Frontal Activity

Cold Fronts and Associated Lows

A frontal zone represents the interaction of two airmasses of differing properties (usually temperature, relative humidity and density). Cold fronts develop when warm air is displaced by cold air at the surface. The cold fronts that affect the

southern areas of Australia, are associated with lows (or temperate cyclones), which generally remain to the south of the continent. On occasions the associated low may move onshore, bringing large amounts of rain. The temperate cyclones and their fronts move northwards from summer to winter producing maximum rainfall during June and July. For the purpose of this classification lows and cold fronts are grouped together for southern Australia.

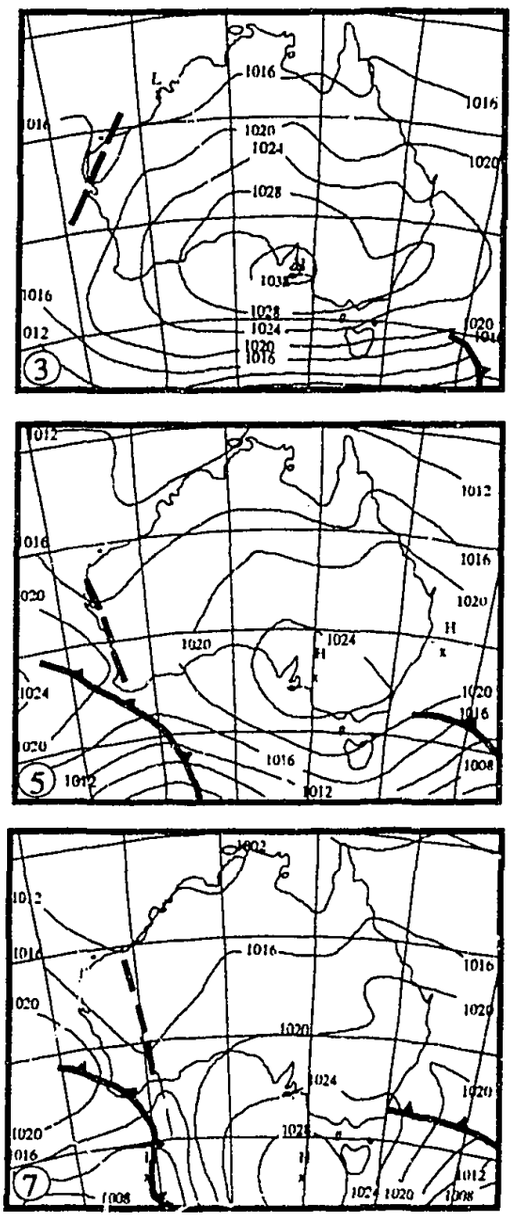

FIGURE 2.9 Sequence of synoptic charts showing the development of a West Coast Trough between the 3rd and 7th of April 1991. A trough developed off the west coast of Western Australia on 3rd of April, deepened on the 4th and 5th of April and began moving eastwards in response to a cold front. On the 6th of April, the trough was stationary over the Goldfields, and eventually disappeared on the 7th. From the Bureau of Meteorology 1991a. *For Figures 2.9 to 2.12 lines are isobars drawn at 4 hPa intervals, thick lines with arrows are cold fronts, dashed lines are troughs.*

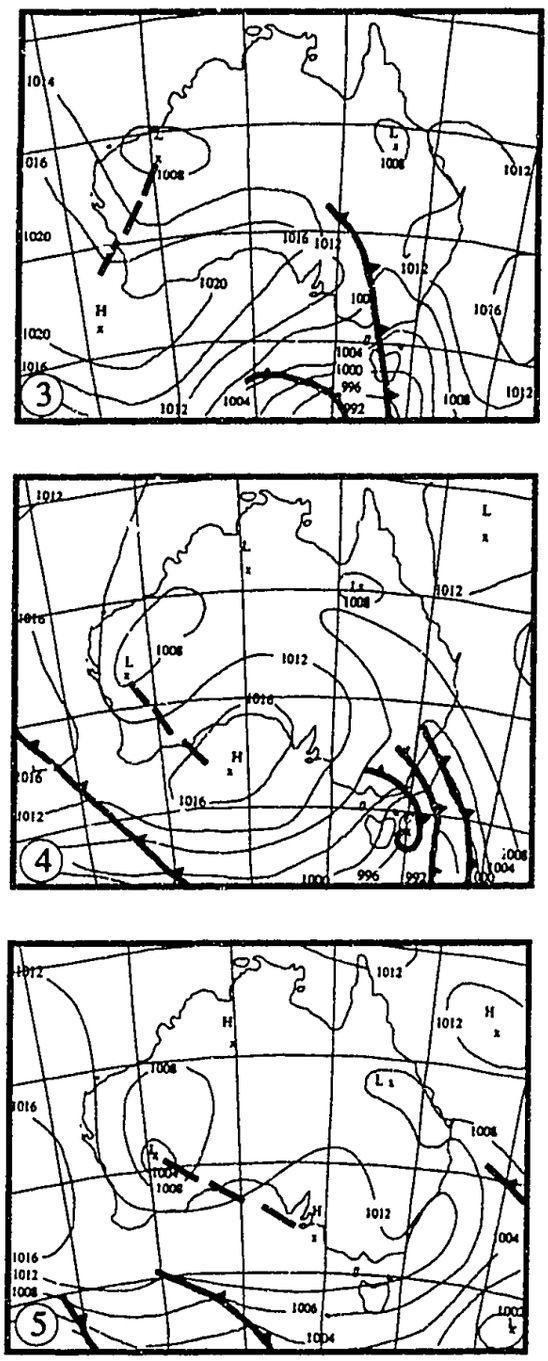

FIGURE 2.10 Sequence of synoptic charts showing the development of an Inland Trough between the 3rd and 5th of December 1991. A trough formed between the Pilbara and lower west coast on the 3rd and moved over the rest of Western Australia producing thunderstorms in the Goldfields and Eucla. From the Bureau of Meteorology 1991b.

Western Australia (Figure 2.11a)

The airmasses that provide the moisture for the cold fronts in Western Australia are most likely the sTm and sPm. Cold fronts affect the coastal regions of Western Australia, generally to the south of Carnarvon, and most frequently during winter. The cold fronts that affect Western Australia are associated with lows that usually pass to the south of the state.

South Australia (Figure 2.11b)

Cold fronts predominantly move from southwest to southeast across South Australia. When the associated temperate cyclone moves onshore, large amounts of rainfall result. The airmasses that produce moisture for cold fronts in South Australia are also sTm and sPm, and the associated lows may occur between the Bight and the eastern margins of the state.

Cut-off Low (Figure 2.12)

A cut-off low develops when a low-pressure system is isolated from the main low-pressure area in the westerlies to the south. A cut-off low only occurred twice during the sampling program in Western Australia, the first time in association with a West Coast trough, and the second time with a cold front. Each time the air involved was sourced from the west of the central west coast (i.e. between Carnarvon and Geraldton). South Australia experienced a cut-off low during Autumn 1994.

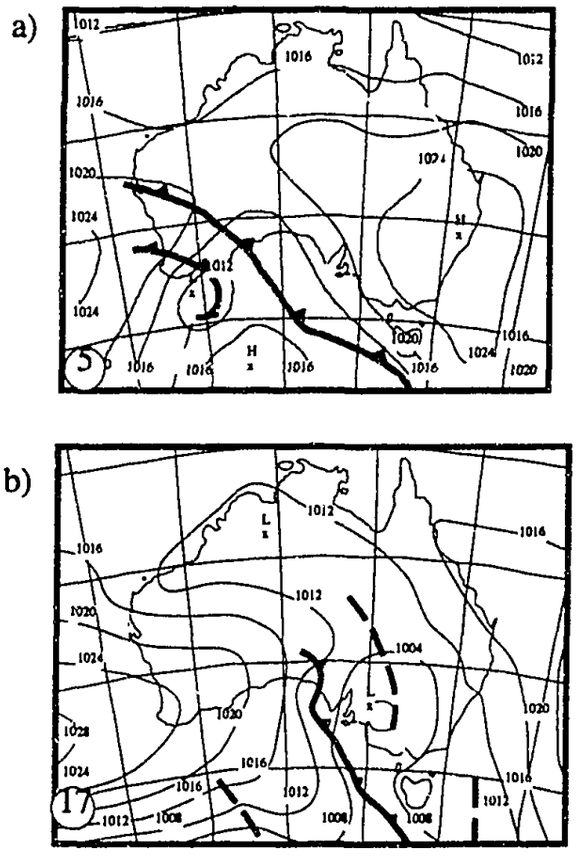

FIGURE 2.11 surface synoptic charts showing cold fronts that affected a) Western Australian the 5th of May 1991 (Bureau of Meteorology 1991c) and b) South Australia on 17th of October 1992 (Bureau of Meteorology 1992b).

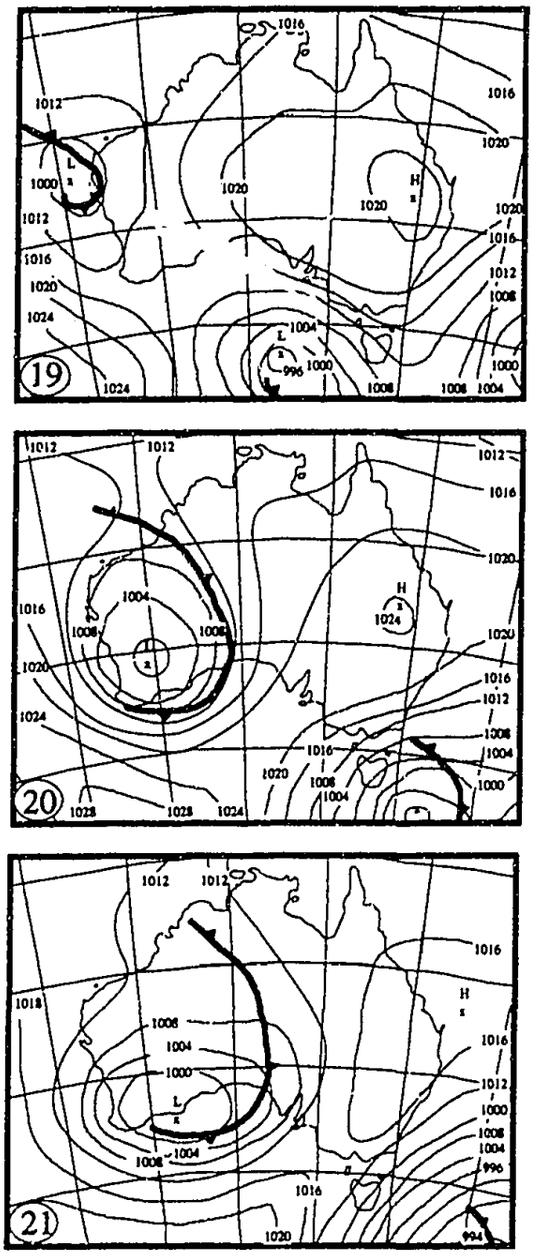

FIGURE 2.12 Sequence of surface synoptic charts showing a cut-off low affecting Western Australia between the 19th and 21st of July 1991. On the 19th a deep cut-off low had developed west of Carnarvon. This produced a vast cloudband that covered much of the southwest of Western Australia. The low had deepened by the 20th and tracked southeast to enter the Great Australian Bight on the 21st. From the Bureau of Meteorology 1991d.

Cloudbands

Middle-Level Cloud Band

Incursions of middle-level moist air from tropical regions may bring heavy rainfall to Australia during winter by producing a cloud band under suitable conditions. An example of a cloud band is the Northwest Cloud Band which regularly forms over Australia during May, June and July. The Northwest Cloud Band develops when upper level troughs that are embedded in the westerlies of the middle latitudes extend into the tropics, drawing moist air from over the Timor Sea to the southeast.

The moist tropical air ahead of the trough is cooled as it is forced to rise over the drier cooler air associated with the approaching trough, and the moisture condenses to form a cloud band. The amount of precipitation depends on the amount of moisture in the airstream and the amount of uplift generated (which depends on the stability of the airmass). For the purpose of this classification, occurrences of the Northwest Cloud Band are noted as middle-level cloud bands. The important feature of this category is the provision of moisture by the Tm airmass. In the case of the Northwest Cloud Band the origin is more specifically west of the Timor Sea.

Middle-Level Disturbance

'Middle-level disturbance' is a generic term sometimes used to explain the formation of weather that cannot be attributed to processes happening near the surface. The lifting mechanisms are generally associated with the presence of a nearby middle-level trough or some related development. The term may at times be used in reference to a middle-level cloudband or cut-off low that does not appear on the surface (Cram, pers comm. 1995).

Application of the Rain-producing Synoptic Classification Scheme

The results of the application of the above classification scheme of rain producing conditions are shown graphically in Appendix A, and summarised in Tables 2.4 and 2.5. These tables show the single rain-producing condition responsible for the production of most rainfall at each Met station during each sample collection period for the WE (Table 2.4) and SN (Table 2.5) arrays.

WE array

The winter season sees the predominant influence of cold fronts on the Met Stations of the western half of the WE array. During winter 91 this influence extends inland to Giles. Thus winter represents periods of influence by marine air masses from the south and southwest. West Coast Troughs are most active during autumn and spring of each year across the array. During summer, inland sites are influenced by tropical airmasses in the form of tropical events. During winter and autumn, inland sites are also affected by middle-level cloud bands and tropical flow. The coastal Met Station is influenced by cold fronts throughout most of the sampling program.

NS Array

Rainfall at the Met Stations from the northern half of the NS array are affected by processes that source tropical air masses north, northwest and north of Australia. The influence of tropical airmasses extends as far south as Tarcoola in the form of

middle-level cloud bands and tropical flow during spring. The southern half of the NS array is affected by cold fronts that can extend as far inland as Coober Pedy during winter and autumn. The southern-most Met Stations are influenced by cold fronts all year round.

2.4 SUMMARY AND DISCUSSION

A classification scheme of synoptic processes that produced rainfall at Met stations close to sampling sites along the WE and SN arrays attributes moisture to airmasses from the tropical north (Tm, sTm), the south and southwest (IsTm, PsTm and sPm) and the Australian continent (Tc). The extent of the influence of these differing airmasses is dependent on time and location.

TABLE 2.4 Major rain producing processes at Met Stations along the WE array.

Station	A91	W91	Sp91	S91	A92	W92	Sp92	S92
Dongara	CF	CF	CF	CF	WCT	CF	CF	nil
Mt Magnet	CF	CF	CF	WCT	WCT+ MLD	CF	WCT	CF
Meekatharra	T+MLD	CF	CF	WCT	T+MLD	CF	CF	TE
Yeelirrie	T+MLD	CF	CF	T	WCT	CF	WCT	WCT
Wiluna	WCT TE	CF+MLCB	WCT	WCT	WCT+ MLCB	MLD	WCT	TE
Carnegie	TE	CF	WCT	T	MLCB	T	WCT	TE
Giles	WCT+ TE	CF	WCT	T+MLD	WCT	T+ MLD	WCT	TE+WCT

CF=Cold Fronts; WCT=West Coast Trough; T=Trough; CoL=Cut-Off Low: MLCB=Middle-Level Cloud Band; TF=Tropical Flow; TE=Tropcial Event; TD=Tropical Depression, MLD=Middle-level Disturbance

The results of this classification will be of use in the interpretation of the major element chemistry and ^{36}Cl data. In terms of the major-element chemistry (Chapter 5), the tropical, south and southwest airmasses may contribute a seawater chemical signature to the rainfall chemistry during periods of maximum influence from these airmasses, eg. winter 91 for the WE array, summer for the northern half for the SN array. Rainfall attributed to West Coast Trough activity may provide a continental or marine signature depending on the source of moisture. In terms of the ^{36}Cl composition of rainfall, these results may be used to explain deviations from the

latitude-dependent predicted fallout of ^{36}Cl to the Earth's surface (Chapter 6). In particular, samples predominantly affected by moisture from the tropical north may be explained in terms of the fallout expected at lower latitudes than the sample location, as samples affected by moisture from the south of Australia may be explained in terms of fallout expected at higher latitudes.

TABLE 2.5 Major rain producing processes at Met Stations along the SN array.

Station	W92	Sp92	S92	A93	W93	Sp93	S93	A94
Darwin	nil	T	MT TD	GL	T	TF	MT	TF
Katherine	nil	T	MT	T	nil	TF	MT	T+TD
Elliott	nil	T	MT	T MLCB	MLCB	MLCB +T	MT	TF
Tennant Creek	nil	T	MT	MLCB +T	MLCB	MLCB +T	T+TD, MT	TF
Alice Springs	MLCB +T	T	T(ne)	MLCB	MLCB +T	T	MLCB	T
Coober Pedy	?	CF	T+TF	CF	MLCB	T	MLCB T+TF T+TD	CoL
Oodnadatta	T	MLCB +T	T+TF	MLCB	CF ?	T	MLCB T+TF T+TD	CoL
Tarcoola	CF	CF	T+TF	CF	CF	CF+T	CF+ MLCB TF	CoL
Kyancutta	CF	CF	CF+T F	CF	CF	CF+T	CF+T	CF
Port Lincoln	CF	CF	T+TF CF	CF	CF	CF CF+T	CF	CF CoL

CF=Cold Fronts; WCT=West Coast Trough; T=Trough; CoL=Cut-Off Low: MLCB=Middle-Level Cloud Band; TF=Tropical Flow; TE=Tropcial Event; TD=Tropical Depression, MLD=Middle-level Disturbance

CHAPTER 3 METHODOLOGY

This chapter describes the methods used during sample collection, sample analysis and interpretation of data. The procedures used to ensure the data are of high quality are also detailed.

3.1 FIELD SAMPLING PROGRAM

Procedures

Bulk depostion precipitation samples were collected from two arrays of rain collectors: one in a west-east transect from the coast of Western Australia inland to Everard Junction in the Gibson Desert, (labelled WE), and the other a south-north transect from Port Lincoln in South Australia to Kakadu in the Northern Territory (labelled SN). The specific sites that make up the transects are shown in Figure 3.1. The collection periods are defined in Table 3.1. Reference to samples in the following text will follow the form site-collection period. For example, 23-Sp91 refers to site 23 (Carnegie) and collection during Spring 91 (September to November 1991).

TABLE 3.1 Season and collection periods for the WE and SN arrays.

Season	Months (inclusive)	Collection Period				
		WE Array		SN Array		
		1991	1992	1992	1993	1994
Autumn	March to May	A91	A92		A93	A94
Winter	June to August	W91	W92	W92	W93	
Spring	September to November	Sp91	Sp92	Sp92	Sp93	
Summer	December to February	S91	S92	S92	S93	

Collection sites along the WE transect were chosen to lie along a narrow band of latitude (between 25°S and 29°S), and to be placed equidistant from both the north and south coasts of Western Australia. It was also important that they were removed from sources of contamination such as localised salt lakes, and anthropogenic pollution in areas of concentrated populations eg. Kalgoorlie and Perth. Collection sites along the SN array adhered to a narrow band of longitude (132°E to 135°E) and encompassed a variety of climates including coastal, semi arid and subtropical. Accessibility to sites was also an important criteria when deciding the location of

collectors. The WE array consisted of ten collectors, spaced approximately 100 km apart. The SN array was made up of eight collectors separated by distances of 200 to 500 km. Descriptions of the collection sites, including details of land use, soil type, local climatic conditions etc, are listed in Appendix B. Both collection arrays operated over a two-year period, the WE array between March 1991 and February 1993, and the SN array between May 1992 and May 1994. Samples were retrieved from the field every three months at times that roughly coincided with the change of seasons. Seasons are defined in Table 3.1.

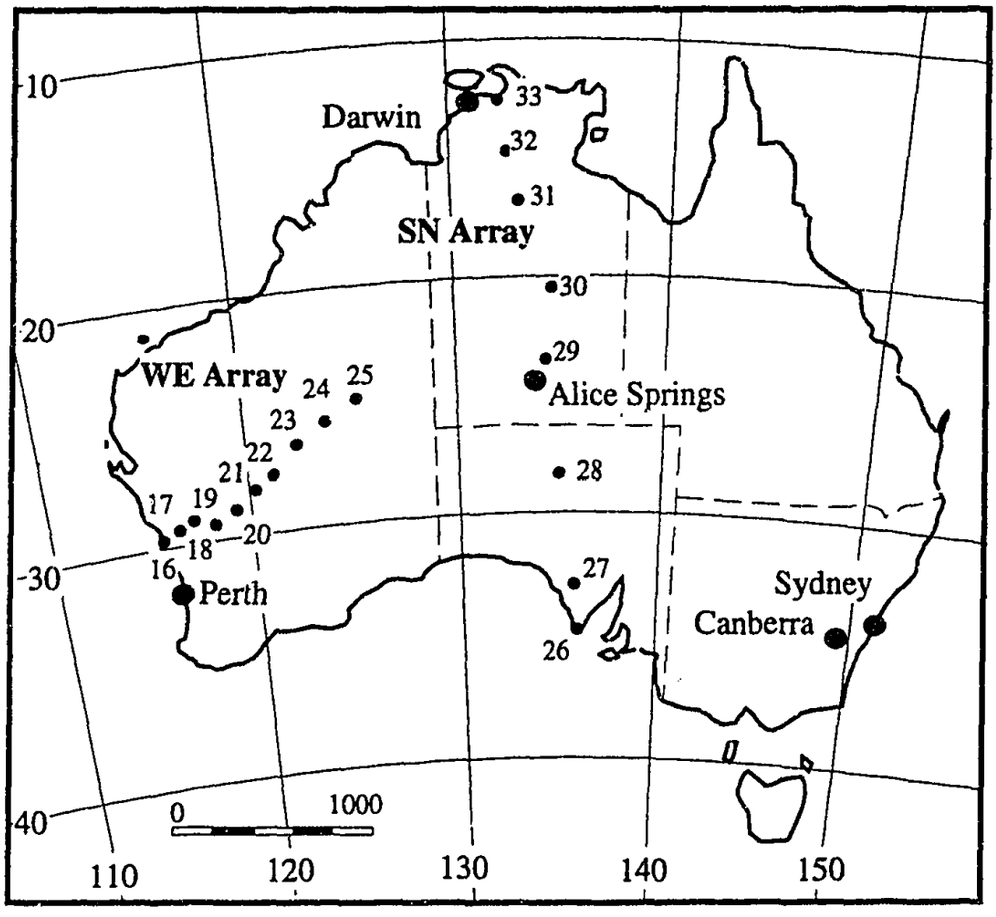

WE Array
site 16 Cliff Head
site 17 Morawa
site 18 Badja
site 19 Iowna
site 20 Barrambie
site 21 Yeelirrie
site 22 Lake Violet
site 23 Carnegie
site 24 Gunbarrel Highway
site 25 Everard Junction

SN Array
site 26 Port Lincoln
site 27 Gawler Ranges
site 28 Wintinna
site 29 Alice Springs
site 30 Tennant Creek
site 31 Dunmarra
site 32 Katherine
site 33 Kapalga

FIGURE 3.1 Location of samples sites on the WE and SN arrays

Precipitation was collected using bulk deposition collectors designed for the project to withstand three months of exposure to extreme wind, rain and heat conditions. The collection vessels consist of two types. The apparatus is shown in Figure 3.2.

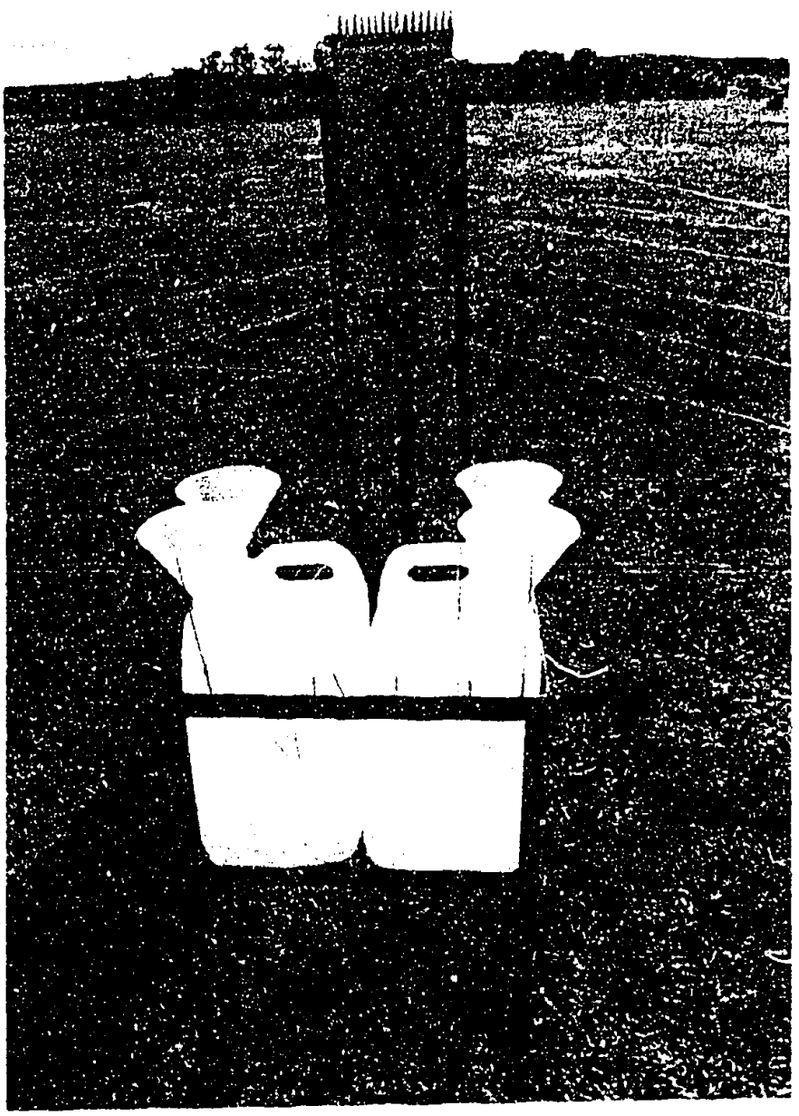

FIGURE 3.2 Photograph of the rain collecting apparatus

The first type consisted of a stainless steel square bin (dimensions 10 x 10 x 60 cm, 30 x 30 x 60 cm or 40 x 40 x 60 cm) and a funnel placed approximately 1.5 m above the ground. Stainless steel mesh (grade 250-300 μm) in the funnel opening prevented large particles such as insects and sand grains from entering the collection vessels. Vertical stainless steel spikes encircled the funnel to prevent birds fouling the samples. Housed in the steel bin was a five-litre borosilicate glass bottle in

which the sample was collected. This will be referred to as the "glass collector" in the following discussion.

The second type consisted of an arrangement of high density polyethylene plastic jerry cans (either five- or ten-litre) and high density polyethylene plastic funnels (average diameter 14.7 cm) placed approximately one metre above the ground. Again, stainless steel mesh was used to reduce contamination. Two jerry cans were deployed during the first half of the WE collection program, and four jerry cans were deployed during the second half of the WE and entire SN collection programs. Throughout the entire program, one of these jerry cans was designated the "paraffin collector" and contained approximately 100 ml of paraffin to prevent water loss by evaporation. At later stages in the sampling program, a third or fourth plastic jerry can was deployed, containing approximately 200 mg of thymol for every litre of sample expected to be collected. Thymol is recommended (Gillett and Ayers, 1991) as a suitable biocide allowing reliable analysis of pH and organic acids, without substantially influencing the major-element chemistry of the samples. However, it was of limited success in this program because of a previously unreported reaction that occurs between thymol and plastic when exposed to sunlight for prolonged periods of time. Finally, one or two plastic jerry cans per site, with no additives, were used to collect precipitation for boron isotope analysis for an independent study, and will be referred to as "boron collectors".

The entire arrangement of collectors was enclosed in a fence to prevent interference from animals, particularly livestock. For the most part this fence arrangement appeared satisfactory. However, at one site on the SN array, a herd of cattle did manage to break through the fence and disturb the collector on one occasion. Table 3.2 summarises the purpose of each collection vessel.

TABLE 3.2 Purposes of different sampling vessels used in the raincollecting arrays.

Collection Vessel	Purpose
glass bottle	general analysis, ^{36}Cl
plastic jerry can with paraffin	measure of volume
plastic jerry can	boron isotopes

Pre-Field Collection Procedures

All field sampling apparatus was cleaned thoroughly before use in the field. The stainless steel bins were scrubbed with laboratory grade detergent, rinsed at least 3

times with deionized water, soaked for 24 hours in deionised water, rinsed at least 3 times, allowed to dry overnight and wrapped in plastic and bubble plastic for safe transport. The glass bottles and stoppers were scrubbed using a special bottle brush, rinsed at least 10 times with Milli-Q® water of 18 μohm resistance and soaked for at least 24 hours with Milli-Q® water. This procedure was carried out at least 3 times. The glass bottles were then dried in an oven overnight and weighed before being sealed in plastic. The cleaning and drying of the glass bottles was carried out in a specially designed Cl-free laboratory at the Research School of Earth Sciences, Australian National University. The plastic jerry cans were rinsed with deionised water at least 3 times, soaked in deionised water for 24 hours, dried in a clean oven, weighed and sealed in plastic. Early in the sampling program, an approximate volume of 100-300 ml of paraffin was added to one of the plastic jerry cans before transport into the field. At later stages, a precise weight of paraffin was added. Jerry cans were only recycled twice, as it was found that the plastic of the jerry can weakened after more than 6 months exposure to sunlight. All cleaning was carried out with disposable gloves, so that hands never came into contact with the sampling vessels.

Field Collection Procedures

All equipment in the field was handled using disposable plastic gloves. Equipment was sealed in plastic for transportation to and from the field.

Post-Field Collection Procedures

Once samples were collected from the field, they were stored at 4°C. All samples were weighed, and from this and the weight of collection vessels before deployment, sample volumes calculated. During the early stages of collection from the WE array, volumes were measured using a graduated measuring cylinder. A 250 ml aliquot was taken from the glass collection vessels for major element, pH and in the early stages of the program, bicarbonate measurement. If the glass bottle was dry (i.e. no precipitation was collected), the bottle was soaked in a precisely known volume of Milli-Q® water (~250 ml) for at least 7 days, and an aliquot of this taken for general analysis. Samples collected in the paraffin collector were separated from paraffin using separator funnels.

Quality Assurance

The aim of the sampling procedure is to collect precipitation samples that are representative of the material being deposited from the atmosphere to the Australian

continent. It is recognised that this is a very difficult task to undertake, even fundamental questions such as what sort of collection surface most closely approximates that of the earth are hard to answer. The procedures used in this project try within the means available to carry out this aim. There are several aspects of the field collection procedure that must be scrutinised with regard to their effect on the chemical composition of the sample collected. In particular, the effect of the collection vessel materials, dry deposition and the assumption of the sample collected under paraffin representing the amount of rainfall collected must be examined. The following discussion looks at each of these issues.

Collection Vessels

The effect of the collection vessel material (i.e. borosilicate glass or plastic) on the chemistry of rainfall sample was investigated by measuring the concentration of various species in Milli-Q® grade water that had been stored in clean collection vessels and exposed to sunlight in the laboratory for approximately 3 months. For both types of collection vessels (glass and plastic) all species concentrations were below the level of detection. Thus it is concluded that the collection vessel type does not contribute to the chemistry of rainfall collected.

Dry Deposition

The nature of the collection vessels (i.e. bulk depositional collectors) means that they collect both wet and dry deposition. Thus the chemistry of the rainfall sample is a measure of material that is deposited both during and between rainfall events. For many investigations the collection of dry deposition is commonly not recommended, and consequently, bulk depositional collection techniques are often disapproved of in rainfall investigations. For example, in a review of deposition monitoring techniques, Erisman et al (1994) cite bulk depositional collectors as a serious source of error for wet depositional measurements. In another review of wet depositional collection techniques, Vet (1991) attributes the reduction in use of bulk depositional collectors in many North American monitoring networks to high measurement uncertainty caused by the unknown and highly variable input of dry deposition. On the other hand, bulk depositional collectors have been used successfully in some wet depositional programs, when located at sites away from direct sources of dry contamination such as seawater, anthropogenic emissions or when sampled over short time periods, eg. 24 hours (Vet 1991).

It is recognised that dry deposition does contribute to the chemistry of rainfall collected in the present investigation. However, this is not seen as a disadvantage

here, as one of the main aspects of this project is an investigation of the accession of material to the Australian continent, whether it be by wet or dry deposition. It would however, be useful to characterise the extent of the effect of dry deposition on rainfall samples collected. A very rough estimate may be made by comparing the deposition of ions in dry samples (i.e. samples for which zero volume of rainfall was collected in both the glass and paraffin collectors) with the average deposition at a site in which rainfall volumes were greater than zero. Unfortunately, only the four sites in the Top End of the SN array experienced zero rainfall. An investigation of the proportion of species contributed by the dry samples (Figure 3.3) shows that there is variation in the amount of dry deposition both between sites and at the same site over different times. This makes it very difficult to generalise about the extent of dry deposition across each array over time.

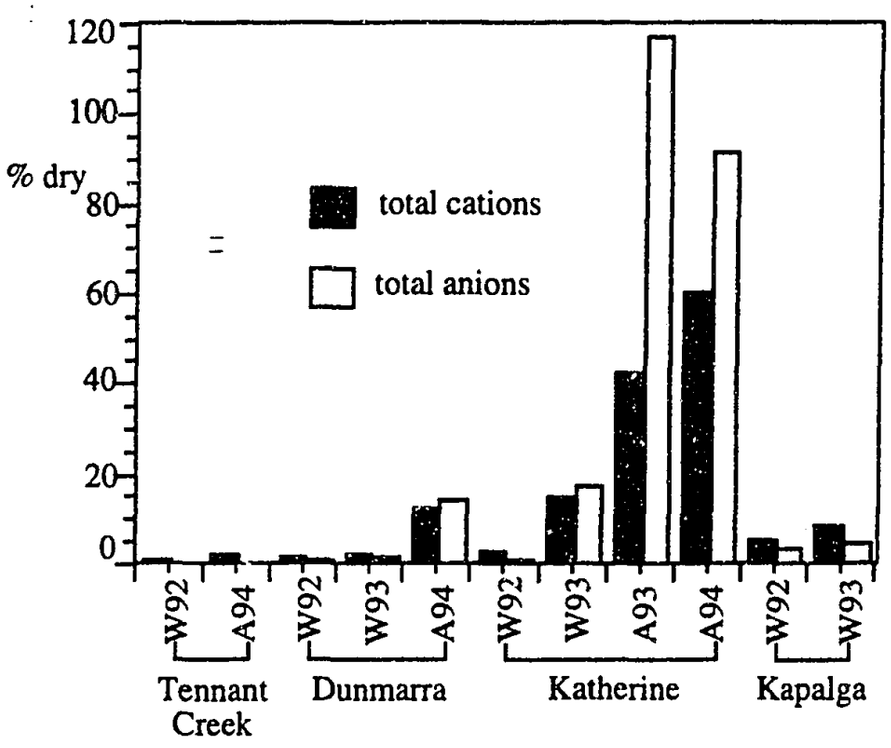

FIGURE 3.3 Dry deposition at northern sites on the SN array (sites 30 to 33). % dry represents the proportion of ions deposited in the dry sample (i.e. nil rainfall) relative to the mean flux of ions deposited at each site. W92 = winter 92, A94 = autumn 94 etc. Calculated from depositional units ($\mu eq/m^2/s$).

In summary, bulk depositional collectors were chosen to be the most practical form of collection vessel for this project, as they are the most suitable method of collection for long periods in remote areas. Both wet and dry deposition is collected in these sampling vessels, and while the extent of dry deposition cannot be quantitatively constrained, it is recognised as a feature of the samples, and will be taken into account during data interpretation.

Evaporation

The paraffin collector is used to measure the volume of rain that has fallen during the collection period (assuming that no evaporation can occur through the 1 cm paraffin layer). An evaporation correction is applied to all data based on the volume of sample measured in the paraffin collector. The effectiveness of the paraffin collector as a measure of unevaporated rainfall has been tested by placing four paraffin collectors with known volumes of Milli-Q® grade water at the most continental site (Everard Junction) on the WE transect, for periods of 3, 6, 9 and 12 months. The results of this experiment are displayed in Figure 3.4, which compares the volumes of Milli-Q® grade water before and after the evaporation experiment over time. If evaporation was occurring, we would expect to see a gradual decrease in volume over time. The absence of a trend of increasing loss of Milli-Q® grade water with increasing time and the agreement within 1 σ error between volumes (except for the first three months, when sample was lost during separation of paraffin, and agreement does occur at 2 σ) indicates that our assumption of no evaporation occurring beneath the paraffin layer is valid.

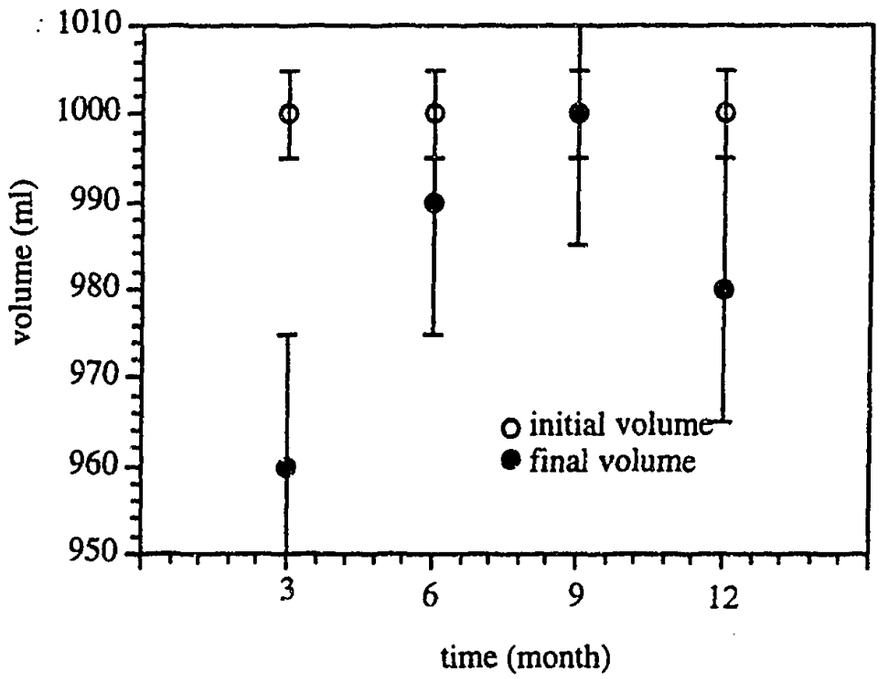

FIGURE 3.4 Evaporation test at Everard Junction (site 25) on the WE array. Four paraffin collectors with known volumes of Milli-Q® grade water were placed at site 25 for periods of 3, 6, 9 and 12 months. The graph shows the volume of water deployed (initial) and the volume of water collected (final). There is no trend of decreasing final volume over time. All final and initial volumes are within 1σ error, except at 3 months when sample was lost during final volume measurement. Error bars represent 1σ error.

The question of how closely evaporation in the plastic jerry can arrangement approximates evaporation in the glass bottle housed inside the stainless steel bin arrangement, is addressed by comparing volumes recovered in each collector. In most situations, when corrected for funnel sizes, the volume collected in the glass bottle is less than that of the paraffin collector (Figure 3.5). However, it is noted that volumes in the glass collectors are not always equal to those found in the jerry cans without paraffin, as would be expected if evaporation conditions were the same in both arrangements. Differences of up to ± 10% are noted, most likely representing the natural level of variability of rainfall deposition in the environment and sampling errors.

3.2 LABORATORY PROCEDURES

Major Elements

Procedures

The analytical techniques used to measure major elements in this project are listed in Table 3.3. Also shown are detection limits and estimated errors for each technique. Standards were prepared gravimetrically using Spec Pure or Analytical Reagent grade primary salts.

Quality Assurance

External examinations of the accuracy of the analytical techniques were performed throughout the program using seawater (Jervis Bay seawater, collected by the Environmental Geochemistry group in February 1986, and diluted by approximately 1000 times to approximate rainwater concentrations), and in the later stages, using a standard reference simulated rainfall material (SRM 2694A-1 and SRM 2694A-11 from the National Bureau of Standards, USA). The reference concentrations of ions in seawater is taken from Millero (1974).

More than one method was available to measure cations, dependent on the stage of the sampling program. Before November 1992 (collections WE A91 to Sp91), all cations were measured by atomic absorption spectrophotometry (AAS)[1]. However the accuracy (relative to seawater) of the AAS techniques was poor for each species, so inductively coupled plasma atomic emission spectrometry (ICPEAS) was adopted for Ca and Mg, and high pressure liquid chromatography (HPLC) for Na and K. At later stages of the program, the HPLC measurement of Ca and Mg also

[1]Collections WE A91, W91 and Sp91 were analysed by E Kiss.

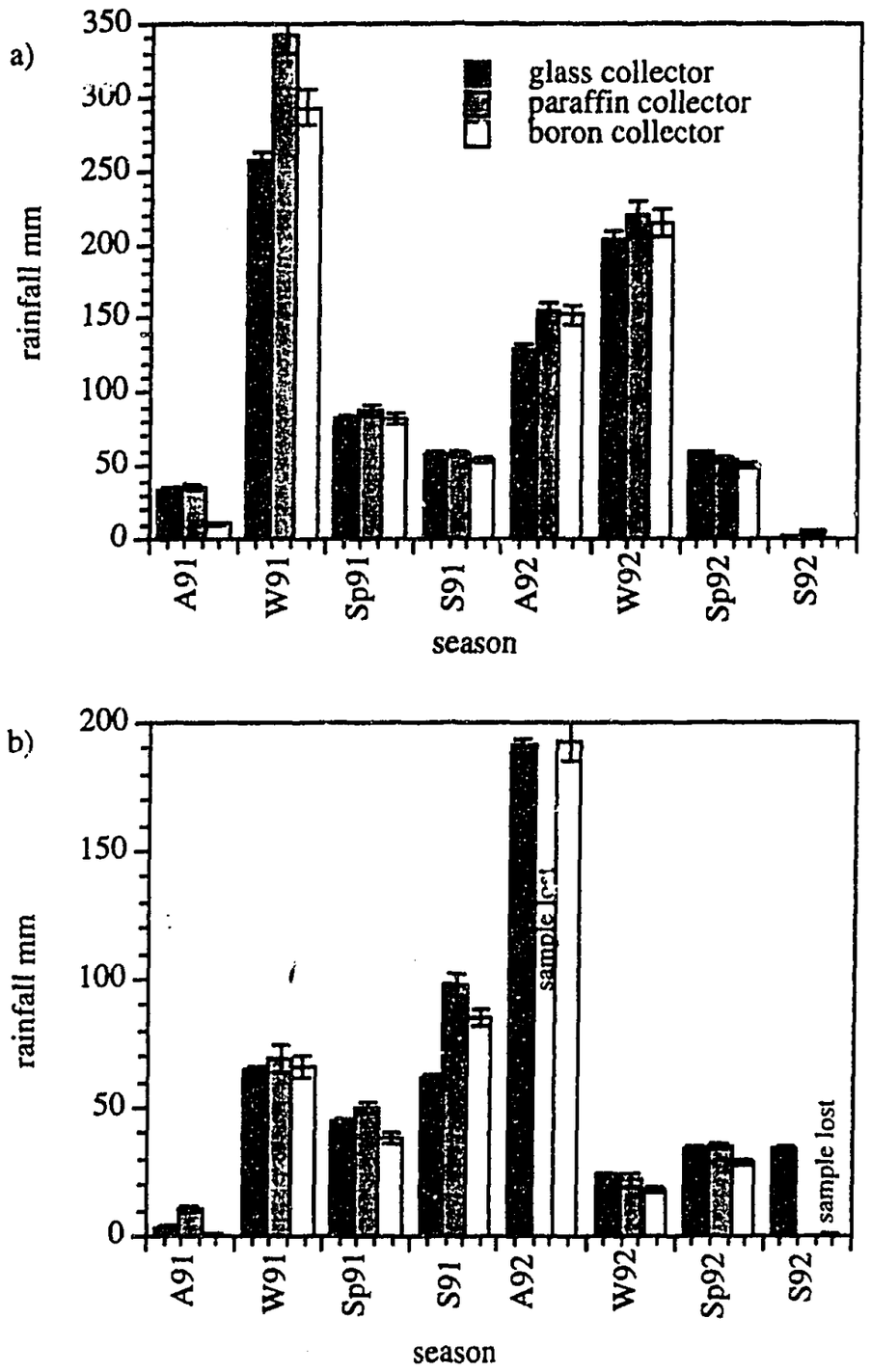

FIGURE 3.5 Comparison of volumes collected by the different collector types (glass, paraffin and boron) at a) site 16 (Cliff Head) and b) site 25 (Everard Junction). Error bars represent 1σ measurement errors. The difference in volumes collected by each collector type is less than 10% (within 1σ error bounds). A91 = autumn 91, W91 = winter 91, Sp91 = pring 91, S91 a= sumrner 91 etc.

TABLE 3.3 Analytical methods, detection limits and accuracy.

Species	Method[i]	Instrument	detection limit µg/ml	accuracy SRM[ii]	accuracy sw [ii]
H	electrode	Solomat 2000	-		
Cl	HPLC	Dionex 4500i[iii]	0.01	1.5%	0.31%
SO_4	HPLC	Dionex 4500i[iii]	0.01	1.4%	0.9%
NO_3	HPLC	Dionex 4500i[iii]	0.01	5.6%	
HPO_4	HPLC	Dionex 4500i[iii]	0.01		
Br	HPLC	Dionex 4500i[iii]	0.01		9.6%
Na	AA	Perkin Elmer 303[iv]	0.02		14.25%
	HPLC	Dionex series 4500i[v]	0.08	5.7%	4.5%
K	AA	Perkin Elmer 303[vi]	0.1		36%
	HPLC	Dionex 4500i[iv]	0.08	5.6%	3.7%
NH_4	HPLC	Dionex 4500ii[v]	0.2	1.0%	
Ca	AA	Perkin Elmer 303[vii]	0.05		32%
	HPLC	Dionex 4500i[viii]		1.1%	5.8%
	ICPAES	RSES high-resolution ICPAES	0.013		3.2%
Mg	AA	Perkin Elmer 303[ix]	0.014		11%
	ICPAES	RSES high-resolution ICPAES	0.002		4.7%
	HPLC	Dionex 4500i[viii]		2.8%	6.2%

i HPLC = Ion Chromatography, AA = Atomic Absorption Spectrophotometry, ICPAES = Inductively Coupled Plasma Atomic Emission Spectrometry: ii calculated by comparing the measured value of a calibration standard to the 'known' concentration:[seawater, Millero 1974; SRM, National Institute of Standards and Technology 1991]: iii ASA4 column; eluant 1.7mmole $NaHCO_3$ and 1.8mmol Na_2CO_3; regenerant 25mmol H_2SO_4: i v wavelength 589nm; flame air:acetylene:v CS10 column; eluant 10mmol HCl and 1mmol DAP.HCl; regenerant 100mmol tetrabutylammoniumhydroxide: vi wavelength 755.5nm; flame air: vii acetylenewavelength 422.7nm; flame acetylene:N_2O: viii CS10 column; eluant 60mmol HCl and 6mmol DAP.HCl; regenerant 100mmol tetrabutylammoniumhydroxide: ix wavelength 285.2nm; flame acetylene:N_2O.

became possible. The accuracy for both the ICPAES and HPLC determinations of Ca and Mg are comparable.

The reproducibility between analytical runs is shown in Figure 3.6, which shows the results of repeated analysis of Jervis Bay seawater over the sampling program, compared with published seawater concentrations (Millero 1974). It can be seen that

Throughout the text Na = Na^+, K= K^+, NH_4=NH_4^+, Ca=Ca^{2+}, Mg=Mg^{2+}, H=H^+, Cl=Cl^-, SO_4=SO_4^{2-}, NO_3 =NO_3^-, HPO_4=HPO_4^{2-} and Br=Br^-

for the major ions of seawater, the analytical techniques have a reproducibility of better than 6.2% between sample runs.

Chlorine-36

Procedures

All sample handling and precipitation of Cl was carried out in a specially designed Cl-free laboratory at the Research School of Earth Sciences, Australian National University. Disposable gloves were used at all stages during sample handling.

Preconcentration

Up to 5 litres of rainwater was filtered through Whatman 54 filter paper, the volume accurately measured and concentrated to approximately 150 ml using a condenser with a 1 litre round-bottomed flask. The pre-concentration stage took approximately two days. The waste from the preconcentration procedure contained no measurable Cl. The concentrate was stored in a 250 ml borosilicate glass bottle until precipitation.

All glassware and equipment used during the preconcentration procedure was cleaned by rinsing with Milli-Q® water (18 μohm) at least 12 times, soaking for 24 hours with very dilute HNO_3, rinsing at least 12 times with Milli-Q® water, soaking for 24 hours in Milli-Q® water, rinsing a least 12 times and drying in an oven. Glassware was then covered with parafilm and stored until use. Scrubbing was commonly required to remove carbon accumulations in the round-bottomed flask. Occasionally, concentrated HNO_3 or laboratory grade detergent was required to remove the residue. A test of the effect of detergent on Cl concentrations was carried out by measuring the Cl concentration of Milli-Q® water that had been soaked in a round-bottomed flask for 7 days which had been washed with the detergent. No measurable amounts of Cl were noted. If the residue could not be removed the round-bottomed flask was discarded. Clean, new boiling chips were used with each sample.

Precipitation

All precipitations were carried out in subdued light or darkness to prevent photodegradation of AgCl. The amount of expected Cl in the concentrate was calculated from the total volume of sample filtered and the concentration of Cl measured by HPLC. If less than 1 mg of Cl was expected, up to 1 mg of carrier was added to the sample. The carrier used was Weeks Island Halite which has a

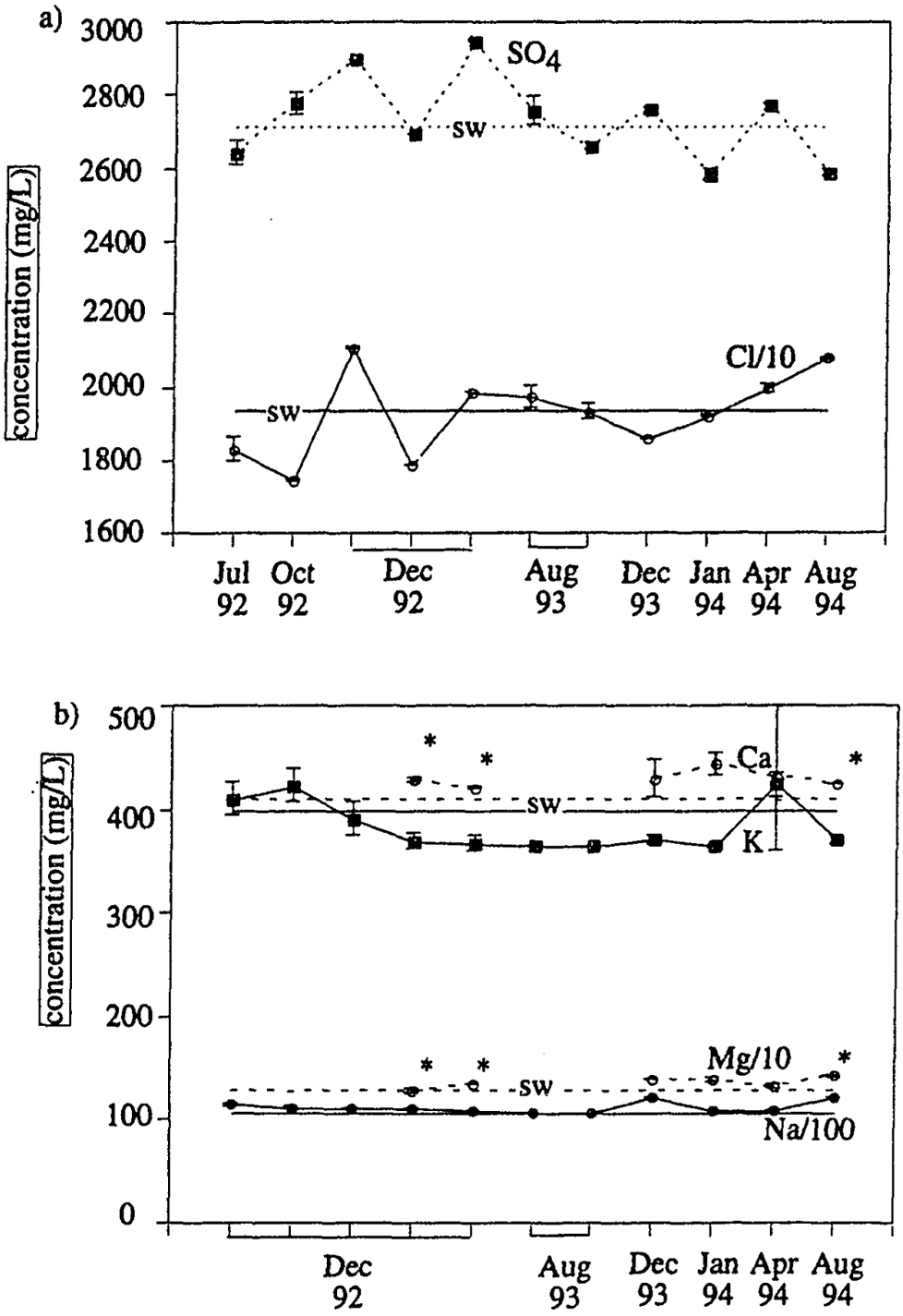

FIGURE 3.6 Concentration of a) major anions and b) major cations measured in Jervis Bay seawater over time. Jervis Bay seawater was used as a standard to measure reproducibilty between analytical runs. Measurements were performed by high pressure liquid chromatography (HPLC), except Ca an Mg values marked with an asterix, which were measured by inductively coupled plasma emission spectroscopy (ICP-AES). The straight lines are published concentrations of the particular element in seawater. Published concentrations taken from Millero 1974. Error bars represent 1 σ error.

negligible $^{36}Cl/Cl$ ratio. The carrier solution was also used to prepare blanks for each batch of precipitations. All carrier additions were precisely measured.

All reagents used during the precipitation procedure were of Spec Pure ($AgNO_3$, $BaNO_3$) or Analytical Reagent Grade (NH_4, HNO_3). Samples were precipitated in batches of 8 to 12. Approximately 100 to 150 ml of concentrated samples were heated in a glass beaker at a low hot plate setting for 1 to 2 hr, by which time the sample was slowly convecting. Some samples, particularly from the Northern Territory turned black upon heating. Five ml of 10% $AgNO_3$ were added to each sample and left to heat further for 30 minutes. After this time a precipitate had formed on the bottom of the beaker. The samples were then allowed to cool, covered with parafilm and left to stand overnight. These were then centrifuged at 2900 rpm for 10 minutes in a 50 ml centrifuge tube. Depending on how much supernatant was present, this process was repeated several times. A bead of AgCl formed in the bottom of the centrifuge tube and this was rinsed twice.

The bead of AgCl was dissolved using 1 ml of concentrated NH_4 solution. In some instances when AgCl remained caked to the beaker (this was particularly common for the blank), NH_4 was used to dissolve the AgCl in the beaker, and this added to the material in the centrifuge tube. The dissolved AgCl was diluted to 40 ml with Milli-Q® water, heated in a water bath for 10 minutes and 5 ml of saturated $BaNO_3$ added. After a further 10 minutes of heating in the water bath, the centrifuge tubes were removed and allowed to stand overnight, by which time a precipitate of primarily $BaSO_4$ (and most likely $BaCO_3$) had formed. The supernatant material was carefully extracted using a disposable cleaned plastic pipette, and transferred to a clean 50 ml centrifuge tube. The precipitate was discarded.

In a 100 ml glass beaker, 15 ml of 2N HNO_3, 10 ml of Milli-Q® water and 5 ml of 10% $AgNO_3$ were heated at a low setting on the hot-plate for 30 minutes. The beaker was removed from the hot-plate and the extracted supernatant material was added. A clean white precipitate of AgCl formed instantly and began to settle. In most cases it was possible to manipulate the formation of this precipitate into a cohesive lump, by tapping the base of the beaker occasionally. After heating for a further hour, samples were removed from the hot-plate, allowed to cool, covered with parafilm and allowed to stand overnight. The clear supernatant material was then carefully poured off and the precipitate centrifuged at 3000 rpm for 5 minutes. This was rinsed, and centrifuged twice. The centrifuge tube and precipitate which had formed a bead in the base of the tube, was dried in an oven overnight. In some

cases, the precipitate did not form a cohesive lump, but a fine powder. This entailed allowing the powder to settle into the base of the centrifuge tube overnight. However, this did result in lower yields.

The dried AgCl bead was then weighed and yields calculated. The AgCl was wrapped in weighing paper and aluminium foil and stored until pressed. Figure 3.7 shows the distribution of yields. The median yield was 77%. Low yields may be attributed to the loss of sample during the final clean-up procedure when AgCl formed a fine powder instead of a cohesive lump. High yields may be attributed to the presence of $BaNO_3$ in the final precipitate.

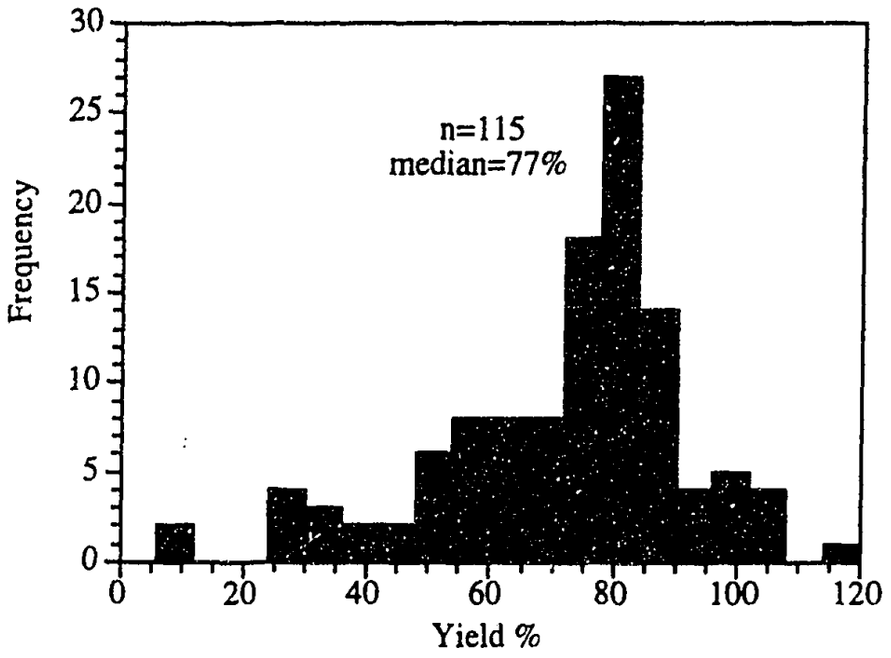

FIGURE 3.7 Yields of AgCl retrieved from the precipitation of AgCl for $^{36}Cl/Cl$ measurements by accelerator mass spectrometry (AMS). Median yield is 77%. Low yields (less than 60%) can be attributed to the formation of a fine powder rather than a cohesive lump during the final stage of precipitation. Yields greater than 100% can be attributed to the presence of $BaNO_3$.

All glassware that had been in contact with AgCl was rinsed with concentrated NH_4 solution, rinsed at least 3 times with Milli-Q® water, wiped with ethanol, rinsed at least 3 times with Milli-Q® water, soaked in very dilute HNO_3 for 24 hours, rinsed 12 times with Milli-Q® water, soaked for 24 hours in Milli-Q® water, rinsed 12 times with Milli-Q® water, dried in the oven, covered with parafilm and stored until use.

Sample Pressing

AgCl was pressed into a AgBr substrate coating the surface of a copper holder. Approximately 10 mg of sample was generally pressed, although one mg was adequate for analysis.

Measurement

Measurement of $^{36}Cl/Cl$ ratios was made on the 14UD Tandem Accelerator Mass Spectrometer in the Research School of Physical Sciences and Engineering at the Australian National University (Fifield et al 1987). The measurement of $^{36}Cl/Cl$ ratios involves the production of 3-5 μA by caesium sputtering. This beam then undergoes pre-acceleration to 128 keV and is mass analysed by a double focussing injection magnet before being focussed into the 14UD accelerator. An electrostatic beam chopper is used to attenuate the stable Cl beam, but is switched off during ^{36}Cl measurement. The negative Cl ions are stripped in the terminal of the accelerator by carbon foils. The resulting positive ions are accelerated a second time to ground at the base of the accelerator and steered around a 90° analysing magnet and onto a detection system comprised of a retractable Faraday cup (where the stable Cl is measured) followed by an ionisation chamber filled with propane in which the ^{36}Cl is detected. A typical measurement sequence consisted of 30 second measurement of ^{35}Cl and ^{37}Cl beam currents followed by a 10 minute counting period of ^{36}Cl, repeated two or three times. The system is set up for final analysis of 154 MeV Cl^{10+} ions in the detector, these high energies allowing clean separation of ^{36}Cl from the isobar ^{36}S and isotope ^{37}Cl, the main sources of interference and background.

Quality Assurance

Blank Measurements

A blank of approximately 10 to 20 mg of Cl, prepared from Weeks Island Halite, was precipitated with each batch to check for contamination during the precipitation process. Table 3.4 shows the $^{36}Cl/Cl$ ratio for each blank measurement. All were at or below 1×10^{-15} $^{36}Cl/Cl$.

Procedural Blank

The entire procedure (i.e. collection, preconcentration and precipitation) was tested for contamination by measuring the $^{36}Cl/Cl$ ratio of Weeks Island halite (50 mg) dissolved in 5 litres of Milli-Q® water and stored in a glass collection bottle in the laboratory for 3 months. The ratio measured was $0.5 \pm 1.0 \times 10^{-15}$ $^{36}Cl/Cl$,

confirming that no ^{36}Cl was being introduced by the preparation procedure or the collection vessel.

TABLE 3.4 $^{36}Cl/Cl$ ratios of Weeks Island Halite precipitated with each batch of samples. The ^{36}Cl counting time for the blank and samples was the same within each batch of measurements (i.e. 20 or 30 minutes). The ratios listed are limits based upon n+1 counts.

Sample batch	$^{36}Cl/Cl \times 10^{-15}$
July 93	0.3±0.3
November 93	0.2±1.1
November 93	0.6±1.1
December 93	0.8±1.2
December 93	0.2±1.0
March 94	0.4±1.0
March 94	0.1±1.0
May 94	0.1±1
November 94	1.0±1.2
November 94	0.4±1.1

Field Sampling

The reproducibility of the sampling procedure was tested by deploying two collectors side by side at site 27 (Gawler Ranges) on the SN array. The ratios measured were 52±5 and 49±5 $x10^{-15}$ $^{36}Cl/Cl$. These values are within the error bounds of each measurements, suggesting that the sampling procedure is collecting a representative sample of ^{36}Cl deposition.

Accuracy

A GEC standard was measured with every batch of 11 samples (1 wheel) run on the accelerator. The GEC standard has been used as a standard for $^{36}Cl/Cl$ measurements at the ANU since 1988 and acts to monitor the precision and accuracy of the AMS measurements. During the course of measurements for this project, the GEC standard displayed no significant deviations from its weighted mean value of 436±2 $x10^{-15}$ $^{36}Cl/Cl$ (Table 3.5).

TABLE 3.5 The $^{36}Cl/Cl$ ratios of the GEC standard measured with each batch of 11 samples. The error is the statistical error.

	GEC1	GEC2	GEC3	GEC4	GEC5
July 93	441±3	441±3	397±11	439±12	
November 93	432±12	436±11	418±12	396±11	
December 93	447±5	417±6	428±13	449±10	
			438±11		
March 94	457±19	447±18	493±20	421±18	
	460±22	447±19	464±19	425±19	
		432±19	451±19		
May 94		484±48	445±17		434±21
November 94		458±19	430±20		412±21
		437±22			416±24

3.3 DATA ANALYSIS PROCEDURES

Data Quality

There are many sources of errors in measurements of precipitation chemistry. These include analytical measurement errors and contamination during sampling (eg. bird droppings, insect infestation, human intervention). The following section contains methods used to identify data that are obviously contaminated or questionable. These data were subsequently excluded from further interpretation.

Ion balance

An initial test of data quality is an ionic balance. This is based upon the assumption that there is an equal number of positive and negative charges in a solution that is in equilibrium. Percentage imbalance is defined as

$$\% \text{ imbalance} = \frac{100 \text{ x (sum of cations - sum of anions)}}{0.5 \text{ x (sum of cations + sum of anions)}} \qquad (3.1)$$

Samples with imbalances of greater than 100% were generally removed from the data set if they also failed the outlier analysis criteria discussed below.

Regression

Regression of cation and anion concentrations provides another means of investigating data quality. Many regression procedures involve fitting a line to a collection of observations, so that the squared deviation of one of the lines is

minimised. In the present investigation, deciding which variable (total anions or total cations) is to be minimised is purely arbitrary. Hence, the reduced major axis technique (Hirsch and Gilroy, 1984) is used here and is recommended by various authors (Keene et al 1986, Ayers and Manton 1991, Gillett et al 1990). This method involves fitting a line that minimises the deviation of observations from both variables. The fitted line is the line for which the sum of the areas of right angles formed by the horizontal and vertical lines from the point to the line is minimised. Hence an equivalence between variables is established. The line is defined by

$$b = y + \frac{sgn(r)sy(m-x)}{sx} \quad (3.2)$$

where b is intercept, m is slope, y is the mean of the y variables, sy the standard deviation of the y variables, x and sx as for y and sy, and sgn(r)=1 if r>0; 0 if r=0; -1 if r<0. This regression procedure is used in the present investigation as a supplementary test to the ion imbalance to check the relationship between the total number of cations and the total number of anions in each sample. In an ideal situation the two variables would be equal, so the ideal line would have a slope (m) of 1 and an intercept (b) of 0. Thus, these parameters will quantify the quality of the data sets.

Outlier analysis

The method of outlier analyses adopted here follows that of Saylor (1992), in which data points that lie outside 2σ from the geometric mean of each chemical species measured were investigated. If justification for the removal of the suspected outlier was found, the data point was removed from the data set. Justification includes visible contamination of the sample by foreign matter.

Multivariate Statistics

With the advent of the relatively simple production of large data sets in atmospheric chemistry investigations, the use of multivariate statistics has increased due to the impracticality of simultaneous assessment of variations between individual components with multiple variables. Many different multivariate techniques have been applied in atmospheric chemistry investigations. The techniques used in this project are factor analysis (FA) and principal component analysis (PCA). The following discussion briefly describes the theory of these techniques and reviews some examples of their application in previous investigations. Finally, the way in which these methods are applied to the data sets in Chapter 5 is discussed.

Theory of Factor Analysis and Principal Component Analysis

A detailed account of the theoretical background to FA and PCA is beyond the scope of this work, and can be found in Davis (1986).

Both FA and PCA are forms of eigenvector analysis, i.e. a correlation matrix (a matrix that is standardised to have a mean of 0 and a variance of 1) is produced which indicates the relationship between pairs of variables. Eigenvector analysis is used to convert the correlation data into multivariate information so that the interrelationships between several variables may be assessed. The first difference between FA and PCA lies in how the eigenvectors are calculated. In FA, eigenvectors are calculated in normalised form and are transformed so that they define vectors whose lengths are proportional to the amount of variation they represent. In PCA, this normalisation does not take place, so that the magnitude of the vector does not represent the amount of variation the component is depicting. Thus factors derived by eigenvalue extraction in FA, and components derived by eigenvector extraction in PCA, will have the same direction, but different loadings. Hence while the proportion of variance accounted for by each factor and component will be the same for FA and PCA, the apparent importance of each variable in the factor or component will differ. The normalisation process carried out during FA has more statistical relevance if data sets with large numbers of cases are used, while PCA is more appropriately used on data sets with low numbers of cases, eg. data sets for individual sites where the maximum number of cases is 8. However, for the entire WE data set for example, (i.e. all ten sites for eight collection periods) the case number is up to 80, and FA can be used.

The extraction of the appropriate number of factors or components to be used is an important step in both FA and PCA. There are various methods employed to do this. The most common is to choose factors with eigenvectors greater than one. The argument for this is based upon the normalization of the variables so that each variable carries a variance of one. Therefore eigenvectors of less than one represent single variables. Many argue that this is not the most appropriate method, and it has been suggested that while eigenvectors of greater than one set a lower limit on the number of factors retained they do not automatically set an upper limit (SPSS 1990). Instead, an investigation of residual correlations (i.e. the difference between correlation coefficient estimated by the FA or PCA and the observed correlation coefficient), and the variance attributable to each factor allows for a more rigorous determination of the number of factors to be used in FA and PCA.

The normalisation of the eigenvectors in FA makes the loadings of variables simpler to interpret. Interpretation is further aided by the rotation step in FA, which represents the second difference between FA and PCA. PCA does not involve a rotation step. Rotation of the factor axes in FA is performed in order to create a simpler structure. Interpretation of factors may be clouded by the position of orthogonal axis in space being constrained by unnecessary axes. Rotation provides a means of removing these unnecessary axes. The rotation method commonly used is varimax rotation, which moves each axis so that projections from each variable onto the factor axis are either near the extremities or origin of the axis. Thus the factor loadings are adjusted so that they are either near ±1 or 0. Variables with loadings close to 1 have a high proportion of their variance explained by that factor, while those that are close to 0 have very little variance explained by that factor.

Previous Uses Of Multivariate Statistics In Atmospheric Chemistry Investigations

Factor analysis is a tool that has been used extensively in recent investigations of rainwater chemistry (eg. Crawley and Sievering 1986, Ayers and Manton 1991, Kessler et al 1992). The purpose of using FA in these investigations was to assess the sources of various components in rainwater. Ayers and Manton (1991) describe the presence of two major sources of rainwater ions from Coffs Harbour and Wagga Wagga: seasalt, dominated by Na, Mg, Cl and SO_4; and a continental source with ions such as K and Ca (characteristic of soil-dust), SO_4 (an oxidation product of anthropogenic emissions), NO_3 (from anthropogenic and soil emission) and NH_4 (from soil and plant emissions of NH_3). Crawley and Sievering (1986), as part of the MAP3S/RAINE precipitation study, determined three sources of ions (seasalt, ammonia/dust soil and an acid factor) in rainwater in the northeastern United States. As a final example, Kessler et al (1992) interpreted four factors to be contributing to rainwater chemistry based on seven years of rainfall data from Texas. These included a Gulf factor (marine origin), a soil factor, an acid factor and an aged aerosol factor.

Zeng and Hopke (1989) used FA to indicate three sources of components to rainfall in Canada; an acid precursor source (SO_2 and NO_x), a Ca and Mg source and a Na and Cl source (marine aerosol). They extended the use of FA further to investigate in more detail the acid precursor source, by incorporating into the FA back-trajectory information. The results of this showed the relationship between the chemical nature of the sources and the geographic regions over which the air parcels passed, pinpointing areas along the east coast of Canada as being the major source of acid precipitation to Ontario.

There are numerous examples of the application of PCA to atmospheric chemistry investigations, in which as for FA, the primary use of PCA has been to determine the source of constituents to precipitation. Smeyers-Verbeke et al (1984) investigated the variations in organic air pollutants in the Netherlands from 1979 to 1981, and interpreted the relationships between pollution and meteorological parameters. They stressed the use of PCA as a simple way to graphically display the total variation of a data set in a few dimensions. Also in the Netherlands, Janssen et al (1989) used eigenvector analysis to investigate the relationships between SO_4, NO_3, Cl and NH_4 concentrations in aerosols; the gaseous components SO_2, NO, NO_2 and O_3, and meteorological parameters. Shaw (1991a) investigated the chemical composition of aerosols from Alaska over a four-year period, and using PCA, found high levels of metallic elements were associated with Arctic airmasses. These airmasses sourced material from Eurasia. Investigation of non-anthropogenic sources in the Alaskan data set, revealed an Al-rich dust, a marine seasalt, and a Br component (Shaw 1991b).

Application

Factor analysis was carried out using the factor analysis program contained in the Statistical Package for Social Sciences (SPSS). The generalised procedure involves determining a correlation matrix followed by extraction of factors using principal component analysis. Finally rotation of the factors allows simpler interpretation of results (SPSS 1990). Principal component analysis was performed using Genstat 5 (Genstat 5 Committee 1989).

Multivariate analysis was carried out on the major-element and ^{36}Cl data sets. Both FA and PCA performed on the same data sets (and subsets) produced the same number of factors or components, explaining the same amount of variance. This is not unexpected when it is considered that FA is really just an extension of PCA. The factor loadings produced by FA were much clearer to interpret than the component loadings produced by PCA. However both techniques are adopted here because of the inability of the SPSS factor procedure to deal with data sets that have smaller case numbers than variables (eg. individual site data subsets).

The use of multivariate techniques in many environmental investigations has been heavily criticised. A major problem lies in trying to determine quantitative input rates of each source and trying to extract more information from the data than there really is. Henry (1987) shows that the lack of physical constraints placed on factor models suggest that the results of many models mean very little as they are based

upon incorrect assumptions. In this study, FA and PCA are used only as a qualitative tool to group variables that have common variances. In conjunction with other arguments it enables an indication of the major sources of components to precipitation across the WE and SN transects and the relationships between ^{36}Cl and major elements.

Graphical Procedures

Graphical techniques are used to investigate the seasonal variations demonstrated by the ^{36}Cl data set. The multivariate techniques discussed above will indicate some general characteristics of the major element data set, such as the source types of chemical constituents to the arrays. Further assessment of these general characteristics will require techniques that pinpoint finer scale details, such as how these sources affect each site, and the change in the influence of these sources over time.

Seawater and soil/dust are two probable sources of constituents to rainfall in unpolluted areas for which we have some idea of chemical composition. The chemistry of seawater is well constrained (eg. Millero 1974). The influence of seawater on the ionic concentration of rainfall can be assessed by comparing the ratios of "characteristic" seasalt ions measured in rainfall with the ratios found in seawater. The concentrations of the characteristic seasalt ions used here are shown in Table 3.6. In many rainfall investigations Na is often assigned as a quantitative tracer of seasalt (eg. Ayers and Manton 1991). By assuming that all Na measured in the rainfall sample is of seasalt origin, we can investigate the influence of seasalt on other ions measured in the rainwater samples and assess the influence of seasalt on non-coastal sampling localities. Using characteristic seasalt ratios the extent of a non-seasalt contribution of the ions for SO_4, K, Ca and Mg can be investigated by looking at the "non-seasalt" (nss) fraction of these ions in rainfall. Non-seasalt fractions are calculated from the following equation

$$\%Cnss = \{ \frac{[(\frac{Cx_{(rw)}}{Na_{(rw)}} - \frac{Cx_{(sw)}}{Na_{(sw)}}) * Na_{(rw)}]}{Cx_{(rw)}} \} * 100 \qquad (3.3)$$

where C is μeq/L of species x (SO_4, Ca, Mg or K) in rainwater (rw) or seawater (sw).

TABLE 3.6 Composition of seawater. From Millero 1974.

species	concentration g/kg
Na	10.76
Mg	1.29
Ca	0.41
K	0.39
Cl	19.34
SO4	2.71
Br	0.07

Figure 3.8 illustrates the use of seasalt versus non-seasalt contributors as will be used in later discussions. In Figure 3.8a, the ratios of Cl/Na and SO_4/Na are shown as a function of distance from the coast for the WE array during winter 1992. The Cl/Na ratio approximates that of seawater across the WE array, while the SO_4/Na ratio increases with increased distance from the coast, reflecting the decreased influence of seasalt on SO_4 at inland sites. This is also displayed in the non-seasalt plot (Figure 3.8b), where nss SO_4 and Ca contribute approximately 40-50% of the SO_4 and Ca at inland sites. Non-seasalt Mg is a minor contributor to the Mg content of precipitation across the array, while nss K is a significant contributor to total K.

Unlike seawater, the chemical composition of soils is not well constrained and can differ markedly from place to place. To overcome this problem, samples of surface soil and dust material were collected from each site, at distances of approximately 10 m to the north, south east and west of each collector. These samples are assumed to represent the locally derived material that enters the rain collector due to local wind movement. Characteristic soil/dust concentrations for each site were measured after leaching the soil/dust material from each site in Milli-Q® water for 2 months. The proportion of soil/dust to Milli-Q® was calculated from the average amounts of undissolved material measured in the rain collectors at each site. The soil/dust composition at each site is given in Appendix C. The rainwater compositions can

then be compared with soil/dust compositions in a similar fashion as the seawater comparisons.

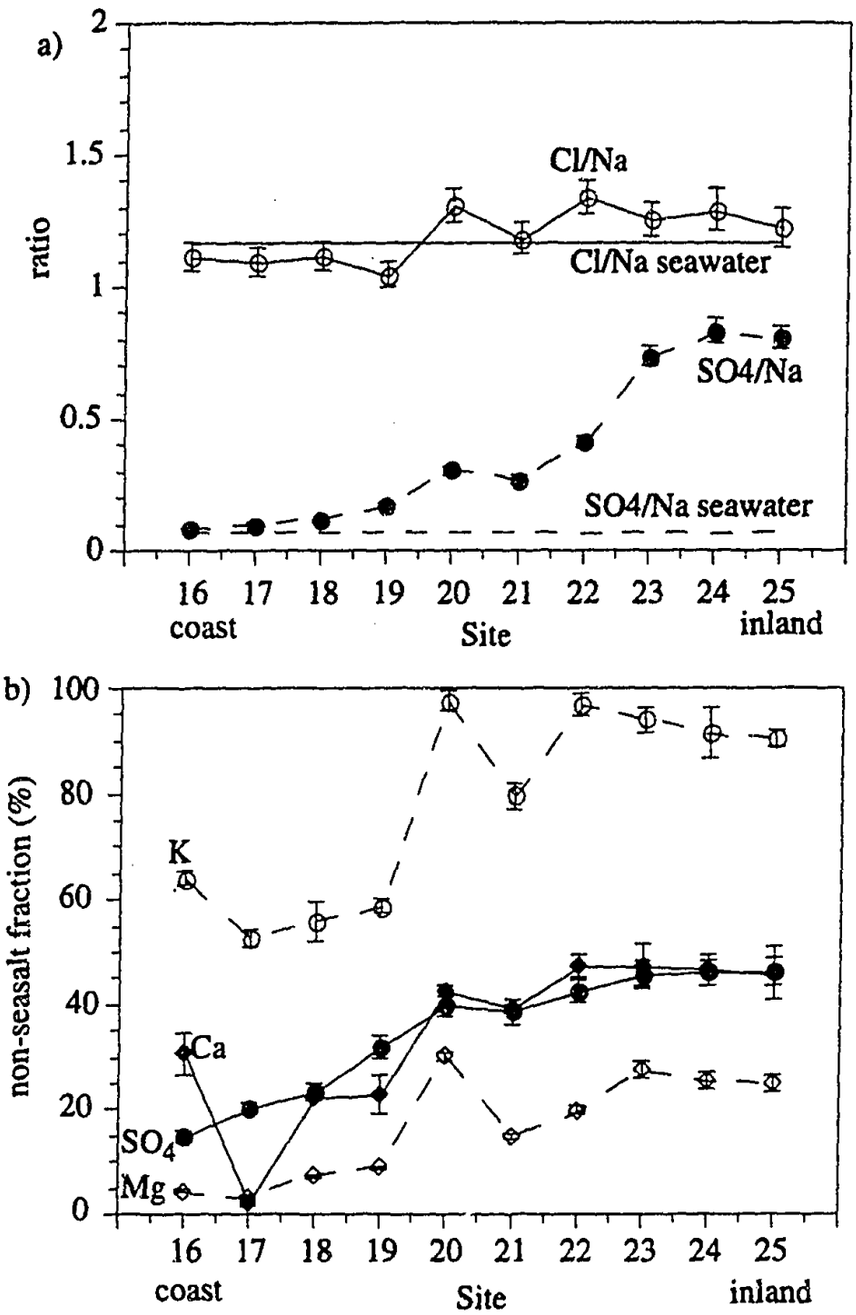

FIGURE 3.8 Examples of a graphical techniques used to interpret spatial and temporal variations displayed by the major-element data sets. a) Ratios of elements to Na (considered to be a conservative seawater tracer) are compared with the ratio of the particular element with Na in seawater. This figure shows the ratios of Cl and SO_4 with Na for the WE array during winter 92. A trend of increasing ratio (i.e. moving away from the seawater ratio) is observed for SO_4 with increasing distance from the coast. Ratios are calculated from depositional units (i.e. $\mu eq/m^2/s$). b) The non-seasalt (nss) fraction represents the proportion of the particular element measured in precipitation of non-seawater origin and is calculated as described in the text. This figure shows the nss fractions of SO_4, K, Ca and Mg in precipitation along the WE array during winter 92. There is a general increase in nss concentration with increasing distance from the coast.

CHAPTER 4 INTRODUCTION TO PRECIPITATION CHEMISTRY

A summary of the current understanding of the formation of precipitation, the incorporation of chemical species into precipitation, and the sources of the species describes the framework from within which results of the present investigation can be interpreted. A summary of previous precipitation investigations in Australia will help place interpretations from the present investigation into context.

4.1 INCORPORATION OF CHEMICAL SPECIES INTO RAINFALL

Rainfall is an important part of the hydrological cycle as it involves the exchange of water and chemical constituents between the atmosphere, oceans and landmasses. Details of the processes involved in the formation of precipitation and the incorporation of chemical constituents in precipitation were given by Pruppacher and Klett (1980) and Warneck (1988), and can be summarised below.

Cloud Formation

Condensation resulting from adiabatic cooling in rising air is responsible for the formation of clouds and precipitation. Uplift of the air parcel occurs by convection, frontal activity or orographic interference (Linacre and Hobbs 1982). Figure 4.1 is a schematic representation of ascending air undergoing adiabatic expansion and cloud formation.

Aerosols are important in cloud formation as they may act as condensation nuclei and provide inorganic salts that make up the ionic chemistry of rainfall. Generally, aerosol particles greater than 0.1 μm will act as cloud condensation nuclei, with the largest particles being used first (Figure 4.2). As an air parcel rises and supersaturation increases, smaller particles become activated. Ice particles will be generated only in clouds at temperatures below -20°C (or 6 km into the troposphere), since special ice-forming nuclei are required to form ice in clouds. Thus in the middle troposphere supercooled liquid water in clouds is common. However all clouds that reach temperatures below 250K host a certain population of ice (Barry and Chorely 1976).

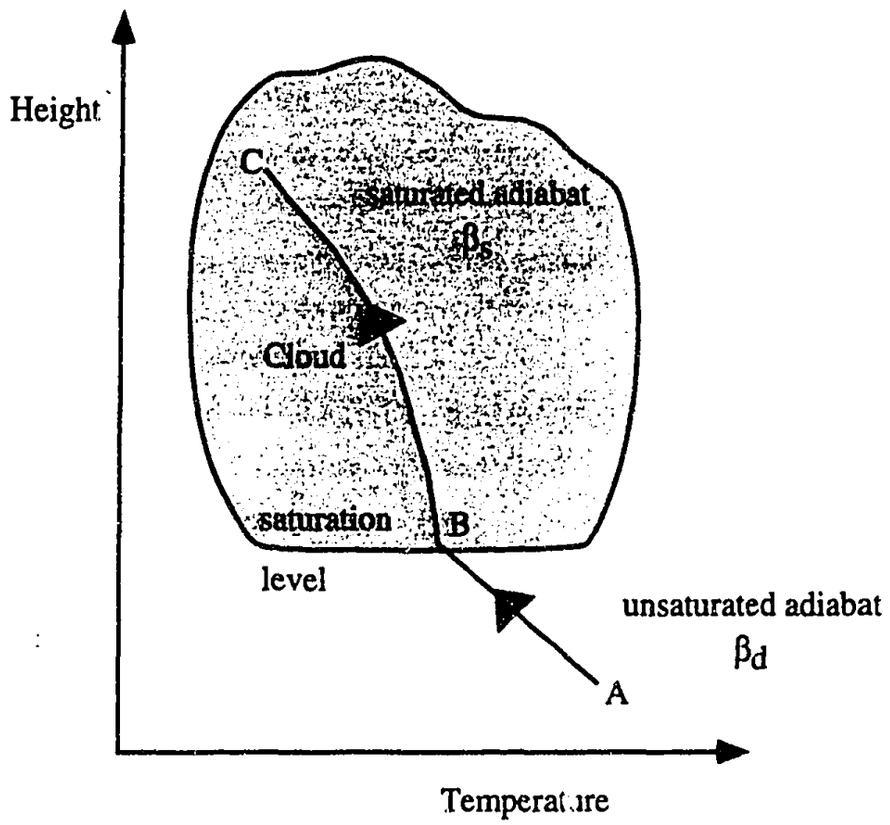

FIGURE 4.1 A schematic diagram showing the ascent of air in the atmosphere and cloud formation. From A to B, air is unsaturated and cools adiabatically (i.e. does not gain or loose heat), the temperature decrease (or adiabatic lapse rate βd) is 9.8K/km. If the air from A to B contains water vapour, it will cool as it rises and if it rises far enough will become saturated. Further rising causes supersaturation, or if nuclei are present, condensation. When condensation takes place, the pressure change is no longer adiabatic since latent heat is released. The latent heat released by condensation offsets cooling due to adiabatic expansion, so that the lapse rate in the cloud βs (from B to C) is less than the lapse rate for the process in the absence of condensation (from A to B).

Rainfall Formation

Not all clouds produce precipitation. In order to produce rain a cloud must form drops with an initial radius of greater than 500μm (Figure 4.2), otherwise evaporation of the drop will occur at the base of the cloud before the drop is able to reach the ground. The formation of rain occurs in two ways: by cold-rain formation and warm-rain formation (Warneck 1988). Cold-rain formation occurs over continental regions where high reaching clouds promote the growth of ice particles in the upper reaches of the cloud. Falling ice particles melt as they descend through warmer layers of the atmosphere. Warm-rain is produced over tropical landmasses and oceans where cloud tops cannot reach 273 K, and involves only the liquid phase, with growth first by coalescence and then condensation.

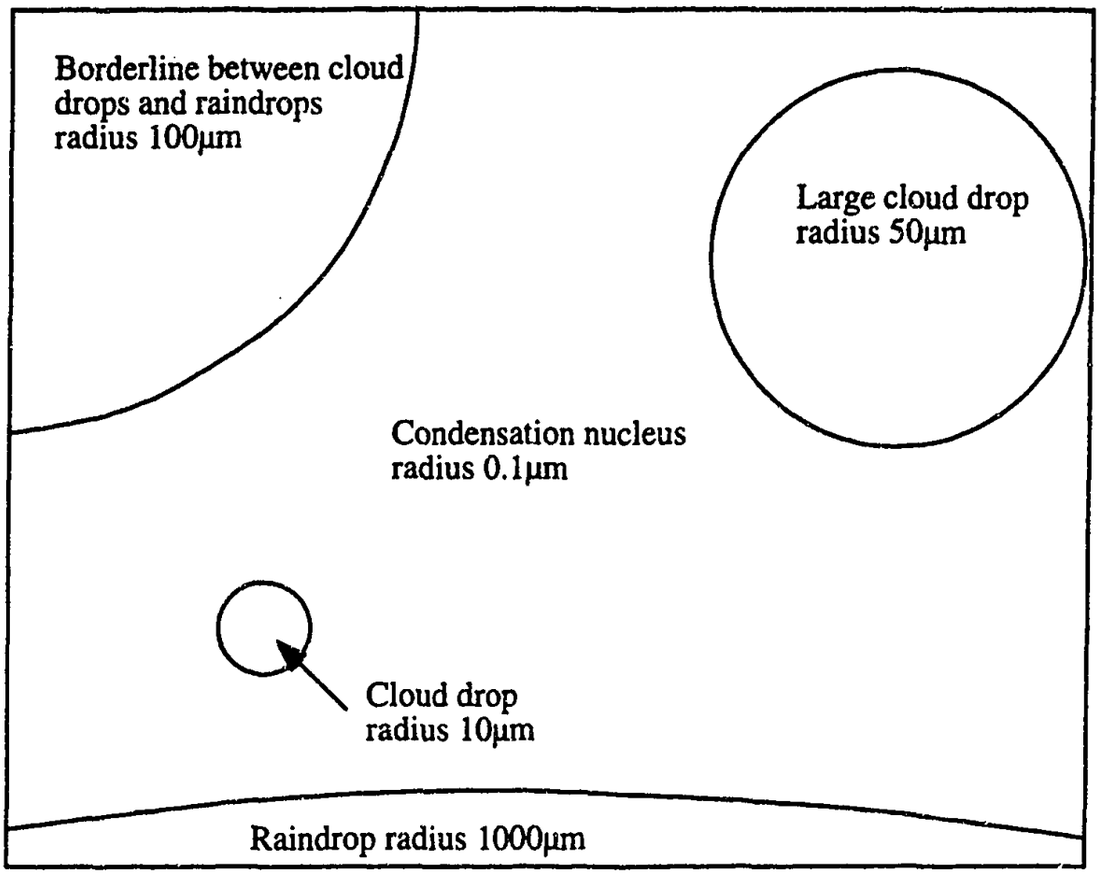

FIGURE 4.2 Schematic diagram showing the size ranges of particles involved in the formation of clouds and rain. After Iribarne and Cho 1980.

The chemical composition of rainfall is governed by the incorporation of aerosols and gases from the atmosphere into cloud and rain drops. This scavenging occurs both within the cloud (within-cloud) and below the cloud (below-cloud), processes that have been termed "rainout" and "washout" (eg. Junge 1963), respectively. The following section describes the processes of aerosol and gas scavenging as they occur within and below the cloud.

Aerosol Scavenging

Within-cloud scavenging of aerosols involves nucleation of aerosol particles with radii greater than 0.2 μm. These make up 60 to 80% of the total air mass (Warneck 1988). Aerosols not used for nucleation once the cloud has formed may join other aerosols and cloud droplets, although this adds very little mass to the cloud. The

aqueous concentration of ionic species resulting from within-cloud scavenging (c_w) is dependent upon the concentration of species in the aerosol (c_a), the liquid water content of the cloud (L) and the scavenging efficiency (E_a) according to:

$$c_w = c_a E_a / L \qquad (4.1)$$

E_a combines the effects of nucleation, Brownian motion and collision capture, but is dominated by nucleation (Junge 1963). Warneck (1988) showed that within-cloud scavenging and precipitation is the dominant process for the removal of particulate matter from the troposphere. Congruency was found in the residence time of particulate matter in the atmosphere removed by within-cloud scavenging and precipitation, and the residence time of bulk aerosols in the atmosphere, as calculated from radioisotope tracers.

Below-cloud scavenging of aerosols involves the incorporation of aerosols by collision capture. The airflow around a spherical drop results in the modification of capture cross section of the falling droplet, since particles follow hydrodynamic streamlines of a droplet (Pruppacher and Klett 1980). The scavenging efficiency becomes a function of the radii of both the water droplet and particle, and may be increased by drop oscillation and electric charge. The efficiency is also increased when a standing eddy develops in the lee of the falling water droplet (common for water droplet radii of 200-600 μm), so that particles escaping frontal collisions are trapped in the rear of the eddy and undergo rear capture. A schematic representation of a falling spherical raindrop is shown in Figure 4.3. Falling ice particles behave in a similar way to water droplets with regards to scavenging efficiencies.

Below-cloud scavenging affects particles in the 2-15 μm range, while within-cloud scavenging incorporates aerosol particles greater than 0.2 μm. Thus below-cloud scavenging enhances elements in precipitation associated with the mineral fraction of the aerosol (eg. Cl, Na, Ca, Mg, K).

Gas Scavenging

The extent to which gases absorb into cloud and rain drops depends on the solubility of the gas in water. Gases and water vapour are incorporated into cloud and water drops at the same rate because of their similar coefficients of molecular diffusion. Within clouds, gases equilibrate quickly with the liquid phase. However, below clouds, gas concentrations are different from those within the clouds so that

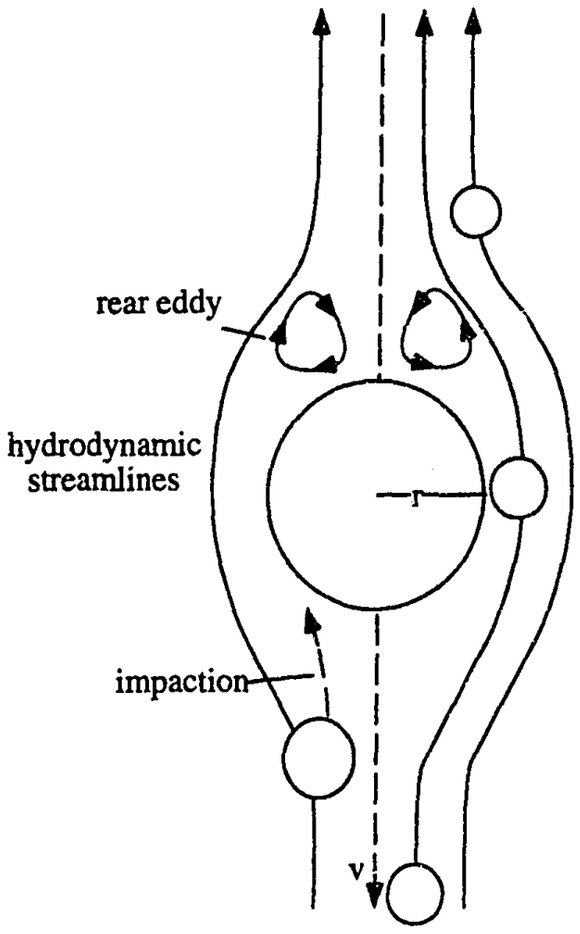

equilibration is a slower process. This governs the difference between within-cloud and below-cloud scavenging of gases.

FIGURE 4.3 Schematic representation of the air flow around a falling sphere. As the water drop falls, particles are incorporated into the drop by collision (or impaction) capture. A drop with radius r falling at velocity v will sweep out all particles in a cylinder πr^2 if the there was not air flow around the spherical drop. The figure shows that the hydrodynamic streamlines around a falling drop modify the capture cross-section of the drop. This modification is accounted for by an efficiency factor which is a function of the radii of both the falling drop and the collected particle. Electric charges and drop oscillation can increase the collection efficiency. Particles escaping frontal collision may be trapped in the rear eddy of the falling drop and undergo capture. After Warneck 1988.

The partitioning of gases between the aqueous and gaseous phases of a cloud is determined by Henry's law and the associated partition coefficients (Warneck 1988). The scavenging efficiencies of most gases are very small, except for water vapour. The residence time of water-soluble gases due to within-cloud removal is dependent on the column density of the gas in the troposphere and the mass flux of the gas from the troposphere. The mass flux of the gas is dependent on average rainfall amount. Slightly soluble gases have long residence times, while permanent gases are not

retained by the ground surface and are soon released back to the atmosphere. Residence times of less than one year require scavenging efficiencies of 2% (eg. H_2O_2).

Within a cloud, acid and base precursors such as SO_2, CO_2, NH_3, HCl and HNO_3 react with water to form ions by dissolution. Dissolution involves two steps, hydration and formation of ions from the hydrate. A third step exists for diprotic acids. For weak acids (SO_2 and CO_2) Henry's Law can be adapted to account for dissolution, and an adapted Henry's Law coefficient determines the degree of gas liquid partition of a substance within the cloud. Weak acid-forming gases are poorly absorbed by cloud water that is of low pH, while weak base-forming gases are poorly absorbed by cloud water that is of high pH. For strong acids (HCl and HNO_3) it is difficult to separate the ion equilibrium constant for H (KH) and the dissociation constant, so Henrys Law is modified to account for the product of the two constants. For pH of 4.5 (the typical value of cloudwater) all HNO_3, HCl and NH_4 is directly scavenged from the gas phase. In order to return HCl and HNO_3 to the vapour phase from solution, liquid water contents would have to be decreased.

A falling droplet below the cloud experiences different conditions from those existing within the cloud. Mass flux occurs in the process of equilibrating to these new conditions. The rate of mass flux is dependent on a number of parameters that include mass molecular diffusion inside and outside of the droplet and transport resistance at the gas-liquid interface. These parameters, combined with the heterogeneous distribution of trace gases, mean that a raindrop falling in a below-cloud region will experience rising gas phase concentrations. Thus the raindrop cannot attain equilibrium and will scavenge only a fraction of the material that it is potentially capable of absorbing. However periods of prolonged rainfall will deplete gas-phase concentrations below a cloud.

Models of the Incorporation of Species into Rainfall

Many models have tried to incorporate some of the complex processes of cloud microphysics and dynamics associated with removal of constituents from the troposphere. For example, Brimblecombe and Dawson (1984) suggested a model in which a species concentration in a cloud is determined by species solubility and liquid water content of the cloud, as based upon thermodynamic partitioning. Qin and Chameides (1986) used a one-dimensional, time-dependent model of a warm precipitating stratiform cloud to determine that the rate of removal of highly soluble species is controlled by transport process rather than thermodynamic processes. The

model of Qin and Chameides was extended to include below-cloud scavenging (or washout) by Lin Xing and Chameides (1990) to compare the relative roles of rainout and washout. The model showed that below-cloud removal dominates within-cloud removal for very soluble gases. This arises because the gas-phase mixing ratio within the cloud is lower than below the cloud, so that the falling droplet leaving the cloud is undersaturated with respect to trace gases below the cloud. Thus more of the soluble gas is able to dissolve into the falling raindrop. The model also showed that during periods of extended rainfall, the rate of wet removal becomes independent of microphysical parameters such as rainfall rate and liquid water content, but is determined by the rate at which new material is transported into the precipitating column.

Cautenet and Lefeivre (1994) developed a model that contrasted the behaviour of gas and aerosol species scavenging (SO_2 gas and SO_4 aerosol) during convective rain over an African equatorial forest. A reduction in aerosol scavenging with increasing rain intensity was found. A difference in scavenging efficiencies according to the origin of the element (i.e. gas or aerosol) was noted, with the dilution effect of increased rain being more important for aerosols than gases. Finally a decrease in atmospheric concentrations of the sulphur species during rainfall was noted.

Likens et al (1984) showed an inverse relationship between rainfall amount and rainfall ionic concentrations at Hubbard Brook, New Hampshire. Rainfall concentrations are also dependent on rainfall type, i.e. convective or frontal (Lacaux et al 1992). Convective showers show the development of rainfall intensity maximum corresponding with a concentration minimum through the course of the rainfall event (Gatz and Dingle 1971). Frontal precipitation events, however, have initially high concentrations which diminish to a constant value that is independent of rainfall amount. Frontal rainfall concentrations are explained in terms of evaporation of raindrops during the initial stages of precipitation and by the removal of scavengable material by below-cloud processes (Warneck 1988).

Summary

The most significant points to arise from the above discussion concerning the incorporation of chemical species into precipitation can be summarised. The bulk of aerosols in the atmosphere are removed by within-cloud scavenging, while below-cloud scavenging enhances the mineral fraction of aerosols in precipitation. Henry's Law controls the absorption of gases by clouds and raindrops. Strong acids are directly scavenged from the gas phase within clouds, and the scavenging of gases in

the below-cloud region is inefficient, except during periods of extensive rain. Modelling studies however, reveal that below-cloud scavenging dominates over within-cloud scavenging for highly soluble gases (Lin Xing and Chameides 1990). Comparison of aerosol and gas scavenging shows a negative relationship between aerosol scavenging and rainfall amount, with the dilution effect of rainfall being more significant for aerosols than gases (Cautenet and Lefeivre 1994).

4.2 SOURCES OF THE CHEMICAL CONSTITUENTS OF PRECIPITATION

The major constituents of precipitation in remote areas are Cl, SO_4, NO_3, Na, K, Mg, Ca, H and NH_4 (eg. Brimblecombe 1986). The concentration of these different constituents is dependent upon both location and time. For example, coastal localities have higher Na and Cl concentrations than non-coastal localities as displayed by Hingston and Gailitis (1976) for Western Australian rainfall. European rainfall shows maximum concentrations of all species during spring, probably due to increased photochemical activity (Brimblecombe 1986). Sources can be described under three headings: seawater, continental dust and acid-base precursors. In addition, phosphate is briefly discussed because of the presence of phosphate measurements in the analytical program.

Seawater

Seawater is an important source of Na, Cl, SO_4, Mg, Ca, K and Br to the atmosphere. Seasalt aerosols are injected into the atmosphere by bubble bursting at the sea surface. (Blanchard and Woodcock 1957). Most of this aerosol is directly returned to the ocean, but approximately 10% can be carried over continents (Andreae 1984). Partial evaporation of water in the seasalt droplet leads to the formation of a brine droplet or solid seasalt particle, which is transported until dissolved. Indeed, salts (eg. NaCl) are important to the production of rainfall since clean air, even under conditions of supersaturation, will not condense water vapour (Barry and Chorely 1976). The equilibrium vapour pressure over small droplets is greater than over plane surfaces; the presence of salts acts to lower the water vapour pressure sufficiently that salt particles act as condensation nuclei.

Continental Dust

Aeolian weathering in arid regions has been shown to inject large amounts of dust into the atmosphere (Ryaboshapko 1983). Soil or dust introduces similar cations as seawater to the atmosphere. However, precipitation strongly influenced by soils will be enriched in Ca and K compared with Na and Mg (Hutton 1968). The composition

of soils is geographically very variable as shown by Moore et al (1983), and is reflected in the wide range of compositions measured in the soil/dust samples from the WE and SN arrays (Appendix C). Extensive amounts of carbonate, sulphate and chloride salts are found in arid to sub-humid soils of Australia (Isbell et al 1983), with salt accumulation occurring when annual precipitation is insufficient to leach soils below 0.7 to 1m depth. Salts also accumulate at the surface when the local water table is at a depth shallow enough to maintain an upward flow of soil solution to the surface where evaporation occurs. Gypsum ($CaSO_4$) is common in a wide range of soils in arid and semi-arid regions. It may be pedogenic or inherited from parent material rich in gypsum such as salt-lake sediments. The common occurrence of salt lakes in Australia, in particular in proximity to the WE array, suggests that salt lakes may be an important source of continental material to the chemical load of precipitation in the present study. Salts such as halite and gypsum form as the latest stable phases during evaporite formation, and therefore are most likely to be available for deflation from the surface.

Acid-Base Precursors

Rainwater is commonly moderately acidic, i.e. the pH is less than 7, and H ions are derived from the dissociation of acids. Acids in the atmosphere include strong acids (HNO_3, HCl, H_2SO_4) and weak acids such as CO_2(aq) and organic acids. Bases in the atmosphere include NH_4. The following discussion describes the sources of each of these acid and base precursors, and these species will subsequently be grouped together as the 'acid-base' balance.

Sulphur

The presence of SO_4 in the atmosphere is due to the injection of seasalt and aeolian weathering salts as described above, as well as the oxidation of SO_2 in the atmosphere. Atmospheric SO_2 is primarily derived from anthropogenic emissions, in particular the burning of fossil fuels. The levels of SO_4 introduced by oxidation of SO_2 therefore depend on the level of industrialisation and the sulphur content of fuel used. The transformation of SO_2 to SO_4 proceeds on time-scales of several hours to days, so that urban concentrations of SO_4 (i.e. near the source of emission) do not differ substantially from regional average concentrations (Ryaboshapko 1983). While the sampling localities in the present study were chosen to lie away from direct sources of anthropogenic emissions, the presence of possible sources of emission need to be borne in mind during interpretation of the precipitation chemistry. It should be noted that Ayers and Gillett (1988a) in a review of

acidification of tropical Australia, estimate that the Mt Isa smelter in Queensland accounts for 70% of total sulphur emissions in tropical Australia.

Another source of sulphur to the atmosphere arises from biological emissions. Sulphur is an element that is essential for the life processes of many biological organisms, and biological emissions occur from both continents (plants, soils, wetlands and biomass burning), and from oceans (eg. dimethylsulphide). For the present study biological emissions may be of particular significance for the northern section of the SN array. Ayers and Gillett (1988a) estimate biological emissions in the north of Australia to be the major natural source of sulphur to the atmosphere.

Volcanic emissions are also an important source of SO_4 to the atmosphere, both during eruptive and non-eruptive stages, emitting both gaseous sulphur and particulate SO_4 (Andreae 1984). For example, SO_2 emissions from the crater lake of Mt Ruapehu in New Zealand during a period of relative inactivity in 1993 were measured at 171 metric tonnes/day (Smithsonian Institute 1993). Australia is flanked to the north and east by a rim of volcanoes. Prevailing wind directions suggest eruptions in areas north of Australia are most likely to affect Australia. The largest volcanic eruption during the sampling program occurred from Pinatubo (Philippines) in June of 1991, where ash was ejected a maximum of 40 km into the atmosphere, with an average ejection height of 10 km over several days (Bulletin of Volcanic Eruptions 1991). Activity from Pinatubo continued on a smaller scale (eg. erupting a column of ash 15 km high in August of 1993), periodically throughout the sampling program. Continued, smaller-scale activity was observed in Papua New Guinea (Manman, Langila and Ullawun), and from Indonesia (Krakatau, Rinjani and Gamalama to name a few).

Chloride

Volatile inorganic Cl (available for the formation of HCl among other Cl compounds) is introduced to the atmosphere by heterogeneous reactions involving seasalt aerosols (Keene et al 1990). Approximately 3 to 20% of Cl is released as vapour from aerosols introduced by bubble bursting at the ocean surface (Cicerone 1981), and this particle-gas conversion process is the major source of gaseous Cl to the global troposphere. The mechanism involved in the particle-gas transformation over continental regions involves the direct volatilization from the seasalt particle at a pH of less than 3 by the incorporation of H_2SO_4 and HNO_3 (Ericksson 1959, Duce (1969), Martens et al 1973) according to the following reactions

$$HNO_3(g) + NaCl\ (p) = HCl(g) + NaNO_3(p) \qquad (4.2)$$

$$H_2SO_4(g) + NaCl(p) = 2HCl(g) + Na_2SO_4(p) \qquad (4.3)$$

The importance of the above acid-base desorption reactions in the marine troposphere is debated, and alternative mechanisms involving reactions of various N gases have been suggested. For example, the reaction of NO_2 with seasalt has been demonstrated as a source of volatile Cl (Finlayson-Pitts 1983) according to the following reaction

$$2NO_2(g) + NaCl(p) = NOCl(g) + NaNO_3(p) \qquad (4.4)$$

where NOCl undergoes photolysis to generate Cl atoms which initiate oxidation of hydrocarbons to produce HCl or hydrolysis to generate OH radicals and HCl. Finlayson-Pitts et al (1989) reported reactions of $ClNO_3$ and N_2O_5 with NaCl to generate Cl vapour. Keene et al (1990) showed that acid-base desorption reactions could account for only 38% of HCl production in the marine atmosphere, and suggested that reaction of O_3 at seasalt aerosol surfaces generates Cl_2, which is rapidly converted to HCl via the photochemical transformation of Cl_2 to Cl radicals. The authors also suggested that HCl was eventually recaptured by the aerosol.

Nitrogen

There are six major processes that supply nitrogen compounds to the atmosphere. These are emissions from soil microbial processes, lightning, combustion of biomass, anthropogenic fuel combustion, fertiliser application and volitilization of ammonia (Galbally 1984).

Soil microbial processes include nitrification (biological oxidation of fixed nitrogen) and denitrification (anaerobic reduction of NO_3^{2-} or NO_2). These processes result in the exchange of NO, NO_2 and NO_3^{2-} at the Earth's surface. The emissions of nitrogen compounds from soils of different ecosystems have been summarised by Galbally (1984). While recognising the need for a larger data base, Galbally has attributed most of nitrogen emissions on a global scale to soil, with a significant proportion involving agricultural land use. Ayers and Gillett (1988a) recognised the complete lack of data on nitrogen oxide emissions from tropical soils, but were able to attribute 7% of emissions of nitrogen compounds to soil in tropical Australia, based on NO fluxes from temperate woodlands in Australia and the area of tropical soil cover.

Lightning produces NO in the atmosphere through the high-temperature combustion of N_2 and O_2 (Chameides et al 1977). NO is then oxidised to NO_3 within a short period of time (i.e. 1 day), scavenged and deposited in rainfall. The global emission of NO_x-N by lightning has been estimated by Galbally (1984) to represent only a small fraction (less than 10%) of the total emissions of nitrogen compounds.

Burning of biomass generates NO, NO_2, NH_3 etc. On a global scale, emission of nitrogen compounds by biomass burning is a small fraction of total nitrogen emissions (Galbally 1984). However in tropical Australia, where anecdotal evidence quoted in Ayers and Gillet (1988) suggests that approximately 30% of tropical Australia is burnt each year, biomass burning provides a substantial proportion of nitrogen emissions (80%).

Anthropogenic sources of nitrogen emissions arise from combustion of fuel, such as in the use of motor vehicles and operation of power stations. Ayers and Gillet (1988a) show that anthropogenic sources of nitrogen emissions account for less than 5% of all emissions in the tropical north of Australia. During coal burning, for example, 1g of NH_3 is emitted for every kg of coal consumed (Robinson and Robbins 1972). The application of fertiliser is also an important anthropogenic source of NH_3 to the atmosphere. Galbally et al (1980) estimate an average of 10% of NH_3 applied as fertiliser in Australia is lost to the atmosphere.

NH_3 is an important species in precipitation because it can neutralise atmospheric acids. The primary sources of NH_3 to the atmosphere are volatilization of NH_3 from animal urine, soils and microbial decomposition (Galbally et al 1980). Volatilization of NH_3 results from the difference in the partial pressure of NH_3 in equilibrium with the liquid phase (in a moist soil or a solution) and that of ambient atmosphere above the soil or solution. Volatilization is controlled by pH, NH_4 concentration, binding of NH_4 to clays, soil buffer capacity, presence of $CaCO_3$, soil moisture, evaporation, turbulence and presence of vegetation. The large area of Australia given over to grazing means that agricultural emissions of NH_3 are significant, sourced from both volatilization of animal urine, soil emissions and fertiliser application (Galbally et al 1980). Soils in ungrazed pasture also emit significant amounts of NH_3, but most of this is absorbed by the growing plants above the soil surface (Denmead et al 1976).

Galbally et al (1980) summarise the emission of NH_3 to the atmosphere for Australia, as mostly being due to rural sources, with 70% due to volatilization of animal urine. Ayers and Gillett (1988a) attribute the lower amount of emissions in tropical northern Australia (10% of Australian-wide emissions) to the lower proportion of agricultural activity that occurs in these regions.

Organic Acids

Organic acids contribute up to 40% of the free acidity of rainfall from Katherine (Galloway et al 1982). Possible sources of organic acids to the atmosphere include volatilization of plant material, photochemical oxidation of hydrocarbons and aqueous phase oxidation of formaldehyde to formic acid (Herlihy 1987).

Phosphate

Information relating to the source of HPO_4 to the atmosphere is scarce. However the most likely source to rainfall would seem to be from fertilisers or bird excreta.

4.3 PREVIOUS RAINFALL STUDIES IN AUSTRALIA

Previous rainfall investigations in Australia have been designed to address several issues. These include: acidic precipitation both in populated areas such as Sydney (Ayers and Gillett 1982, Ayers et al 1987), the Hunter Region (Bridgeman et al 1988a, Bridgeman et al 1988b) and Newcastle (Avery 1984), and remote areas such as Northern Australia (Noller et al 1990, Gillett et al 1990); baseline level monitoring, as part of Global Precipitation Chemistry Network (GPC; Galloway et al 1982, Likens et al 1987) and Baseline Air Pollution Monitoring Network (BAPMoN; Ayers and Ivey 1988, Ayers and Manton 1991); and the accession of salts to the Australian landmass and the subsequent effects of salinity (Teakle 1937, Hutton and Leslie 1958, Hingston and Gailitis 1976, Blackburn and McLeod 1983, Farrington and Bartle 1988, Farrington et al 1993).

The present investigation is concerned with unpolluted background precipitation. Thus the following review of previous rainfall investigations in Australia will focus on those studies from remote areas, in particular areas that coincide with sample localities used in the present investigation. A review of acid precipitation investigations from urban areas of Australia is given by Bridgeman (1990). All sites discussed in this section are shown in Figure 4.4, and results of previous relevant investigations are listed in Table 4.1.

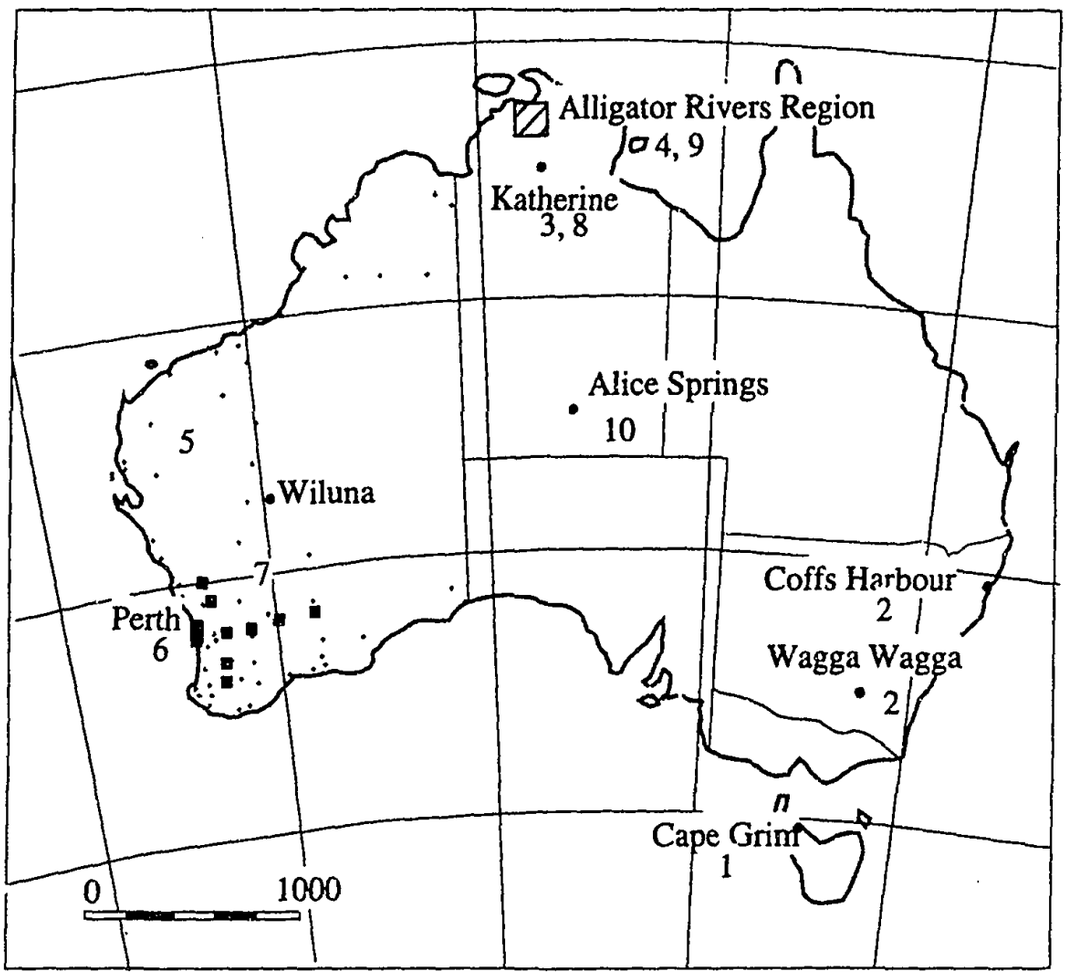

1 Ayers and Ivey 1988
2 Ayers and Manton 1991
3 Galloway et al 1982
Likens et al 1987
Galloway et al 1992
4 Noller et al 1986
Ayers and Gillett 1988b
Gillett et al 1990
Noller et al 1990
5 Hingston and Gailitis 1976
6 Farrington and Bartle 1988
7 Farrington et al 1993
8 Wetselaar and Hutton 1962
9 Noller et al 1985
10 Hutton 1983

FIGURE 4.4 Location of previous precipitation investigations discussed in the text. The small crosses in Western Australia mark sample localites from Hingston and Gailitis 1976. The shaded box in Western Australia marks the Gnangara Mound area from Farrington and Bartle 1988. Squares in Western Australia mark sample localities from Farrington et al 1993.

Baseline Monitoring

Investigations into background levels of constituents in rainfall include research in both maritime and continental areas. An important maritime location included in the BAPMoN project is at Cape Grim in Tasmania. Ayers and Ivey (1988) noted high seasalt loadings and extreme wind speeds were found to cause soil components to concentrate in the rainwater samples, affecting pH, K and Ca concentrations. Acidity values were also thought to be affected by seasalt alkalinity. Also as part of the BAPMoN project, Ayers and Manton (1991) compared a coastal site (Coffs Harbour) with a continental site (Wagga Wagga). Both sites were influenced predominantly by seawater, the extent of which was dependent on wind direction. A continental source was also recognised at both sites, and at Wagga Wagga, NH_4 was interpreted to have a biological source, attributable to the extent of agriculture in the vicinity of Wagga Wagga.

Acidity Investigations in Northern Australia

As part of the GPC Network, precipitation at Katherine in the Northern Territory has been extensively investigated. Precipitation at Katherine has been found to be acidic (eg. Galloway et al 1982) measured a mean pH of 4.78), with 64% of acidity attributed to organic acids (Likens et al 1987) sourced from the extensive burning that occurs at the beginning of the wet season. Thus as the wet season progresses, the amount of burning decreased and hence there were less organic acids emitted to the atmosphere, ultimately decreasing the free acidity of rainfall as the wet season continued (Galloway et al 1982). Airmass trajectories were used to determine that airmasses from the northeast were the most important trajectory in terms of deposition. The contribution of ions from anthropogenic sources was found to be small, with non-seasalt SO_4 concentrations at Katherine an order of magnitude lower than sites in eastern North America. No evidence was found to suggest that lightning contributed to the nitrate concentration in rainfall at Katherine (Likens et al 1987).

Acidity in precipitation from the Alligator Rivers Region in the Northern Territory for the wet season of 1982/1983 (Noller et al 1990) has also been attributed to the presence of organic acids. Strong correlations between H and NO_3 were found and excess concentrations of SO_4 could not be attributed to anthropogenic emissions, in particular from the Ranger Uranium Mine. Rainfall events were separated into monsoonal and non-monsoonal, based on the presence of the monsoonal trough over Northern Australia. It was found that monsoonal rain showed relative concentrations

of Ca, Mg, Na and K that approximate those of seawater. In further work at Alligator Rivers (Gillett et al 1990), non-monsoonal rainfall was found to be more acidic than monsoonal rainfall. Anthropogenic emissions from the Mt Isa smelter in Queensland, while not being completely ruled out as a source of non-seasalt SO4 to rainfall at Jabiru, were found to have only a very minor influence. The source of organic acids was speculated to be from bushfires or photochemical OH oxidation of reactive biochemical emissions such as isoprene. Continued investigations during the 1984/1985 wet season (Gillett et al 1990) revealed the organic acids, formic, acetic and propionic acids to be responsible for 74% of free acidity in the rainfall. It was also suggested that HCl may be a contributor to acidity.

Cloudwater and rainwater samples were taken from the Alligator Rivers Region and Katherine during the wet season of 1985/1986 (Noller et al 1986, Ayers and Gillett 1988b). Cloudwater was found to be highly acidic (pH less than 4) and the solute concentrations of cloudwater and rainwater were consistent if the expected variations in cloud liquid water between precipitating and non-precipitating clouds were taken into account. Systematic variations in the rainwater/cloudwater ratios of formic and acetic acid suggested that these solutes exist below the cloud in the gaseous phase. However, cloud acidity was high only 100m above the base of the cloud, suggesting that most acids are incorporated directly from boundary layer air during cloud nucleation.

Accession Investigations

The initial investigations of rainfall chemistry in Western Australia to address the issue of the source of salts in soils and groundwaters suggested a cyclic source rather than a geological source of salts (Willsmore and Wood 1929, Teakle 1937). Hingston and Gailitis (1976) used bulk-depositional collectors to investigate the accession of salts to 59 sites across Western Australia between 1973 and 1974. Concentrations of solutes in coastal rainfall were found to be an order of magnitude greater than at inland sites. Regional differences in volume weighted non-seasalt ionic compositions have been explained in terms of the proximity of the sampling site to other sources, for example the amount of dissolved salts in rainfall collected from Wiluna was about twenty times that of nearby locations, and was attributed to a large salt lake (Lake Way) located 10 km south of Wiluna (Hutton 1983). The greater accession of oceanic salts to sites in the southwest relative to those in the north of the state was thought to have been an important factor in the development of salinity in the southwest of the Western Australia. It is now recognised however,

that land management practices are also a big determining factor in the development of salinity (Peck et al 1983). Therefore, the more extensive agriculture in the southwest of the state is probably an important factor in the increased development of salinity in that region.

Farrington and Bartle (1988) looked at chloride concentrations in bulk deposition north of Perth between 1982 and 1986 in order to use the accession of chloride to the Gnangara groundwater mound to assess recharge rates for groundwater supplying the mound. Chloride composition was shown to decrease with increasing distance from the coast, and annual accession over the period of measurement was considerably lower than recorded during 1973 and 1974 by Hingston and Gailitis (1976). The difference was attributed to the lower incidences of winter and spring storms during the 1982 to 1986 sampling season. It was suggested that Cl accession increases when strong westerly onshore winds are able to transport oceanic spray further inland.

A regional bulk-depositional collection program in the southwest of Western Australia was established by Farrington et al (1993) between 1989 and 1992, to improve the available information on the regional balance of dissolved salts by looking at spatial and temporal variation in the accession of major ions in rainfall. This information could then be used to develop strategies to reduce salinity. The results confirmed that the atmospheric deposition of major ions from rain was principally controlled by distance from the coast. At inland sites important sources of material to rainfall were also soil, smoke, plant debris and industry. The lakes and drainage systems associated with the sampling localities are saline and therefore may have been a source of terrestrial salt. Excessive non-seasalt Ca concentrations at coastal sites were attributable to aeolian dust originating from calcareous dunes, and at inland sites, from gypsum in salt lakes. The annual variation in Cl accession was attributed to differences in weather patterns and to rainfall amount.

In an investigation of nutrient accession to Katherine during the wet season, Wetselaar and Hutton (1962) reported low concentrations of soluble material, despite high rainfall amount. It was concluded that the material found in rainwater at Katherine represented input from the terrestrial cycle rather than true accession. Noller et al (1985) showed that half of all nutrients were deposited in the Alligator Rivers region of the Northern Territory during the early transition period between the wet and the dry season (November to February in this particular wet season). The input of nutrients was found to be lower or similar to those of drier tropical locations,

and NH_4 and NO_3 were found to be of terrestrial origin. A recycled terrestrial origin was also attributed to components of bulk-depositional precipitation 100 km north of Alice Springs, collected between 1957 and 1962 (Hutton 1983). The high Ca/Cl ratios (twenty times that of seawater) and similar ratios of Ca, Na, Mg and K to Todd River water, led to the suggestion that rainfall at this site was heavily influenced by the Todd River. Thus rainfall at Alice Springs did not represent true accession, but represented a small return of a larger net loss of material suspended in the atmosphere as dust.

Summary

The above review of previous rainfall chemistry investigations in Australia highlights the lack of comprehensive information about the spatial and temporal properties of precipitation chemistry that affects the remote areas of the Australian continent. This investigation addresses these deficiencies by sampling from far-reaching arrays over two years. The arrays span a variety of climates, and the seasonality of sampling allows insight into the affects of different meteorological and climatic processes in producing precipitation. Several of the localities in the present investigation overlap with those of previous studies. Thus the results from this study will add to the Australian precipitation chemistry data base, as well providing the first data on precipitation chemistry from some areas of Australia.

CHAPTER 5 MAJOR ELEMENTS

The aims of investigating the major-element chemistry of precipitation from the present study are two-fold. In a general sense, the data from remote localities will provide information on baseline levels of constituents in unpolluted atmospheres, and will add to the sparse data base of precipitation chemistry from Australia. Of particular relevance to the present investigation however, is that an understanding of the major-element chemistry and the processes that affect it at different times and locations around Australia, will provide a basis upon which ^{36}Cl data can be interpreted.

Since the initiation of the sampling program in March of 1991, a total of 148 samples have been collected. Each sample was analysed for Cl, SO_4, NO_3, HPO_4, Br, Na, K, NH_4, Ca, Mg and pH, and the data split into two groups, those from the WE array (80 samples) and those from the SN array (68 samples). Following data quality checks outlined below, the data for 7 samples have been removed from the WE data set leaving 73 samples for detailed analysis, and 11 samples have been removed from the SN data set, leaving 57 samples for detailed analysis. The complete data set is listed in Appendix D.

5.1 DATA QUALITY

The data are subject to scrutiny with respect to their representativeness of precipitation in the collection area over the collection period. The following discussion applies the ion imbalance, regression and outlier analysis techniques described in Section 3.3 to each data set. Samples were only removed from the data set if they failed all the data quality checks. Thus, for example, while the dry samples from the northern section of the SN array had ion imbalances of greater than 100%, they satisfied the outlier analysis check, and were retained in the data set.

Ion Imbalance

Tables 5.1 and 5.2 display the ion imbalances for each sample collected from the WE and SN arrays respectively. Samples from the WE array with imbalances of greater than 100% are removed from the data set and are listed in Table 5.3. In each case, the imbalance can be attributed to contamination during sampling, eg. infestation of ants or the presence of algal matter, and are reflected by excessive amounts of cations, in particular NH_4.

TABLE 5.1 Ion imbalances for the WE array. Bold values highlight imbalances greater than 100%.

Site	Collection Period							
	A91	W91	Sp91	S91	A92	W92	Sp92	S92
16 Cliff Head	0	5	-1	41	14	24	11	-2
17 West Morawa	-17	-15	-20	6	32	11	79	-1
18 Badja	-3	-0.6	-37	26	59	12	31	15
19 Iowna	-48	13	-32	**122**	26	15	45	-14
20 Barrambie	-28	-42	-20	-23	**124**	90	45	-10
21 Yeelirrie	-17	-49	-9	-42	34	6	43	64
22 Lake Violet	-22	-64	-26	-17	37	25	25	29
23 Carnegie	-16	-74	-5	-6	30	35	12	81
24 Gunbarrel	-75	-88	-42	**146**	20	10	**124**	83
25 Everard Junction	-50	-91	-65	**127**	31	-10	**139**	**123**

TABLE 5.2 Ion imbalances for the SN array. Bold values highlight imbalances greater than 100%.

Site	Collection Period							
	W92	Sp92	S92	A93	W93	Sp93	S93	A94
26 Port Lincoln	3	58	7	-58	11	16	28	14
27a Gawler Ranges	13	61	30	40	25	31	5	88
27b Gawler Ranges					24	29	10	84
28 Wintinna	-9	40	20	58	-16	23	38	67
29 Alice Springs	14	32	**131**	-12	17	11	24	26
30 Tennant Creek	70	22	**197**	**104**	19	33	86	93
31 Dunmarra	**112**	35	75	**105**	91	37	**100**	57
32 Katherine	**132**	**104**	64	61	**125**	**117**	40	92
33 Kapalga	91	70	82	24	**126**	**148**	90	**169**

An apparent high ionic imbalance may also occur for samples where ionic strengths are at or near to analytical detection limits, where poorer precision can exaggerate differences. This is illustrated for the WE array in Table 5.4. Low total ionic strength for each season gives higher occurrences of imbalances greater than 50%. In comparison, the site at Cliff Head (site 16) exhibits a high ionic strength and nil

imbalances greater than 50%. This has been noted elsewhere (Ayers and Manton 1991).

TABLE 5.3 Samples removed from the WE data set, ion imbalances and reasons for removal.

Sample	Ion Imbalance %	Reasons for Removal
19-S91 Iowna	122	growth of algae
24-S91 Gunbarrel	146	insect infestation
25-S91 Everard Junction	127	insects and algae
20-A92 Barrambie	124	insects
24-Sp92 Gunbarrel	124	ant infestation
25-Sp92 Everard Junction	139	ant infestation
25-S92 Everard Junction	123	ant infestation

TABLE 5.4 Relationship between total ionic concentration and ionic imbalance for samples from the WE array.

Site	Mean total ions µeq/L	Imbalance				
		<10%	10 to <20%	20 to <50%	50 to <100%	>100%
16 Cliff Head	975	4	2	2	0	0
17 Morawa	220	2	3	2	1	0
18 Badja	176	2	1	3	2	0
19 Iowna	170	0	3	4	1	1
20 Barrambie	231	0	1	5	1	1
21 Yeelirrie	87	2	1	4	1	0
22 Lake Violet	175	0	1	6	1	0
23 Carnegie	93	2	2	2	2	0
24 Gunbarrel	69	1	1	2	2	2
25 Everard Junction	85	0	1	2	2	3

Table 5.5 displays the samples that have been removed from the SN data set. As in the WE data set, each of these samples can be directly attributed to contamination during the sampling program. Sample 26-A93 displays a very high concentration of SO_4 which acts to produce a high negative imbalance. While no obvious source of contamination was observed in the sample, the outlier analysis that follows justifies

the removal of this sample from the data set. It should be noted that dry samples with imbalances of greater than 100% have not been removed, and the reasons for this are shown in the following section.

Several features noted in the ion balances for the SN data set are shown in Table 5.6. Firstly there is a predominance of positive imbalances (i.e. indicating higher cation concentrations than anion concentrations). Secondly, the more northerly sampling localities in the array (sites 30 to 33) show a higher occurrence of imbalances of greater than 100%. These two features may reflect the absence of the measurement of all anions in the analytical program. The most likely missing anions are organic acids. Organic acids have been measured in rainfall from tropical regions (Noller et al 1990) where they have been found to be a major anion. However, organic acids were not measured in the present investigation as steps taken to preserve the organic acids in the sample during field collection were unsuccessful (Section 3.1) and the facility to measure organic acids as part of the analytical program did not exist at the Research School of Earth Sciences, Australian National University. The absence of rainfall during the non-monsoonal period in the northern half of the array is another feature that can be correlated with the higher occurrence of ion imbalances in the more northern section of the array. Finally, as seen in the WE array, low ionic strengths in some samples are correlated with increased ionic imbalances (Table 5.6).

TABLE 5.5 Samples removed from the SN data set, ion imbalances and reasons for removal. Cases marked with an * are removed because a reliable record of the volume of rain for the sampling period was not recorded due to the inappropriate design of the collector for that particular season.

Sample	Ion Imbalance %	Reasons for Removal
26-A93 Port Lincoln	-58	elevated SO_4 (?)
29-S92 Alice Springs	131	ants nest
30-S92 Tennant Creek	197	field site disrupted
30-A93 Tennant Creek	104	algae
31-S92 Dunmarra	75	field site disrupted
31-A93 Dunmarra	105	algae
32-S92 Katherine	64	unknown volume*
32-Sp93 Katherine	117	field site disrupted
33-S92 Kapalga	82	unknown volume*
33-Sp93 Kapalga	148	ash/algae
33-A94 Kapalga	169	ash

TABLE 5.6 Relationship between total ionic concentration and ion imbalances for samples from the SN array.

Site	mean total ions µeq/L	Imbalance				
		<10%	10 to <20%	20 to <50%	50 to <100%	>100%
26 Port Lincoln	1137	2	3	1	2	0
27a Gawler Ranges	383	1	1	4	2	0
27b Gawler Ranges	383	1	0	2	1	0
28 Wintinna	242	1	2	3	2	0
29 Alice Springs	202	0	4	3	0	1
30 Tennant Creek	549	0	1	2	3	2
31 Dunmarra	131	0	0	2	3	3
32 Katherine	578	0	0	1	3	4
33 Kapalga	147	0	0	1	4	3

Regression

Figure 5.1 shows the plots of total cations versus total anions for the WE and SN arrays. All samples are shown on the plots, including those removed from the data which failed to meet the ion balance criteria above. Also shown on the plots is the regression line derived using the reduced major axis technique. The results of the reduced major axis regression are also shown in Table 5.7. The data set used in these regressions does not include data with ionic imbalances of greater than 100%. In an ideal situation, where all ions are accounted for and analytical error does not exist, a regression slope of unity and intercept of zero will be attained. The results listed in Table 5.7 show a very high correlation coefficient between anions and cations for the WE data set, and a calculated slope and intercept close to the ideal situation at the 68% confidence interval (within twice the standard error). The coefficient of correlation for the SN data set is lower than for the WE data set, reflecting the high imbalances introduced by the dry samples. However, the slope and intercept of the regression fall within the bounds of an ideal situation at the 68% confidence interval (within two times the standard error), as is shown in Figure 5.1 where the data fall in the area bounded by the upper and lower 2σ limits rather than on the reduced major axis regression line.

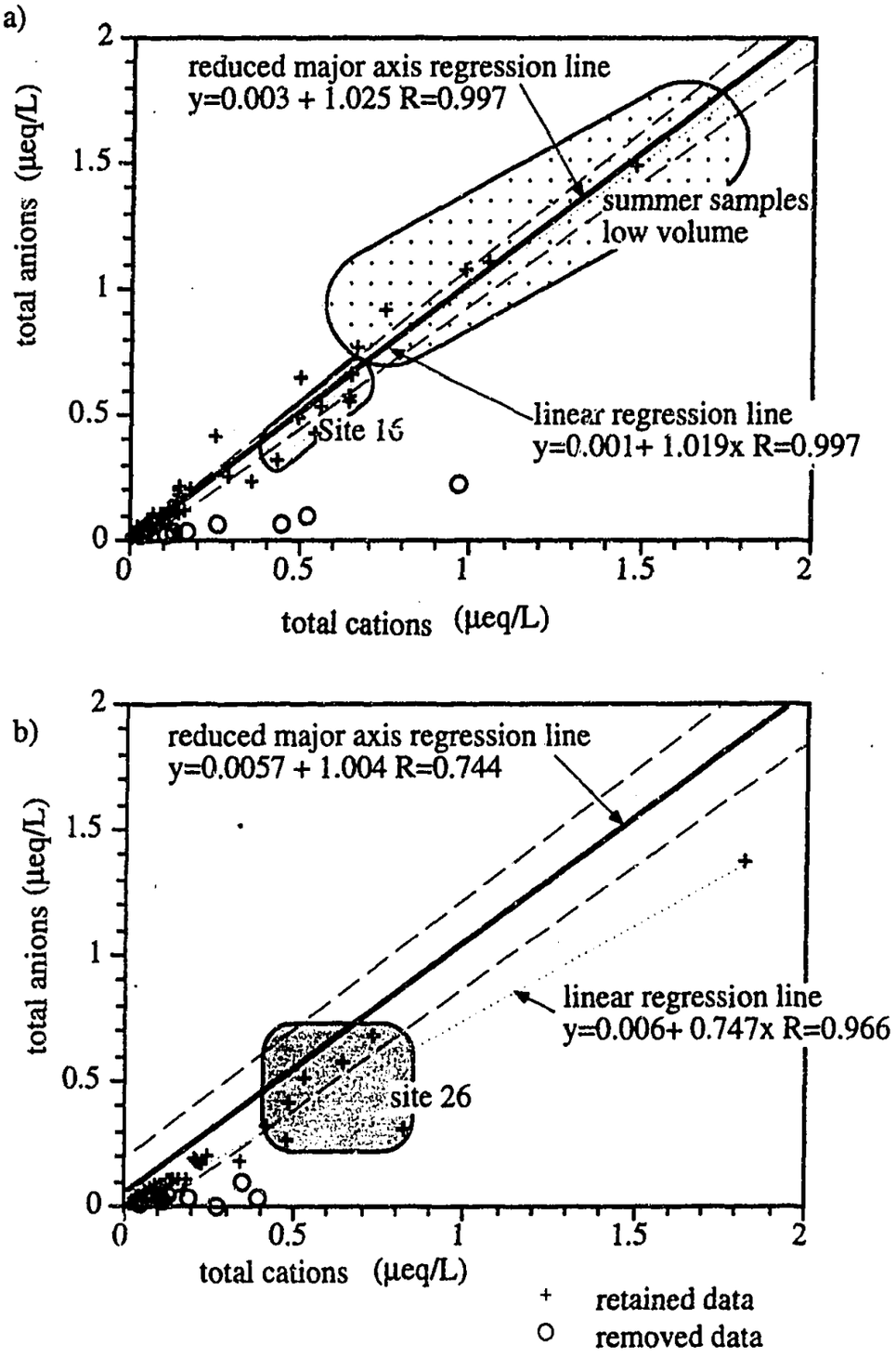

FIGURE 5.1 Total anions versus total cations (μeq/L) for a) WE Array and b) the SN Array. The reduced major axis regression lines are shown as solid thick lines, and the 2σ errors as thin short-dashed lines. For comparison, the linear regression line is also shown, as the thin dotted line. For the SN data set, the reduced major axis line passes through the data points within the bounds of the 2σ error for the line, and there is poor agreement between the reduced major axis and linear regression lines. This lack of agreement most likely reflects the low correlation coefficient for the reduced major axis regression (R=0.74) which occurs because of the high ionic imbalances introduced by the dry samples from the NS array.

TABLE 5.7 Statistics for reduced major axis regression on WE and SN data sets.

Statistic	WE Array	SN Array
number of data points	73	58
slope (std error)	1.025 (0.026)	1.004 (0.033)
intercept (std error)	0.003 (0.008)	0.057 (0.071)
correlation coefficient	0.99	0.74

Outlier Analysis

The geometric means used in the outlier analysis do not use the data removed during the ionic imbalance calculation. Samples with individual ionic concentrations that differ from the geometric mean by greater than 2σ for the WE array are listed in Table 5.8. As expected, these include all the samples with imbalances of greater than 100%. The remaining samples 21-Sp91 and 23-Sp91 represent samples of very low rainfall amount and hence have elevated concentrations of ionic species. However, because of the good balance between anions and cations in these samples, as shown in Table 5.1, these samples are not removed from the data set. Samples with individual ionic concentrations that differ from the geometric mean by greater than 2σ for the SN array coincide with those listed in Table 5.5, that have already been removed from the data set. Dry samples fell within 2σ of the geometric mean, justifying their inclusion in the SN data set.

TABLE 5.8 Samples that lie outside 2σ of the geometric mean for each site.

sample	ion imbalance %	rainfall mm
19-A92 Iowna	122	30
24-A92 Gunbarrel	146	38
25-A92 Everard Junction	127	98
20-W92 Barrambie	124	268
24-Sp92 Gunbarrel	124	23
25-Sp92 Everard Junction	139	35
25-S92 Everard Junction	123	34
18-S92 Badja	15	3
21-Sp91 Yeelirrie	-9	0
23-Sp9 Carnegie	-5	0

5.2 GENERAL RELATIONSHIPS

A summary of the minimum, maximum and means for each site on the WE and SN arrays, expressed in units of total deposition ($\mu eq/m^2/day$) is given in Appendix E. A typical frequency distribution of ionic species for each array is shown in Figure 5.2 for Cl which reveals a skewed distribution towards lower concentrations. Figure 5.3 confirms that the distribution displayed by the ions is approximately log-normal, a feature that has previously been noted by other workers (eg. Saylor et al 1992). The relative magnitude of ionic species over the entire WE array is Cl > Na > SO_4 > Ca > NO_3 > Mg > H > NH_4 > HPO_4 > Br. The general relative magnitude of ionic species for the SN data set is Cl, Na > SO_4, Ca, Mg > K, HPO_4, NO_3, NH_4 > Br. NH_4 displays locally high concentrations eg. at sites 30 (Tennant Creek) and 32 (Katherine). Ionic pair correlations and rainfall amount for each array are listed in Table 5.9 and 5.10. High affinities (greater than 0.5) are displayed between most species for the WE data set except H, HPO_4 and NH_4. The low affinities of these latter ions may be due to the influence of biodegradation on the concentration of these species. Good correlations are displayed between Cl, SO_4, Na, Ca and Mg in the SN data set. K displays good correlations with Ca, Mg, and HPO_4, and NO_3 correlates well with Ca, SO_4 and H (inversely). Both H and rainfall amount show negative correlations with all species.

TABLE 5.9 Table of ionic pair correlation coefficients for the WE array. Bold values highlight correlations of greater than 0.4.

	rain	H	Cl	SO_4	NO_3	HPO_4	Br	Na	K	NH_4	Ca	Mg
rain	1											
H	-.17	1										
Cl	-.02	-.38	1									
SO_4	-.30	-.16	**.79**	1								
NO_3	-.37	.07	.28	**.72**	1							
HPO_4	-.18	-.27	.35	**.42**	.31	1						
Br	-.08	-.11	.57	**.56**	.31	.29	1					
Na	-.11	-.37	**.98**	**.84**	.38	.39	**.59**	1				
K	-.27	-.40	**.59**	**.75**	**.48**	.40	.30	**.66**	1			
NH_4	-.05	-.27	-.01	.00	.02	.03	-.16	-.04	.31	1		
Ca	-.3	-.39	**.77**	**.86**	**.58**	**.42**	**.52**	**.82**	**.77**	.18	1	
Mg	-.17	-.40	**.95**	**.85**	.40	.37	**.54**	**.97**	**.72**	.01	**.88**	1

TABLE 5.10 Table of ionic pair correlation coefficients for the SN data set. Bold values highlight correlations of greater than 0.4.

	rain	H	Cl	SO_4	NO_3	HPO_4	Br	Na	K	NH_4	Ca	Mg
rain	1											
H	.14	1										
Cl	-.34	-.25										
SO_4	**-.59**	-.24	**.75**	1								
NO_3	**-.68**	-.13	.31	**.59**	1							
HPO_4	-.20	-.38	.25	.28	.22	1						
Br	.01	.19	**.57**	.44	.17	.25	1					
Na	-.35	-.27	**.97**	**.82**	.38	.22	**.56**	1				
K	**-.48**	-.31	**.45**	.50	.37	**.67**	.33	**.44**	1			
NH_4	-.03	-.33	-.04	.11	-.03	**.42**	-.24	-.08	.37	1	.	
Ca	**-.53**	**-.47**	**.87**	**.75**	**.51**	.39	.33	**.84**	**.57**	.09	1	
Mg	-.37	-.37	**.93**	**.78**	.37	.31	.53	**.95**	**.60**	.01	**.88**	1

The correlations give a general idea of the sources of ionic constituents to precipitation. For example, correlations between Cl, Na, Mg, Ca, K and SO4 suggest a seawater origin, while a continental source of material would be indicated by similar correlations, but with elevated concentrations of K and Ca. The inverse correlation of rainfall volume with all species is a commonly noted feature of rainfall chemistry (Lindberg 1982, Khwaja and Husain 1990, Saylor et al 1992). One possible explanation involves a 'washout' effect of the rain cloud during initial stages of the rain period. This initially concentrated rainfall is then diluted if deposition continues. Saylor et al (1992) invoked in-cloud and below-cloud removal of aerosols during brief showers that occur after periods of dryness as a mechanism for concentrating ions in low rainfall amounts. As discussed in Chapter 4 other workers have recognised the significance of precipitation type, i.e. frontal or convective. For example, Likens et al (1984) suggest that evaporation below the cloud at the leading edge of a frontal storm may lead to increased concentrations of ions during the initial stages of a period of rainfall.

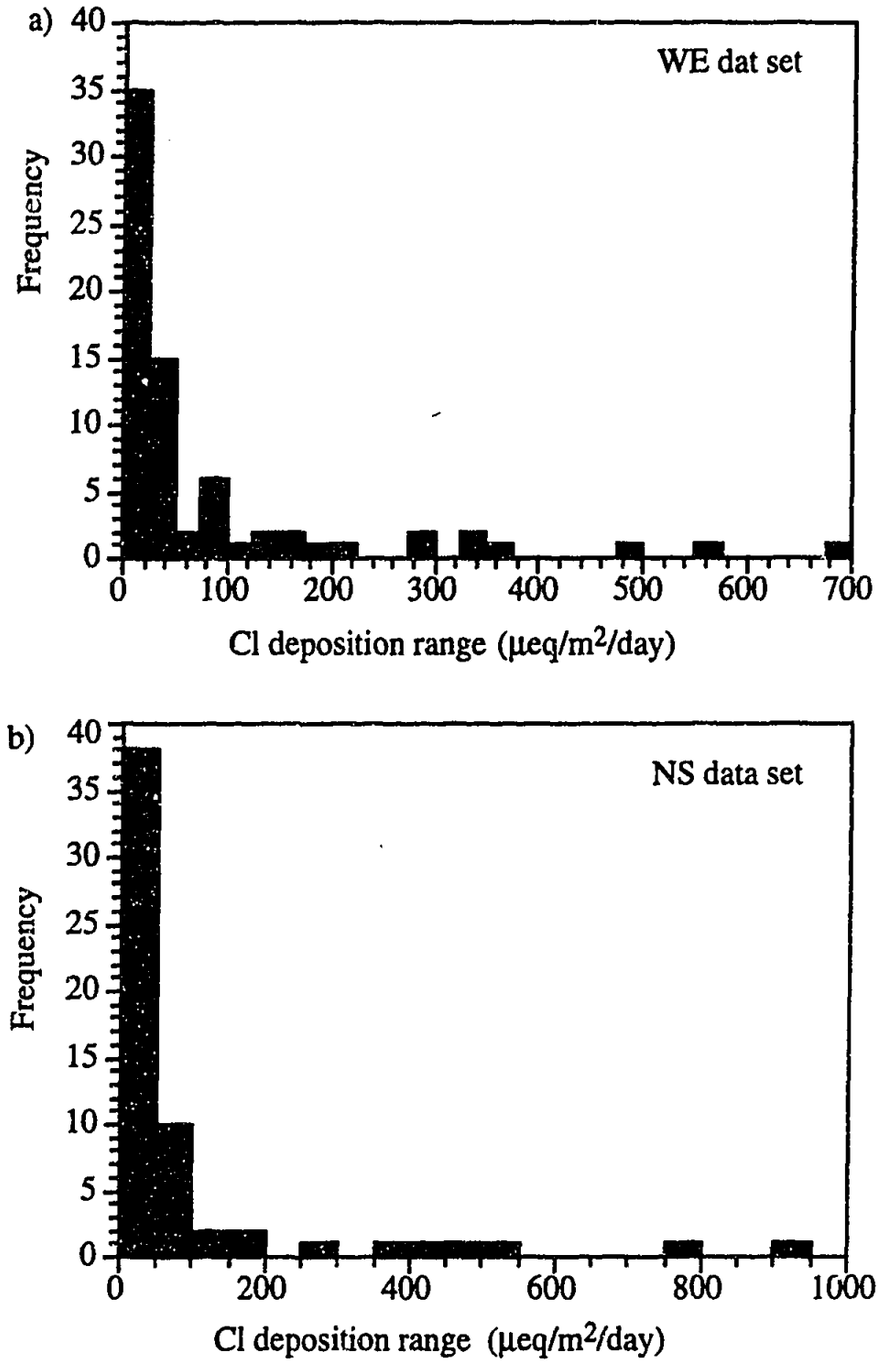

FIGURE 5.2 The frequency distribution of Cl deposition for a) all samples in the WE data set (n=73) and b) for all samples in the SN data set (n=57), remaining after data quality tests. The distribution is skewed towards lower concentrations. A similar pattern of distribution is displayed by the other major elements.

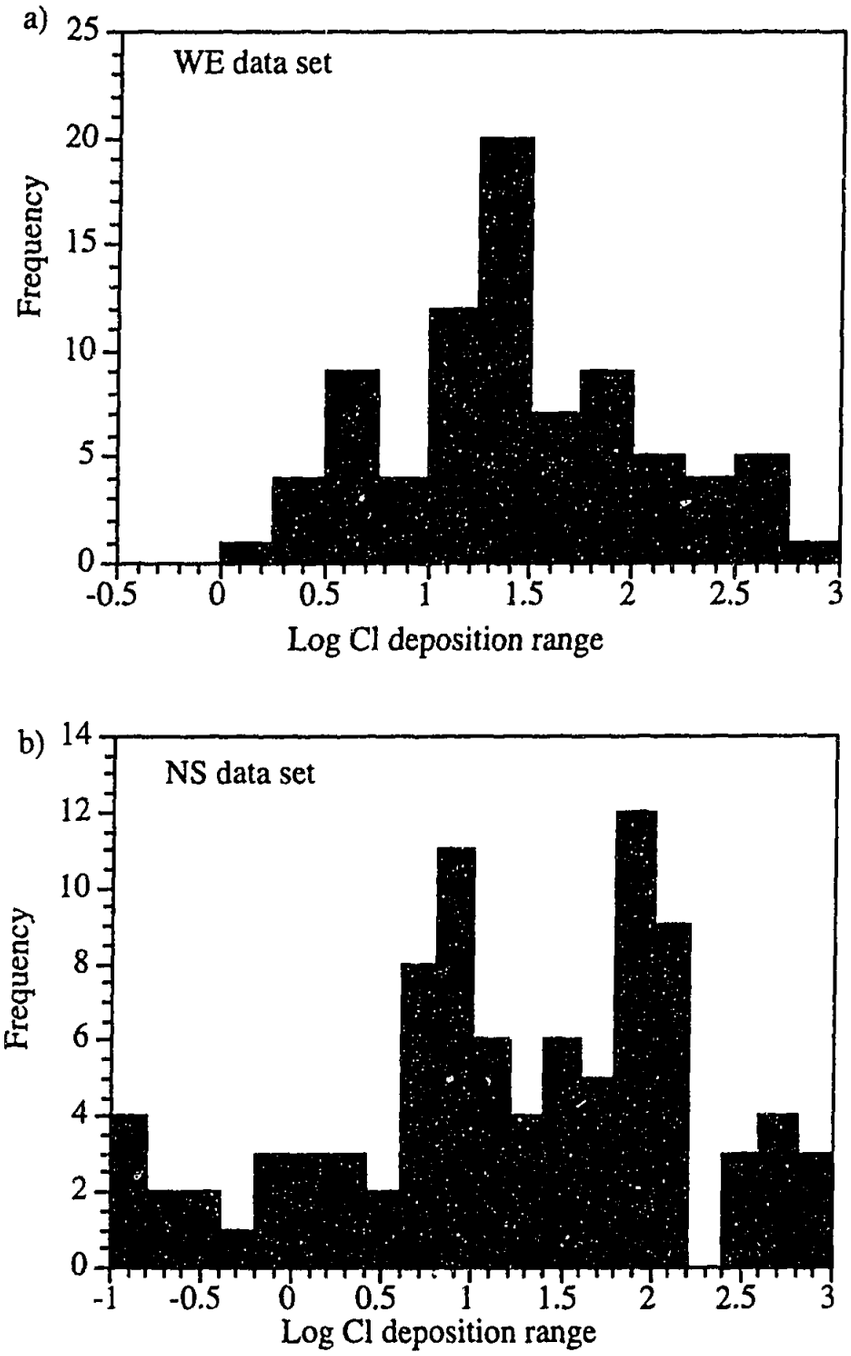

FIGURE 5.3 The logarithmic transformed frequency distribution of Cl deposition for a) the WE Array data set (n=73) b) the SN data set (n=57).

Spatial and Seasonal Variations

WE Array

Ionic fluxes generally decrease with increasing distance from the coast (Figure 5.4).

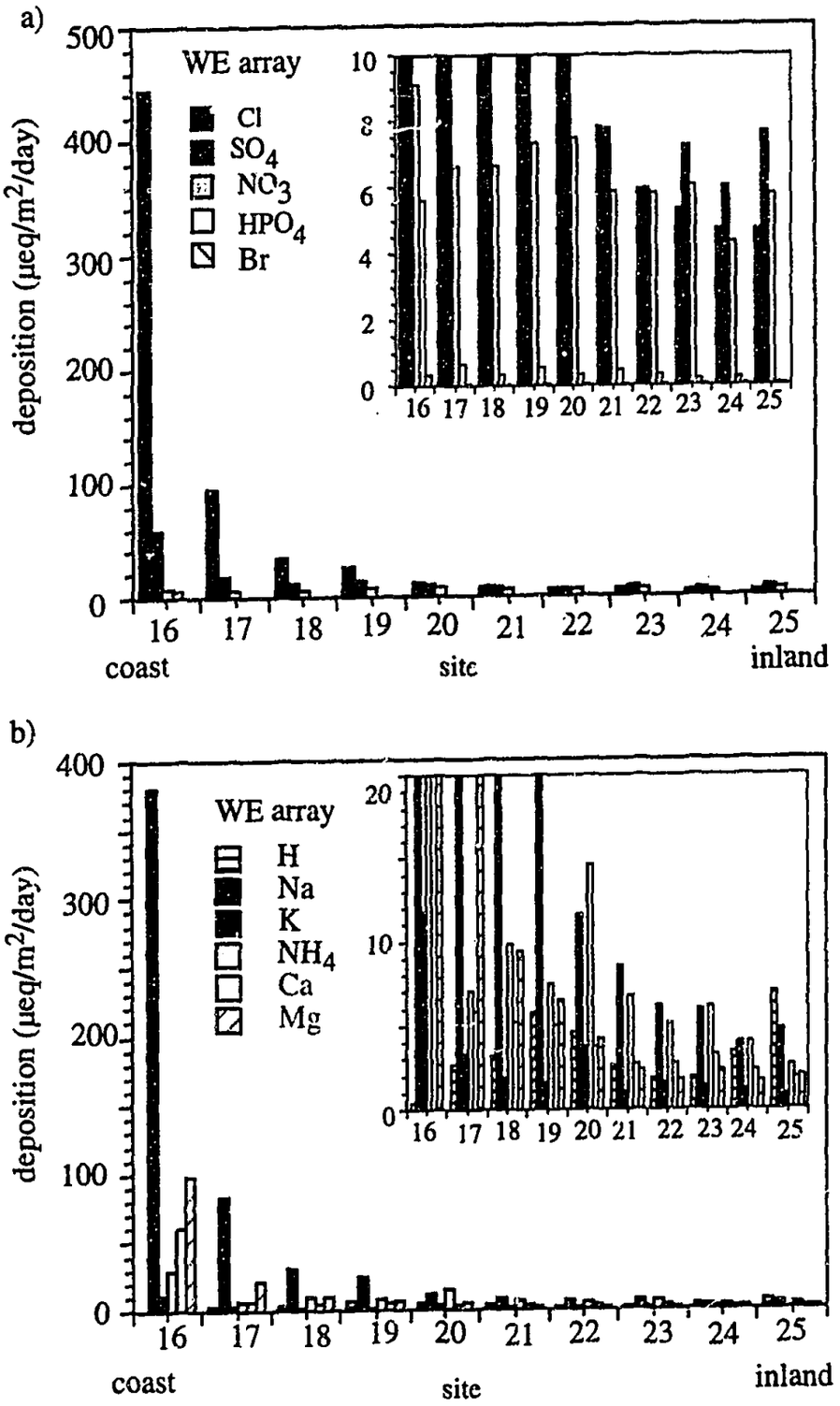

FIGURE 5.4 Mean deposition of a) anions and b) cations for the WE Array. Insets show spatial variations of ionic species with low deposition rates. Coastal localities have higher deposition rates than inland localites. See Figure 3.1 for site number localities.

This trend most likely reflects the decreasing influence of seawater on rainfall composition at continental sites. The general seasonal distribution of ionic fluxes over time is summarised in Figure 5.5. Maximum values occur in winter of each year, and minimum values in summer and autumn, reflecting the influence of rainfall volume on deposition. When individual ions are investigated (Figure 5.6) it can be seen that the above variation pattern is predominantly followed by Na, Mg, and Cl, ions characteristic of seawater. This may suggest there is a change in the influence of seawater on rainfall composition with time. The influence of seawater as a source of material to the chemistry of rainfall across the WE array is discussed in more detail later in this chapter.

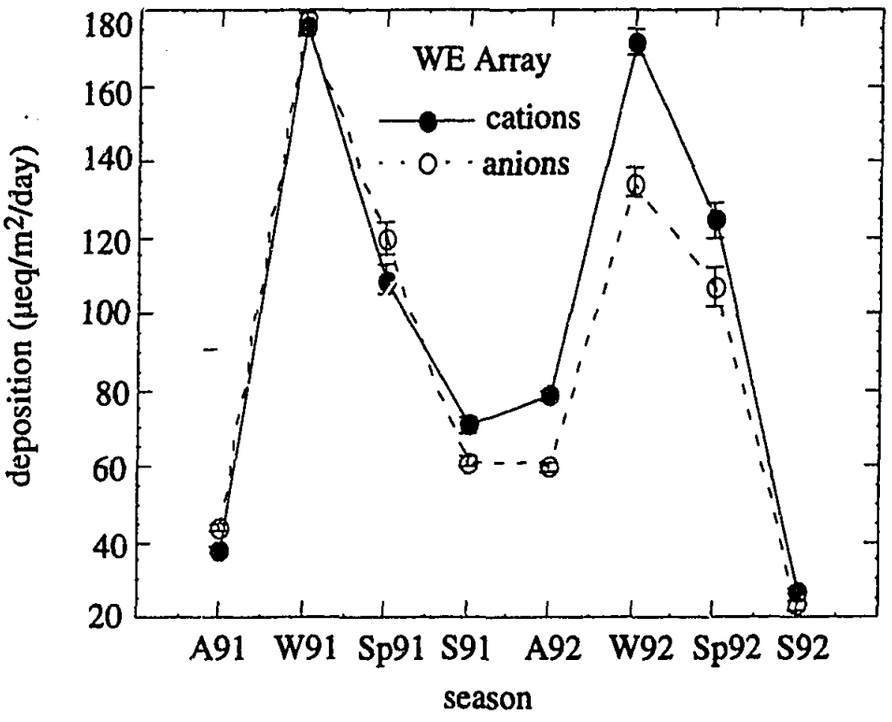

FIGURE 5.5 Seasonal variations in the deposition of total cations and anions for the WE array. A91=autumn 91, W91=winter 91, Sp91=spring 91, S91=summer 91 etc.

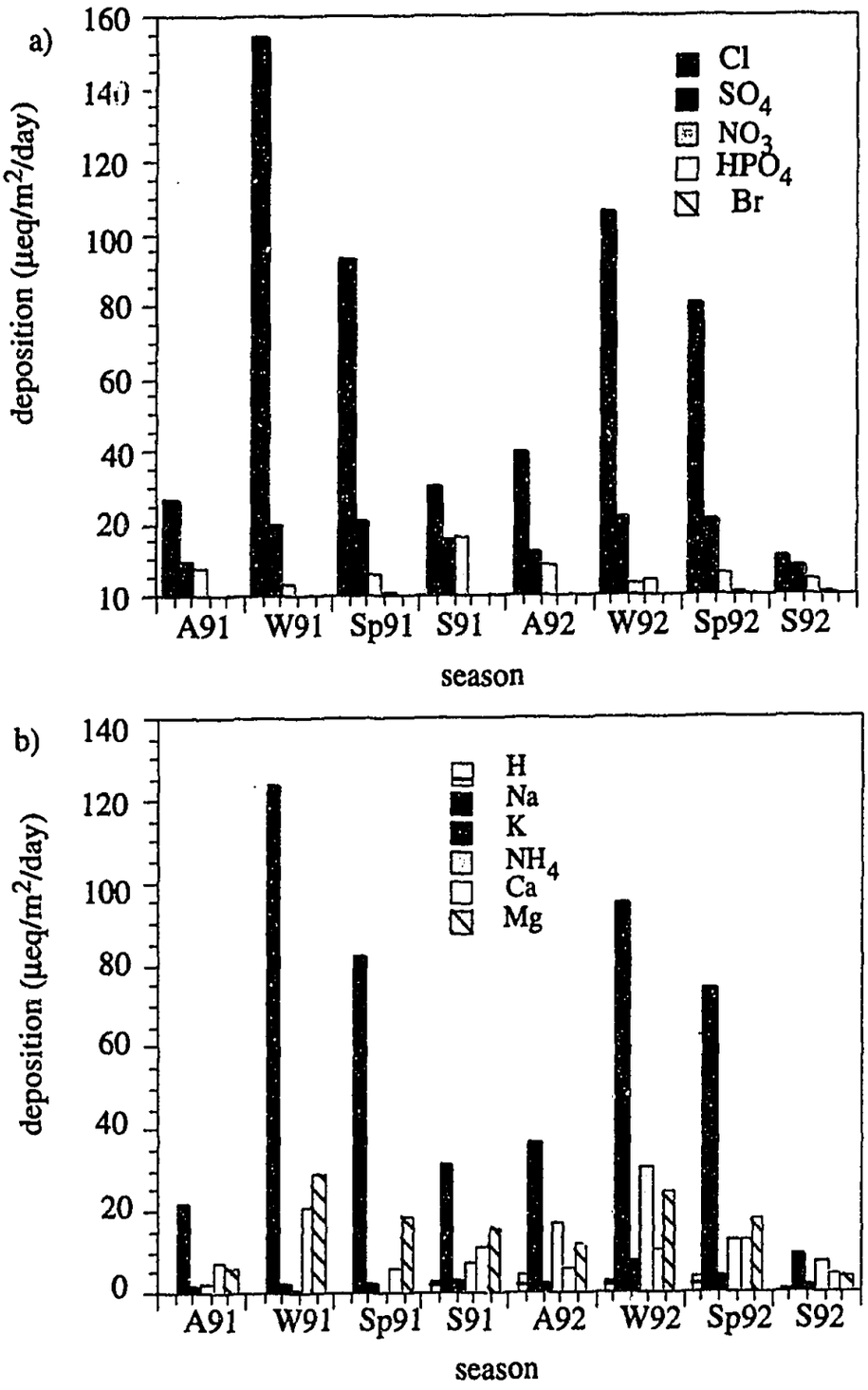

FIGURE 5.6 Mean seasonal deposition of a) anions and b) cations for the WE Array. A91= Autumn 91, W91=Winter 91, Sp91=Spring 91, S91=Summer 91 etc.

SN Array

Figure 5.7 show spatial variation of ionic deposition for the SN array.

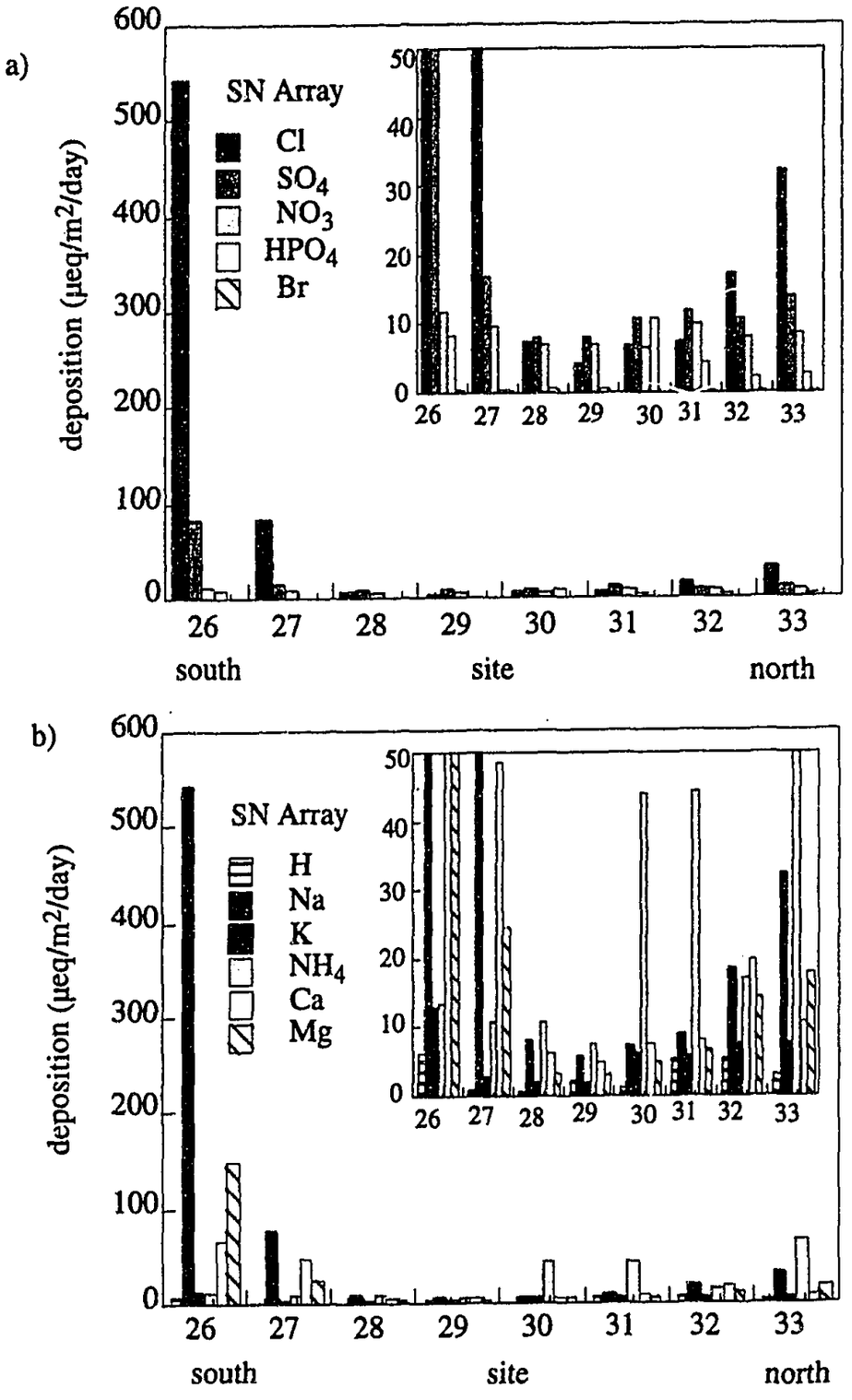

FIGURE 5.7 Mean deposition of a) anions and b) cations for the SN Array. Insets show spatial variations of ionic species with low deposition rates. See Figure 3.1 for site number locations.

The most obvious pattern displayed by both cations and anions is for very high deposition rates at the southern coastal site, (26 Port Lincoln), decreasing inland, and increasing at the most northern site 33 (Kapalga). This pattern again most likely reflects the influence of seawater at the coastal margins of the continent. When the inland sites are examined in more detail (Figure 5.7) a change in the significance of major chemical species is noted at sites 28 (Wintinna), 29 (Alice Springs), 31 (Dunmarra) and 32 (Katherine). At these sites anions, SO_4 and NO_3 become as, or more, significant as Cl, and cations NH_4, Ca and Mg become comparable to Na. This again reflects the limited influence of seawater to deposition at these inland sites, where if it were significant, Na and Cl would be the most important species as at site 26 (Port Lincoln). The high flux of NH_4 at sites 30, 31 and 33 most likely reflects the high level of biological activity as expected in tropical regions.

The mean total ion deposition for each season is shown in Figure 5.8 for the southern and northern section of the SN array. Deposition in the south of the array is greater than in the north. Maximum deposition occurs in the south during spring 92, and the relatively high deposition that occurs during winter of each year, represent the importance of winter rainfall in the south of the array. Maximum deposition rates occur during the summer seasons in the north of the array, while minimum deposition occurs during winter of each year, reflecting the control of the monsoonal rainfall on deposition. When individual ions are investigated (Figure 5.9), it can be seen that the above seasonal variation patterns are predominantly followed by Na and Cl in the south of the array. In the north of the array the pattern is dominated by Cl, Na, SO_4, NO_3 and NH_4.

5.3 MULTIVARIATE RELATIONSHIPS

Multivariate analysis is performed on total and subsets of WE and SN data sets to isolate the sources of ionic constituents in precipitation, by grouping ionic species with similar variances. The background, theory and previous examples of the application of factor analysis (FA) and principal component analysis (PCA) are given in Section 3.3.

The application of FA to the data from both arrays reveals the influence of three major sources/processes that control the ionic composition of precipitation collected in the present investigation. These are termed a mixed seawater/continental source, acid-base balance factor and biodegradation.

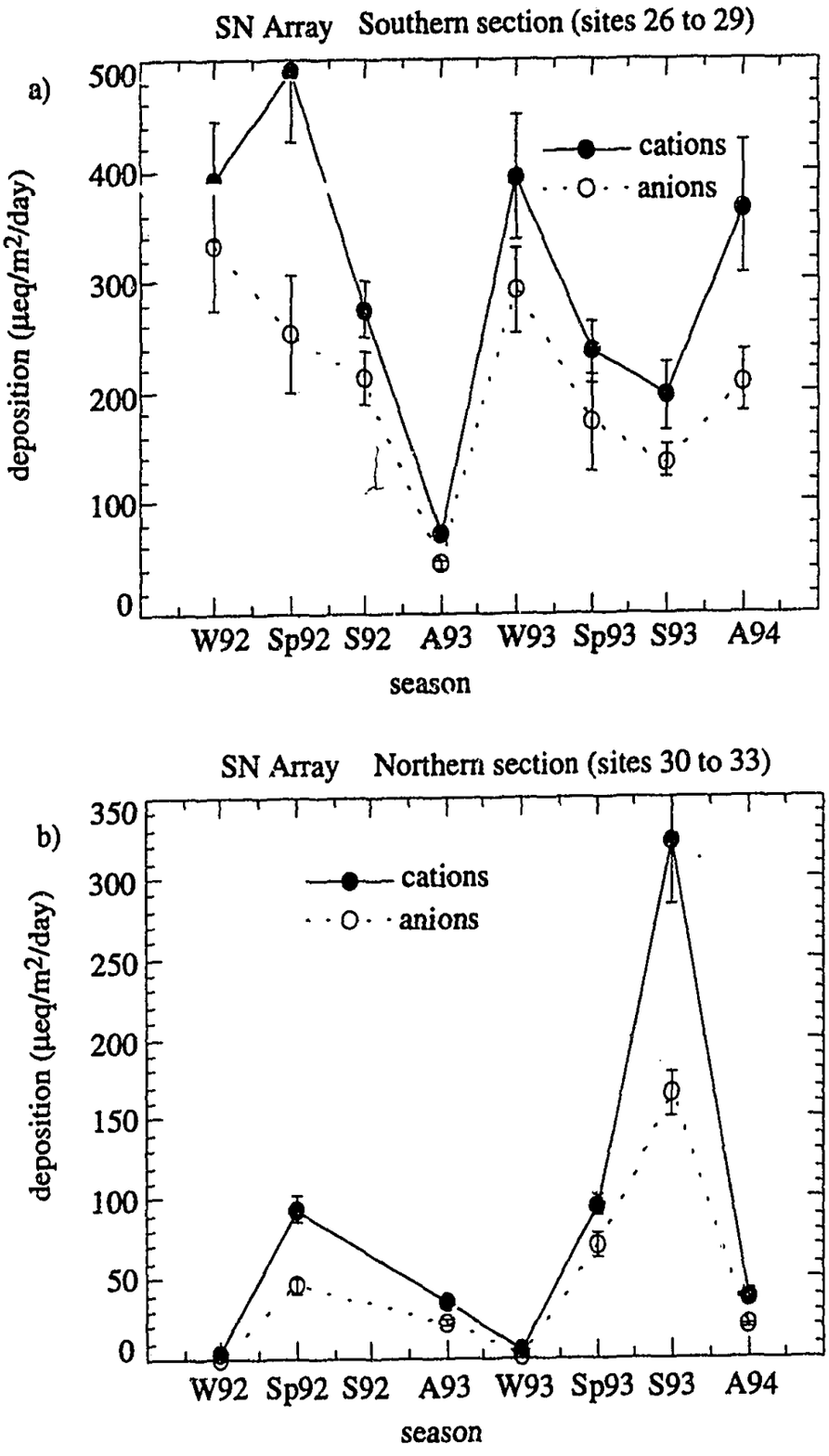

FIGURE 5.8 Seasonal variations in the deposition of total cations and anions for a) the southern section of the SN array and b) the northern section of the SN array. W93=winter 93, Sp93=spring 93, S93=summer 93, A93=autumn 93 etc.

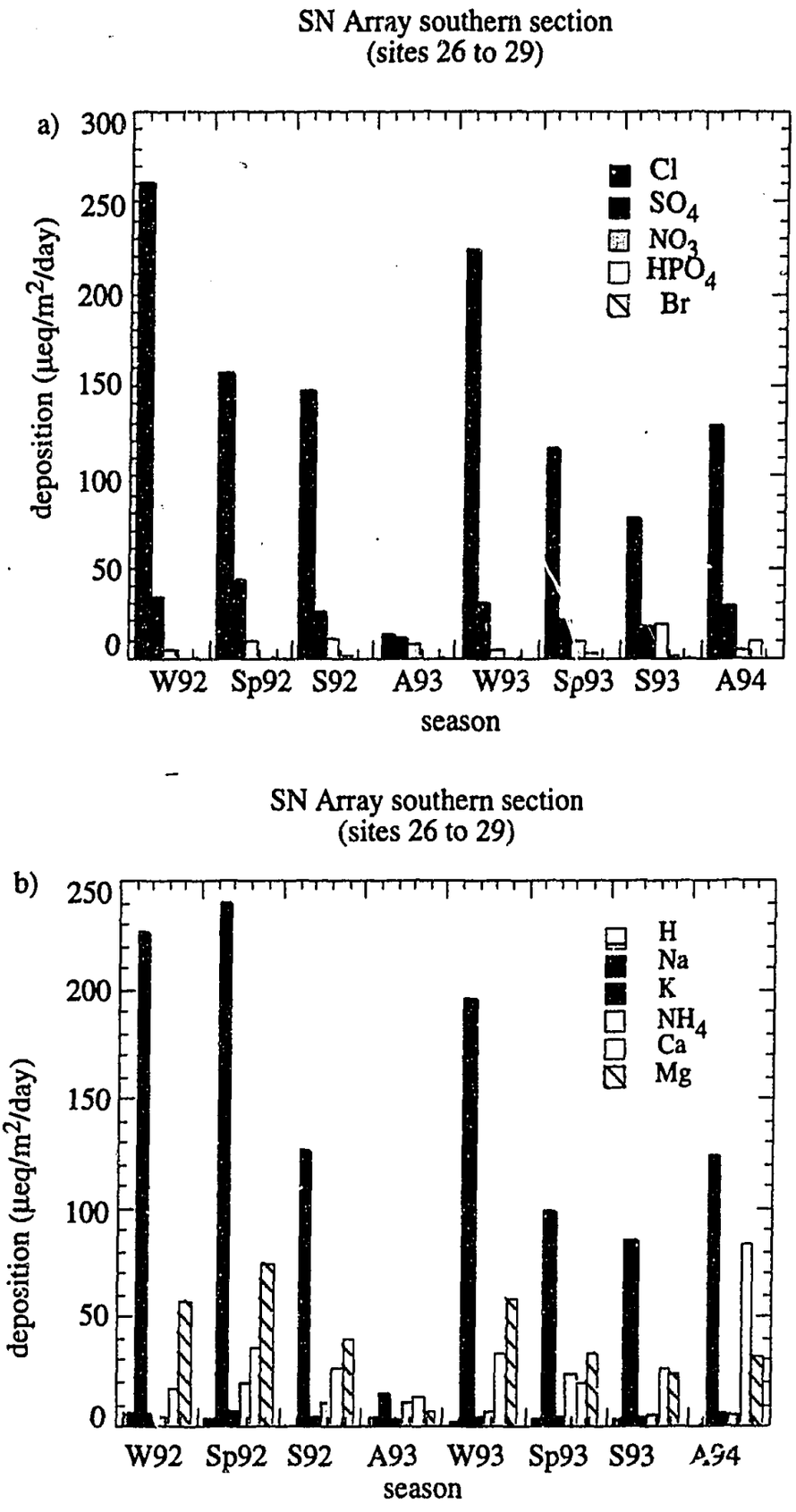

FIGURE 5.9 Mean seasonal deposition of a) anions and b) cations for the southern section of the SN array and c) anions and d) cations for the northern section of the SN array. A93= Autumn 93, W93=Winter 93, Sp93=Spring 93, S93=Summer 93 etc.

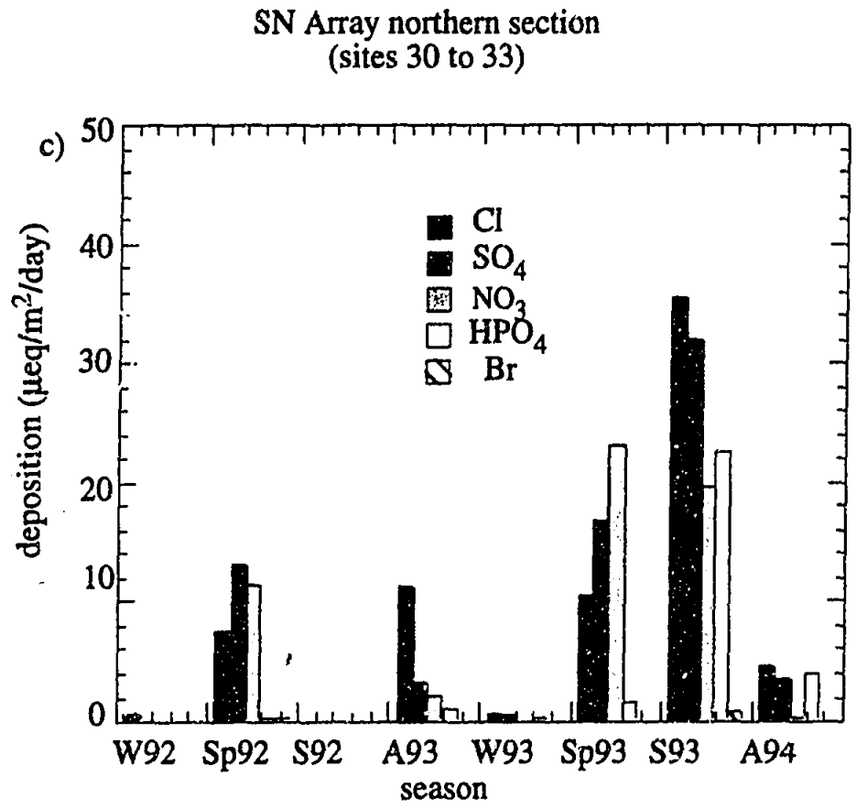

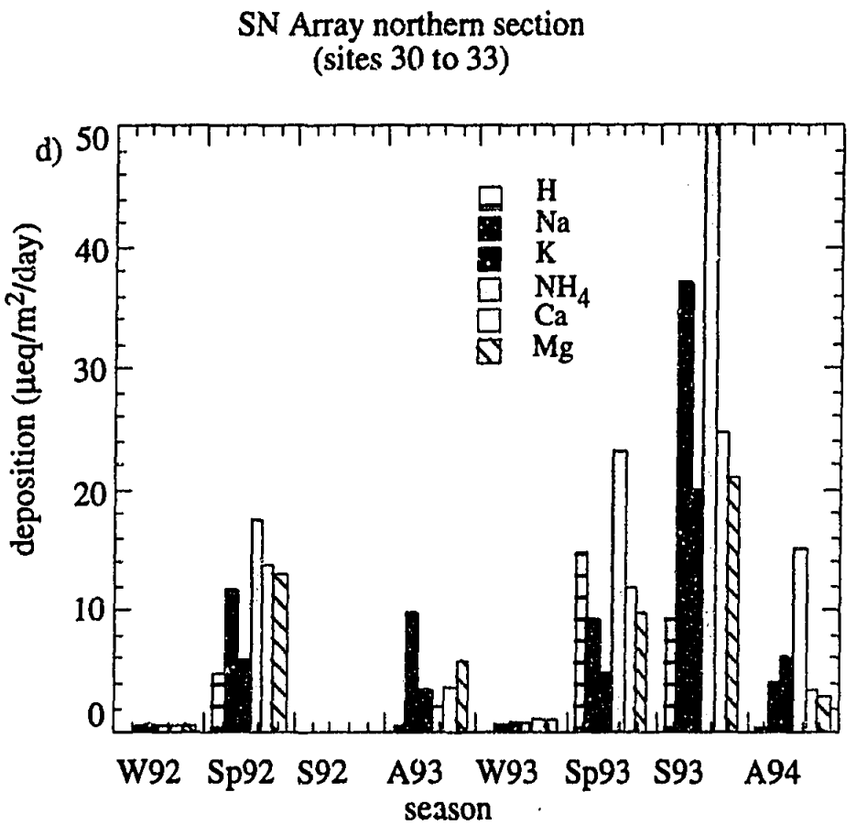

FIGURE continued

The seawater/continental source defines common variation between Cl, Na, Mg, SO_4, Br, Ca and K. FA is generally unable to distinguish between the two end-members of this source, although dividing the data into subsets (eg. coastal and non-coastal) shows higher loadings of seawater constituents (Cl, Na and Mg) with respect to continentally sourced ions (eg. Ca and K) in coastal subsets. The natural acid-base balance factor groups all or some of NO_3, SO_4 and H. Biodegradation groups NH_4, H, K and HPO_4. HPO_4 may also indicate agricultural input in the form of fertiliser, and may be particularly significant in the southern section of the SN array where agricultural activities are concentrated. Note that the assignment of sources based upon species groupings is a subjective process.

The significance of the influence of each of the three factors differs between data sets and subsets, and in some cases a factor may be described in terms of a combination of sources. For example, a mixed seawater/continental/biodegradation source may be invoked to explain the grouping of Cl, Na, Mg, SO_4, Ca, K, NH_4 and H.

Principal component analysis is applied to subsets made up of data for individual sites and isolates the same three sources/processes as FA performed on the larger data sets.

Within the framework provided by the three factors described above the following discussion describes details of the application of FA and PCA to the WE and SN data sets (and subsets of these). Because of the approximately log-normal distribution of the data described above, all multivariate analyses are performed on log-transformed data. Factor loadings of greater than 0.4 are considered to be significant, following the technique of Crawley and Sievering (1986).

Factor Analysis of the WE Data Set

The results of the FA of the total WE data set are shown in Table 5.11. The three factors described above explain 78% of the variance in the data set. High loading of seawater components (i.e. Na, Cl and Mg) in the mixed seawater/continental factor indicates the predominance of seawater in this mixed source. The presence of Br in the acid-base balance factor most likely reflects the low concentration of this ion (usually less than the level of detection) at all sites except the coastal site 16 (Cliff Head), and is therefore most likely an artifact of the measurement technique. The relationships between the factor loadings of each species can be more clearly seen in the factor loading diagrams of Figure 5.10. In these plots factor loadings are plotted as co-ordinates. Species that have high loadings on a single factor will cluster along the end of the axis of that factor, eg. Cl, Na and Mg for factor 1. Species that cluster

near the origin have small loadings on both factors, eg. Na, Cl and Mg for factor 2 and 3. Species that plot between two axes may be explained by two factors, eg. K for factors 1 and 3.

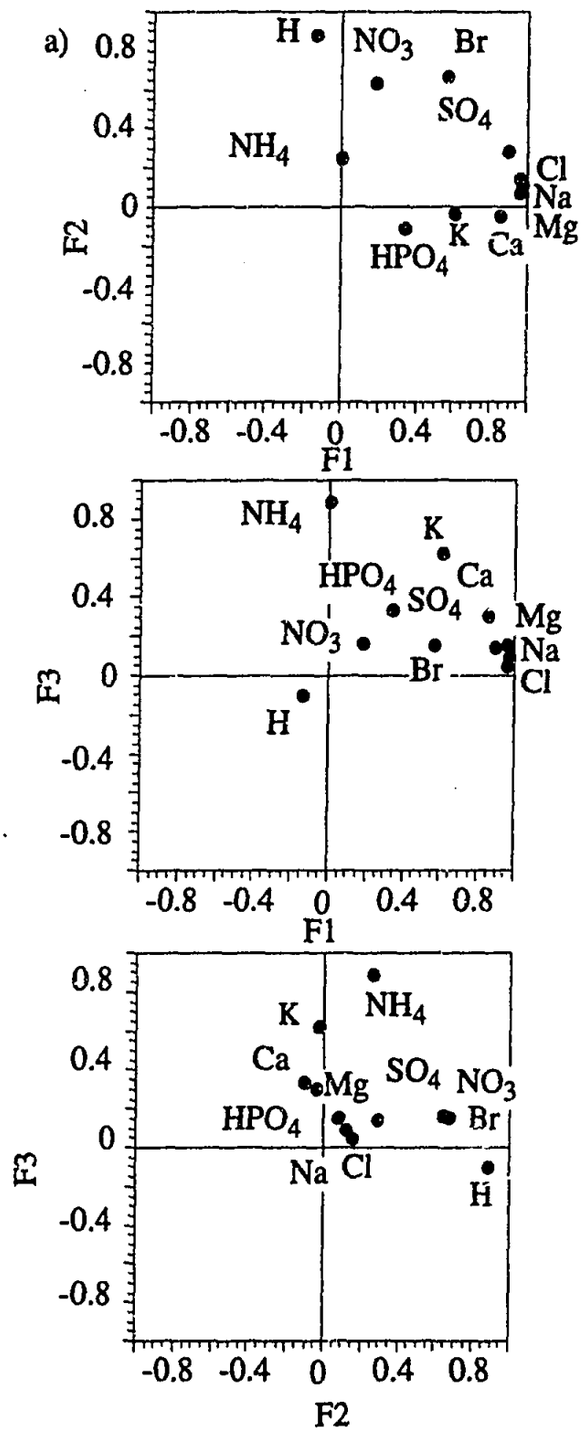

FIGURE 5.10 Factor loading plots for data from the WE array. F1, F2 and F3 represent factor 1, factor 2 and factor 3. Species that have high loadings on a single factor cluster along the end of the axis for that factor, eg. Na, Cl and Mg have high loadings on F1. Species that cluster near the origin, have small loadings on both factors in the plot, eg. Na, Cl and Mg for F2 and F3. Species that plot between two axes may be explained in terms of two factors, eg. K for F1 and F3.

TABLE 5.11 Factor loadings for the WE data set (n=73). Bold values highlight loadings of greater than 0.4.

Factor	Factor 1	Factor 2	Factor 3
% variance	52.9%	14.9%	9.9%
eigen value	5.8	1.6	1.1
H	-0.14	**0.89**	-0.10
Cl^-	**0.96**	0.15	0.06
SO_4	**0.90**	0.29	0.15
NO_3	0.18	**0.64**	0.17
HPO_4	0.34	-0.11	0.34
Br	**0.56**	**0.67**	0.16
Na	**0.97**	0.11	0.10
K	**0.61**	-0.03	**0.63**
NH_4	0.00	0.26	**0.90**
Ca	**0.86**	-0.04	0.31
Mg	**0.96**	0.08	0.16
source/process	seawater/continental	acid/base balance	biodegradation

The results of this FA suggest the major source of ionic constituents to WE precipitation is of mixed seawater/continental origin. The relationship between the continental and seawater source may be further investigated by dividing the data set into coastal and non-coastal data sets based on the proximity of the sample location to the Western Australian coast, and comparing factor loadings for each data subset. Coastal localities were chosen to lie within 200 km of the coast, (after Simpson and Herczeg 1994), so include sites 16 (Cliff Head) to 18 (Badja). Inland sites include the remaining sampling localities, i.e. 19 (Iowna) to 25 (Everard Junction). It should be noted here and for elsewhere in this section that dividing the larger data set into subsets (i.e. coastal and non-coastal) has the effect of increasing the uncertainties associated with FA, because the number of cases is reduced.

The results of FA performed on the coastal and non-coastal data subsets are summarised in Table 5.12 and detailed in Appendix F. The results are similar to the FA performed on the entire WE data set. However, the factor loadings of species in the mixed seawater/continental source are greater for the coastal data subset suggesting that at non-coastal sites the remaining two factors are also important to the variance of these species. The high loading of all species into F1 for the coastal data subset may be showing the predominance of seawater as a source at the coast, as is intuitively suggested by the coastal locality of these sampling sites.

TABLE 5.12 Summary of FA performed on coastal and non-coastal data subsets. Ionic species are listed in order of decreasing factor loadings.

	Factor 1	Factor 2	Factor 3
% variance	59%	13%	10%
Coastal	Mg, Cl, Na, SO_4, K,	H, NO_3, Br	NH_4
n=24	Ca, Br, HPO_4		
source/process	seawater/continental	acid-base balance	biodegradation
% variance	42%	16%	14%
Non-coastal	Na, Mg, Cl, SO_4,	NH_4, K, Ca, NO_3	H, NO_3
n=49	Ca, NO_3		
source/process	seawater/continental	biodegradation/continental	acid-base balance

Principal Component Analysis on the WE Data Set

The change in emphasis of each species in the three factors between the coastal and non-coastal data subsets can be further investigated by looking at principal component loadings that are calculated when the data set is divided into individual sites. PCA is used to calculate the principal component loadings as outlined in Section 3.3. The results of PCA on data sets of each site are shown in Figure 5.11 and summarised in Table 5.13. The sites display variance explainable by three or four components. The loading of species in the fourth component for sites 19 (Iowna) to 23 (Carnegie) represent duplications of one of the three sources/processes described by FA, thus Figure 5.11 shows only three components. Of note in Figure 5.11 are both negative and positive component loadings, which provide additional information with regards to the importance of each component to a particular species. For example, Site 20 (Barrambie) shows highly negative loadings for species in PC2 (H, SO_4, NO_3, NH_4 and Ca), suggesting the acid-base balance, biodegradation and possibly a gypsum (Ca and SO_4) input, while high positive loadings of Na and Cl may suggest halite input.

All sites are characterised by a high loading of most species into PC1. At sites 16 (Cliff Head) to 19 (Iowna), 23 (Carnegie) and 25 (Everard Junction) the loading of species in PC1 suggests a mixed seawater/continental origin. However, the high loadings of H and NO_3 in PC1 for sites 20 (Barrambie), 21 (Yeelirrie), 22 (Lake Violet) and 24 (Gunbarrel) suggest a mixed continental/acid-base balance. The

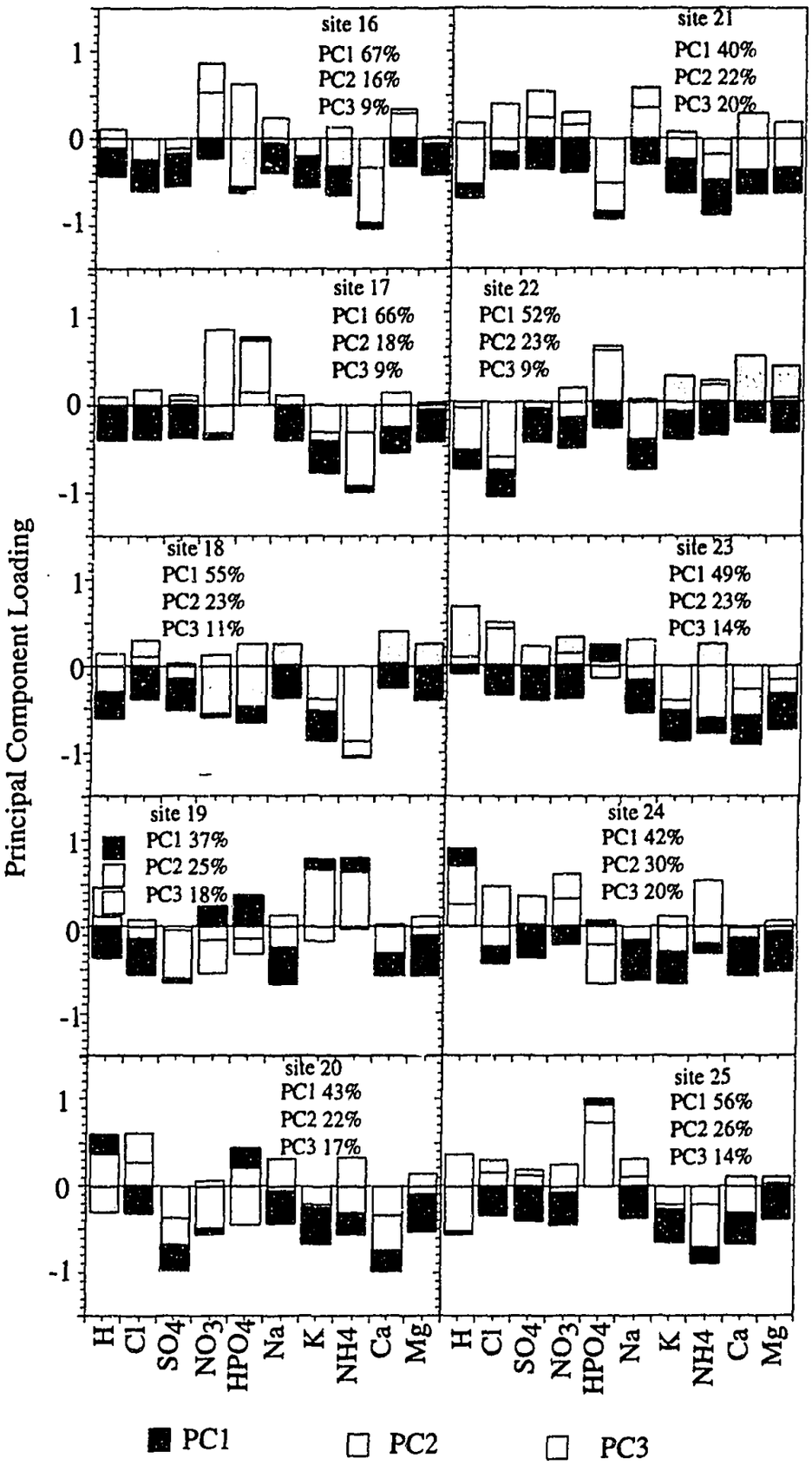

FIGURE 5.11 Principal component loadings for individual sites along the WE array. PC = principal component loading. See Figure 3.1 for site number localities

extent of this influence at each site differs however, as suggested by the differences in variation explained by PC1 at each site (Table 5.13). As distance from the coast increases, the amount of variance explained by this mixed continental seawater source decreases from 66% at the coastal site to 37% at site 19 (Iowna). Sites 23 (Carnegie) and 25 (Everad Junction) display the influence of a mixed seawater/continental source, explaining approximately 50% of variance at these sites.

The loading of species amongst the three PCs at inland sites, 20-25 (Barrambie to Everard Junction), may be interpreted as showing the stronger influence of continental sources of material to precipitation. For example, at site 20 (Barrambie), PC2 shows high negative loadings of Ca, SO_4, NO_3 and H, and high positive loadings of Na and Cl, suggesting a mixed acid/base and continental source. The continental source in this case appears to be supplying halite. Other sites where a salt-lake source of material may be inferred include site 21 (Yeelirrie) and 22 (Lake Violet) where PC2 has high loadings for Ca and SO_4, suggesting a gypsum source, and PC3 has high loadings for Na and Cl, suggesting a halite source. Site 23 (Carnegie) also shows high loadings of Na and Cl for PC3. The importance of salt lakes as sources of material to these inland sites is not surprising when the number of salt lakes in the proximity of the WE array is considered, and will be important in the discussions of ^{36}Cl compositions of Chapter 6.

TABLE 5.13 Summary of variances attributable to each PC for the WE data set.

site	% variation PC1	% variation PC2	% variation PC3	% variation PC4
16 Cliff Head	67	16	9	
17 Morawa	66	18	9	
18 Badja	55	23	11	6
19 Iowna	37	25	18	10
20 Barrambie	43	22	17	8
21 Yeelirrie	40	22	20	8
22 Lake Violet	52	23	9	9
23 Carnegie	49	23	14	7
24 Gunbarrel	42	30	20	
25 Everard Junction	56	26	14	

Acid-base balances and sample biodegradation are also significant at each site, being more so at inland sites than coastal localities.

Factor Analysis of the SN Data Set

Two factors explain 85% of the variance displayed by the SN data set (Table 5.14 and Figure 5.12). The first factor (74%) suggests mixed seawater/continental and biodegradation, and the second (11%), acid-base balances. Again, the high loading of Br in the second factor is most likely an artifact of the below-detection-level of Br at all sites except the coast, as described for the WE data set. The continental component of this mixed source may include an agricultural input, as suggested by the high loading of HPO_4 in factor 1.

TABLE 5.14 Factor loadings for SN data set (n=57). Bold values highlight loadings of greater than 0.4.

	factor 1	factor 2
% variation	73.5	10.6
eigen value	8.1	1.2
H	0.08	**0.94**
Cl	**0.85**	0.35
SO_4	**0.89**	0.33
NO_3	**0.74**	**0.50**
HPO_4	**0.85**	-0.23
Br	**0.76**	**0.60**
Na	**0.87**	0.37
K	**0.89**	0.15
NH_4	**0.76**	0.14
Ca	**0.90**	0.26
Mg	**0.89**	0.35
source/process	continental/seawater/ biodegradation	acid-base balance

The extreme differences in rainfall regimes experienced by the southern and northern sections of the SN array (i.e. the northern section experiences summer rainfall while the southern section experiences winter rainfall), suggests it may be useful to divide the SN data set into northern (30-33) and southern (26-29) sites. The northern data set is further subdivided into wet and dry sampling periods. The dry periods are

times when the prevailing wind direction is from the southeast (i.e. off the continent). The wet periods represent monsoonal and transitional monsoonal activity. The transitional monsoon periods are marked by the monsoonal trough existing north of the latitude of Jabiru (Gillett et al 1990) and therefore are also represented by southeasterly winds. However, as discussed in Chapter 2, the monsoonal period involves winds from the northeast. Thus dividing the northern data subset into wet and dry periods may provide some information about the effect of the monsoon on precipitation chemistry. The southern data subset is also further divided, into coastal (sites 26 and 27) and inland (sites 28 and 29) data subsets, to assess the effect of seawater input to these localities.

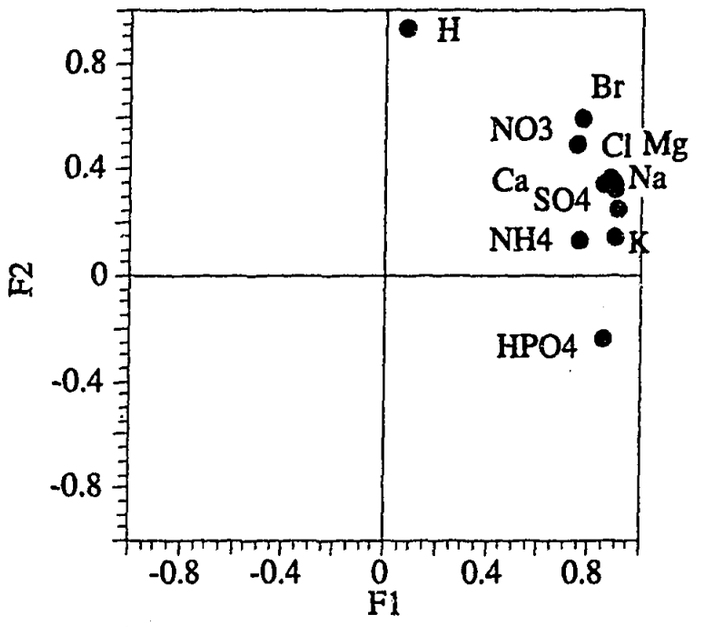

FIGURE 5.12 Factor loading plot for all data from the SN array.

Northern Subset

The results of the FA on the northern data subsets are summarised in Table 5.15 and detailed in Appendix F. A mixed seawater/continental and biodegradation source explains most of the variance for each data subset. Little effect on the overall variance explained by each factor is observed for the wet data set. The dry data set, however, has a lower amount of variance explained by the two-factor model (85%) than does the wet or complete northern data set (93%). The loading of individual species in each factor also differs between data subsets. High loadings of seawater species (i.e. Na, Cl and Mg) in the second factor for the wet data subset suggest an isolation of the seawater source associated with monsoonal and transitional monsoon deposition. This is not surprising since monsoonal precipitation moisture is derived from tropical marine air masses, as discussed in Chapter 2. It is also not surprising

that the distinct seawater source of wet deposition explains only a very small proportion of the variance in the wet data subset, and indicates the influence of southeasterly winds during transitional periods when wet deposition occurred.

TABLE 5.15 Summary of FA performed on northern, northern wet and northern dry data subsets. Ionic species listed in order of decreasing factor loadings.

	Factor 1	Factor 2
% variance northern subset (all seasons) n=24 source/process	82% K, Na, Mg, Cl, Ca, HPO_4, SO_4, NH_4, NO_3 seawater/continental and biodegradation	12% H, NO_3 acid-base balance
% variance wet samples (n= 14) source/process	81% HPO_4, K, NH_4, SO_4, Ca, Cl, Na, Mg, NO_3 biodegradation and mixed continental seawater	12% H, NO_3, Mg, Na, Ca, Cl SO_4 acid-base balance and seawater
% variance dry samples n=11 source/process	77% Na, Cl, Mg, Ca, K, HPO_4, NH_4, NO_3 seawater/continental and biodegradation	8% H, HPO_4, NO_3 acid-base balance

Southern Subset

The results of the FA performed on data subsets from the southern section of the SN array are summarised in Table 5.16 and detailed in Appendix F. Three factors explain the variance of the data sets, with the loadings of ionic species again suggesting the sources/processes discussed throughout this section. The high loading of HPO_4 in the third factor may represent an agricultural input.

Isolation of seawater from the mixed seawater/continental source is again noted when the southern data set is divided into coastal and non-coastal subsets. The negative loading of Ca in the second factor may represent the neutralising property of $CaCO_3$, evidenced by the presence of carbonate crusts on dunes in the vicinity of the coastal site 26 (Port Lincoln). The non-coastal data subset shows lower magnitude in loadings of species for factor 1 than for the coastal data subset,

indicating the importance of factors 2 and 3 on the variance of the species in the non-coastal data subset.

TABLE 5.16 Summary of FA performed on northern, northern wet and northern dry data subsets. Ionic species listed in order of decreasing factor loadings.

	Factor 1	Factor 2	Factor 3
% variance southern subset (all sites) n=34 source/process	61% Mg, Cl, Na, Ca, SO_4, K mixed seawater/continental	12% H, NO_3, Br, SO_4, K acid-base balance and continental?	10% HPO_4, NH_4 biodegradation
% variance Coastal n=19 source/process	57% Mg, Na, Cl, SO_4, K, Br, H, Ca seawater/continental	16% H, NO_3, HPO_4, -Ca acid-base balance	16% -NH_4, HPO_4, NO_3, Ca biodegradation
% variance Non-coastal n=15 source/process	60% Cl, Na, Mg, NO_3, Cl, NH_4, Ca seawater/continental	18% H, SO_4, Mg, K, NO_3 acid-base balance and continental	10% HPO_4, K, NH_4, Ca biodegradation

Principal Components in the SN data set

PCA performed on individual site data sets show very similar results to the FA for the various groups of data. Results of PCA on individual site data sets are shown in Figure 5.13 and summarised in Table 5.17.

Variance at the southern sites can be explained by three components. The coastal site (26 Port Lincoln) has a PC1 with high loadings of seawater species, while PC2 represents mixed acid/base continental source with the neutralising role of Ca as sourced from calcareous dunes inferred by the high loading of Ca in this component. The third PC has high loadings of acid-base and biodegradation species. Site 27 (Gawler Ranges) has similar loadings of species in the three components, although the seawater component is less significant in explaining the variance. At site 28 (Wintinna), most of the variance can be explained in terms of a continental source and acid-base balance. A mixed seawater/continental source makes up PC2 which is almost as significant as PC1, and PC3 represents a continental (possibly agricultural)

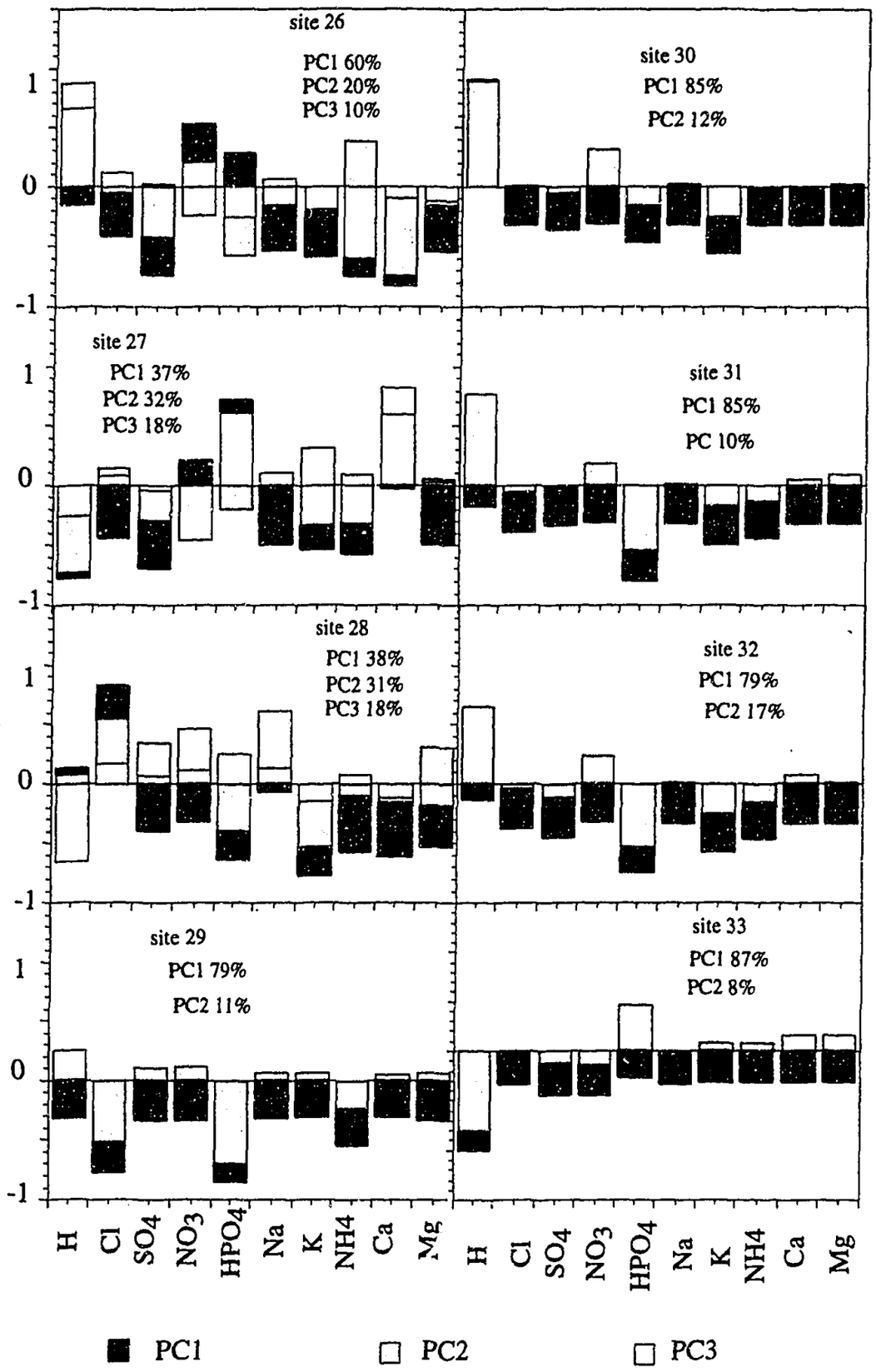

FIGURE 5.13 Principal component loadings for individual sites along the SN array. PC= principal component.

source. Sites 29-33 (Alice Springs to Kapalga) display two principal components, comprising a mixed continental/seawater/biodegradation origin and acid-base balances. The amount of variance explained by each component ranges between 79 and 87% for PC1, and 8 to 11% for PC2.

TABLE 5.17 Summary of variances attributable to each PC for the SN data set.

site	% variation PC1	% variation PC2	% variation PC3
26 Port Lincoln	60	20	10
27 Gawler Ranges	37	32	18
28 Wintinna	38	31	18
29 Alice Springs	79	11	
30 Tennant Creek	85	12	
31 Dunmarra	85	10	
32 Katherine	79	17	
33 Kapalga	87	8	

The results of multivariate analyses performed on the SN data set reveal that variations are primarily controlled by the variations that occur in the northern half of the array. This is suggested by the similarity between results of FA analysis on the entire data set and the results of PCA on the northern most individual sites 29-33 (Alice Springs to Kapalga). The northern sites of the array are influenced primarily by mixed continental/seawater/biodegradation sources. During periods of monsoonal and transitional precipitation, a seawater factor can be isolated in the variation displayed by the northern sites, but this factor is only responsible for a very small amount of variation during the wet season. The southern localities are influenced by three factors; a mixed seawater/continental source, acid-base balances and biodegradation. The coast proximal sites 26 (Port Lincoln) and 27 (Gawler Ranges) show the influence of a seawater source which contributes to a large proportion of variance (30-60%).

5.4 SPATIAL AND SEASONAL VARIATIONS

The results of multivariate analyses show that there are three major processes that affect the composition of rainfall across the arrays; the influx of a mixed seawater/continental source, natural acid/base balances in the atmosphere and decomposition of the sample between deposition and collection from the field. The following discussion assesses each of these processes in more detail.

Mixed Seawater/Continental Source

The most significant source of material to the rain collectors along the WE and SN arrays is of mixed seawater/continental origin. The results of dividing the WE data set and southern section of the SN data set into coastal, non-coastal and individual sites, suggests that the relative input of a seawater and continental source is dependent on sample locality. The mean seasonal patterns of depositional flux, described in Section 5.2, suggest that there is a seasonal dependency in the supply of most species to the collectors. The following discussion uses simple graphical techniques described in Section 3.3 to carry out a detailed investigation of the variations displayed by this mixed seawater/continental source over space and time.

Spatial Variations along the WE Array

The mean ratios of Cl, SO_4, K, Ca and Mg to Na at each site on the WE are shown in Figure 5.14. Also plotted are the ratios of these species in seawater. As expected, the coastal locality (site 16 Cliff Head) displays ratios found in seawater, suggesting the coastal rainwater samples represent diluted seawater. The Cl/Na ratio displays a decrease with increasing distance from the coast, while each of the ratios of the other ions to Na show an increase. The decreasing Cl/Na ratio with increasing distance from the coast may be attributable to the addition of continental soil or dust material that has a Cl/Na ratio lower than that of seawater, or to the liberation of Cl and H (to produce gaseous HCl) by H_2SO_4. This latter process has been used to explain depletions of Cl in marine aerosols of up to 12% (Warneck 1988). The inland sites of the WE array (site 20 Barrambie to site 25 Everard Junction) display depletions of up to 18%, suggesting that both processes are acting to decrease the Cl/Na ratio as distance from the coast increases. In addition, attributing the trend mostly to the input of non-seasalt aerosol material with low Cl/Na ratios agrees with the trend of increasing ratios displayed by SO_4, K, Ca and Mg ratios with Na with increasing distance from the coast. Thus, seawater may be the main source of Cl to the rain collectors, while the ions SO_4, K, Ca and Mg are influenced by an additional source at non-coastal localities. The very low concentrations (i.e. near the detection level of instrumentation) of Br in rainfall at non-coastal localities also suggests seawater to be the sole source of Br to the array. However, because of the low concentrations and therefore high errors, Br is excluded from the following discussion.

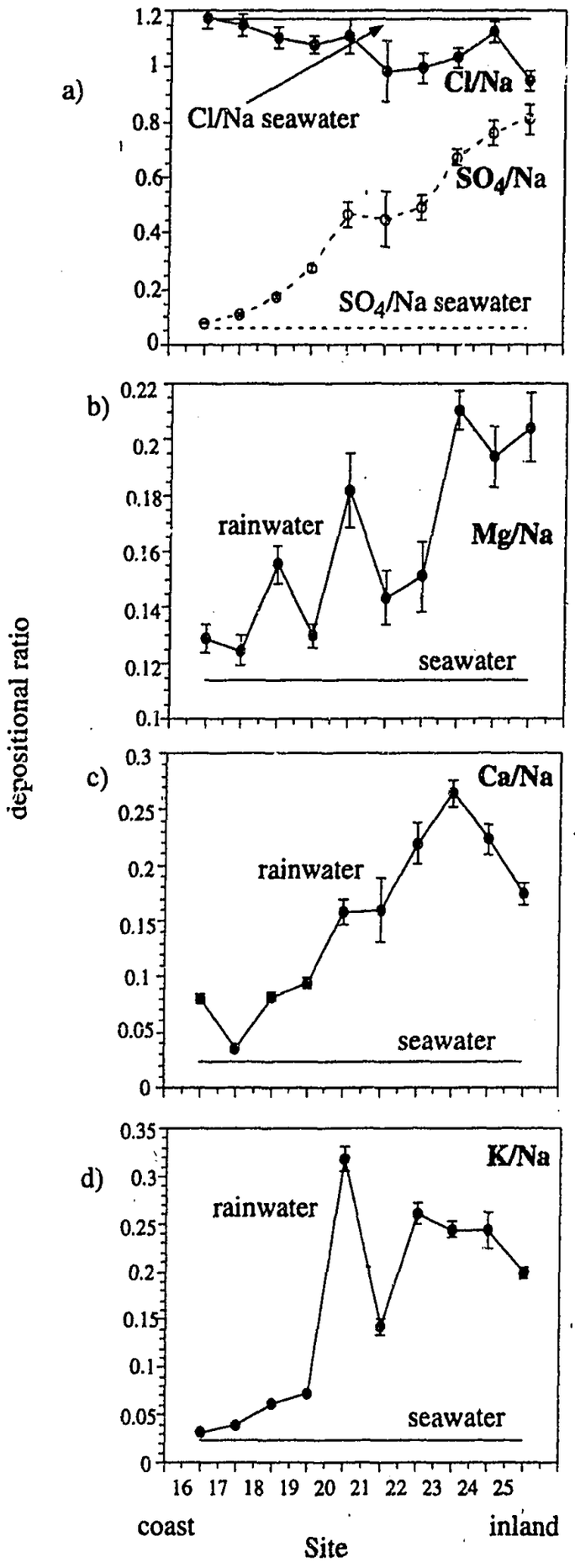

FIGURE 5.14 Mean Ratios of a) Cl and SO_4, b)Mg, c) Ca and d) K with Na for sites along the WE array compared with the ratios found in seawater. Seawater ratios calculated from Millero 1977. Ratios calculated from depositional units ($\mu eq/m^2/day$). See Figure 3.1 for site number names.

The non-seasalt source for SO_4, K, Ca and Mg to the rain collectors can be further investigated by looking at the "non-seasalt" (nss) fraction of these ions in rainfall (as defined in Section 3.3). Figure 5.15 displays the percentage of the nss ions as a function of distance from the coast for the WE array. In general, nss ions increase with increasing distance from the coast, with nss SO_4 and nss Ca reaching a steady state of between 40-50% at approximately 400 km from the coast. The percentage of nss K at inland sites reaches values of close to 90%, while nss Mg remains below 30% at inland sites. These patterns may suggest that the source of K to inland sites is almost exclusively from a source other than seawater, while seawater remains an important source of Mg at inland sites, and the ions SO_4 and Ca are influenced by a mixture of sources, one of which is seawater.

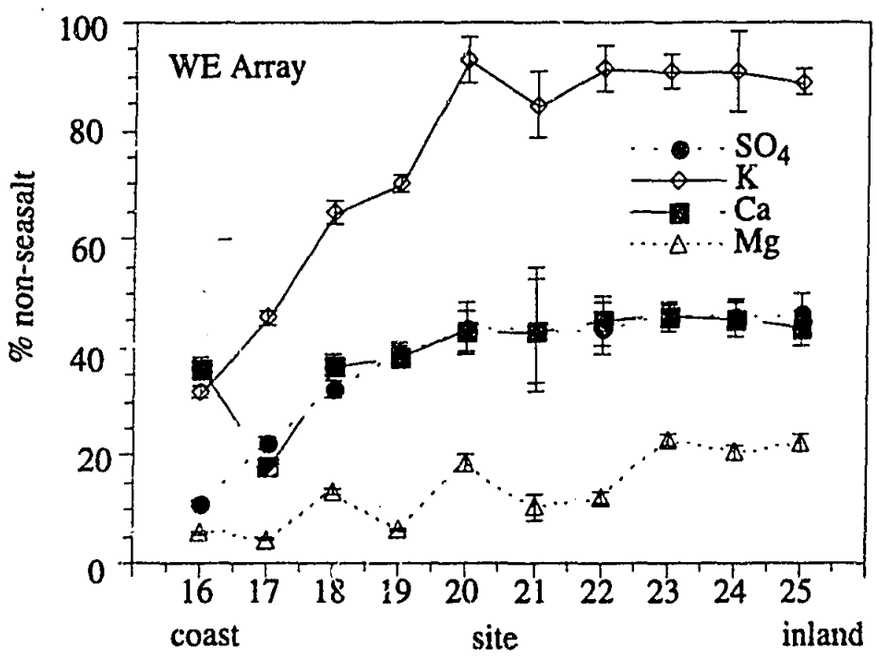

FIGURE 5.15 The mean non-seasalt proportions of SO_4, Ca, Mg and K for sites along the WE array. See Figure 3.1 for site locations.

Comparisons of mean ratios of Cl, SO_4, Na, K and Mg with Ca in rainfall and soil/dust samples collected from each site on the WE array are shown in Figure 5.16. Further evidence of the importance of seawater to the concentrations of Cl, Na and Mg can be seen with the decreasing of ratios of these elements to Ca as distance from the coast increases. The ratios generally move closer to those of the soil/dust compositions at inland sites, though SO_4/Ca in rainwater remains greater than in soil/dust compositions across the entire array, and no relationship can be discerned between rainfall and soil/dust K/Ca ratios.

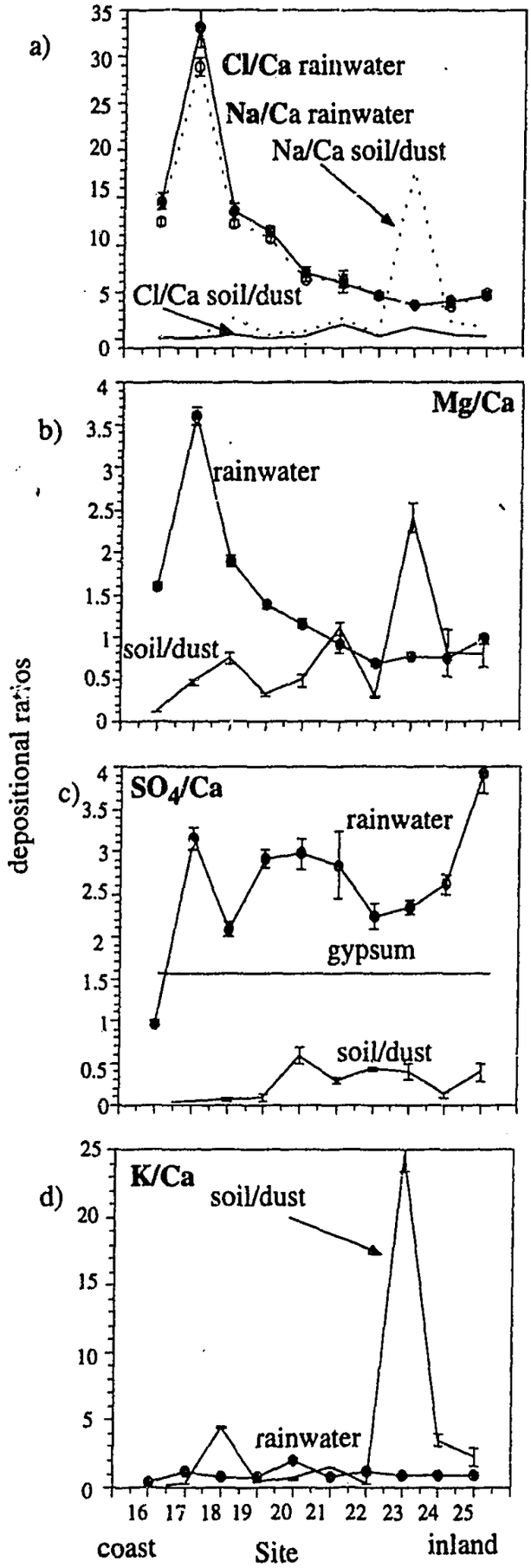

FIGURE 5.16 Mean ratios of a) Cl and Na, b) Mg, c) SO_4, and d) K with Ca for sites along the WE array compared with the ratios found in soil/dust collected at each site. Ratios calculated from depositional units ($\mu eq/m^2/day$). See Figure 3.1 for site localities.

Spatial Variations along the SN Array

The mean ratios of Cl, SO_4, K, Ca and Mg to Na at each site on the SN are shown in Figure 5.17. Site 26 (Port Lincoln), the southern coastal site, shows with ionic concentrations that approximate those found in seawater. The remaining sites show an increase in ratios (Cl shows a decrease) relative to seawater in a northward direction, suggesting the importance of a non-seawater source at these non-coastal sites. At the northern end of the array, ratios begin to fall closer to that of seawater, reflecting the influence of seawater at site 33 (Kapalga).

The non-seasalt fractions for sites along the SN array are shown in Figure 5.18. All nss concentrations show an increase from site 26 (Port Lincoln) to inland sites and a slight decrease at sites 32 (Katherine) and 33 (Kapalga). The relatively high nss fractions shown at site 33 suggest that seasalt is less important to the chemistry of precipitation than a non-seasalt source. This supports the work of Ayers and Gillett (1988a) who found high levels of non-seasalt Ca, Mg and SO_4 in rainfall at Jabiru. Despite site 33 (Kapalga) being within 100 km of the north coast of Australia, and the prevailing northwest winds during the monsoon, the high non-seasalt fractions represent the predominance of southeasterly winds during the non-monsoon periods. Thus, this locality may be considered continental rather than maritime.

The mean ratios of Cl, SO_4, K, Na and Mg to Ca, are compared with local soil/dust ratios for each site along the SN array in Figure 5.19. The importance of seawater to site 26 can be inferred from this plot by the high ratios of Cl, Na and Mg. An increase from the generally low ratios at inland sites to values seen at site 33 (Kapalga) also points to the importance of seawater at this site. The ratio of K with Ca increases from north to south, and SO_4 to Ca ratios approximate that of gypsum.

Simpson and Herczeg (1994) looked at the relative abundances of Ca and Na in rainfall from southeastern Australia in order to investigate the input of resuspended soil to precipitation. High Ca/Na ratios (greater than unity) were considered to represent a significant regional dust input, since Ca salts such as $CaCO_3$ and $CaSO_4.2H_20$, tend to be the first salts to precipitate out of soils. The WE data set all show Ca/Na ratios of less than 0.5 and sites along the SN array show mean Ca/Na ratios of less than 0.5. However several individual samples display ratios greater than 1, suggesting the influx of resuspended soil material. These samples include sites from both the north and south of the array, and represent some of the seasons of low to nil rainfall.

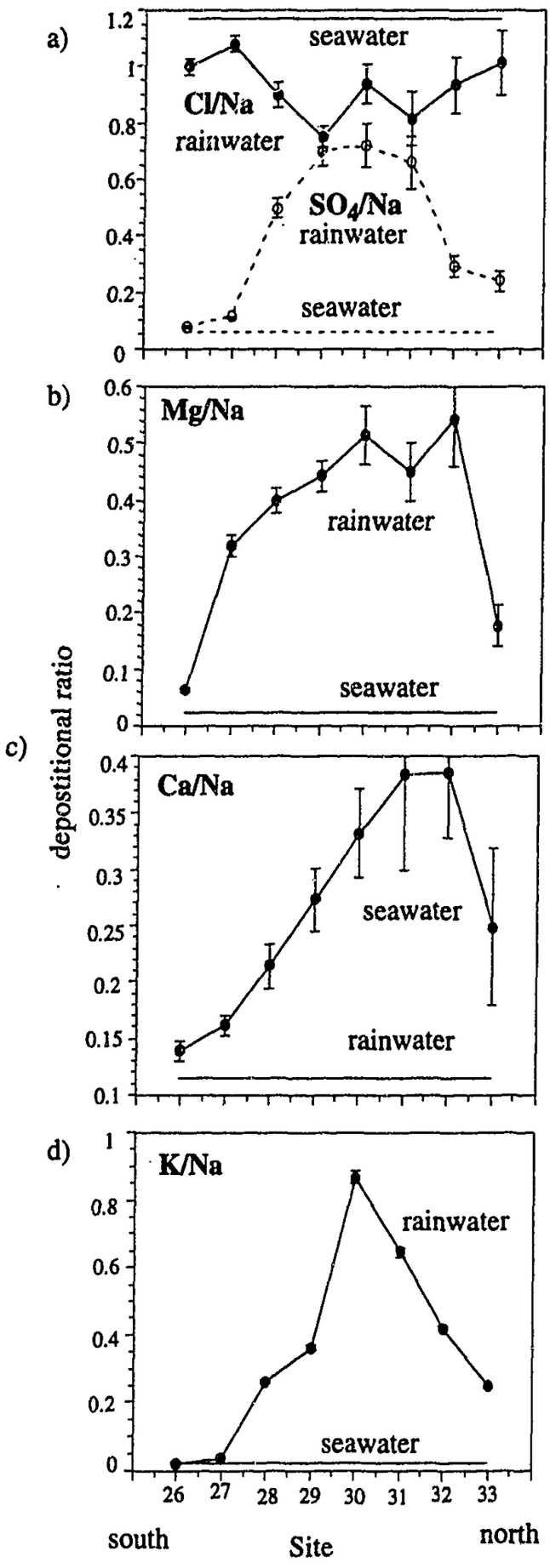

FIGURE 5.17 Mean Ratios of a) Cl and SO_4, b) Mg, c) Ca and d) K with Na for sites along the SN array compared with the ratios found in seawater. Seawater ratios calculated from Millero 1977. Ratios calculated from depositional units ($\mu eq/m^2/day$). See Figure 3.1 for site locations.

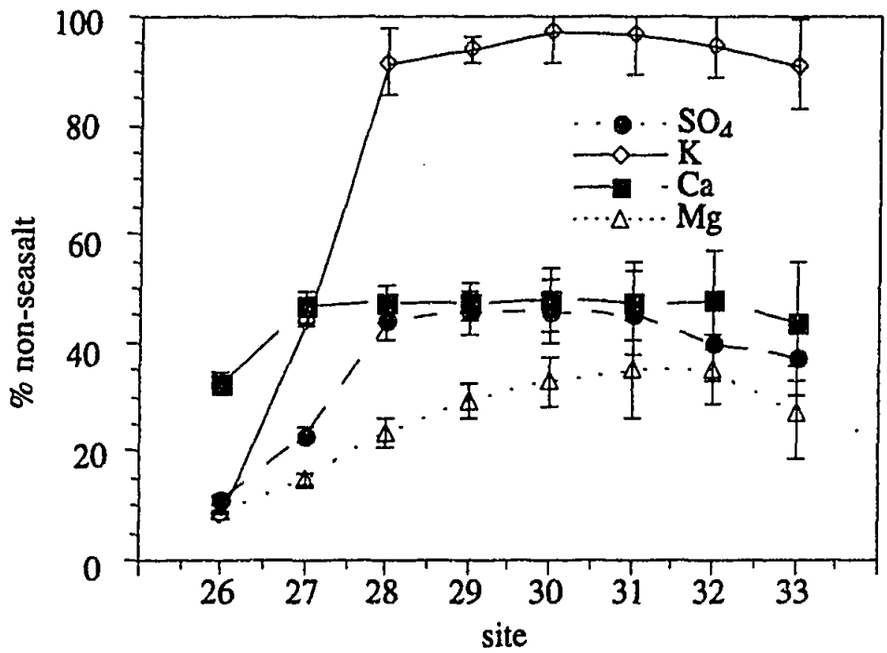

FIGURE 5.18 The mean non-seasalt proportions of SO_4, Ca, Mg and K for sites along the SN array. See Figure 3.1 for site localities.

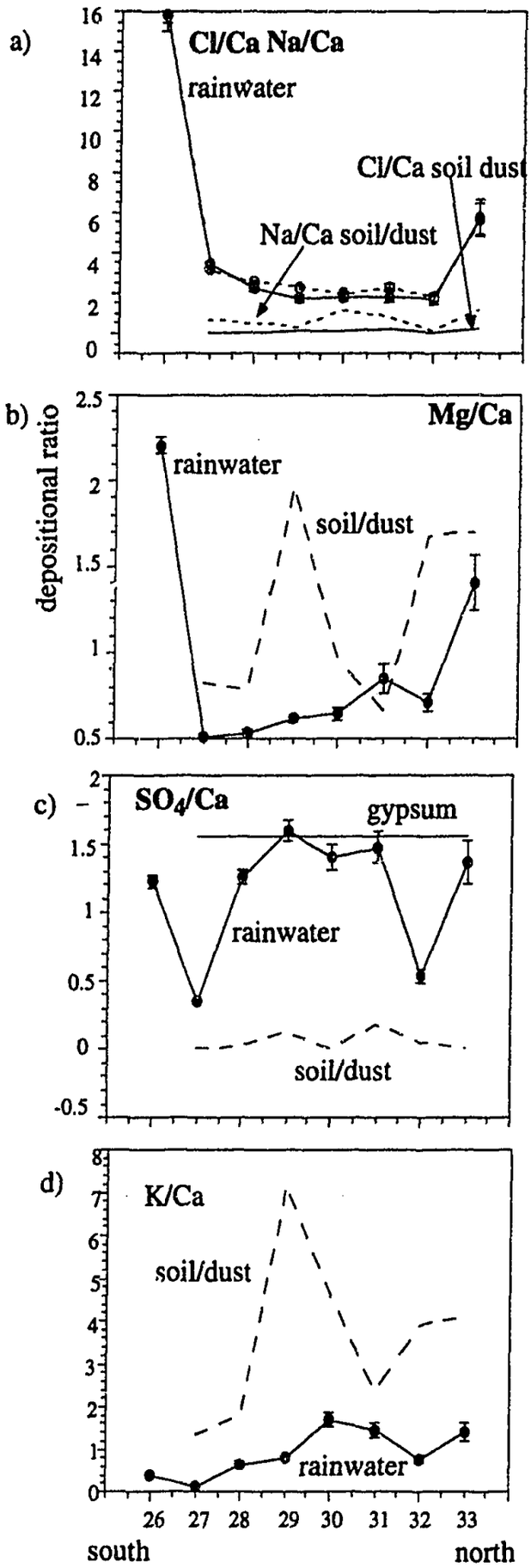

FIGURE 5.19 Mean ratios of a) Cl and Na, b) Mg, c) SO_4, and d) K with Ca for sites along the SN array compared with the ratios found in soil/dust collected at each site. Ratios calculated from depositional units ($\mu eq/m^2/day$). See Figure 3.1 for site localities.

Seasonal Variations

Seasonal changes in the influence of seawater as a source of material to rainfall at each site can be investigated by looking at the ratios of various species to Na and Ca at each site over time. The plots shown in Figure 5.20 show the ratios of Cl, SO_4, K, Mg, Ca and Na with Na and Ca for sites 16 (Cliff Head), 21(Yeelirrie) and 23 (Carnegie) along the WE array and Figure 5.21 shows the same ratios for sites 26 (Port Lincoln), 30 (Tennant Creek) and 33 (Kapalga) along the SN array. Also shown are the seawater ratios of these species, the local soil/dust ratios at each site, and the Cl/Na ratio of halite and SO_4/Ca ratio of gypsum.

Calcium is assumed to be of continental origin. Thus when a continental source is predominant at a site, increased supply of Ca leads to a decrease in the ratio of other species with respect to Ca. Hence low Ca ratios are generally interpreted as representing increased continental source influence. Low Ca ratios are often matched by Na ratios higher than that of seawater, suggesting an alternative source to seawater is adding all species except Na. The exception is when the Cl/Na ratio falls below that of seawater, indicating that the alternative source is then also adding Na. The local soil/dust ratios shown in the plots do not represent the end-member composition of the continental source, but rather, the composition of rainfall that would arise if soil/dust from the site in question were to enter the collector. The halite and gypsum ratios also do not represent the end-member composition of the continental source, but are shown on the plots as references for possible input of salt lake material to the rain collectors at each site. Because the concentration of seawater is well known, and we therefore have better constraints on the seawater source, the ratios are summarised in Figure 5.22 in terms of the dominance of a seawater source. During some collection periods, the behaviour of the different ratios is inconclusive or contradictory. Such cases are marked with a slash in Figure 5.22. For cases where analyses are missing, no results are shown.

As expected, site 16 (Cliff Head) is dominated by a seawater source throughout most of the sampling program, except for summer of each year and autumn of 91. An investigation of the synoptic patterns (Figure 5.23) reveals the dominance of cold front activity in association with rainfall at Dongara meteorological observation station (approximately 50 km north of site 16) throughout the sampling program. A similar trend is displayed by site 26 (Port Lincoln) on the SN array (Figure 5.24). Cold fronts affecting Western Australia and South Australia, involve air masses that are sourced from the south or southwest, i.e. of marine origin.

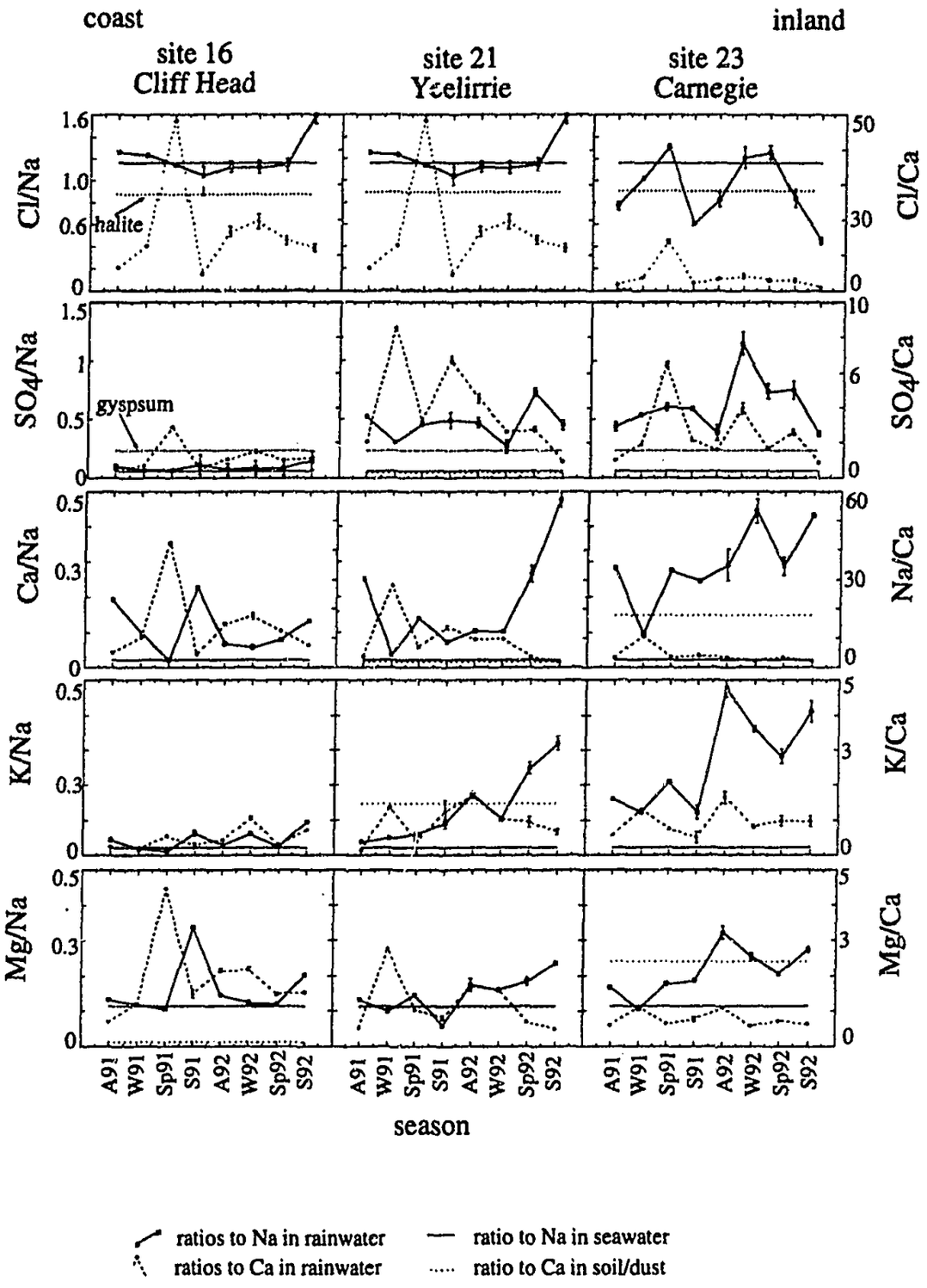

FIGURE 5.20. Seasonal variations in the ratios of Cl, SO_4, Ca, K and Mg to Na, and Cl, SO_4, Na, K and Mg to Ca for sites 16, 21 and 23 on the WE array. Circles with the solid line are ratios to Na in precipitation. Circles with the dashed line are ratios to Ca in precipitation. The solid horizontal line is the ratio to Na in seawater (from Millero 1974). The dashed horizontal line is the ratio to Ca in soil/dust at the site. The left vertical axes are scales for the Na ratios. The right axes are scales for the Ca ratios. In the SO_4/Na and SO_4/Ca plots the dotted line is ratio of SO4/Ca in gypsum. In the Cl/Na and Cl/Ca plots the dotted line is the ratio of Cl/Na in halite.

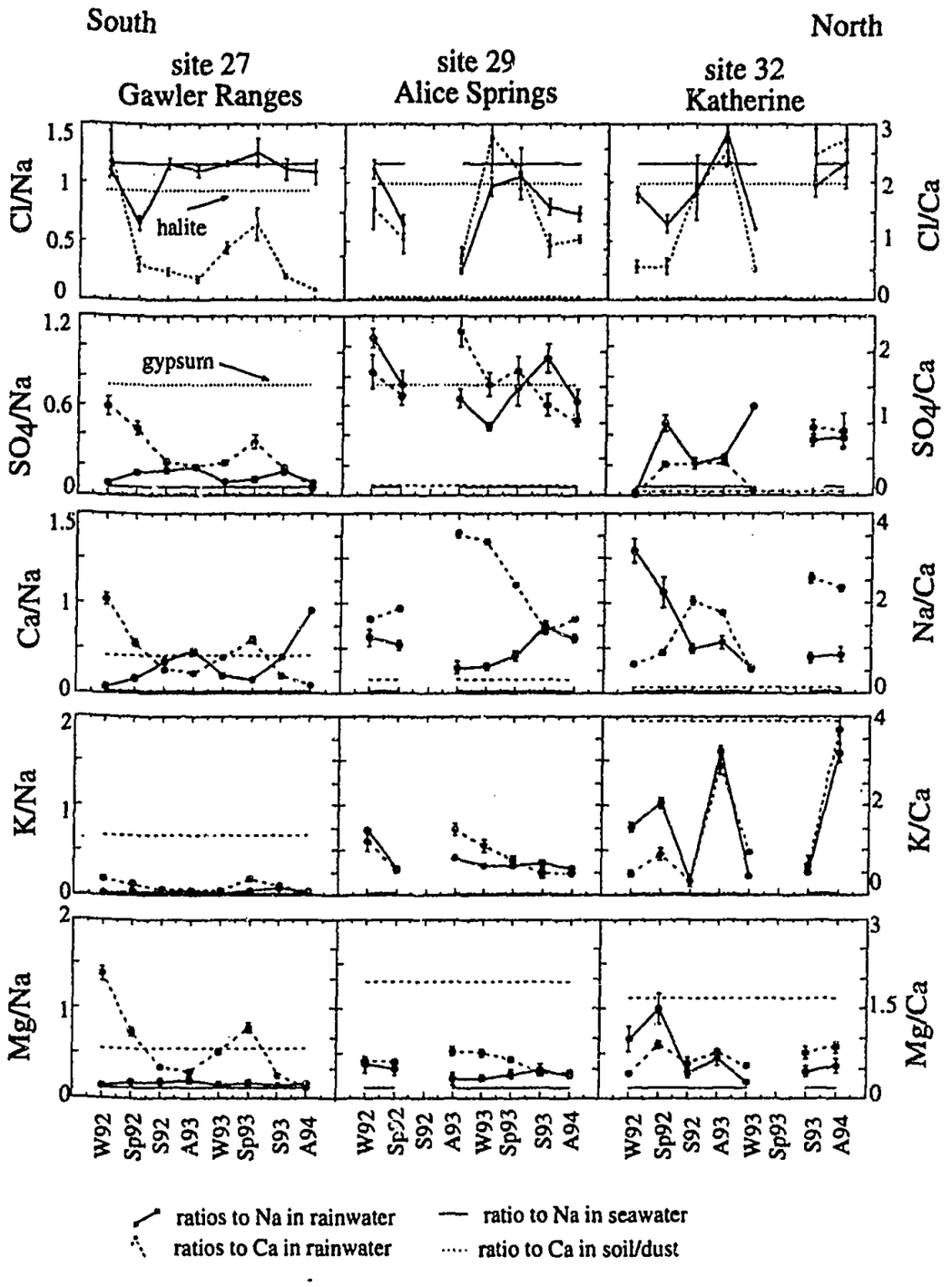

FIGURE 5.21. Seasonal variations in the ratios of Cl, SO_4, Ca, K and Mg to Na, and Cl, SO_4, Na, K and Mg to Ca for sites 27, 29 and 32 on the SN array. Circles with the solid line are ratios to Na in precipitation. Circles with the dashed line are ratios to Ca in precipitation. The solid horizontal line is the ratio to Na in seawater (from Millero 1974). The dashed horizontal line is ratio to Ca in soil/dust at the site. The left vertical axes are scales for the Na ratios. The right axes are scales for the Ca ratios. In the SO_4/Na and SO_4/Ca plots the dotted line is ratio of SO4/Ca in gypsum. In the Cl/Na and Cl/Ca plots the dotted line is the ratio of Cl/Na in halite.

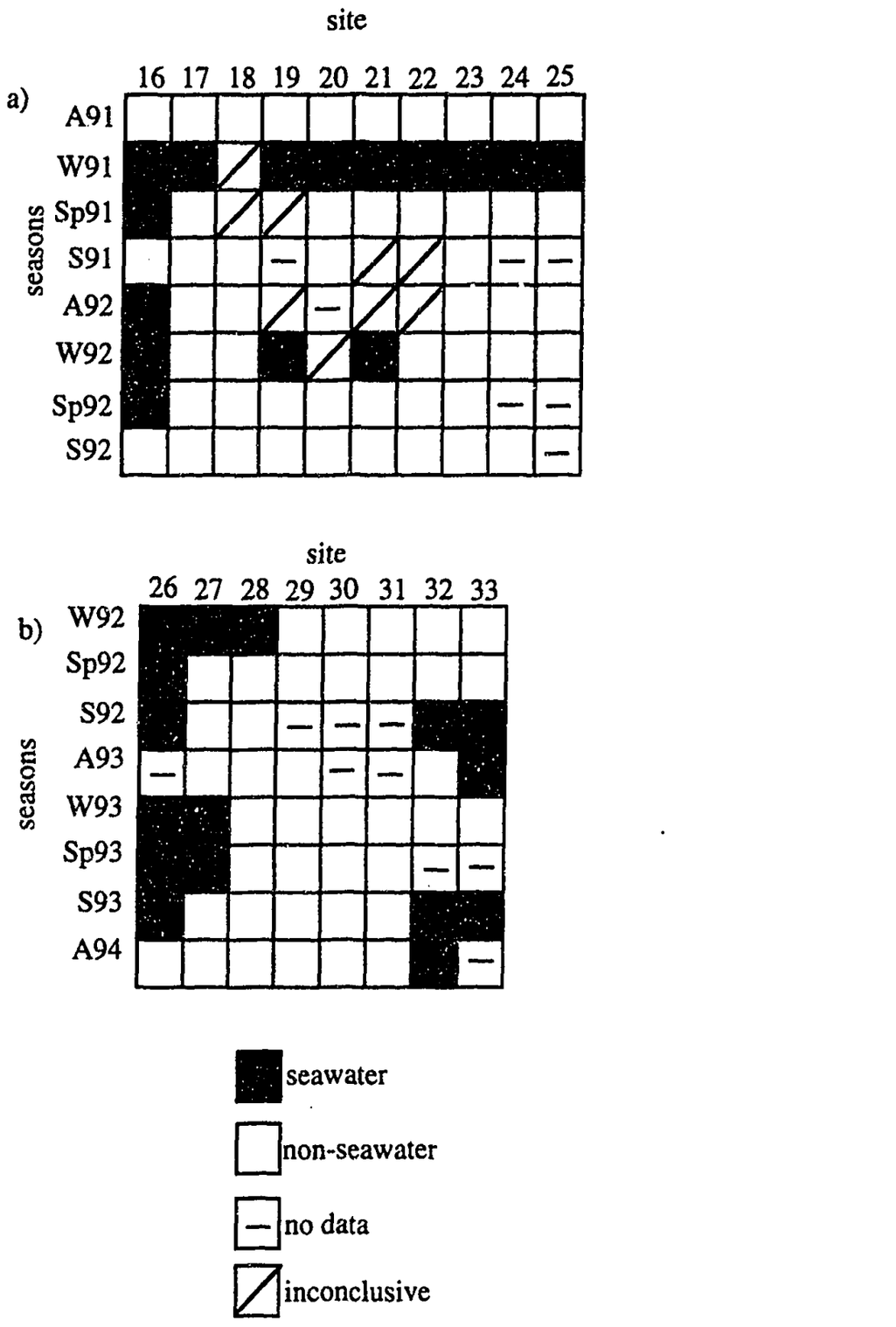

FIGURE 5.22 Summary of seasonal variations in terms of the dominance of a seawater source for a) the WE array and b) the SN array.

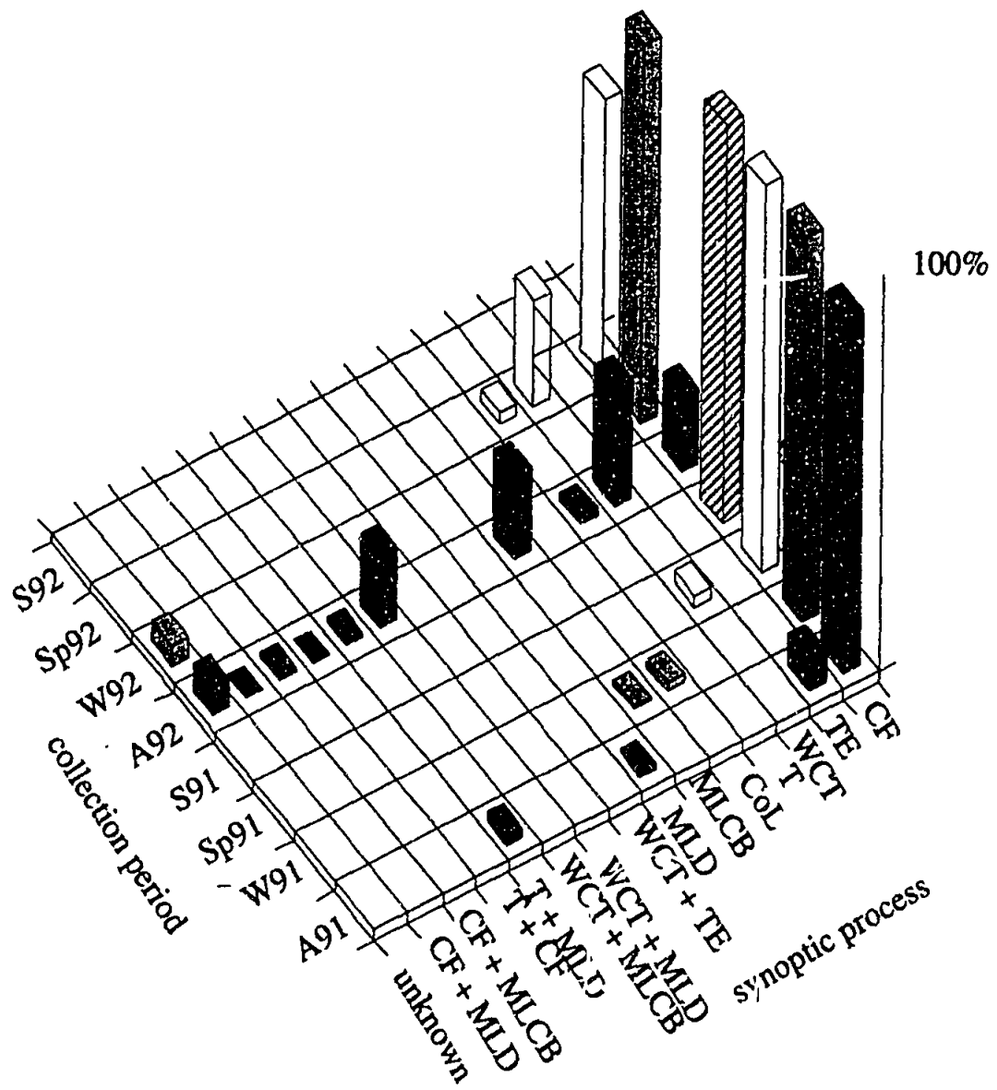

FIGURE 5.23 The percentage of rain attributable to different synoptic processes (defined in Chapter 2) during each collection period at Dongara (Met station closest to site 16, Cliff Head). CF = cold front, TE = tropical event, WCT = West Coast Trough, T = trough, CoL = cut-off low, MLCB = middle-level cloud band, MLD = middle-level disturbance. A91 = autumn 91, W91 = winter 91, Sp91 = spring 91, S = summer 91 etc. Note that throughout most of the sampling program rainfall at Dongara was associated with cold fronts.

The dominance of the seawater source at all sites along the WE array during winter 91, including the most inland site, Everard Junction (site 25), is unexpected. An investigation of the synoptic patterns for each meteorological observation station across the WE array (Figure 5.25), again reveals that a high proportion of rainfall for winter 91 is associated with cold front activity. The more coastal sites 17 (Morawa), 18 (Badja), 19 (Iowna) and 21(Yeelirrie) also display seawater source dominance during winter 92, again corresponding to periods of enhanced cold front activity. The remaining sites show dominance of a non-seawater source throughout the sampling program (except during winter 91 as described above).

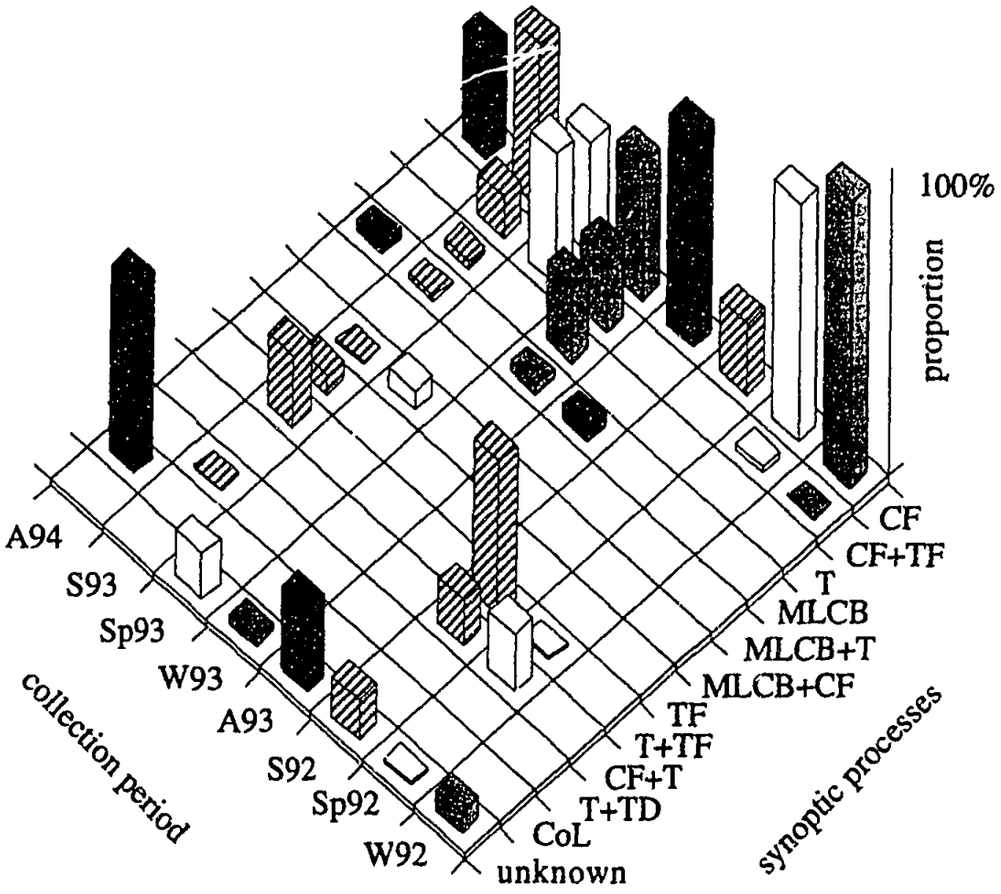

FIGURE 5.24 The percentage of rain attributable to different synoptic processes (defined in Chapter 2) during each collection period at Port Lincoln (Met station closest to site 26, Port Lincoln). CF = cold front, TF = tropical flow, WCT = West Coast Trough, T= trough, CoL = cut-off low, MLCB = middle level cloud band. A92 = autumn 92, W92 = winter 92, Sp92 = spring 92, S92 = summer 92 etc. Note that throughout most of the sampling program rainfall at Port Lincoln was associated with cold fronts.

Sites 27 (Gawler Ranges) and 28 (Wintinna) along the SN array display the dominance of a seawater source during winter of each year, and non-seawater dominance during autumn of each year. Between autumn and winter there is a gradation towards seawater dominance. The distinction between the influence of seawater and non-seawater sources is less obvious as distance from the coast increases. Sites 29 (Alice Springs), 30 (Tennant Creek) and 31 (Dunmarra) do not experience the dominance of a seawater source during any stage of the sampling program (Figure 5.22). The contradictory nature of many of the Na and Ca ratios may suggest something about the non-seawater source and possible changes in its composition. The SO_4/Ca ratio approximates that of gypsum at various times during the sampling program. Sites 32 (Katherine) and 33 (Kapalga) show a high ratios of Na during winter of each year, and minium Na ratios during summer. This represents the dominance of continental material bought to the collectors by the southeasterlies that characterise the dry season in the north of Australia. During the

summer, when northerlies associated with the monsoon become more important, the ratios move closer to those of seawater (Figure 5.26).

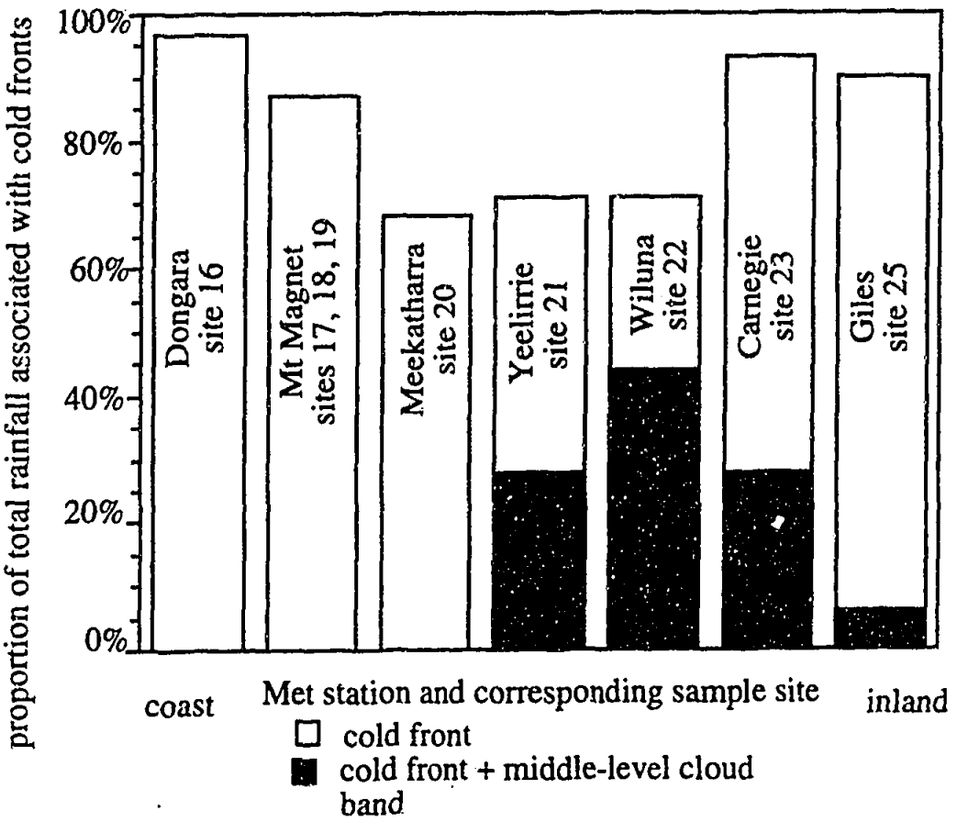

FIGURE 5.25 Proportion of total rainfall at Met stations along the WE array associated with cold fronts during winter 1991.

These results are not unexpected, i.e. seawater compositions in rainfall correspond to increased cold front activity. Thus rainfall during winter of 1991 is mainly of marine origin, even as far inland as Everard Junction (1800 km from the coast). However, it is surprising that the tropically sourced rainfall does not have a marine signature (we would expect to see seasons and sites dominated by tropical events or middle level cloud bands eg. Site 22 (Lake Violet) during summer 92, to display a seawater dominance). This may represent the extent of the land mass over which the airmass must pass, therefore adopting a continental signature, or may be an artefact of the three-month sampling period. The results from the SN array support these speculations. During the summer seasons, the north of Australia experiences both monsoonal (ie marine-sourced airmasses) and transitional monsoonal (i.e. continental airmass from the southeast of the continent). This is represented by the data from sites 33 (Kaplaga) and 32 (Katherine) displaying only weak seawater signatures.

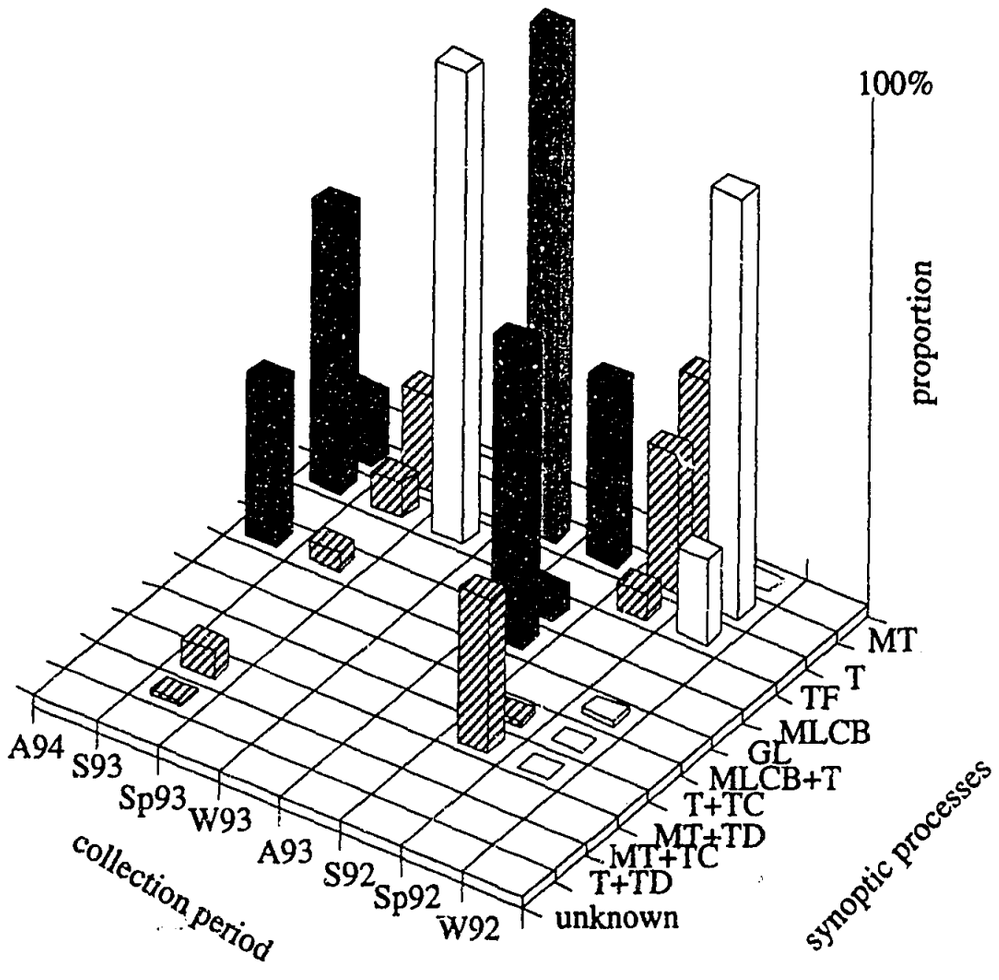

FIGURE 5.26 The percentage of rain attributable to different synoptic processes (defined in Chapter 2) during each collection period at Darwin (Met station closest to site 33, Kapalga). MT = monsoon trough, T = trough, TF = tropical flow, GL = Gulf Lines, MLCB = middle level cloud band, TC = tropical cyclone. A92 = autumn 92, W92 = winter 92, Sp92 = spring 92, S92 = summer 92 etc. Note that throughout most of the sampling program rainfall at Darwin is associated with synoptic processes sourced from the topical north of Australia.

Acid-Base Balance and Biodegradation

The results of multivariate analysis on the total WE data set show that 25% of variation in the data set may be explained in terms of the acidity of the sample, or a combination of acidic anions and biodegradation. Acid-base balances account for 10% of variance in the overall SN data set and northern subset of the SN data set, and 12-20% variance in the southern subset of the SN data set. Input of an agricultural source and biodegradation, are only found in the southern data subset and accounts for approximately 10% of variation. For the purpose of the following discussion, acid-base balance and biodegradation are grouped together as it will be seen that the effects of both processes produce the acidity measured in the samples.

Rainfall acidity has been shown to change within ten days of sample deposition in wet precipitation samples (Vesely 1990). We would expect changes in pH to occur even sooner in bulk depositional collectors used in the present investigation. Thus the pH values measured in this project may not reflect the true H concentrations of rainfall as deposited. Instead, the pH levels of the samples may represent processes that occur after deposition of the sample eg. biodegradation. The high positive ion imbalances for the SN data set suggest the presence of an unmeasured species in the precipitation samples, possibly organic acids. Herlihy (1987) showed formic and acetic acids to be very unstable, and readily utilised by microorganisms in precipitation for their growth. Both formate and acetate are also known to be intermediate metabolic products. Thus the presence of organic acids may influence the extent of biodegradation and thus the acid-base balances of precipitation. Unfortunately, organic acids were not measured in the present study for the reasons outlined in Chapter 3. Despite this however, we do see H showing variances with inorganic acid ion NO_3, and at particular sites with SO_4, NH_4 and HPO_4.

WE Array

There have been many previous investigations into acidic precipitation, especially in polluted areas, eg. Ayers and Gillett (1984). These investigations often directly link acid precipitation to sources of anthropogenic emissions of SO_2, NO_x and hydrocarbons. The remoteness of the sampling localities in the present investigation, however, minimises the effect of anthropogenic sources along the WE array.

As described in Chapter 4, the natural sources of NO_3 to rainfall may include biogenic emissions, biomass burning and lightning. The NOx emission rates for temperate grassland and agricultural land as taken from Galbally (1984) are listed in Table 5.18. While many of the localities along the WE array are situated on agricultural land predominantly used for grazing, the number of domestic grazing animals per acre is very low because of the poor suitability of the land in the arid regions of the array for grazing. Thus it seems more useful to compare emission rates from temperate grassland systems than from agricultural systems. It should be noted that there is a complete lack of information regarding the emission of NOx from desert areas. When agricultural emissions are ignored, the major contributors of NOx are soil emissions and lightning.

TABLE 5.18 Emission of NOx (g $N/m^2/a$) after Galbally 1984.

source	Emission
soil emissions temperate grassland	-0.006-0.08
soil emissions agricultural	0.04-0.26
biomass burning	0.003
lightning	0.05

The importance of lightning on the supply of NO_3 can be investigated by comparing the mean depositional flux of NO_3 for each season with the lightning. Figure 5.27 attempts to correlate between the total number of lightning flashes per day for Western Australia and the NO_3 fluxes for each sampling season. Maximum NO_3 deposition during summer 91 is matched by maximum number of lightning flashes, and there is a generally sympathetic trend between NO_3 deposition and lightning flash counts. Summer 92 does not fit into this general pattern however, with extremely high lightning counts being matched by average NO_3 deposition. This may be a function of the low rainfall amount during summer 92 (less than 0.5 mm/day), reflecting the dependence of flux on rainfall amount, or may be due to processes that occur after sample deposition that involve the consumption of NO_3.

Natural sources of SO_4 include seawater and gypsum from salt-lake material. Ayers and Gillett (1988a) suggest that SO_2 introduced by biogenic emissions or biomass burning may be significant precursors to acidification in tropical Australia. It is likely that these sources are much less significant in the semi-arid, and therefore less densely vegetated area of the WE array than is the seawater or gypsum source.

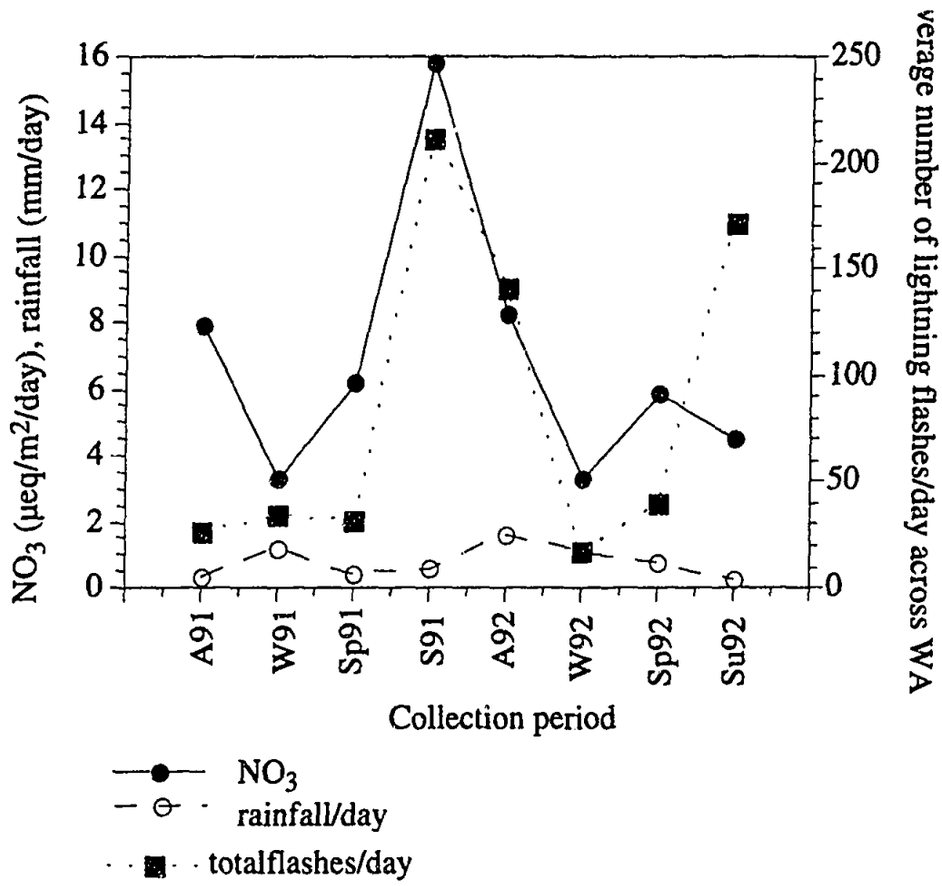

FIGURE 5.27 Deposition of NO_3 and rainfall per day for sites along the WE array and average number of lightning flashes for 10 lightning observation stations across Western Australia plotted as a function of seasons. There is a stronger relationship between rainfall per day and NO_3 deposition than between lightning flashes per day and NO_3 deposition. Monthly records of lightning flashes were obtained from the Bureau of Meteorology. The observation sites for WA include Albany, Geraldton, Kalgoorlie, Kununurra, Meekatharra, Moora, Perth Airport, Port Hedland and Three Springs. Observations are made using lightning flash counters. For the purpose of this work, total lightning flash counts per day is calculated by adding all lightning flashes recorded at all observation stations for each sampling period and dividing by the number of days in each sampling period.

Vesely (1990) investigated the change in H, NO_3 and NH_4 in rainwater samples over time, under various conditions of sample treatment and storage. He described bioconsumption as being caused by microbially induced oxidation of NH_4 (nitrification), which consumes NH_4 and produces NO_3 and H, or the assimilation of NH_4 into organic matter, which consumes NH_4 and produces H. Once all the NH_4 is consumed, or if initial NH_4 values were low, bioconsumption of NO_3 then proceeds, consuming NO_3 and H. These processes were found to occur at a greater rate under warmer conditions. An investigation of the depositional fluxes of NH_4 and H for each season for the WE data set, shows that H fluxes are constant throughout most of the sampling program, while NH_4 concentrations decrease during summer and

spring of each year (Figure 5.28). This suggests that NH_4 is being consumed during warm months, but other processes have a stronger effect on controlling the deposition of H. Because of the common association of NH_4 and K displayed in multivariate analyses, K deposition is also shown on Figure 5.28. High depositional fluxes of K are matched by high deposition of NH_4. The absence of a strong relationship between H, NH_4 and NO_3, as suggested by the work of Vesely (1990), indicates that either bioconsumption involves assimilation of NH_4 into organic matter, rather than the nitrification reaction, or that the supply of N_2O via lightning is far greater than that produced by bioconsumption, so that the bioconsumption of NO_3 is being swamped.

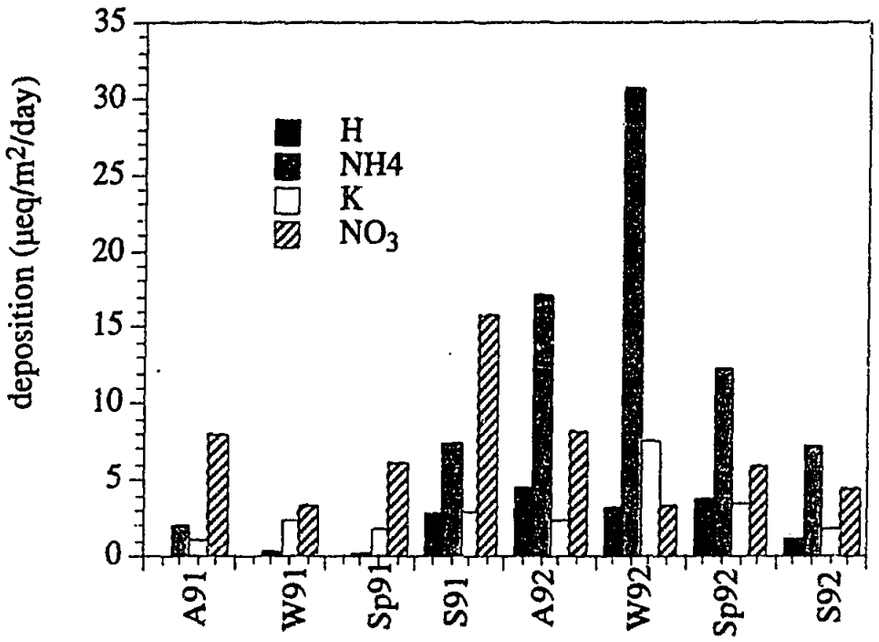

FIGURE 5.28 Seasonal variation in the deposition of H, NH_4, K and NO_3 for the WE array.

SN Array

As for the WE data set, the acid-base balance process in the SN data set is represented primarily by co-variance between H and NO_3. However, depending on the data subset used, SO_4, HPO_4, K, Ca and NH_4 may also vary in accordance with the more typical acid-base species. Anthropogenic sources of NO_3 and SO_4 to precipitation along the SN array cannot be completely discounted, because of the proximity of major areas of settlement to some of the collection sites; in particular Port Lincoln is 30 km north of site 26, Alice Springs is 100 km southwest of site 29,

and Katherine is 25 km south of site 32. As none of these settlements support industries that would emit large quantities of SO_2 or NO_x, the major anthropogenic emissions from these settlements would most likely be from motor vehicle use. However, the results of this work are insufficient to do more than acknowledge that anthropogenic sources of SO_4 and NO_x may play a small part in the acid-base balance of precipitation along the SN array.

Northern Subset

The northern data subset sees the covariance of H and NO_3 in the acid-base balance factor. Natural sources of NO_3 to tropical Australia have been summarised by Ayers and Gillett (1988a) and are listed in Table 5.19. The major input of nitrogen shown in Table 5.19 appears to be from biomass burning. This is because tropical Australia is prone to bushfires, both controlled burns and wildfires. It should be noted that site 33 is located at the CSIRO Kapalga research station where one of the major areas of research is the effect of burning on tropical ecosystems (Hurst et al 1994). While the collector was located in a natural fire compartment (i.e. no fires were deliberately lit), the adjacent compartments were burnt in late May-June (early burning), progressively (fires in late May-June followed by a series of fires as vegetation dries out downslope towards permanent water), and in September (late burning). The late burns were usually very hot, while the early burns were patchy and low temperature. Figure 5.29 shows the flux of NO_3 during all seasons at site 33 and the dates of burning in the adjacent compartments. While no relationship can be discerned between the dates of burning and NO_3 flux at site 33, the fact that burning occurs throughout most of the sampling program suggests that biomass burning should be an important source of nitrogen emissions in the north of the array.

TABLE 5.19 Summary of N inputs (tonnes/year) for northern Australia, after Ayers and Gillett (1988a).

source	input (tonnes/year)
biomass burning	388,000
soil emissions	33,000
lightning	23,000
anthropogenic (power stations, cars)	22,000

A comparison of NO_3 depositional fluxes and lightning flash rates at observation stations at Darwin and Tennant Creek are shown in Figure 5.30 There is a very strong correlation between deposition of NO_3 at site 33 (Kapalga) and lightning rate

at Darwin. The relationship between NO_3 deposition and lightning rate at Tennant Creek (site 30) is weaker but is still present. A direct relationship is also observed between lightning flash rate and rainfall amount. This has been observed by the Bureau of Meteorology (Ayers and Gillett 1988a). The absence of a strong relationship between lightning flash rate and NO_3 concentration (μeq/L) in rainfall, however suggests that the relationship between deposition of NO_3 and lightning flash rate displayed in Figure 5.30 primarily reflects the relationship between rainfall amount and lightning flash rate.

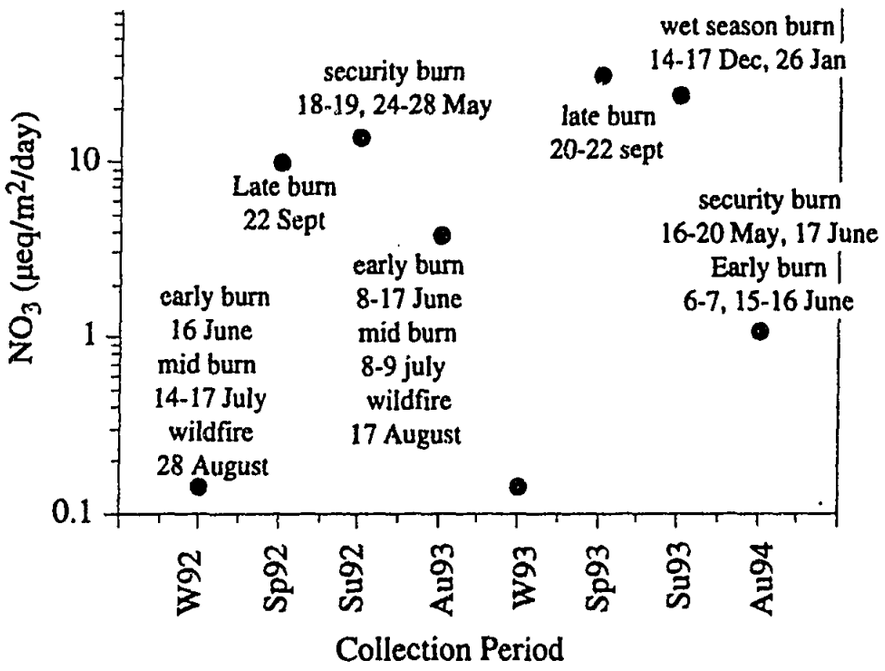

FIGURE 5.29 NO_3 deposition at Kapalga (site 33) and times and types of burns in adjacent compartments of the Kapalga Research Station. Burning occurred throughout the sampling program.

From the present study, the acid-base balances in the northern half of the SN array reflect the supply of NO_3 to the atmosphere by both biomass burning and lightning flash production of NO. While soil and vehicle emissions may also be important, there is insufficient evidence to discuss the extent of the importance of these sources. However, the clear relationships between lightning flash rates and NO_3 deposition, and the extent of burning throughout most of the sampling program suggest that lightning flashes and biomass burning are the most significant sources of NO_3 to the north of the SN array.

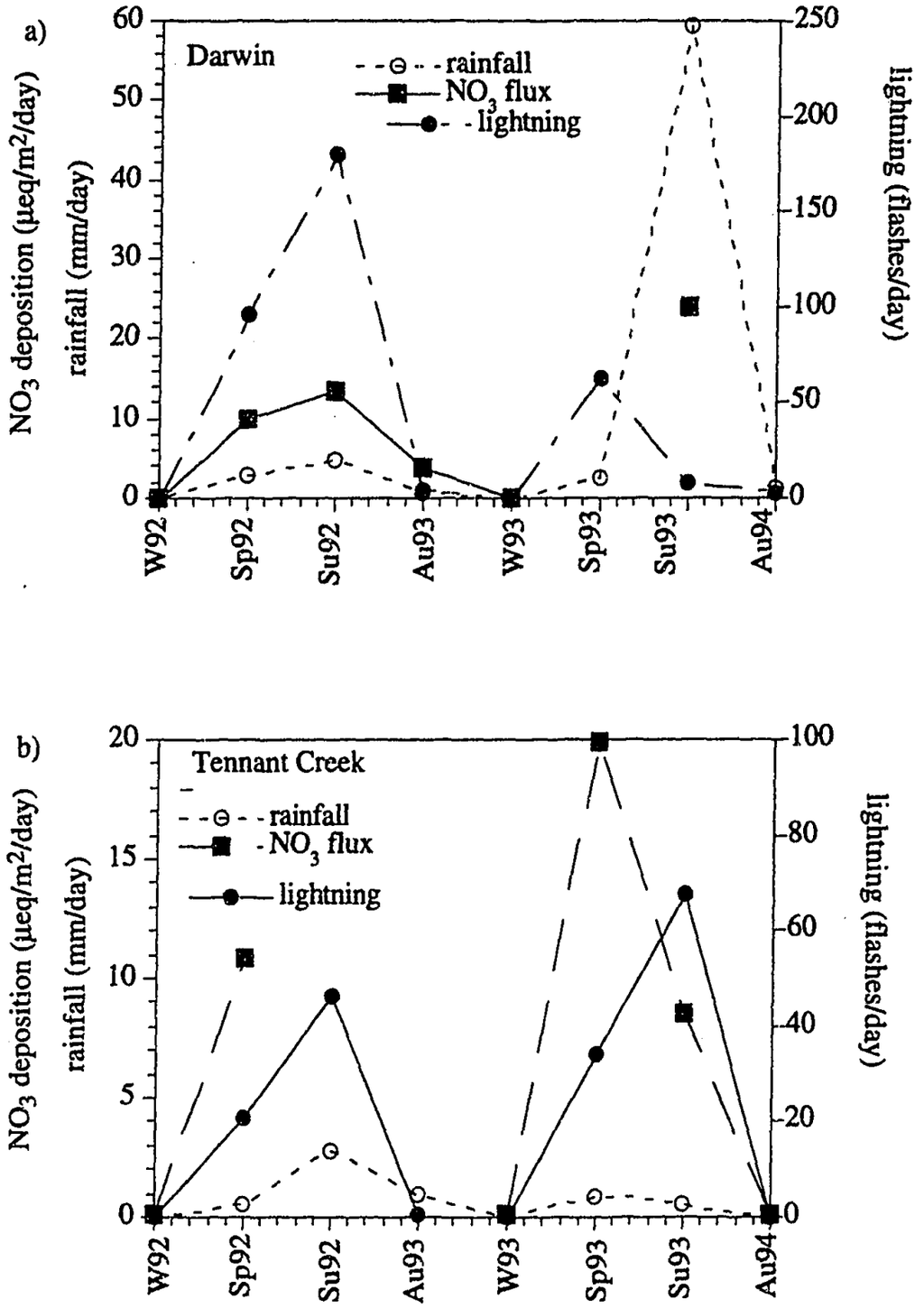

FIGURE 5.30 Mean NO_3 deposition, rainfall per day and lightning flashes per day for each season at a) Darwin and b) Tennant Creek. The postitive relationship between all three factors at each site suggests lightning to be a source of NO_3 in the north of Australia.

Southern Subset

The acid-base balance factor for the southern sites of the SN array explains variance primarily between NO_3 and H, with SO_4 and K also being significant. A comparison of lightning flash rates and NO_3 deposition for site 26 (Figure 5.31) reveals a very poor relationship, suggesting that lightning flash is not a major source of NO_3 to precipitation in the south of the SN array. Burning is also not as extensive in the south of the array as in the north. Thus, these two sources (burning and lightning) that are considered to be significant to the supply of NO_3 in the north of the array, do not appear to be significant in the south of the array, and the importance of soil, plant and anthropogenic emissions can only be suggested by default. SO_4 also has high loadings in this factor (except in the coastal data), and is most likely sourced from seasalt. Thus at coastal sites, the variance of SO_4 with other seawater-supplied species masks the variance of SO_4 with the acid-base balance species.

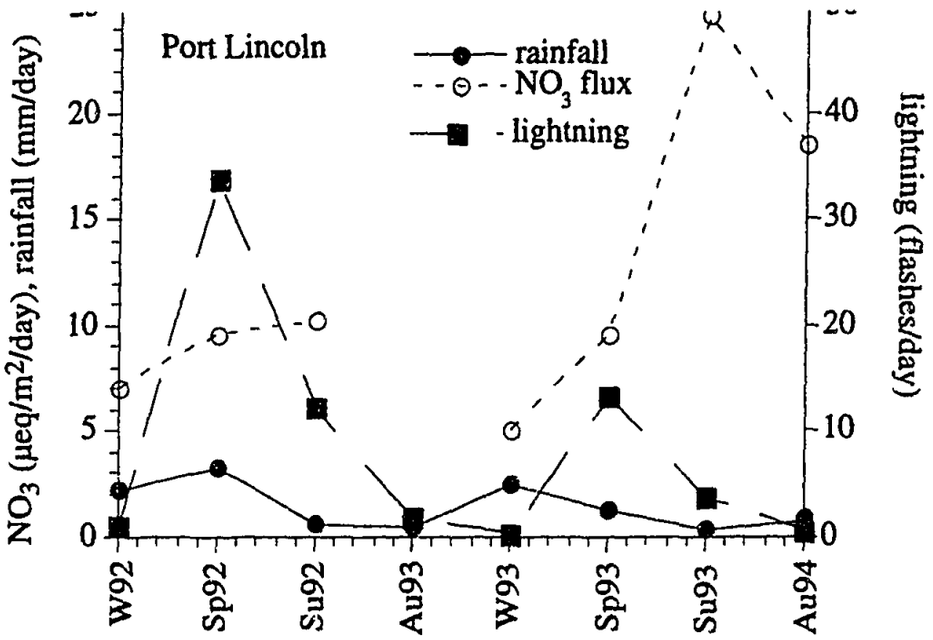

FIGURE 5.31 Mean NO_3 deposition, rainfall per day and lightning flashes per day during each season at Port Lincoln (site 26) in South Australia.

Biodegradation and a supply of agricultural material that group NH_4 and HPO_4 are suggested by the third factor of the multivariate analysis carried out on the southern subset of the SN data set. The agricultural source is not unexpected when it is considered that the southern sites of the SN array are located in areas of high density grazing. As discussed in Chapter 4, one of the largest sources of NH_3 to the atmosphere involves volatilization of animal urine. All sites in the southern section of the SN array are used for sheep and cattle grazing, with the highest density of domestic animals on the SN array, occurring on the property on which site 26 (Port

Lincoln) is located. The negative correlation of NH_4 with other species with high loadings in this factor may represent biodegradation of the sample. The source of HPO_4 is most probably fertiliser.

5.5 SUMMARY AND DISCUSSION

The major-element chemistry of precipitation from the WE and SN array shows the main influence on the composition of precipitation from remote areas of Australia is the mixing between a seawater and continental source. At most sites along the two arrays it is difficult to distinguish between the separate end-members of this source, except at coastal localities where seawater dominates the chemistry of precipitation. However, the influence of seawater can be discerned at non-coastal sites in association with favourable synoptic conditions, such as cold frontal activity in southern and western Australia during winter, and monsoonal activity in northern, Australia during summer. The continentally-derived end-member is most likely composed of re-suspended soil/dust material, including salt lake and calcareous dune components. In the south of the SN array where agriculture is intense this continental source may also include a fertiliser component. The chemistry of precipitation across Australia is also affected by an acid-base balance factor, the components of which are derived from natural sources such as biogenic emissions, biomass burning and lightning flash production. The nature of the collection program means that biodegradation is also a feature of rainfall chemistry.

Results from the major-element chemistry of precipitation provide information important for Chapter 6, in particular in the interpretation of $^{36}Cl/Cl$ ratio anomalies.

WE Array

Three processes affect the composition of rainfall along the WE array: the supply of a mixed seawater/continental source, acid-base balances and bioconsumption of the sample between deposition and sample collection. The extent of the influence of each of these factors is dependent on locality and/or season. Further, due to the well constrained composition of seawater, differences in the influence of the mixed continental/seawater source can be discussed in terms of the dominance of seawater and otherwise derived aerosols. The coastal site is dominated by a seawater source throughout most of the sampling program, while the effect of the seawater source at inland sites is dependent upon season. This seasonal dependence can be linked to weather patterns, eg. with increased cold front activity being conducive to the

transportation of seawater great distances inland, eg. as far as 1800 km to Everard Junction during winter 1991.

The acid-base balance describes the variations displayed in H and NO_3. Nitrate is supplied to the atmosphere by natural sources, including biogenic emissions of soils and via lightning strikes. The deposition of NO_3 is also dependent on season, and is associated with increased lightning occurring during summer of 1991. The third factor arises from biodegradation of the sample. This really represents modification of the rainfall after its deposition, rather than a possible source of influx of constituents to the sampling vessels. Biodegradation is also dependent on season, with maximum biodegradation occurring during warm seasons.

As discussed in Chapter 4, many of the previous investigations into the chemistry of precipitation of Western Australia have been concerned with the accession of salts to the landmass. The results from the present investigation can most usefully be directly compared with the results of Hingston and Gailitis (1976) who carried out a comprehensive investigation of 59 sites throughout WA, many of which coincide with sites in the present investigation. Figure 5.32 shows a figure from Hingston and Gailitis displaying the pattern of deposition of Cl (kg/ha) across Western Australia. Also shown on the diagram are the average deposition rates measured at each site in the present investigation. It can be seen that deposition measured in the present study falls within the ranges defined by the Cl isochrones calculated by Hingston and Gailitis dependent on locality. As in other investigations of rainfall chemistry from the southwest of the state (Farrington and Bartle 1988, Farrington et al 1993), deposition in the present investigation is lower than was measured in the southwest of Western Australia by Hingston and Gailitis. It has been suggested that Cl accession increases at inland sites when strong westerly onshore winds are able to transport oceanic seaspray inland (Farrington and Bartle 1988). This is supported in the present investigation by characteristically seawater compositions of precipitation up to 1800 km inland associated with enhanced cold frontal activity during winter months.

SN Array

Four processes affect the composition of rainfall along the SN array: supply of a seawater/continental source, acid-base balances, supply of an agricultural source material and biodegradation. The effect of these processes on the north and the south of the array is quite different. Sites in the north of the array have a large proportion of variance that can be explained in terms of a mixed

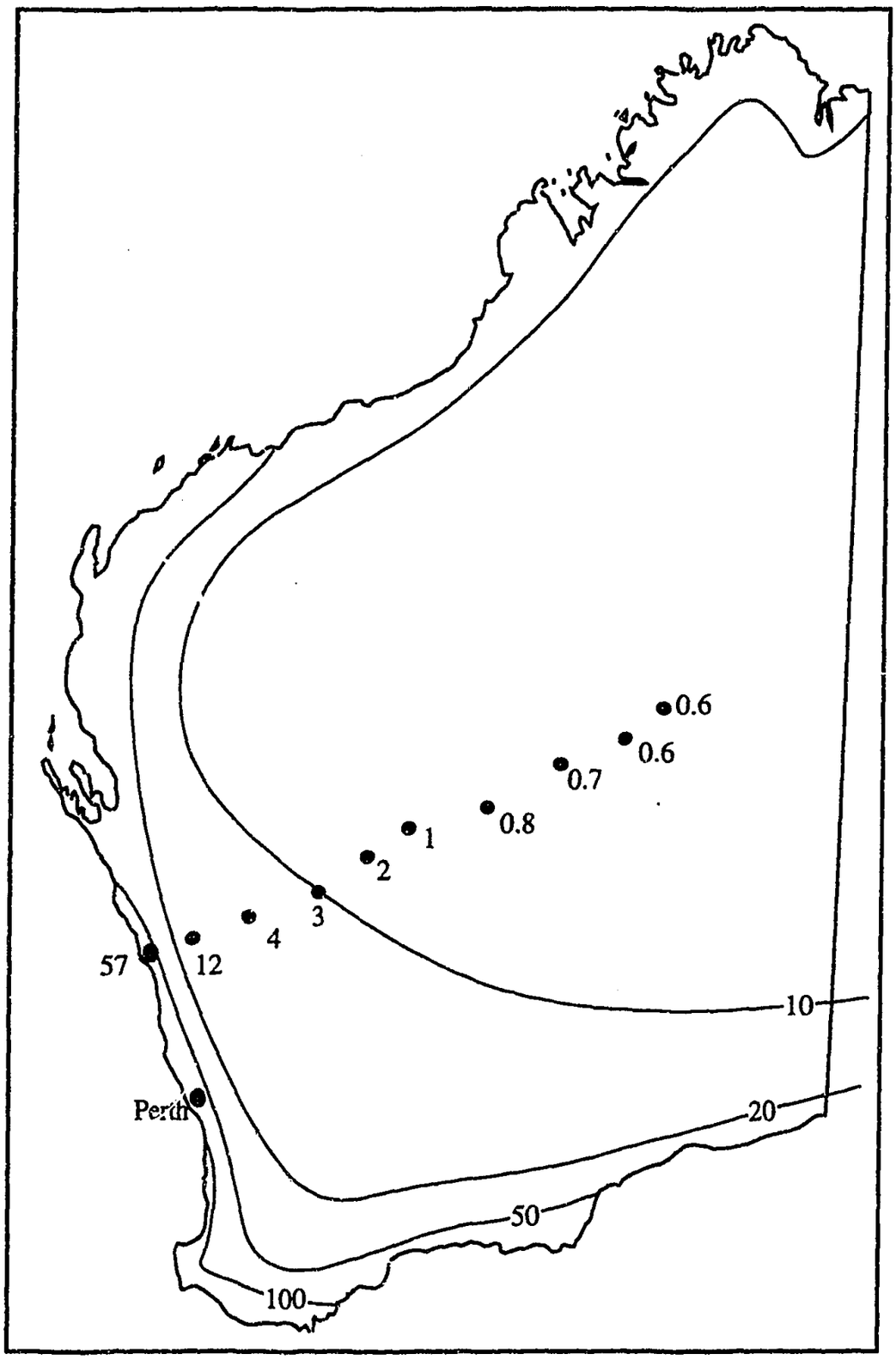

FIGURE 5.32 The mean Cl deposition rates for sites along the WE array (in kg Cl/ha) and the isochrons calculated from the investigation of Hingston and Gailitis 1976. The WE array shows broad agreement with the isochrons.

seawater/continental source. During the monsoonal period, seawater can be separated from the mixed seawater/continental source, but this only explains a small amount of variance. The extent of seawater influence from the north coast of Australia can only be seen as far inland as site 32 (~200 km), and only during the summer season when the monsoon occurs. Acid-base balances explain less than 20% of variance in the north of Australia, and are described by variation between H and NO_3. A seasonal variation in the supply of NO_3 to precipitation can be related to lightning flashes and rainfall amount in the north of Australia.

Sites in the south of the SN array are influenced by three factors, a mixed seawater/continental source, acid-base balances and a mixed agricultural input/biodegradation factor. The seawater source can be isolated for coastal sites 26 (Port Lincoln) and 27 (Gawler Ranges), and seawater can be seen to influence the composition of precipitation as far inland as site 28 (Wintinna) during winter of each year, in accordance with the strong influence of cold frontal precipitation from the south coast of Australia at this time of year. The acid-base factor is defined by covariance between H, NO_3, SO_4 and Ca, representing the supply of SO_4 by seasalt and the neutralising effect of $CaCO_3$ at the coastal locality. A mixed agricultural/biodegradation factor is suggested by covariance of HPO_4, NH_3, Ca and K.

It is difficult to make direct comparisons between previous investigations and the present investigation despite the extensive number of investigations into precipitation in the north of Australia (Table 4.1), due to of the difference in sample collection techniques. The present investigation uses bulk-depositional collectors and therefore incorporates both wet and dry deposition, while previous investigations in the Alligator Rivers Region (eg. Noller et al 1990, Gillett et al 1990) and Katherine (Galloway et al 1982, Likens et al 1987) looked at wet-only deposition. This means that comparisons of the rate of deposition of material between the different studies is unrealistic. However, some general comparisons can be seen between the various investigations: i) the large cation excesses over anions in the present study may be interpreted to suggest the presence of large amounts of organic acid anions as seen in previous studies (eg. Galloway et al 1982). ii) the importance of seawater as a source of material to monsoonal rain as suggested by Likens et al (1987) and Noller et al (1990), is supported in the present investigation, although, the tropical airmasses are modified of their marine character after movement 300 km inland. iii) contrary to previous investigations, is the correlation between lightning flash rates and NO_3 depositional flux shown strongly in the north of the SN array. This good correlation

most likely reflects the strong relationship displayed between lightning flash rate and rainfall amount (Ayers and Gillett 1988a).

Results from the Alice Springs collector (site 29) can be compared with those of Hutton (1983) for a site 100 km north of Alice Springs. Table 5.21 shows that concentrations measured in the present investigation are much lower than the volume weighted mean for 1958 to 1962 measured by Hutton. Also of note is the higher average amount of rainfall recorded during the present investigation. An individual rainstorm measured on 13/11/58 has a similar rainfall volume to the present investigation, and it can be seen from Table 5.21 that the concentrations measured in the present investigation are much more comparable to the high rainfall sample collected in 1958. This suggests that the difference displayed between the mean concentrations is a artifact of the rainfall volume.

TABLE 5.21 Comparison of a previous precipitation investigation at Alice Springs with the present investigation.

Investigation Alice Springs	rainfall mm	Cl µeq/L	SO_4 µeq/L	Na µeq/L	K µeq/L	Ca µeq/L	Mg µeq/L
13/11/58 (Hutton 1983)	30	4	20	8	2	20	10
*vwm 1957-1962 (Hutton 1983)	14	25	<30	28	9	32	23
1992-1994 (Present investigation)	55	6.3	12.2	8.6	3.1	9.6	4.8

* vwm=volume weighted mean

CHAPTER 6 CHLORINE-36

This chapter describes ^{36}Cl in precipitation from remote areas of Australia. It begins with a review of the production and fallout mechanisms of ^{36}Cl from the atmosphere (both natural and anthropogenic), followed by a description of observations. The chapter is concluded with a discussion of the observations and implications of this work for atmospheric and hydrologic investigations.

6.1 CHLORINE-36 PRODUCTION AND FALLOUT

Chlorine-36 is produced in the atmosphere and lithosphere by various reactions. In the atmosphere, it is formed by the cosmic ray spallation of ^{40}Ar. During the detonation of a thermonuclear device in a marine environment, neutron capture of ^{35}Cl may also inject large quantities of ^{36}Cl into the atmosphere as a single pulse (Schaeffer et al 1960). Within the top 2 m of the Earth's surface, cosmic ray spallation of ^{39}K and ^{40}Ca produces ^{36}Cl. Below 2 m, negative muon induced reactions become an important source of ^{36}Cl. At greater depths in the crust (>50 m), neutrons produced by U and Th decay and subsequently captured by ^{35}Cl are the dominant source of ^{36}Cl. Cosmic ray spallation in the upper few metres of the ocean produces large amounts of ^{36}Cl (30 atoms/m^2/s). However the $^{36}Cl/Cl$ ratio of oceanic water is low ($<1x10^{-15}$) due to dilution during oceanic circulation (Andrews and Fontes 1992).

This project is concerned with atmospherically produced ^{36}Cl, but production in the lithosphere may also contribute to groundwater systems. In general however, this contribution is very small compared to atmospheric production.

Natural Production and Fallout

Most of the production of ^{36}Cl by cosmic ray spallation occurs in the stratosphere with less than 40% occurring in the troposphere (Lal and Peters 1967). Stratospherically produced ^{36}Cl mixes with stable Cl (sometimes termed dead Cl), usually of marine and terrestrial origin in the troposphere, and it s beli ed that this mixed aerosol, containing ^{36}Cl and stable Cl, is quickly washed out as wet or dry precipitation. The residence time of aerosols in the troposphere has been calculated to be about one week (Turekian et al 1977).

The latitudinal dependence of ^{36}Cl fallout has been calculated by Lal and Peters (1967). Their values, which were based on production from ^{40}Ar alone, ranged from 5 atoms/m^2/s near the equator to a maximum of 28 atoms /m^2/s at 40°N, with a mean of 11 atoms/m^2/s. Onufriev (1968) suggested that neutron activation of ^{36}Ar should produce an additional fallout of 5 atoms/m^2/s. Accordingly, Bentley et al (1986a) reproduced the shape of the fallout curve of Lal and Peters (1967), but adopted a mean fallout of 16 atoms/m^2/s. More recently however, the cross sections for the neutron activation reaction of ^{36}Ar have been measured (Jiang et al 1990) and shown to result in negligible ^{36}Cl production. Best modern estimates (Andrews and Fontes 1992) use a mean fallout of 11 atoms/m^2/s. The most recent fallout curve dependent on geographic latitude is shown in Figure 6.1 and is taken from Andrews and Fontes (1992). This shows a reduction in the values reported in Bentley et al (1986a) by a factor or 11/16 and reproduces the curve of Lal and Peters (1967).

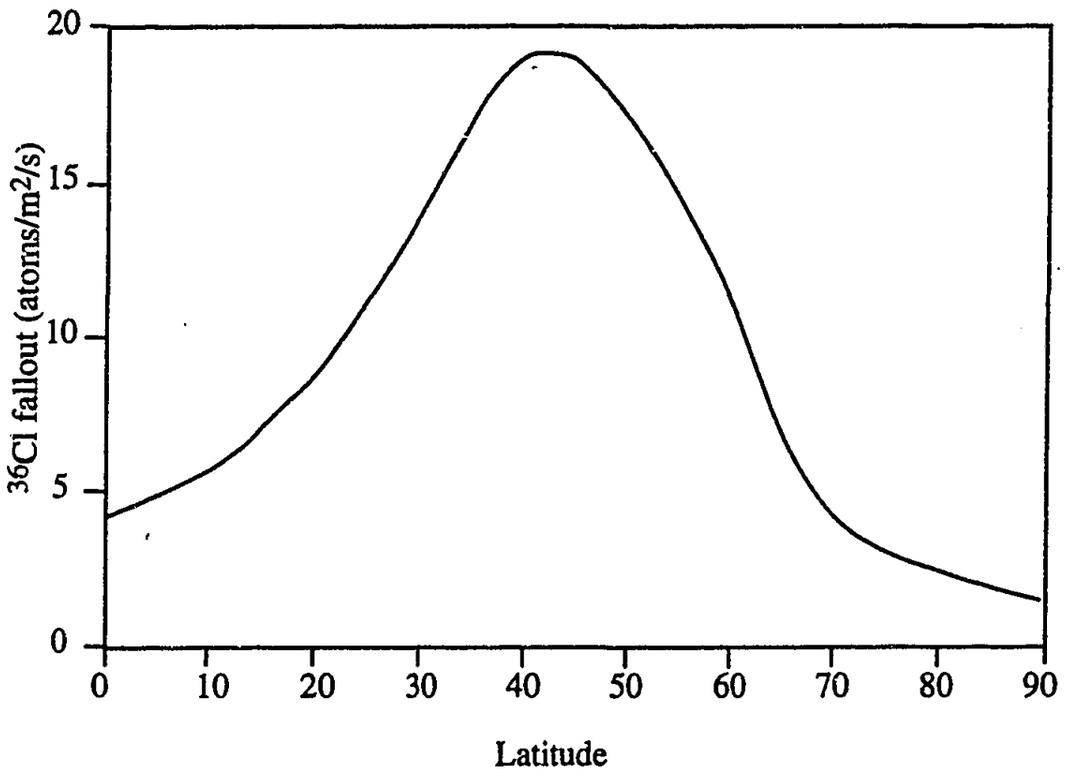

FIGURE 6.1 The pattern of fallout of ^{36}Cl as a function of latitude. From Andrews and Fontes 1992.

The latitudinal dependence of ^{36}Cl fallout has two components: i) variation due to the effect of the Earth's dipole and ii) variation due to the atmospheric transfer between the stratosphere and troposphere.

Geomagnetic Dependence

Cosmic ray fluxes to the Earth's surface are affected by the Earth's magnetic field. The geomagnetic dipole field of the Earth prevents charged particles below a certain rigidity (the ratio of the particle's momentum and charge) from penetrating into the atmosphere. The shielding effect is greatest at the equator, and decreases towards the magnetic poles. At geomagnetic latitude λ the minimum rigidity $R(\lambda)$ which can penetrate the atmosphere is given by

$$R(\lambda) = R_0 \cos^4\lambda \qquad (6.1)$$

where R_0 is the magnetic rigidity at the equator. Thus when a particle's rigidity at a certain latitude λ is less than $R(\lambda)$, it is unable to reach the atmosphere.

Variations in the flux of cosmic rays to the Earth's surface have been noted in association with the 11-year sun spot cycle (Lal and Peters 1962). It is well established that cosmic ray intensity decreases with increasing solar activity (Figure 6.2). Lal and Peters (1962) suggest that the average eleven-year cycle produces a fluctuation of about ±5% around mean global production of cosmogenic isotopes, and that the emission of high energy particles in solar flares may offset reduced isotopic production during periods of strong solar activity (i.e. during the sunspot maxima). Solar flares may also be responsible for major changes in the flux of cosmic rays to the Earth's surface (Lal and Peters 1962). Solar flares involve the emissions of high-energy particles from the sun and are rare even at the height of sun spot activity.

Transfer Between Atmospheric Domains

While the production of ^{36}Cl in the stratosphere is dependent upon geomagnetic latitude (Lal and Peters 1967), geographic latitude controls the transfer of stratospheric ^{36}Cl to the troposphere and the dispersion of the mixed aerosol in the troposphere. The most effective processes of transfer between the stratosphere and the troposphere involve mean meridional circulation dominated by Hadley circulation and large-scale eddy transports associated with the jet streams (Reiter 1975). Hadley cell circulation carries tropospheric air into the stratosphere at tropical latitudes and stratospheric air into the troposphere at middle and high latitudes (see Figures 2.1 and 2.2).

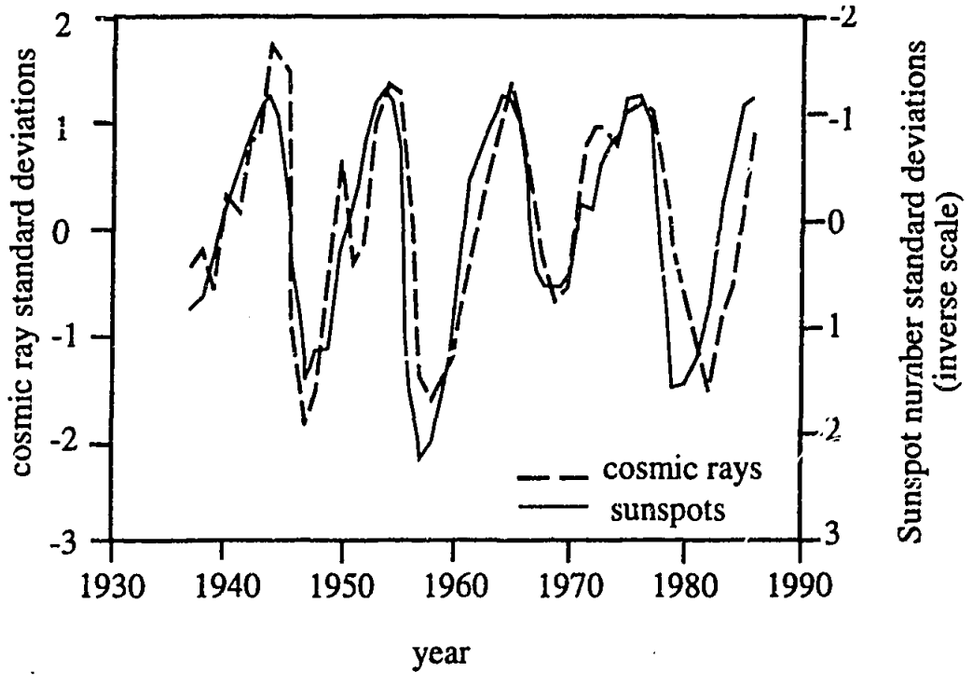

FIGURE 6.2 Comparison of groundlevel cosmic ray flux secondary-particle fluxes with sunspot number over the past 150 years. Cosmic ray fluxes are recorded by ionisation chambers and neutron monitors. The amplitudes are given in units of standard deviations (i.e. the number of standard deviations the value is from the normalised mean). All data points represent annual mean values. The correlation factor is -0.8. From Beer et al 1991.

Air circulation in the vicinity of the jet streams promotes air mass transfer from the stratosphere to the troposphere. Figure 6.3 shows a schematic north-south cross section through a jet stream. The tropopause is defined by the thick line. At the jet stream core, the tropopause cannot be defined and a gap appears. A frontal zone extends from the tropopause section on the right of the diagram into the lower troposphere. Circulation relative to the position of the jet stream causes air from the stratosphere to extrude into the frontal zone (as shown by the curved arrow). This process is also known as tropospheric folding (Danielsen 1968, Reiter 1975). Jet streams occur in the 30-50° latitude belt (subtropical jet stream) and more regularly in the 50-60° latitude belt (the stronger subpolar jet stream) where they are associated with cyclones (See chapter 2).

The combination of mean meridional circulation and large-scale eddy transports result in the transfer of 73% of the mass of the stratosphere, i.e. 38% by mean meridional flow, 15% from the northern hemisphere to the southern hemisphere, and 20% by large-scale eddy transport (Reiter 1975). Thus, maximum transfer of air from the stratosphere to the troposphere occurs in the middle latitudes (35-40°).

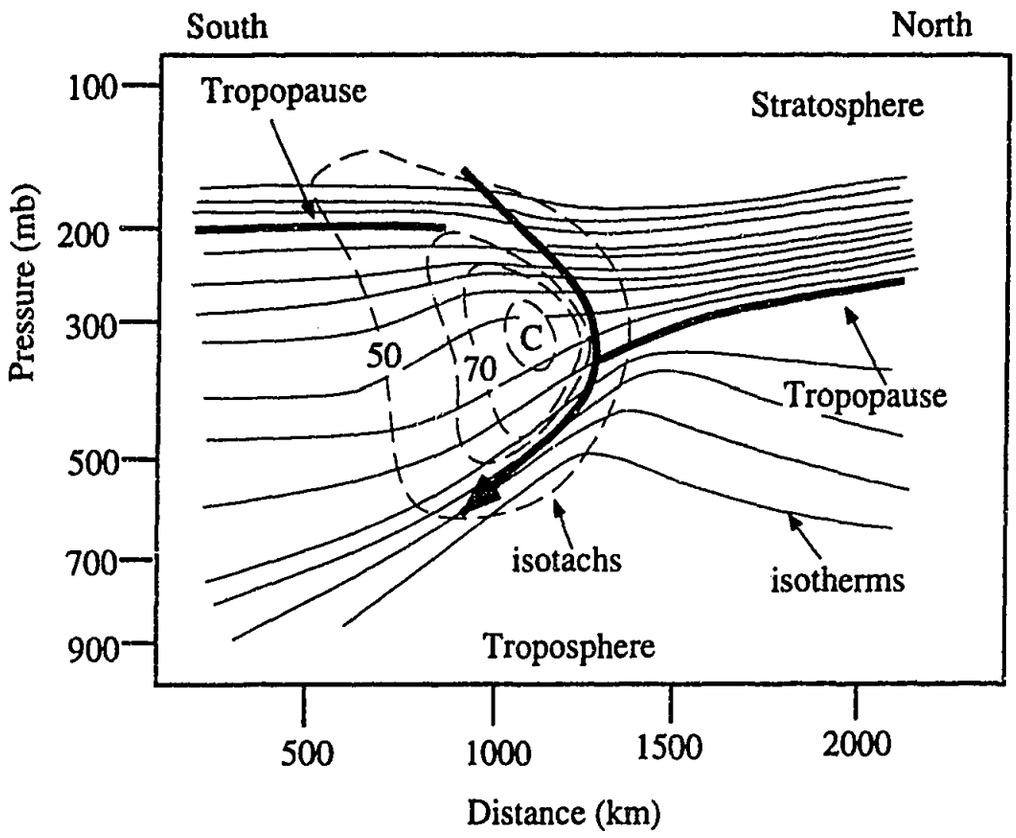

FIGURE 6.3 South-north cross section through a jet stream. Isotachs (lines of constant wind speed m/s) are shown as dashed lines, isotherms of potential temperature (temperature an air parcel would assume if compressed adiabatically to 1 bar) are solid lines. Tropopause is the solid thick line. The flow of air through the jet stream is the thick curved arrow. C is the core of the jet stream. After Warneck 1988.

Another significant mechanism of transfer of stratospheric air mass involves seasonal adjustments in the height of the mean tropopause level. This leads to changes in the mass of air contained in the stratosphere (Staley 1962), and is seen as a net flux (upwards or downward) of stratospheric air. Increased tropopause heights in the warmer seasons, promote inclusion of stratospheric air into the troposphere, where trace species such as ^{36}Cl can be scavenged. In addition for ^{36}Cl, more cosmic rays can penetrate the troposphere, enhancing the production of tropospheric ^{36}Cl. Based upon seasonal measurements of tropopause heights made at four different latitudes in the northern hemisphere, it was suggested that seasonal variations in the height of the tropopause results in transfer of 10% of the mass of the stratosphere (Reiter 1975). Small-scale eddy transport across the tropopause eg. penetration of thunderstorm cells into the lower stratosphere, result in transfer of less than 10% of material between the stratosphere and troposphere.

Air is also transferred across the interhemispheric tropical convergence zone (ITCZ) between the northern and southern hemispheres. Exchange between the two hemispheres occurs by eddy diffusion in the equatorial troposphere. However, most exchange occurs by seasonal shifts in the ITCZ, which lies to the north of the equator in July and may lie to the south of the equator in January, in the vicinity of Australia. The displacement is greatest over the Indian Ocean, highlighting the importance of the monsoon for interhemispheric exchange (Figure 2.2).

Warneck (1988) summarises movement of airmasses through the different atmospheric domains in terms of a four-box model, where the stratosphere and troposphere of each hemisphere belong to a separate box. The exchange rates shown in Figure 6.4 are summarised by Warneck from various tracer observations (including CO_2, $^{14}CO_2$, ^{185}W, ^{144}Co, ^{137}Cs, ^{54}Mn, ^{85}Kr, ^{90}Sr and meteorological data). This model treats the northern and southern hemispheres the same, i.e. assumes that the rate of stratospheric/tropospheric exchange is the same in both hemispheres.

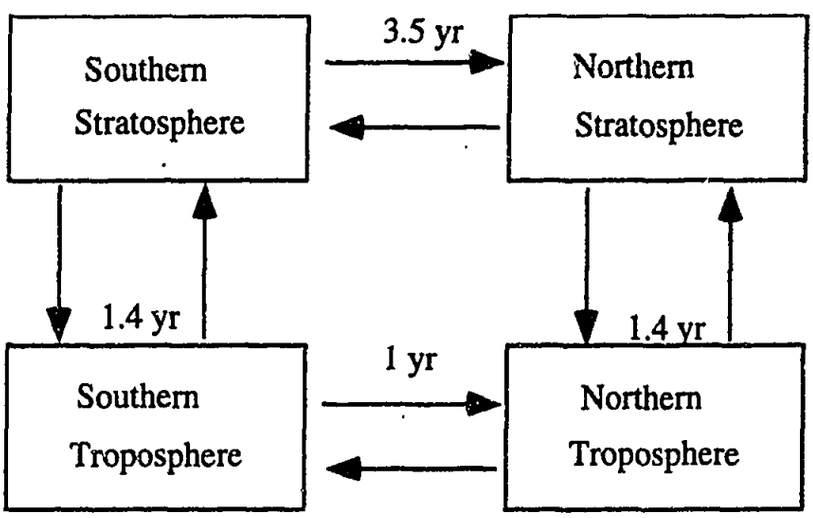

FIGURE 6.4 Standard four-box model of the atmospheric reservoirs and the rate of exchange between reservoirs. After Warneck 1988.

However, asymmetry in the exchange of material between the stratosphere and troposphere in the northern and southern hemispheres has been noted in several studies involving a variety of tracers. For example, the fallout of ^{90}Sr in the southern hemisphere was lower than in the northern hemisphere after atmospheric bomb tests (Lal and Peters 1962, Figure 6.5). Measurements of ^{10}Be in northern hemisphere precipitation also appear to be greater than in southern hemisphere precipitation. Raisbeck et al (1979) measured a deposition rate of 4.2 $x10^{-2}$ atoms $^{10}Be/cm^2/s$ at 39°N, and more recent measurements have been in agreement with

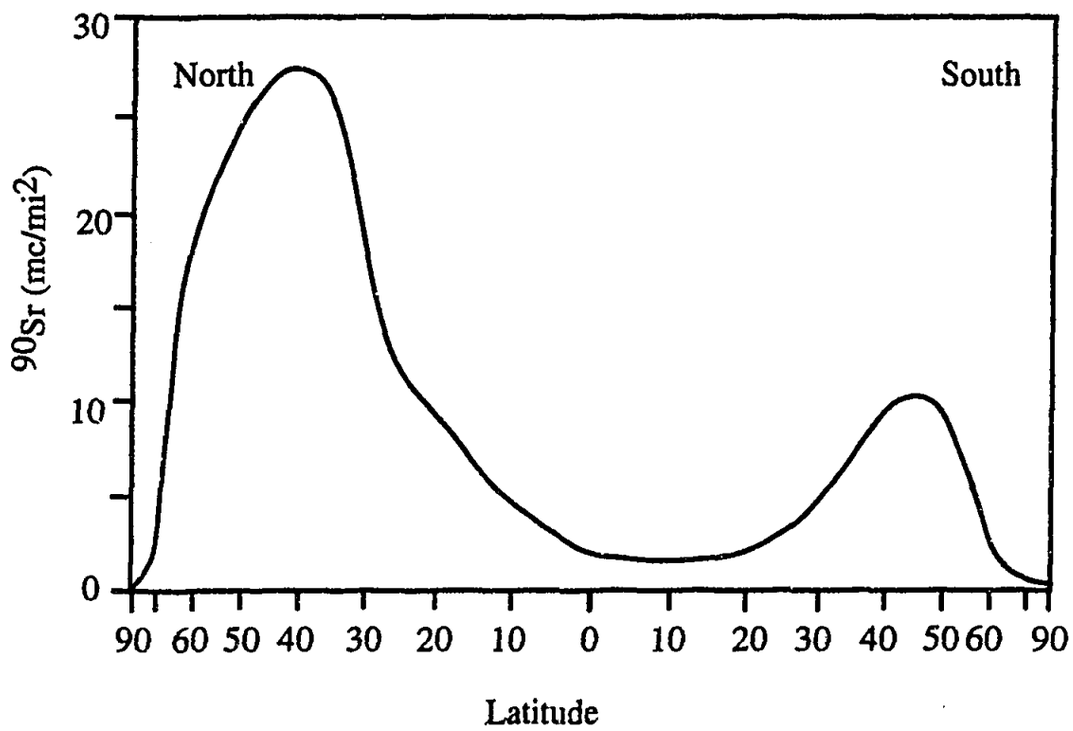

FIGURE 6.5 The fallout pattern of ^{90}Sr from the stratosphere in the northern and southern hemisphere. From Lal and Peters 1962.

this value (eg. 6.9 x10^{-2} ^{10}Be atoms/cm^2/s measured in precipitation at 40°N by Knies 1994 and 4.4 x10^{-2} ^{10}Be atoms/cm^2/s for continental sites in the US measured by Monaghan 1985/1986). A surface snow sample from Antarctica (Raisbeck et al 1978), however, gives a lower rate of deposition (3.1 x10^{-3} ^{10}Be atoms/cm^2/s), ten times lower than measured in Greenland ice. This extremely low value was attributed to the low rate of precipitation at the Antarctic site.

Investigations into the meridional distribution of ozone in the troposphere also highlighted this asymmetry between the hemispheres (Fabian and Pruchniewicz 1973). Peaks in ozone mixing were observed for northern hemisphere subtropical and high latitudes, while only occasional peaks were observed in the southern hemisphere subtropical latitudes. These peaks trace the latitudinal ranges where enhanced stratospheric/tropospheric exchange occurs in association with tropopause folding events. Figure 6.6 shows the mean ozone injection from the stratosphere as a function of latitude, based upon flight data (Fabian and Pruchniewicz 1973). Pruchniewicz (1973) attributed the asymmetry observed between northern and southern hemisphere ozone levels to the lower efficiency of the southern

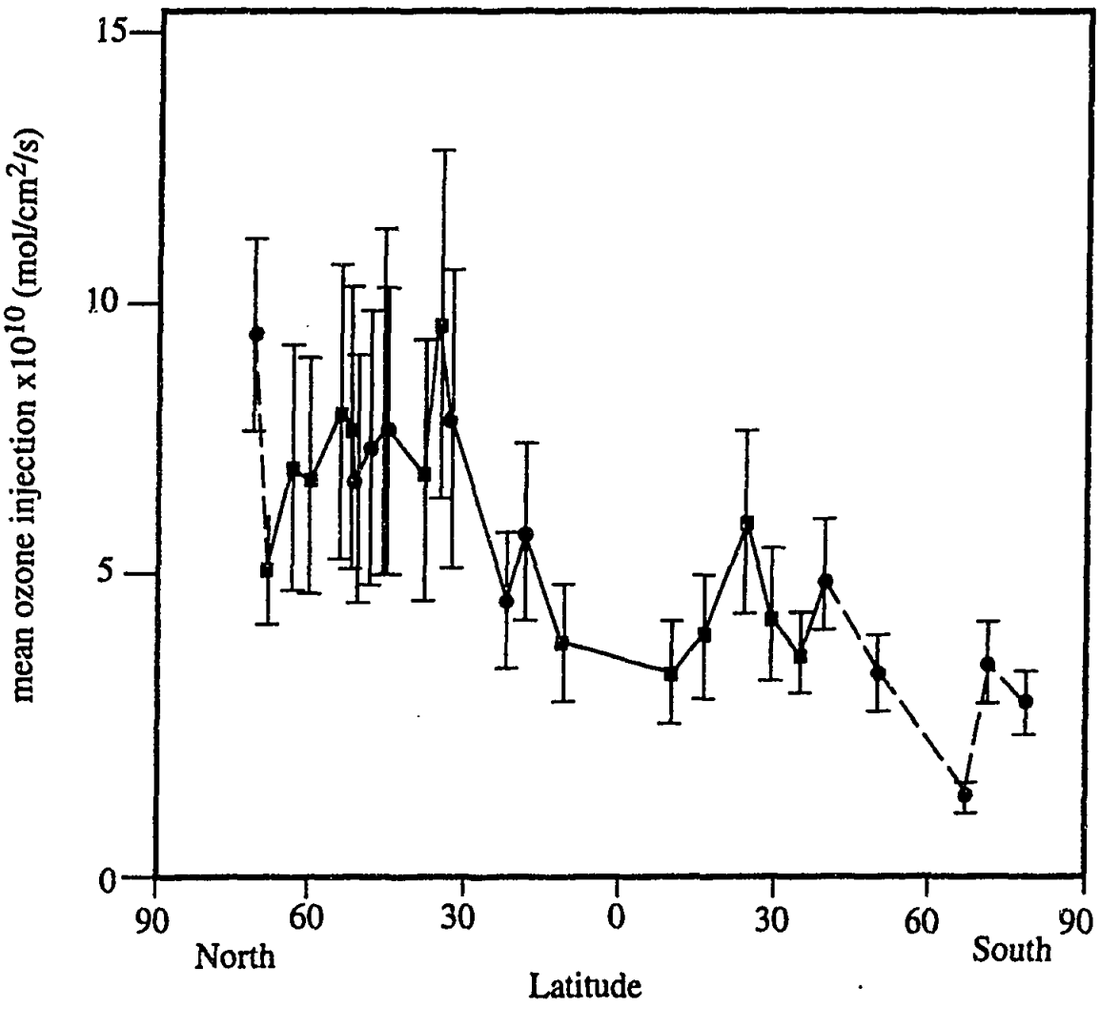

FIGURE 6.6 Mean ozone injection from the stratosphere as a function of latitude. From Faiben and Pruchniewicz (1977).

hemisphere gap region in transferring ozone from the stratosphere to the troposphere.

Holton (1990) used climate data to model the rate of flux of material between atmospheric domains and found transfer in the northern hemisphere to be 50% greater than in the southern hemisphere. In extratropical regions, poleward and downward transport of aerosols was found to be most robust during winter, and stronger in the northern hemisphere than in the southern hemisphere (Hitchman et al 1994). Robinson (1980), Holton (1990), Follows (1992) and Yulaeva et al (1994) attributed the enhanced poleward and downward transport of air during winter in the northern hemisphere to a more pronounced driving lower stratospheric wave. Lower stratospheric stationary waves are generated by orographic and thermal forcing in the troposphere, the effects of each process being equally important (Gill 1982, Smith 1979).

Orographic Forcing

Figure 6.7 shows a schematic representation of the role of mountains in producing stationary waves. Mountain waves have been observed, eg. in the Rocky Mountains and the Tibetan Plateau (Lilly et al 1974) and modelled (see Smith 1979 for a review of planetary-scale mountain wave models). Manabe and Terpstra 1974, used a complex three layer model to show that the disturbance to zonal air flow is stronger in the presence of mountains. Smith and Davies (1977) used a simpler two-layer model to show that in the absence of mountains recurring transient disturbances in the middle latitude wind flow occurred. In the presence of mountains large amplitude standing waves were produced, and the amplitudes of the transient waves decreased.

The smaller area of land mass and therefore lesser amount of topography in the southern hemisphere mean that less orographic production of stationary waves occurs in the southern hemisphere. This factor contributes to the reduced amount of lower stratospheric wave driving in the southern hemisphere.

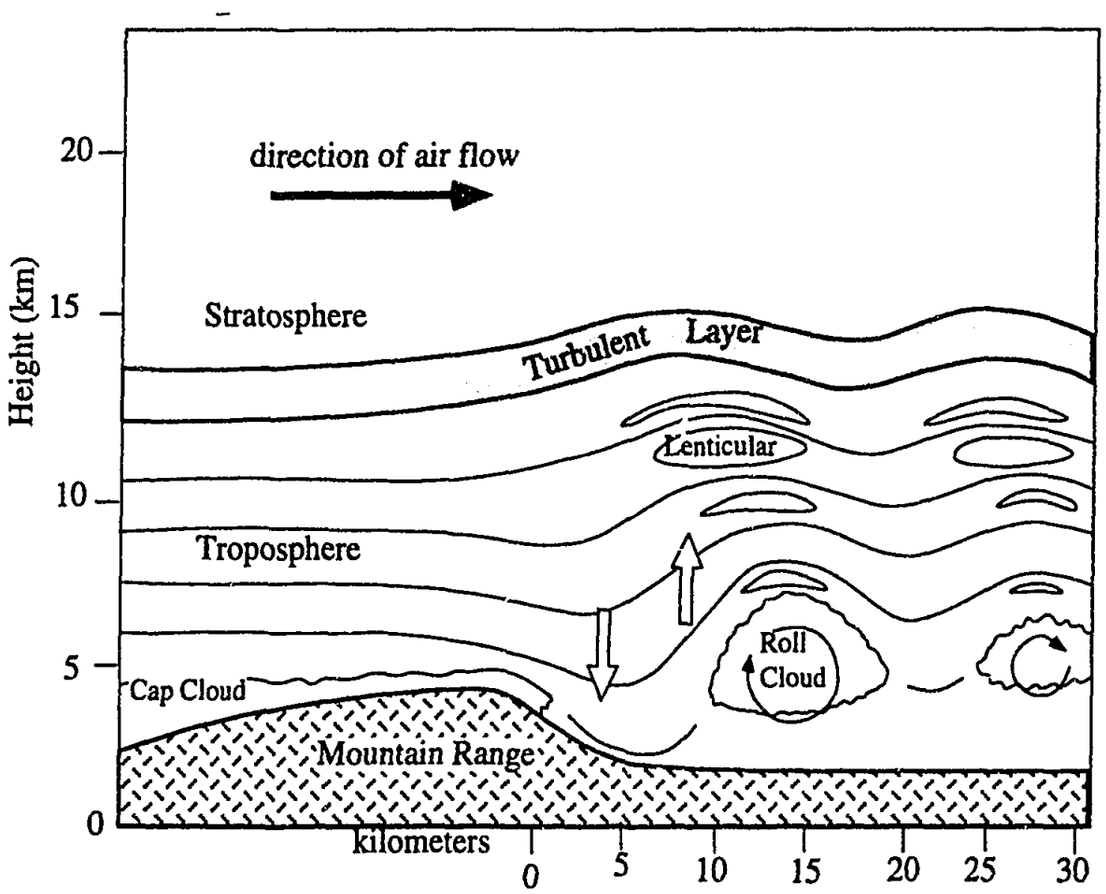

FIGURE 6.7 Schematic representation showing the formation of turbulence in the lower stratosphere by air flowing over mountains to produce mountain waves. After Gossard and Hooke 1975.

Thermal Forcing

Waves are able to propagate vertically if a uniform mean wind (U) is below a critical velocity (Uc), where Uc is dependent on the zonal and meridional components of the wave, the Coriolis effect, buoyancy and height. Arising from this transmission criteria, upward propagation of waves is forbidden in easterly and strong westerly winds (Plumb 1989).

Stationary waves have high amplitudes in the northern hemisphere during winter and are absent during summer. During the southern hemisphere winter, stationary waves have high amplitudes at the beginning and end of winter, but collapse in mid-winter. The behaviour of the southern hemisphere stationary waves is therefore not simply a reflection of tropospheric forcing, but can be explained in terms of the transmission criteria described above. During the southern hemisphere mid-winter westerly winds are too strong to permit vertical propagation of stationary waves. A feedback mechanism seems to exist in which the difference in the mid-winter wind regimes of the two hemispheres arises from the difference in thermal structure of the two hemispheres. The temperature of the southern hemisphere polar night is lower than that of the northern hemisphere polar night (Figure 6.8a). Departures from radiative equilibrium arise from differences in wave transport (Andrews 1989). Therefore the differences in geopotential heights between the two hemispheres in winter (Figure 6.8b) arise from the difference in wave transport, with the southern hemisphere waves being weaker.

Summary

In conclusion, the enhanced lower stratospheric wave driving in the northern hemisphere arises from the greater amount of orographic forcing, a consequence of the greater amount of land mass in the northern hemisphere. Differences in the thermal structure of the two hemispheres are also significant, giving rise to differences in mean zonal winds between the two hemispheres during winter. In the southern hemisphere, the mid-winter westerlies are stronger and therefore inhibit vertical propagation of the stationary waves. In the northern hemisphere, wave propagation in mid-winter is enabled as a result of the reduction to the mean westerlies by the waves themselves (Plumb 1989).

The ^{36}Cl prediction curve of Lal and Peters (1967) is constructed on the basis of the southern hemisphere representing a mirror image of the northern hemisphere in a similar way to the atmospheric box models discussed above. However, for the transfer of many species from the stratosphere to the troposphere (eg. ozone, ^{90}Sr)

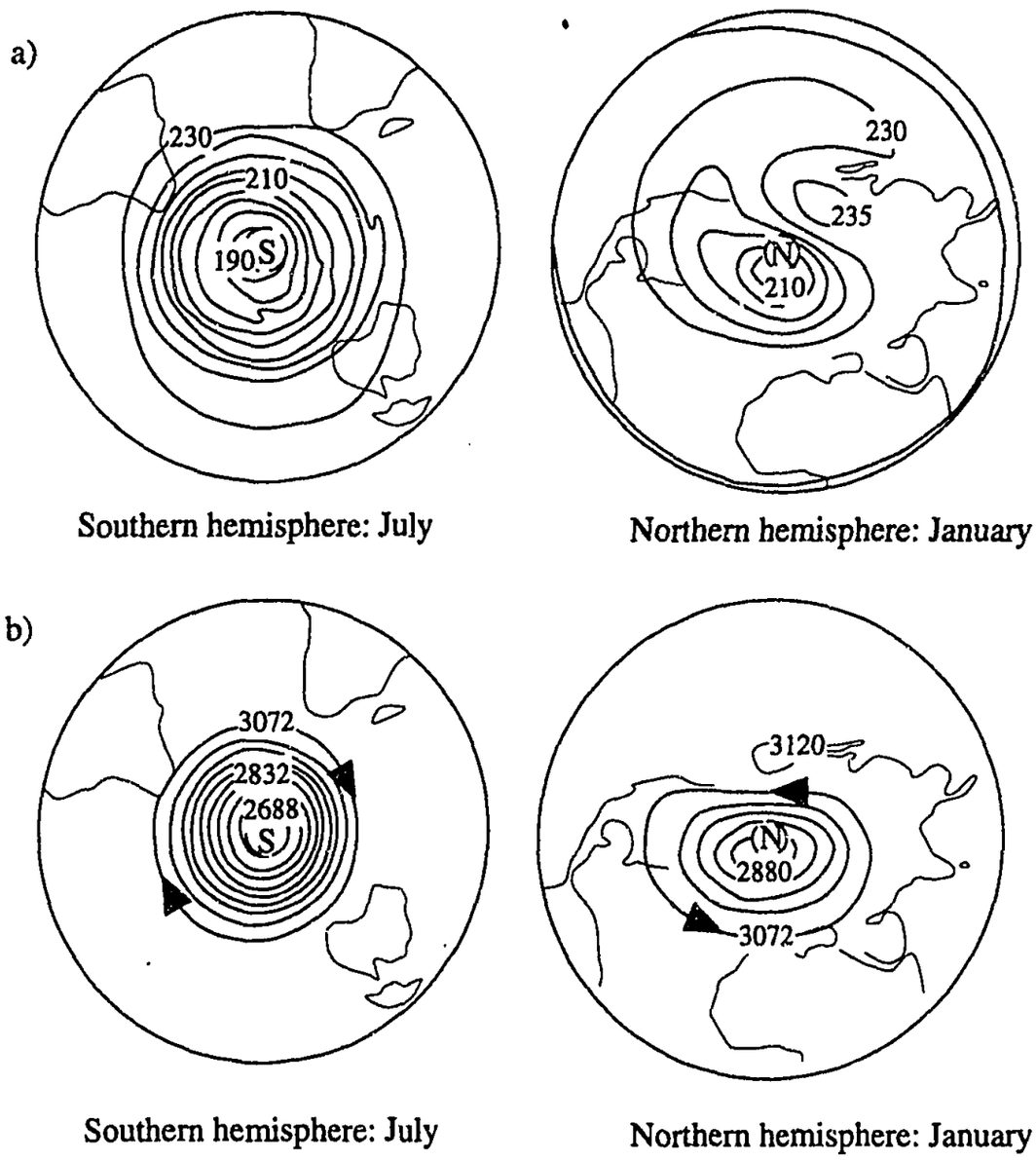

FIGURE 6.8 Polar stereographic maps of a) monthly averaged temperature (K) at 10 mb and b) monthly averaged geopotential height fields at 10 mb during winter in both hemispheres (i.e. July in the southern hemisphere and January in the northern hemisphere). Geopotential height field is calculated from the geopotential/9.8 m/s^2. Geopotential at a certain height in the atmosphere is the amount of work required to move a unit mass from sea-level to that height. Note the zonal symmetries displayed by both parameters for the southern hemisphere winter. Arrows in b) represent direction of geostrophic flow.

this is not the case, and up to 50% less transfer appears to occur in the southern hemisphere. This difference may be reflected in the fallout of ^{36}Cl, with lower values being observed in the present investigation than those measured for the northern hemisphere.

Anthropogenic Production and Fallout

During the 1950s large amounts of ^{36}Cl were injected into the stratosphere by thermonuclear weapons tests in marine environments. Chlorine-36 was produced by the neutron capture of ^{35}Cl in seawater. This injection of ^{36}Cl has become known as the 'bomb pulse'. The bomb pulse was characterised by fallout levels that peaked at 1,000 times the background levels in middle latitudes and occurred between 1953 and 1964 (Schaeffer et al 1960, Bentley et al 1982). The elevated ^{36}Cl levels associated with the bomb pulse are recorded in the Dye-3 Greenland ice core (Elmore et al 1982, Suter et al 1987, Synal et al 1990), the Camp Century ice core (Elmore et al 1987), soils from New Mexico (Phillips et al 1988) and Australia (Fifield et al 1987), and groundwaters from Ontario (Bentley et al 1986a). At Maralinga in South Australia, the site of British nuclear weapons tests during the 1950s, localised $^{36}Cl/Cl$ ratios of up to 10^{-11} occur (Bird et al 1991).

In the Dye-3 Greenland ice core, ^{36}Cl levels in 1957 corresponded to 500 times the background level (Elmore et al 1982, Suter et al 1987). Synal et al (1990) used the data from the Greenland ice core to develop a model of atmospheric bomb-produced ^{36}Cl, and calculated a residence time of 2±0.3 years for bomb-produced ^{36}Cl in the stratosphere. Bentley et al (1982) modelled ^{36}Cl fallout from nuclear tests by using estimates of ^{36}Cl injection into the stratosphere from individual explosions as input for an atmospheric box model. The model was calibrated using the ^{36}Cl concentrations in rainfall reported by Schaeffer et al (1960). In general, good agreement was found between the model and the ^{36}Cl levels found in the Dye-3 Greenland ice core.

As the levels of ^{36}Cl associated with the bomb pulse are so much greater than background levels, the bomb pulse is a useful environmental tracer, eg. in the study of hydraulic flow and dispersive mixing in groundwater investigations. The long half-life of ^{36}Cl eliminates ambiguities that result from decay and dispersive mixing when other radionuclides, such as tritium are used.

Results obtained from the Dye-3 Greenland ice core showed that ^{36}Cl produced during the weapons tests of the 1950s was influencing precipitation until as late as 1985 (Suter et al 1987). While the present-day ^{36}Cl fallout levels have again reached pre-nuclear weapons testing levels, neutron capture of ^{35}Cl associated with nuclear technology may occur on a local scale, eg. nuclear reactor or processing operations. For example, operation of the HIFAR reactor at Lucas Heights, Sydney

Australia has produced ratios up to 10^{-11} on the reactor site (Bird et al 1991). These levels are not considered an environmental hazard. Much more significantly, nuclear reactor accidents such as Chernobyl, have released considerable amounts of ^{36}Cl into the environment (Andrews and Fontes 1992).

6.2 PREVIOUS ^{36}Cl PRECIPITATION INVESTIGATIONS

The first measurements of ^{36}Cl in rainfall were from Long Island, USA, during the period of nuclear weapons testing in the 1950s (Schaeffer et al 1960). As discussed above, levels of ^{36}Cl were several orders of magnitude above background levels. These large values were measured in a screen-wall counter, a technique whose detection limit is too high to measure background levels of ^{36}Cl. With the refinement of AMS, it has become possible to measure much lower levels of ^{36}Cl. For example, Elmore et al (1979) measured ^{36}Cl concentrations in seawater and surface waters from North America with a background level of $3x10^{-15}$ $^{36}Cl/Cl$. Finkel et al (1980) measured ^{36}Cl in ice, rain and upper seawater levels in Antarctica. Variations of up to three orders of magnitude were observed in snow and firn and were attributed to the effects of atmospheric mixing and scavenging, or to radioactive decay of ^{36}Cl in the very old ice. A rainfall sample measured by Finkel et al (1980) showed ^{36}Cl levels lower than rainfall collected during the early 1960s, showing the decrease in atmospheric ^{36}Cl derived from nuclear weapons tests.

Investigations of anthropogenic levels of ^{36}Cl in ice-cores were discussed in the previous section. Pre-bomb ^{36}Cl concentrations of ice from the Dye-3 Greenland ice core were also measured and found to be 3 to 5 times greater than predicted from production rate calculations (Suter et al 1987). In contrast, the global fallout rate of ^{36}Cl estimated from measurements of Antarctic ice (Nishiizumi et al 1979, Finkel et al 1980 and Nishiizumi et al 1983) were close to the predicted calculations. (Table 6.1). Reliable ^{36}Cl fallouts of between 10 and 14 atoms/m^2/s can be deduced from the ^{36}Cl concentrations measured in the surface ice samples when snow deposition rate and latitude are taken into account.

Chlorine-36 has been used as a tool to model evapotranspirative loss from the upper Jordan River catchment (Magaritz et al 1990). Stable Cl concentrations and $^{36}Cl/Cl$ ratios of several water bodies were compared with those of precipitation, and were found to experience between 40 to 90% evapotranspirative loss. The representative precipitation sample was Mt Hermon snow (latitude 32.5°N), which had a ratio of 1589 ± 12 $^{36}Cl/Cl$ and was calculated to be made up of less than 1% of bomb-produced ^{36}Cl.

TABLE 6.1 Concentration of ^{36}Cl in ice from Antarctica and the estimated ^{36}Cl fallout calculated from A=fc/s (from Nishiizumi et al 1979), where A is ^{36}Cl concentration (atoms/kg of ice), f is fallout, c is latitude scaling factor (0.4 at 70°) and s is snow deposition rate (5 cm/y) .

sample	^{36}Cl atoms/kg of ice ($x10^6$)	^{36}Cl fallout (atoms/m^2/s)	Reference
Yamato Mountains	2.5	9.9	Nishiizumi 1979
Allan Hills	2.6±0.1	10.3	Finkel 1980
	7.5±0.3*	30	
	2.8±0.2	11.1	
	3.6±0.2	14.2	
Siple Firn	8.7±0.8**	34	
Allan Hills (0-12 cm)	3.38±0.2	13.4	Nishiizumi 1983
Yamato Mountains c-8	3.17±0.22	12.6	

*higher snow accumulation rate

** remelting of old ice near the surface of the ice sheet (based on field evidence) may have allowed incorporation of bomb ^{36}Cl in the modern ice

Herut et al (1992) investigated the ^{36}Cl composition of Cl-rich rainwater (defined as having greater than 2.9 meq/L Cl) from Israel. A positive strong correlation between $^{36}Cl/Cl$ ratio and Cl concentration was interpreted as a solute relationship defined by mixing between two endmembers, sea-spray with a low $^{36}Cl/Cl$ ratio and Cl-rich marine-dust aerosol with a high $^{36}Cl/Cl$ ratio.

Hainsworth (1994) measured the ^{36}Cl levels in monthly rainfall from Maryland, USA. Seasonal changes in the flux of ^{36}Cl were observed, with a maximum in the northern hemisphere spring reflecting the seasonal changes in stratospheric-tropospheric mixing. Wet-only collectors were compared with bulk depositional collectors, and dry deposition was estimated to account for 25% of flux to the site, being significant during periods of low rainfall. The mean depositional flux at the Maryland site was 59±8 ^{36}Cl atoms/m^2/s, three times greater than that predicted for latitude 38°N, but in accordance with the fallouts measured in the pre-bomb Dye-3 Greenland ice cores (Suter et al 1987).

Ratios of $^{36}Cl/Cl$ ratios in surface waters from the Susquehanna River basin (Pennsylvania) and groundwaters from the Aquia Aquifer (Maryland) were found to be 3 to 5 times higher than predicted by Bentley et al (1986a). Hainsworth (1994)

recalculated the depositional pattern of $^{36}Cl/Cl$ for the USA based upon the deposition pattern of ^{90}Sr. The model included latitudinal and longitudinal variations in ^{36}Cl deposition. The longitudinal variations arise due to the effect of topography on stratospheric/tropospheric mixing. The recalculated $^{36}Cl/Cl$ deposition pattern agreed with that of Bentley but values were two times greater than Bentley's. Bulk-deposition samples were collected from six sites in eastern USA and one site in central northern USA. The measured $^{36}Cl/Cl$ ratios agreed with the predictions of Hainsworth for the eastern sites, but were anomalously high for the central site (i.e. measured at 4220 $x10^{-15}$, when predicted to be between 1200 $x10^{-15}$ and 1600 $x10^{-15}$ by Hainsworth). Measured fluxes were two times greater than Hainsworth's predictions and stable Cl was two times greater than measurements from the National Atmospheric Deposition Program. These discrepancies were attributed to a combination of oversampling, recycling of crustal material and dry deposition. A global production of 40 atoms/m^2/s was suggested, almost four times greater than that predicted by Lal and Peters (1967).

Knies (1994) measured ^{36}Cl, ^{10}Be and ^{7}Be from wet deposition in Illinios, USA. Fluxes of each isotope correlated with precipitation amount. The mean flux of ^{36}Cl was measured to be 67±5 ^{36}Cl atoms/in^2/s, approximately four times that predicted even when dry deposition of 15% was taken into account.

In summary, measurements of ^{36}Cl in precipitation from the northern hemisphere suggest a ^{36}Cl fallout that is 3-5 times greater than predicted by Lal and Peters (1967). The few published values of ^{36}Cl in the southern hemisphere (i.e. Antarctic ice measured by Nishiizumi et al 1979, Finkel et al 1980 and Nishiizumi et al 1983) suggests a fallout that is only slightly higher than the predictions of Lal and Peters (1967), i.e. a factor 3 less than in the northern hemisphere. Data from the present investigation allows a detailed examination of the discrepancy between northern and southern hemisphere fallout estimates.

6.3 CHLORINE-36 INVESTIGATIONS IN AUSTRALIA

There have been many $^{36}Cl/Cl$ measurements made on samples from various parts of the Australian environment. These have all been measured by the AMS group in the Research School of Physical Sciences and Engineering at the Australian National University with the exception of early measurements on the Great Artesian Basin (Bentley et al 1986b). Some early results are reported in Fifield et al 1987, Davie et al (1989) and Bird et al (1991), although a substantial body of data is awaiting

publication. The following discussion will focus on those studies for which the atmospheric deposition results from the present investigation may be of particular relevance.

The present study has relevance to groundwater investigations, as precipitation provides the means of input of ^{36}Cl to groundwater systems. The Great Artesian Basin showed the application of ^{36}Cl to date groundwater greater than 1 Ma (Bentley et al 1986b). The Great Artesian Basin occupies one fifth of the area of Australia, and is located in central and northeastern Australia. Recharge to the basin occurs along the coastal ranges of northeast Australia, and outflow emerges near Lake Eyre in central Australia. Ages of the groundwater ranged between less than 100,000 years and greater than 1 Ma, and were in agreement with age estimates from hydraulic models. The $^{36}Cl/Cl$ ratio was found to be constant in the recharge area and decreased smoothly away from the recharge zone. The $^{36}Cl/Cl$ ratio at the recharge zone was used as an estimate of the initial $^{36}Cl/Cl$ ratio required in the age calculation.

Davie et al (1989) used $^{36}Cl/Cl$ ratios to identify chlorides of different origins in groundwater from the Mallee region of the Murray-Darling Basin, southeastern Australia. Isotope ratios were found to increase in the direction of flow. This trend was opposite to that expected based upon probable relative ages since recharge, and was interpreted as the influx of saline groundwater along the flow path. The generally low $^{36}Cl/Cl$ ratios and the associated increases in Cl along the flow lines were interpreted as the percolation of rainwater downwards at several places within the aquifer.

A major increase in stable Cl concentration and falling $^{36}Cl/Cl$ ratios was noted in the downflow (from east to west) direction of the Lachlan Fan area of the Murray-Darling Basin (Bird et al 1989). The young age of the groundwater (<<300,000 years) ruled out decay as being an explanation of this increase. Instead, evaporation and dissolution of a constant ratio chloride was invoked as a cause.

Simpson and Herczeg (1994) reinterpreted data on the stable Cl concentration of rainfall from eastern Australia and concluded that it consisted of up to 50% recycled Cl. It was recognised that this has implications for the calculated $^{36}Cl/Cl$ ratios as a function of distance from the coast for the Murray-Darling basin. If marine Cl accounts for only half of the Cl in rain, the $^{36}Cl/Cl$ ratio would be twice that calculated for Cl that is 100% marine in origin if the $^{36}Cl/Cl$ composition of the

recycled component is comparable with recent precipitation rather than the low ratios typical of seawater. The present investigation may tell us something about the recycled Cl component by comparing the measured ratio with a recalculated ratio based upon latitude and distance from the coast.

Salt lakes provide a source of recycled Cl to precipitation. Relatively low ratios (30-60x10^{-15}) are found in salt lakes mainly from Western Australia (Fifield et al 1987). The lack of variation in the ratios as a function of location, and the similarity of the average ratio to granites, was interpreted as weathering of surface rocks as being the main source of ^{36}Cl to the salt lakes. However, further investigations of the ^{36}Cl content of halite from Western Australian salt lakes found that ^{36}Cl/Cl ratios in halites from salt lakes in Western Australia showed increasing ratios with increasing distance from the coast (Chivas et al 1994). The present investigation, by measuring precipitation of ^{36}Cl in the vicinity of the Western Australian salt lakes, may provide further insight to this suggestion of the source of ^{36}Cl to salt lakes.

The results of previous investigations of ^{36}Cl in the Australian landscape highlight several areas in which basic measurements of ^{36}Cl are necessary in order to fully interpret existing ^{36}Cl data. For example, although good agreement was found between predicted ^{36}Cl/Cl ratios of precipitation and measured values of ^{36}Cl/Cl in recharge waters in the Mallee area of the Murray-Darling Basin (Davie et al 1989), recharge ratios in the Lachlan River region were higher than the calculated values (Bird et al 1989). This was also the case for the Great Artesian Basin (Bentley et al 1986b). Thus there is a need for more information on the Cl and ^{36}Cl precipitation rates as a function of latitude and distance from the coast. Bird et al (1991) also speculated that the ^{36}Cl/Cl ratios in tropical rainfall would be low because of the very high rainfall carrying marine Cl. Recycled solids in rainfall from inland Australia would be expected to contribute to high ^{36}Cl/Cl ratios in meteoric fallout at inland sites.

The investigation of the ^{36}Cl in precipitation from the two arrays established in this research project provides some of the basic information required to fully interpret existing ^{36}Cl data. The WE array allows an investigation of the change in ^{36}Cl/Cl ratios with changing distance from the coast. The SN array allows an assessment of the latitudinal dependence of ^{36}Cl fallout. Both arrays provide information on the seasonal variations of the ^{36}Cl in precipitation.

6.4 THE DATA SET

The ^{36}Cl data set is made up of 115 (of a possible 144) values spread over the 18 sites that make up the WE and SN arrays. Samples excluded from the data set include those removed during the major-element data quality checks (Chapter 5) and those which experienced problems during collection and subsequent manipulation, eg. northern sites along the SN array during summer 1992 are excluded because an accurate rainfall record was not measured due to a fault in the rain-collector design. The data set is listed in Appendix G.

6.5 OBSERVATIONS

In the following discussion, fallout of ^{36}Cl is in atoms/m^2/s. Stable Cl concentration is in μeq/L (unless stated otherwise) and ^{36}Cl concentration is in units of atoms/L.

Spatial variations

Mean $^{36}Cl/Cl$ Ratios

The mean ratios of $^{36}Cl/Cl$ as a function of distance from the coast, are shown in Figure 6.9 for both the WE and SN arrays. The mean stable Cl concentrations at each site are also shown on the plots. The WE array shows an increase in the $^{36}Cl/Cl$ ratio with increasing distance from the coast. A similar trend is observed for the SN array from the southern and northern coasts. It should be noted that the mean north coastal ratios (eg. at sites 32 and 33) greatly exceed those measured at an equivalent distance from the western coast of the WE array (eg. sites 16, 17 and 18) and from the southern coast of the SN array (sites 26 and 27). The increase in $^{36}Cl/Cl$ ratio with increasing distance from the coast is matched by a decrease in stable Cl. This trend reflects the influence of marine chloride at coastal localities and the decreasing influence with increasing distance from the coast.

Mean Stable Cl Concentrations

The relationship between $^{36}Cl/Cl$ and distance from the coast reflects the decreasing influence of stable Cl of marine origin with increasing distance inland. Figure 6.10 shows the rapid decrease of Cl concentration in rainfall with increasing distance from the coast for the WE and SN arrays. The relationship between Cl concentration of precipitation and distance from the coast has been discussed, both world wide (Junge 1963) and for Australia (Hutton 1976). Junge (1963) showed that wet and dry removal of salt by in-cloud and below-cloud scavenging (calculated from salt residence times in the atmosphere and wind directions) were insufficient to explain

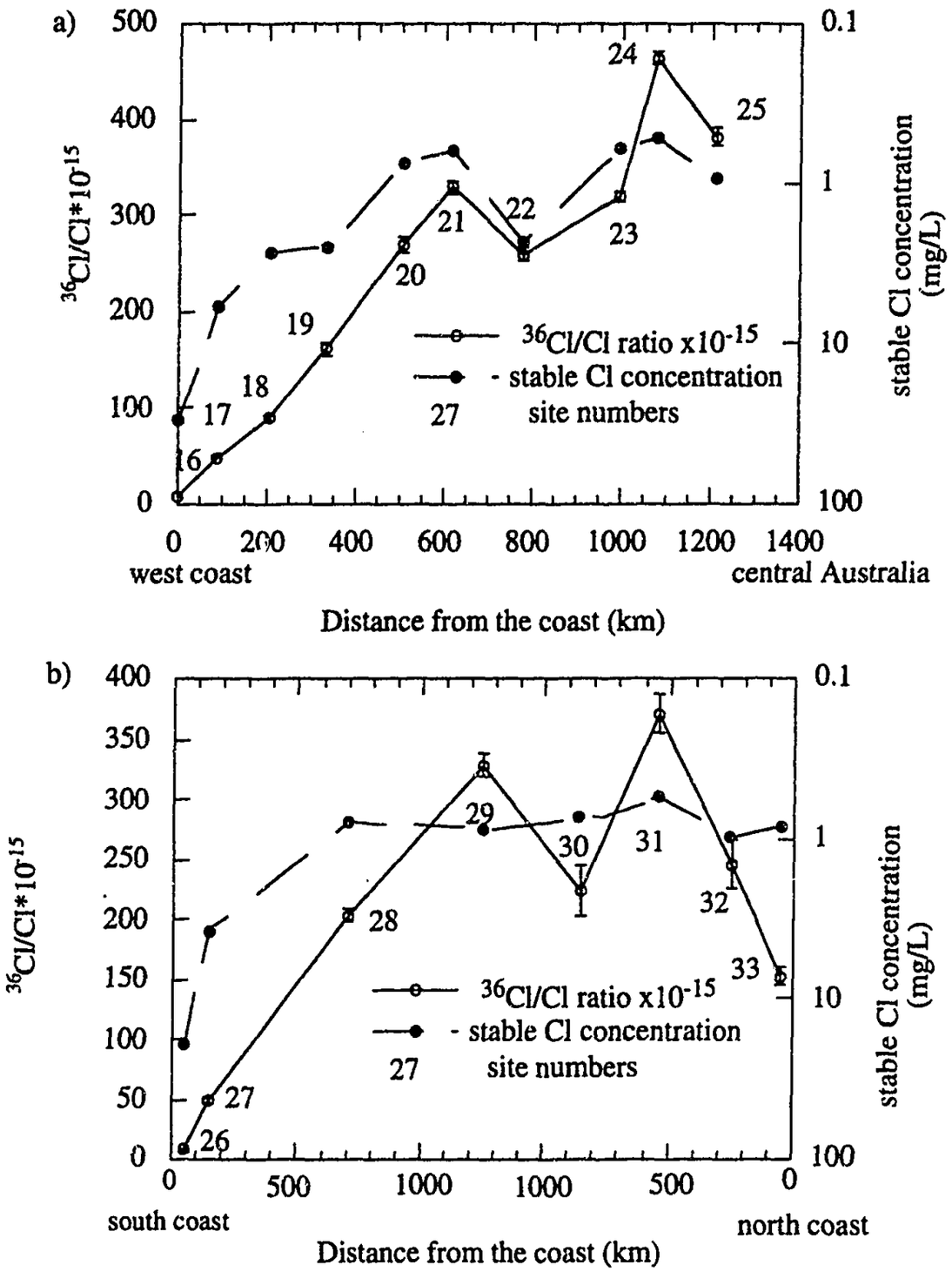

FIGURE 6.9 Mean ^{36}Cl/Cl ratios and stable Cl concentrations as a function of distance from the coast for a) the WE array and b) the SN array. Coast for a) is Leeman, WA b) is Port Lincoln SA for the southern section of the SN array and Finke Bay, NT for the northern section of the SN array. Note that the stable Cl axis is reversed. Mean ratios and stable Cl concentrations are calculated from seasonal means (see text).

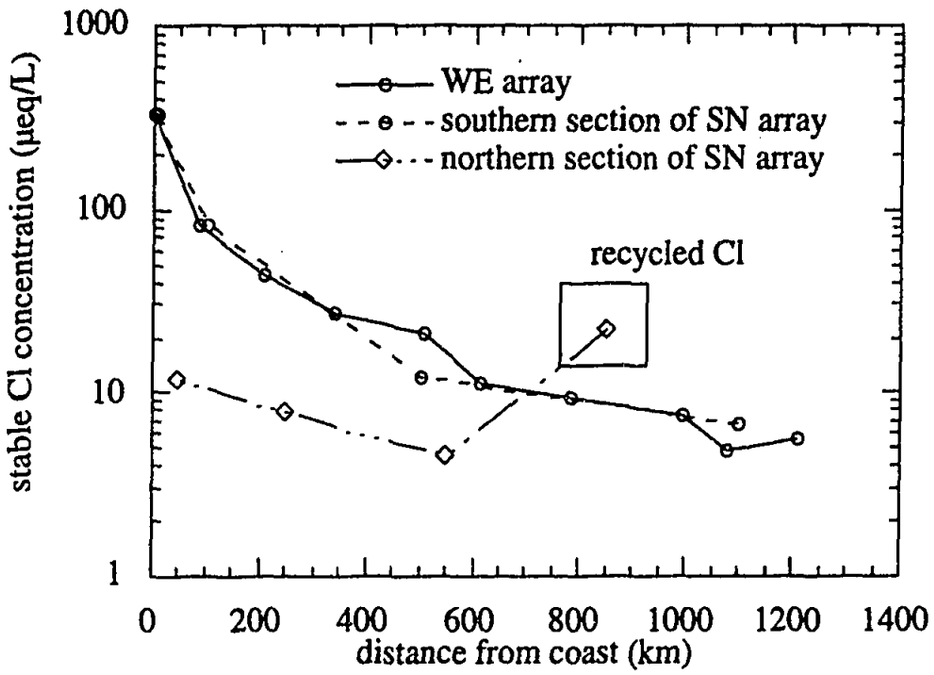

FIGURE 6.10 Mean stable Cl concentrations as a function of distance from the coast. Coast for the WE array is Leeman, WA, coast for the southern section of the SN array is Port Lincoln, coast for the northern section of the SN array is Finke Bay, NT. Mean stable Cl concentrations are calculated from the seasonal means.

the dramatic decrease in rainfall Cl concentration with increasing distance from the coast for Europe, USA and Australia. Instead this dependence was explained in terms of increased convective mixing of marine air masses moving inland. Mixing results in a decrease of salt concentration in subcloud layers, and therefore a decrease in salt concentrations in rainfall. At coastal sites, where convective mixing has not begun, the airmass is not well mixed so that Cl is available for easy removal by in-cloud and below-cloud deposition. As the airmass moves inland, convective mixing occurs and salts are distributed vertically through the airmass. Thus, less Cl is available in the in-cloud and below-cloud regions, so that concentrations in rainfall decrease. The distance from the coast where vertical distribution becomes uniform is marked by a plateau of Cl concentrations, and this distance is dependent upon the original vertical salt profile, which varies with geographical location.

Previous Models

The rate of decrease of Cl concentration in rainfall with distance from the coast has been shown for Australia to follow the form (Hutton 1976)

$$y = 0.99d^{-1/4} - 0.23 \qquad (6.2)$$

where y is volume weighted mean concentration of Cl in μeq/L and d is distance from the coast in km. For data from Victoria (Hutton and Leslie 1958) this gave a good fit with r^2= 0.992, n=24. Restrictions necessary for the application of this equation include the removal of sites influenced to a large extent by terrestrial sources, exclusion of sites with annual rainfall less than 500 mm, sampling over at least 12 months and removal of sites greater than 300 km from the coast. The regression form of Hutton's equation was applied to the data from Western Australia of Hingston and Gailitis (1976) in Isbell et al (1983), and gave different constants i.e.

$$\text{southwest WA: } y = 0.724d^{-1/4}-0.09 \quad r^2 = 0.855 \qquad (6.3)$$

$$\text{northwest WA: } y = 0.14d^{-1/4}-0.02 \quad r^2 = 0.687 \qquad (6.4)$$

Mean annual Cl concentration in rainfall for southwest Western Australia (Farrington et al 1993) was shown to follow the following relationship

$$Cx = Cmin + (Cmax-Cmin)e^{-\lambda x} \qquad r^2 = 0.975 \qquad (6.5)$$

where Cx is the concentration of Cl at distance x km (mg/L), Cmax is the concentration of Cl at coast, Cmin is the concentration of Cl at the most inland site, x is the distance from coast (km) and λ is the spatial decay constant. This exponential decay function was then used to predict the amount of Cl accession in southwestern Western Australia.

The regression equations described by Hutton (1976) and Farrington et al (1993) are applied to data for the WE and SN arrays in Figure 6.11. Also shown in Figure 6.11 are the equations for data from north-west and south-west of Western Australia from Hingston and Gailitis (1976) reported in Isbell et al (1983). Figure 6.11 shows that neither regression form adequately fits the data for the WE and SN arrays. However, the WE data set, falls between the curves defined for the south-west (curve A) and northwest (curve B) of Western Australia. This reflects the location of sampling sites on the WE array which are between those of the northwest and southwest of Western Australia as sampled by Hingston and Gailitis (Figure 6.12). A trend of decreasing Cl concentration in rainfall from the south to the north of the State is suggested. The sites along the northern section of the SN array display lower concentrations than those observed for the north-west of Western Australia by Hingston and Gailitis (1976). The northern sample locations of the SN array are further north than those of Hingston and Gailitis (Figure 6.12), supporting the

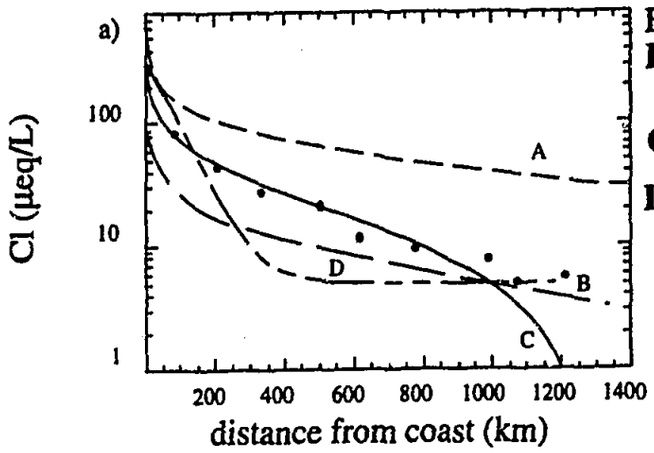

Equations of best fit C Hutton's form, D Farrington's form

C y= $489d^{-1/4}$ -82 r=0.979

D y= 4.9 +$333.1e^{-0.015d}$ r=0.718

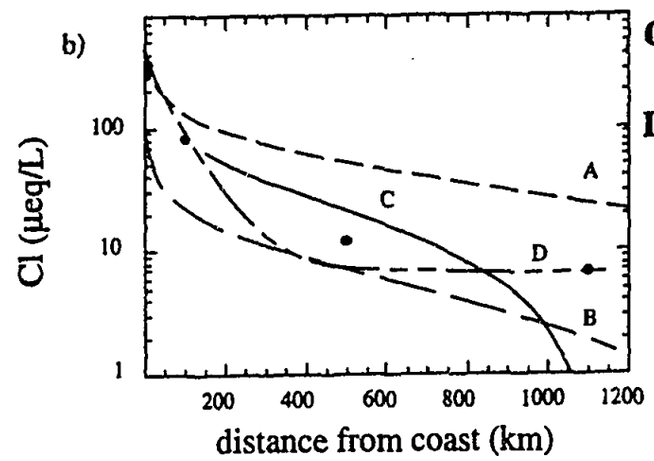

C y= $559d^{-1/4}$ -97 r=0.981

D y= 6.7 +$326.3e^{-0.0136d}$ r=0.974

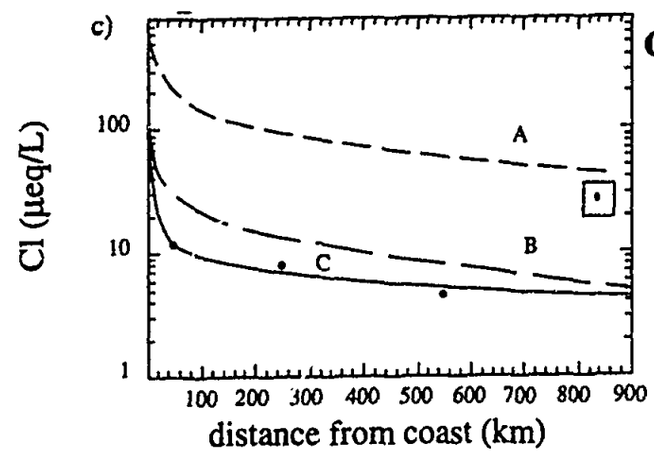

C y= $39d^{-1/4}$ -3 r=0.936

Hutton (1976) form

A y = 724 $d^{-1/4}$ - 90 South-west WA (Hingston and Gailitis 1976)

B y = 140 $d^{-1/4}$ -20 North-west WA (Hingston and Gailitis 1976)

C y= $ad^{-1/4}$ -b

Farrington et al (1993) form

D y= Cmin + (Cmax-Cmin) $e^{-\lambda d}$

FIGURE 6.11 Mean stable Cl concentrations versus distance from the coast for a)WE array, b) southern section of SN array and c) northern section of SN array. Cl concentrations are fitted to equations of Hutton (1976) and Farrington et al (1993). Coast for a) is Leeman, WA, b) is Port Lincoln, SA and c) is Finke Bay, NT.

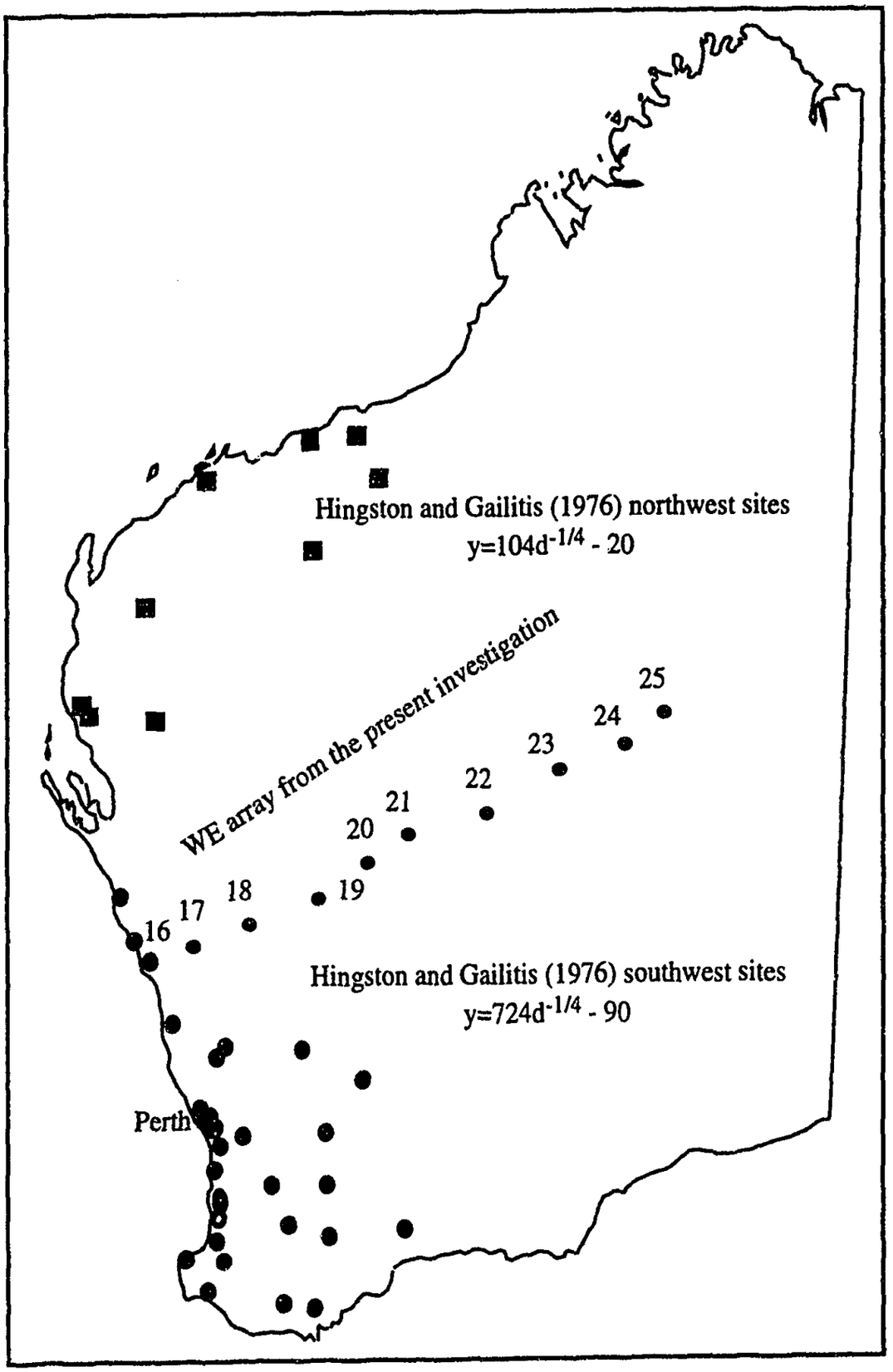

FIGURE 6.12 Map showing the location of the WE array with respect to the northwest (squares) and southwest (circles) sampling sites of Hingston and Gailitis (1976).

suggestion of decreasing Cl concentration of rainfall from the south to the north of Australia. The site at 850 km inland in Figure 6.11c, which is displaced from the regression curve is most likely influenced by recycled Cl.

The data is more adequately explained in terms of a two-exponential equation of the form

$$y = A_1 e^{-d/\lambda 1} + A_2 e^{-d/\lambda 2} \qquad (6.6)$$

where A_1 and A_2 are fitting parameters, $\lambda 1$ and $\lambda 2$ are decay constants and d is distance from the coast. Figure 6.13 shows the WE and southern section of the SN array fitted to this equation.

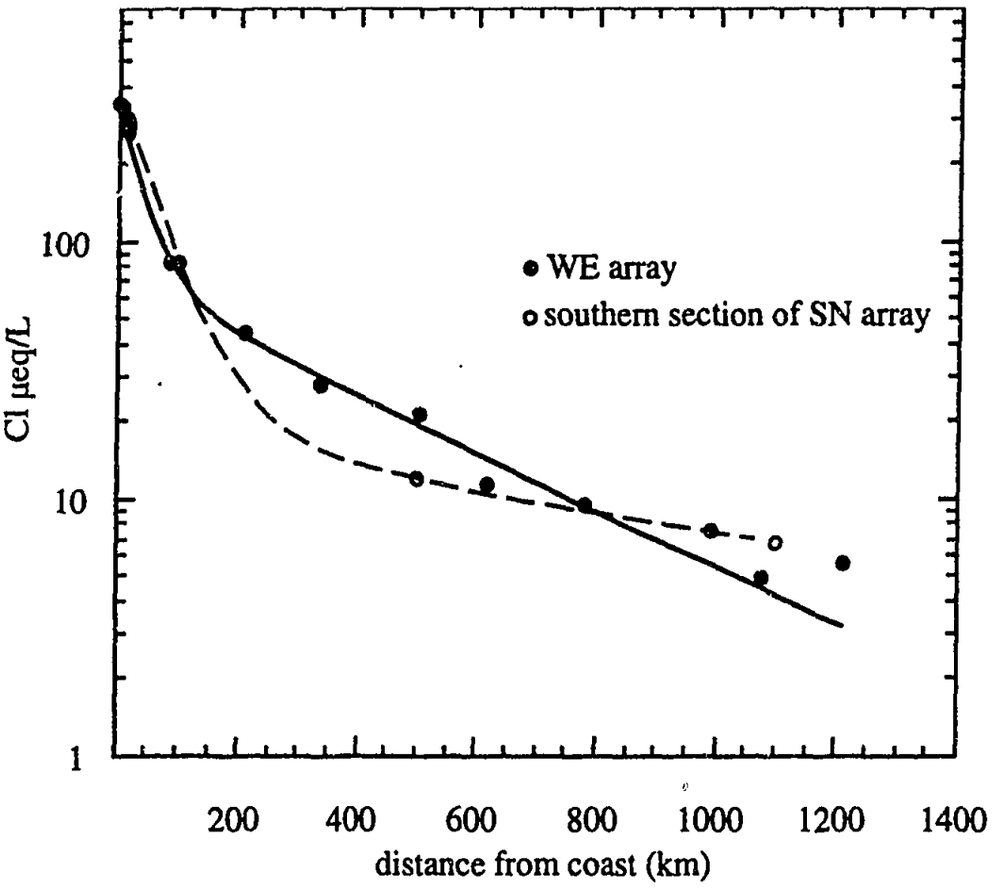

FIGURE 6.13 Stable Cl concentration versus distance from the coast for the WE array (filled circles) and southern section of the SN array (unfilled circles) with a double exponential fit applied to the data. The fit to the WE data (solid line) follows the equation

$$y = 69.4 \exp^{(-d/394.9)} + 284.0 \exp^{(-d/37.1)} \quad \chi^2=16$$

The fit to the southern section of the SN array data (dashed line) follows the equation

$$y = 19.4 \exp^{(-d/1036.9)} + 357.7 \exp^{(-d/58.4)}$$

(Note that a $\chi 2$ could not be calculated because of the lack of degrees of freedom that arises from having only four data points for the southern section of the SN array).

The good fit between the data and the equation suggests that there are two processes influencing the Cl concentration of rainfall as a function of distance from the coast, one that causes rapid decay of Cl concentrations, and the other a slow decay. There are two possible combinations of processes that may cause this two-fold decay of Cl concentrations with distance from the coast: i) the enhanced mixing of airmasses moving inland as discussed above and ii) differences in the rate of removal of Cl aerosols and Cl gas from marine and continental airmasses. The rapid decay of Cl concentrations at the coastal regions represent the removal of Cl in aerosols, introduced to the atmosphere by bubble-bursting at the ocean surface. The second, slower decay process represents the removal of Cl introduced to the atmosphere by volatilisation of Cl from aerosols by strong acids (this process is discussed in Section 6.6). It seems likely that the decreasing Cl concentrations with distance from the coast is influenced by both of the above situations.

Mean ^{36}Cl Fallout

The mean fallouts of ^{36}Cl at each site as a function of latitude are shown in Figure 6.14. Also shown on Figure 6.14 is the predicted fallout curve for the latitudes sampled in this project (Lal and Peters 1967, Andrews and Fontes 1992). In order to minimise the influence of missing values on the mean calculations, mean ^{36}Cl fallouts are calculated from the mean of fallouts for each season (winter, summer, spring and autumn).

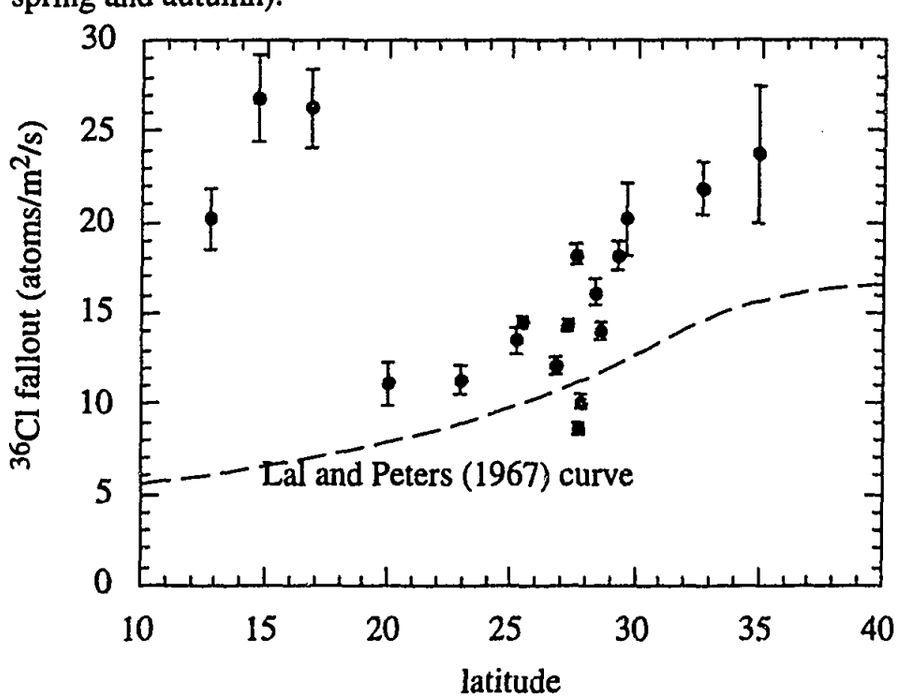

FIGURE 6.14 Mean ^{36}Cl fallout as a function of latitude. Also shown is the predicted fallout curve of Lal and Peters (1967). Error bars represent propagation of standard errors. Mean ^{36}Cl fallouts are calculated from seasonal mean fallouts (see text).

With the exception of the three northernmost points, the data appear to agree with the general shape of the predicted curve, although the predicted curve appears to underestimate the fallout by about 40%. The anomalously large values for sites from the north of the SN array (latitude 12°-18°) reflect the large fallouts during summer (monsoonal period) for these sites, and will be discussed in detail in the following section. A more detailed comparison between predicted and measured fallout values is given in the Discussion (Section 6.6).

Seasonal Variations

The seasonal variations of $^{36}Cl/Cl$ ratios, ^{36}Cl fallout and ^{36}Cl concentration, rainfall amount and stable Cl concentration for each site on the WE and SN arrays are displayed in Figure 6.15. Each value represents the mean value for each season over two years. Where there are missing values (as discussed in Section 6.4), the value in the plot represents single measurements. At site 25 during summer and site 33 during spring, there are no measurements available.

Investigating the trends displayed by $^{36}Cl/Cl$ ratios, ^{36}Cl fallout, ^{36}Cl concentration, rainfall amount and stable Cl concentration over time provide information concerning the processes that effect the ^{36}Cl composition of precipitation. While exceptions exist, the following discussion describes the general trends displayed by the different variables and attempts to explain the processes that may produce these correlations. From the data, a positive correlation is observed between rainfall amount and ^{36}Cl fallout and a negative correlation between rainfall amount and ^{36}Cl concentrations. $^{36}Cl/Cl$ ratios exhibit both positive and negative correlations with ^{36}Cl and stable Cl concentration, reflecting the site dependent input of ^{36}Cl and stable Cl. This is corroborated by a lack of correlation between ^{36}Cl concentration, stable Cl concentration or $^{36}Cl/Cl$ ratio with ^{36}Cl fallout.

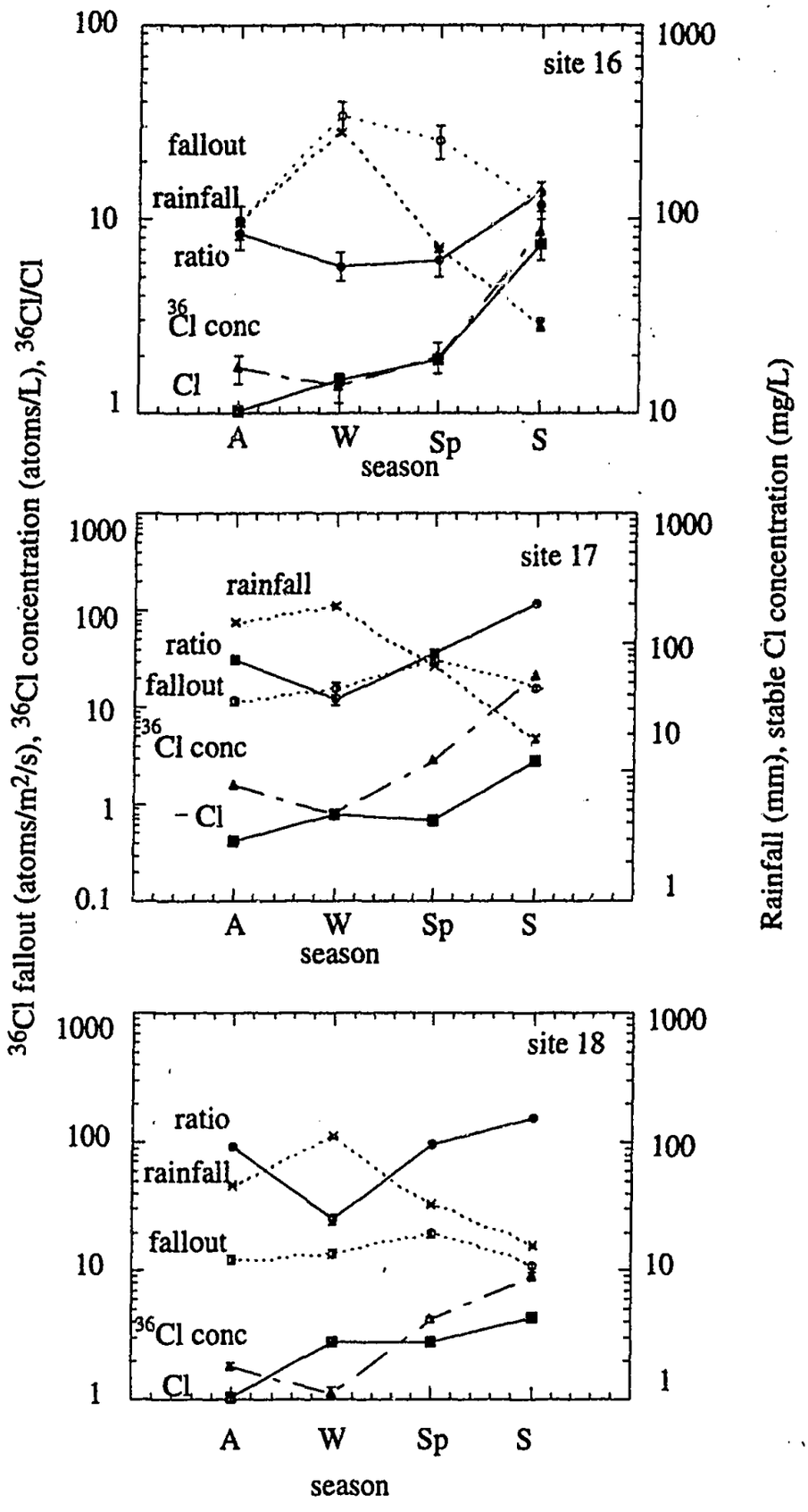

FIGURE 6.15 Seasonal variations displayed by ^{36}Cl fallout, ^{36}Cl concentration, $^{36}Cl/Cl$ ratio, stable Cl concentration and rainfall amount at each sampling site. A=autumn, W=winter, Sp=spring, S=summer. Values represent the mean for each season over the sampling program.

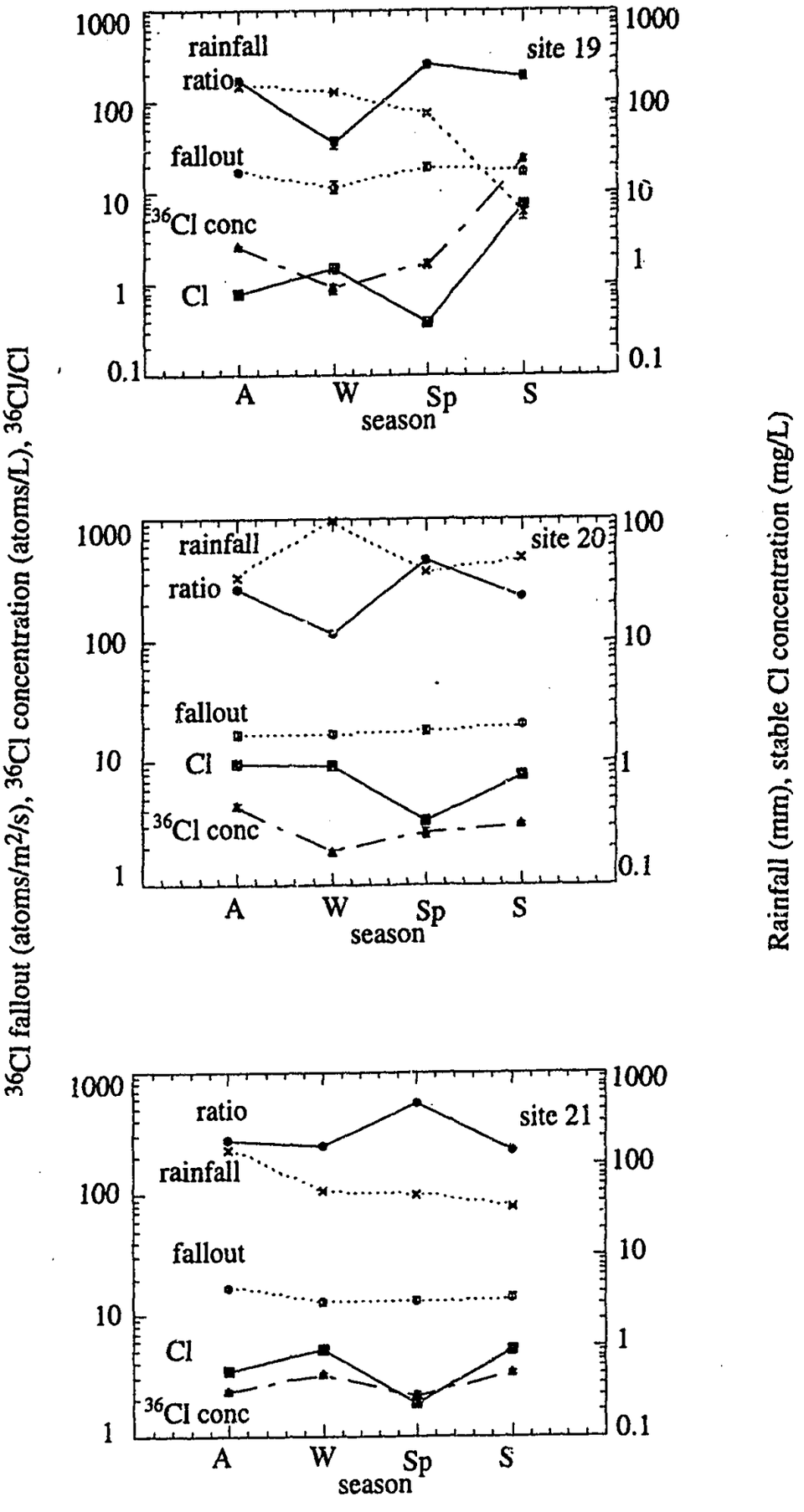

FIGURE 6.15 continued

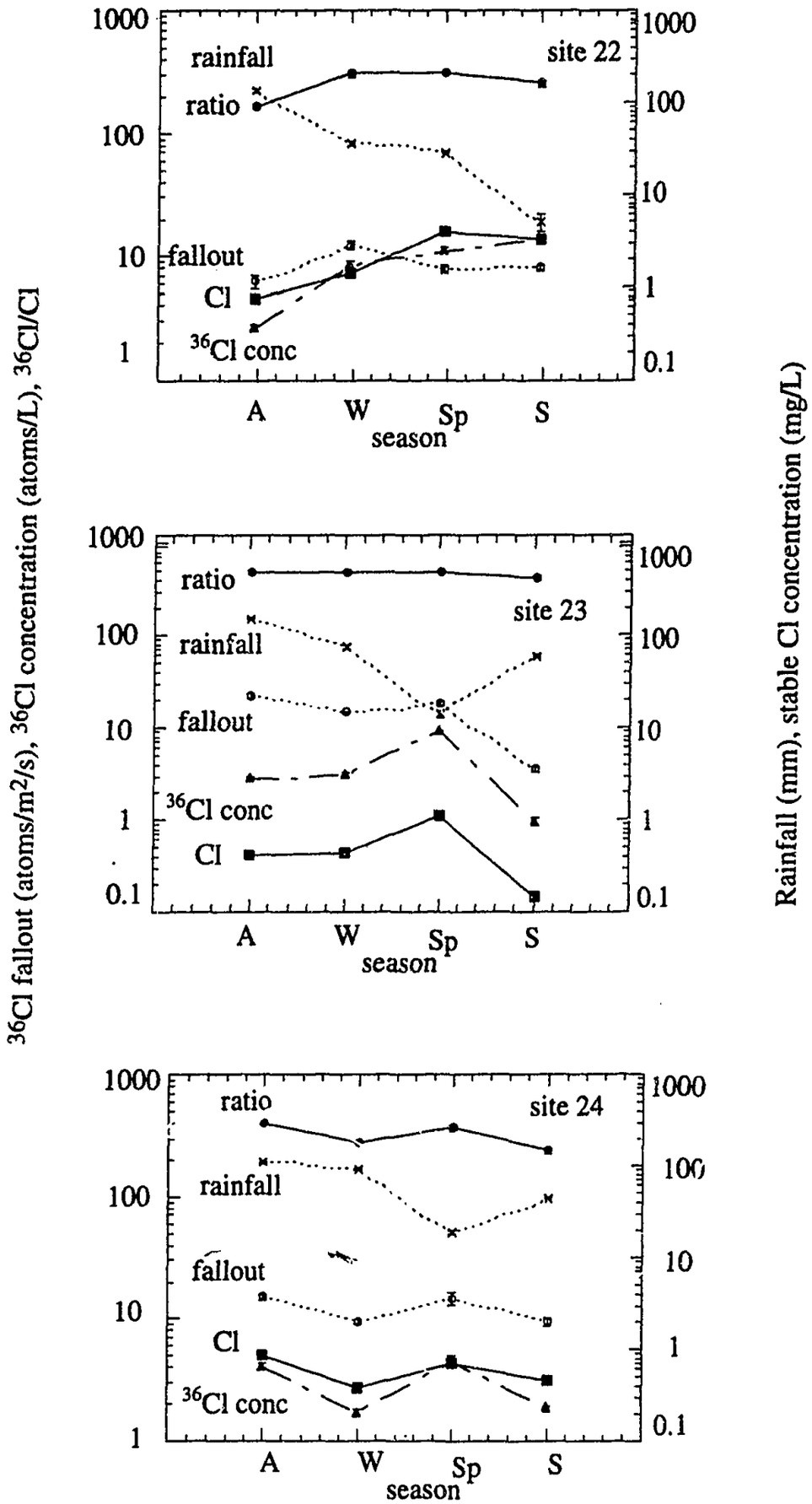

FIGURE 6.15 continued

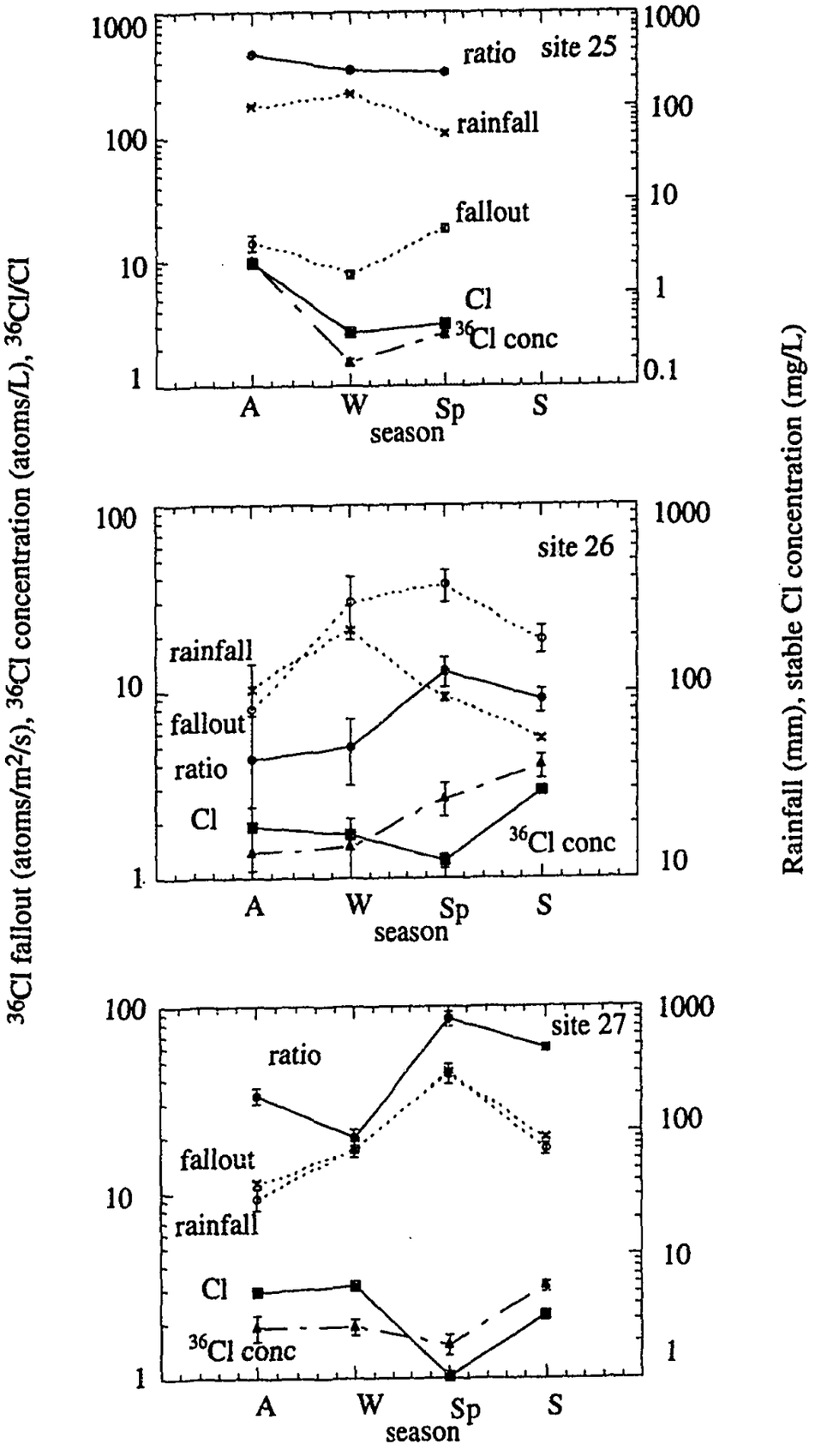

FIGURE 6.15 continued

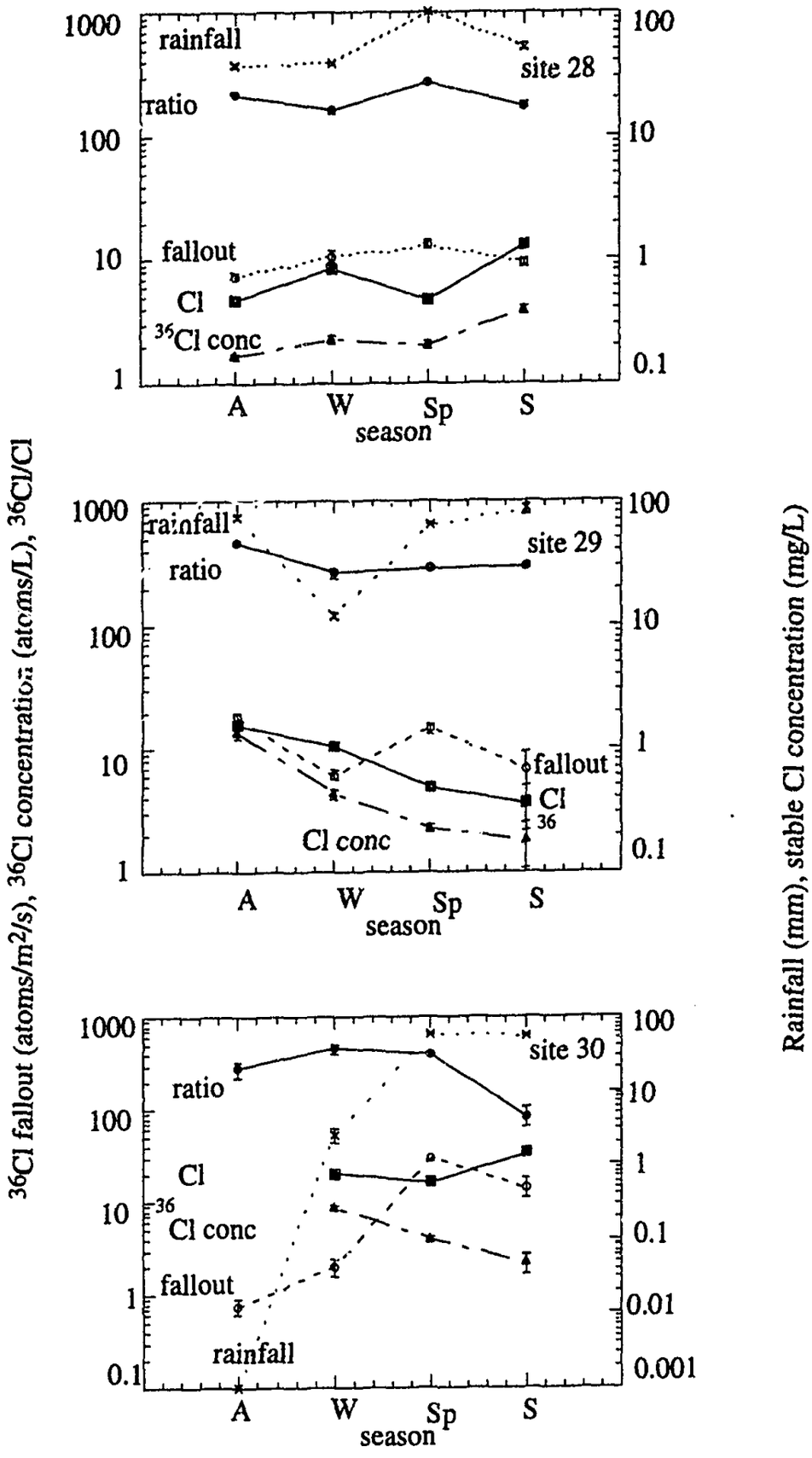

FIGURE 6.15 continued

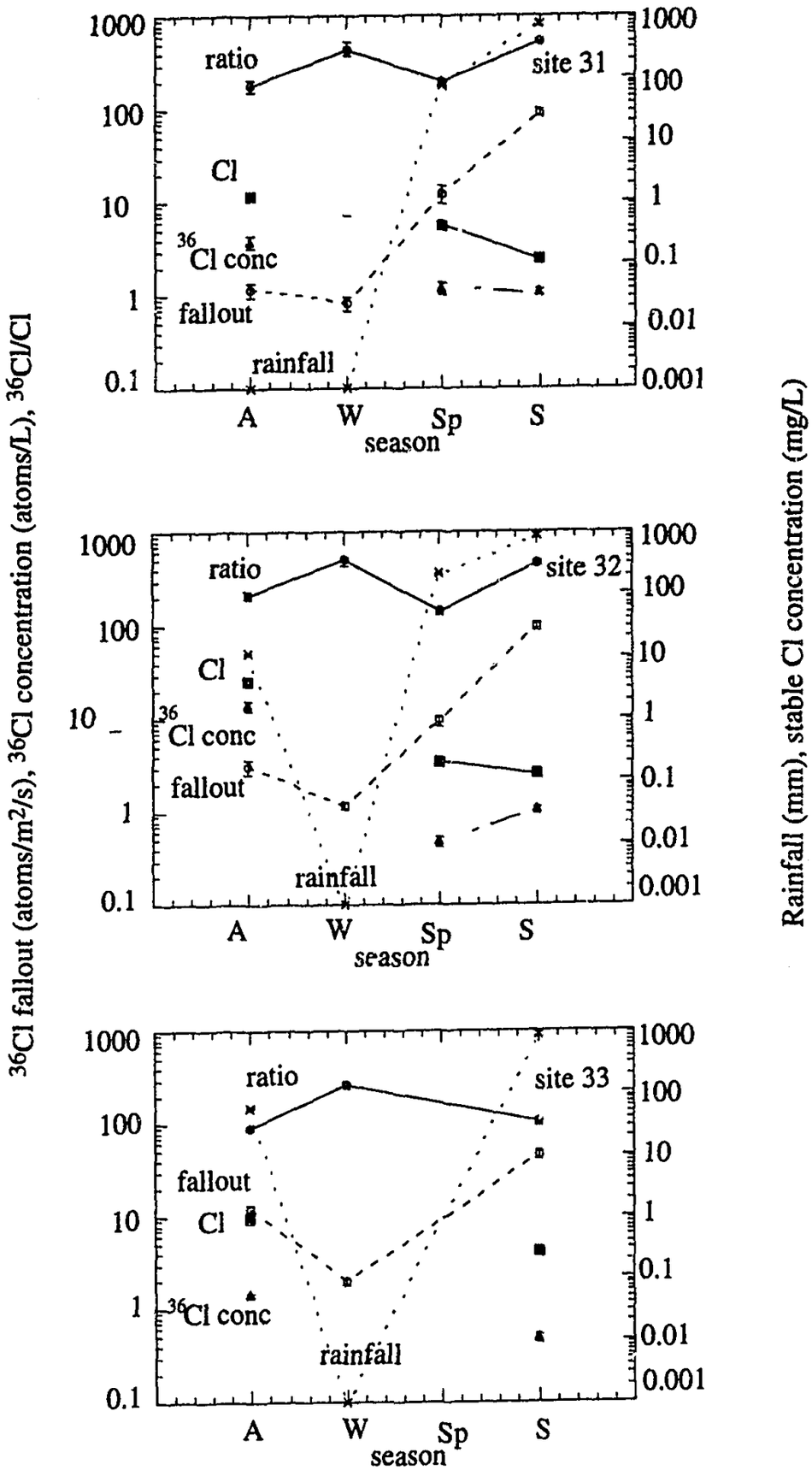

FIGURE 6.15 continued

Chlorine-36 Fallout

The general seasonal trends displayed by ^{36}Cl fallout can be seen in Figure 6.16 which shows the mean ^{36}Cl fallout for each season for sites along the WE array, and northern and southern sections of the SN array. The WE and southern section of the SN array display maximum fallout during spring. High spring fallouts are in accordance with the findings of Hainsworth et al (1994) for rainfall in Maryland, USA (latitude 38°N). It was suggested that this enhanced fallout may be due to an increase in transfer of stratospheric air to the troposphere that occurs as the tropopause rises during spring to its maximum height during mid-summer (Reiter 1975). The elevated tropopause allows transfer of stratospheric ^{36}Cl as well as the penetration of cosmic rays into the troposphere, increasing the production of tropospheric ^{36}Cl. If this mechanism were the sole cause of enhanced $^{36}Cl/Cl$ ratios, it is expected that summer ratios would also be high, which is not observed. The same behaviour for summer fallouts was observed by Hainsworth et al (1994) who were equally puzzled by this inconsistency.

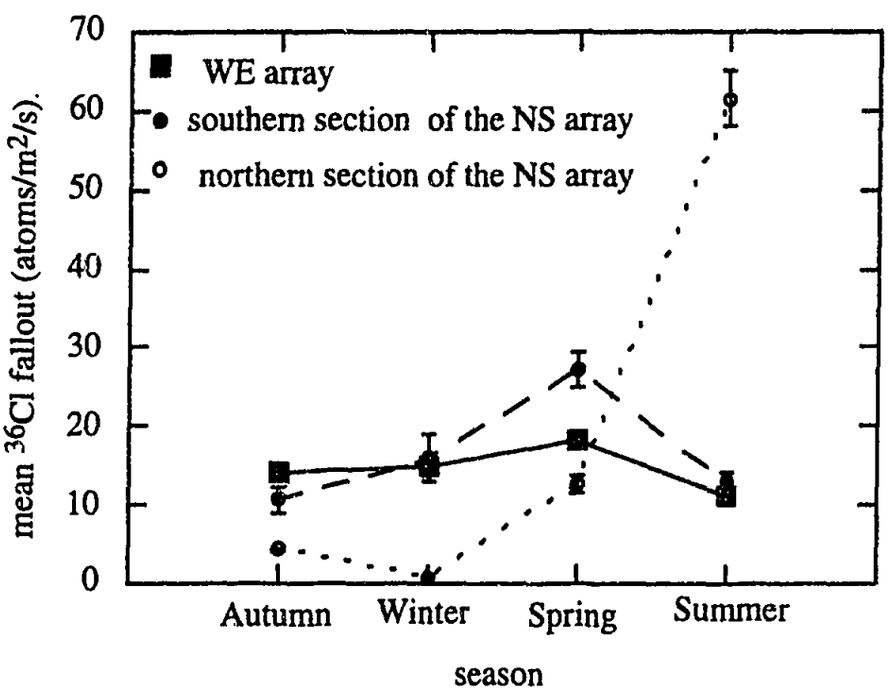

FIGURE 6.16 Mean ^{36}Cl fallout for each season along the WE array, northern section of the SN array and southern section of the SN array. Maximum fallout occurs during spring on the WE and southern section of the SN array, reflecting the change in tropopause height during spring. Maximum fallout occurs during summer on the northern section of the SN array, reflecting direct entrainment of stratospheric ^{36}Cl during convective cumulus activity associated with the monsoon.

The northern section of the SN array displays maximum fallout during summer. However, the fact that high fallouts during summer are restricted to the northern

section of the SN array where the monsoon dominates, suggests that raising of the tropopause during summer is not the main cause of enhanced summer fallout. Instead, entrainment of stratospheric air during convection may be invoked (Reiter 1975). Equatorial Indonesia is known as a fountain region where troposheric air is injected into the stratosphere (Newel and Gould-Stewart 1981), so that tall cumulus clouds exclusively generated near Indonesia sometimes penetrate above the tropopause allowing exchange between the troposphere and the stratosphere (Danielsen 1982, Kley et al 1982).

Rainfall Amount Versus Fallout

In many instances, rainfall amount and fallout variations with season follow similar trends, eg. sites 16-19 (Cliff Head to Iowna) on the WE array, and all sites along the SN array (Figures 6.15).

The positive correlation between rainfall and fallout can be seen in a plot of the two variables for the complete data set (Figure 6.17a). The linear correlation coefficient is 0.47. The dependence of the relationship on array is shown by the difference in correlation when data from the two arrays are separately analysed. Data for the SN array shows a higher correlation coefficient (Figure 6.17b) than data from the WE array (Figure 6.17c).

The more distinct positive relationship between rainfall and fallout displayed by the sites from the SN array most likely reflects the extreme rainfall regimes that sites along this array experience (i.e. nil rainfall in the northern half of the array during winter, and up to 800 mm during summer). Rainfall along the WE array is less variable over time so that the influence of rainfall on fallout appears to be less dramatic. The mechanism for the high fallout along the northern section of the SN array during summer has been discussed above in terms of high-reaching cumulus convective activity.

Sites 20 -25 (Barrambie to Everard Junction) along the WE array do not display a sympathetic trend between rainfall and fallout with season (Figure 6.15). The similarity in trends displayed by fallout, Cl concentration and/or ratio suggest that at these sites rainfall does not control fallout of ^{36}Cl. Instead the supply of ^{36}Cl and Cl (where the sympathetic trends between ratio and Cl suggest the two are sourced from a similar process) is more dominant.

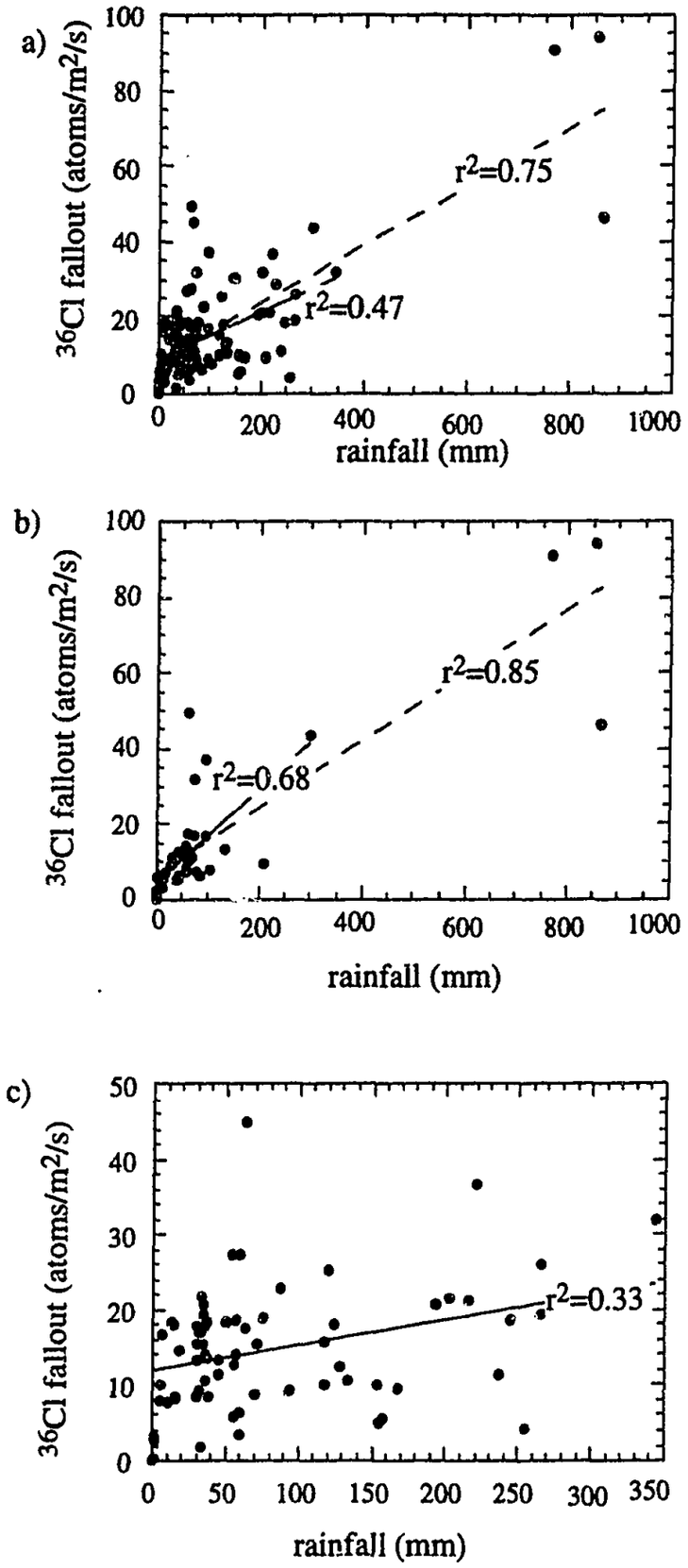

FIGURE 6.17 Fallout of ^{36}Cl versus rainfall amount. a) WE and SN data sets, b) SN dataset, c) WE data set. For figures a and b, full line is the correlation for data with rainfall greater than 700 mm removed and the dashed line is the correlation for all data.

Rainfall Amount Versus ^{36}Cl Concentration

Figure 6.18 shows an inverse relationship between rainfall amount and ^{36}Cl concentration of precipitation. This is in agreement with the behaviour displayed by the major-element concentrations and rainfall amount described in Chapter 5. At coastal localities, ^{36}Cl concentration and stable Cl concentrations show similar trends, but this disappears at non-coastal localities. The relationship between ^{36}Cl and rainfall amount will be discussed further in the Discussion (Section 6.6).

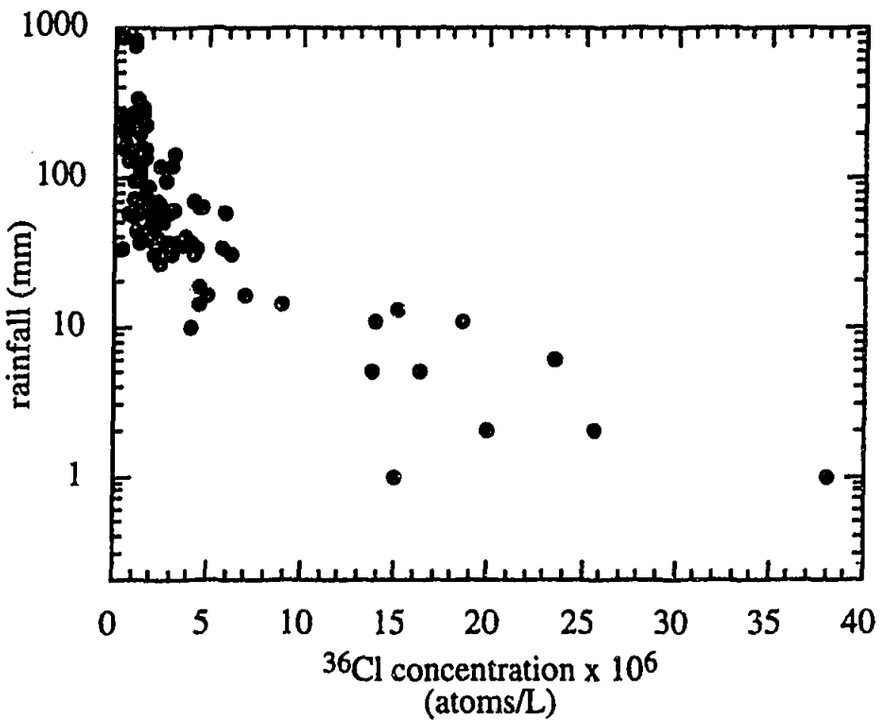

FIGURE 6.18 Rainfall versus ^{36}Cl concentration for all data. The negative correlation displayed between rainfall and ^{36}Cl concentration is in agreement with the behaviour displayed between the major-element concentrations and rainfall amount in Chapter 5.

$^{36}Cl/Cl$ Variations

The seasonal trends displayed by the $^{36}Cl/Cl$ ratio and the stable Cl concentrations of precipitation in Figure 6.15 show variable patterns: sympathetic (eg. high ratios and high Cl, or low ratios and low Cl) and antipathetic (eg. low ratios and high Cl or high ratios and low Cl). The sympathetic trends represent changes in the supply of ^{36}Cl and Cl which have the same magnitude of effect on both species. Conversely, the antipathetic relationships represent independent changes in the supply of ^{36}Cl and Cl. Low ratios and high Cl compositions suggest a supply of stable Cl that has a low ^{36}Cl composition. High ratios and low Cl suggest a supply of Cl that has a high ^{36}Cl composition. Figure 6.19 displays a schematic representation of the processes

that may affect the $^{36}Cl/Cl$ ratio. The following discussion suggests possible explanations for the seasonal variations in $^{36}Cl/Cl$ ratios.

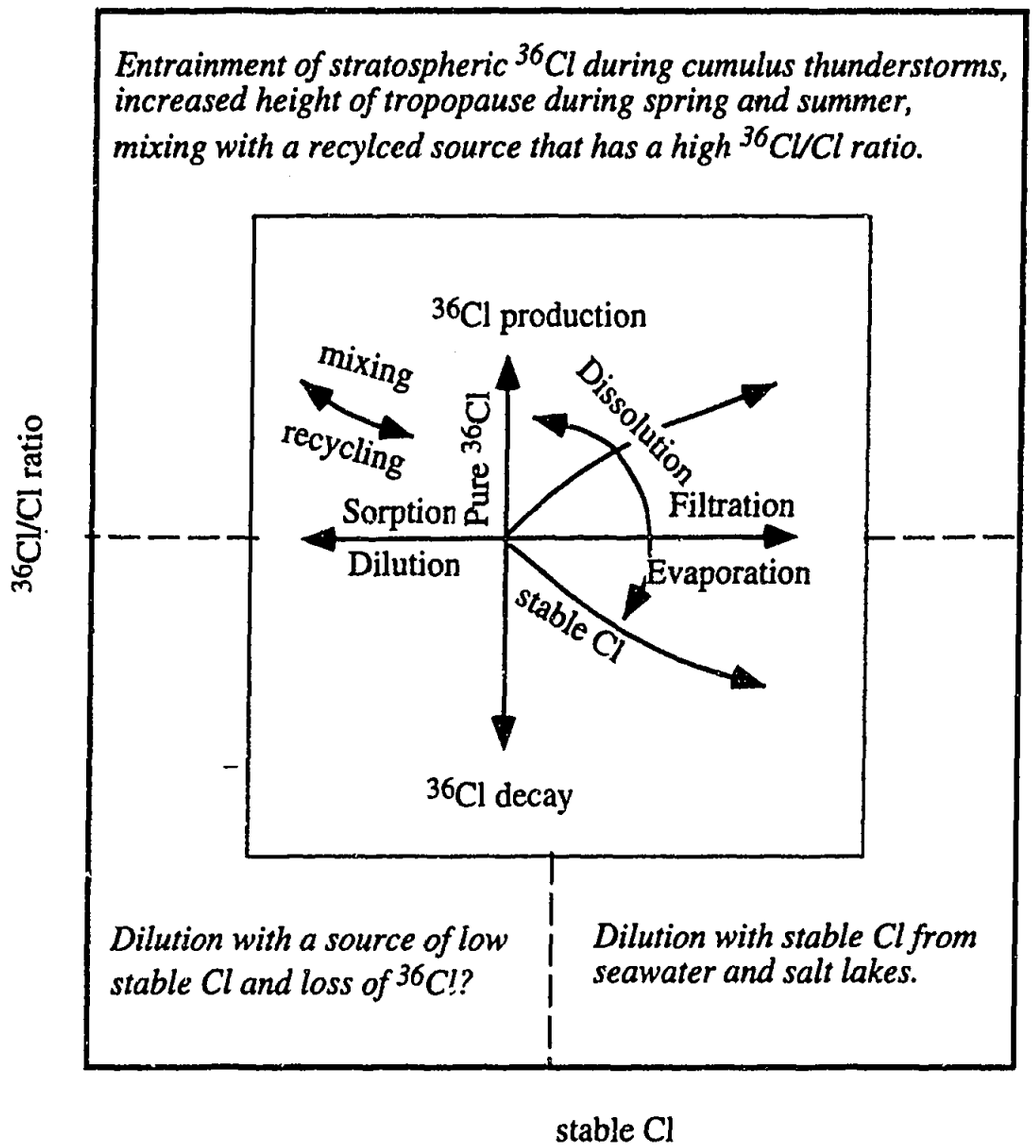

FIGURE 6.19 Schematic diagram of the processes that control the distribution of ^{36}Cl in the environment. Italics describe processes relevant to ^{36}Cl in precipitation.

Low ratios

Low $^{36}Cl/Cl$ ratios that occur in association with high Cl concentrations represent precipitation that has been diluted with Cl with negligible or significantly lower ^{36}Cl composition. The two major sources of this Cl for the present sampling program are seawater and salt-lake material.

a) Seawater

Chapter 5 showed that sites along the WE and SN arrays displayed major ion ratios (eg. Cl/Na, SO_4/Na, Mg/Na) characteristic of seawater during certain seasons.

These seasons of influx of seawater could be tied into the prevailing rain producing synoptic processes described in Chapter 2. The coastal sites 16 (Cliff Head) and 26 (Port Lincoln) displayed seawater ratios throughout most of the year; all sites along the WE array displayed seawater ratios during winter 91 and sites 16 to 21 (Yeelirrie) during winter of 1992.

Low $^{36}Cl/Cl$ ratios and high Cl concentrations are exhibited by the coastal sites 16 and 26 throughout the year, by sites 17 (Morawa) to 20 (Barrambie) along the WE array during winter, and by sites 27 (Gawler Ranges) and 28 (Wintinna) along the SN array during winter. Thus seawater Cl is acting to decrease the $^{36}Cl/Cl$ composition of precipitation at these sites during these times.

b)Salt Lakes

An additional source of Cl that acts to dilute $^{36}Cl/Cl$ ratios at non-coastal localities may be Cl of salt lake origin. Salt lakes are especially common on the WE array and there are a number of salt lakes that may influence the $^{36}Cl/Cl$ ratio of precipitation at inland sites of the WE array (Figure 6.20). There are a number of instances where low ratios and high stable Cl compositions of rainfall can be correlated with surface wind directions that support influx of Cl from a salt lake to a collection site. These are summarised in Table 6.2 and include :

1) Site 20 (Barrambie) during summer; the predominant frequency of surface wind directions at Meekatharra for each summer season are from the southeast (Appendix H) and Lake Mason is situated 30 km towards the east-southeast of the collector site.

2) Site 21 (Yeelirrie) during summer; the predominant frequency of surface wind directions at Yeelirrie are northeast-east-southeast and Lake Way lies 50 km to the northeast of collector 21.

3) Site 24 (Gunbarrel) and 25 (Everard Junction) during winter of 92; the prevailing wind directions at Giles are southeast-south and north and Lake Gillen is located 100 km to the southeast of collector 24 and Lake Breaden is located 100 km to the southeast of site 25.

It should be noted that there are numerous small unmapped salt lakes throughout Western Australia which may also supply stable Cl to the collectors. In addition, the presence of recycled salt in soils may also be a source.

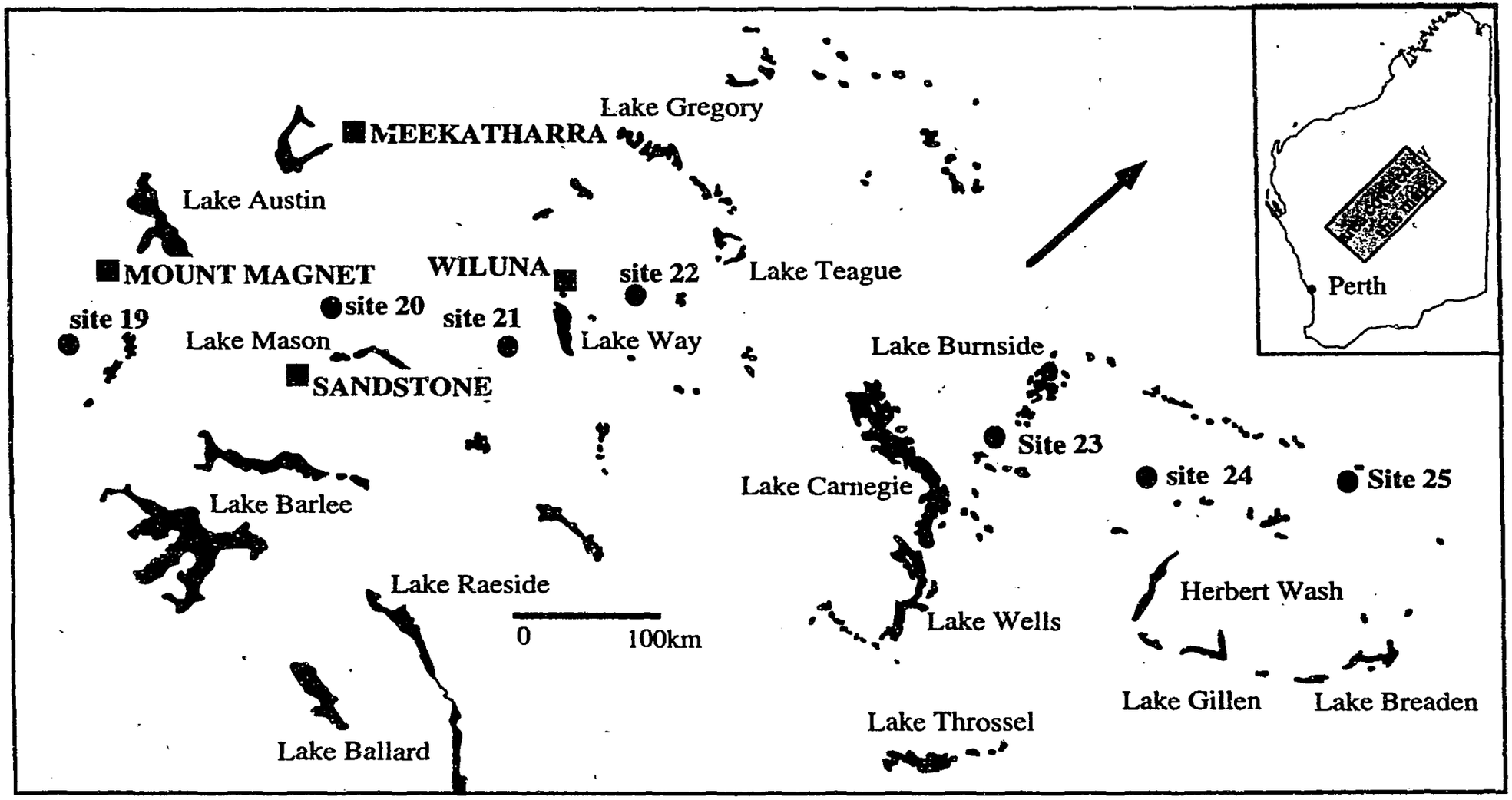

FIGURE5.20 Salt Lakes on the WE array. Circles are sample sites. Squares are Met stations. Location of the area is shown in the inset.

TABLE 6.2 Mean wind direction at sites along the WE array displaying low $^{36}Cl/Cl$ ratios and high stable Cl concentrations, and the salt lakes that may be a source of stable Cl.

Site	Met Station	Season	Wind direction	Lake
20	Meekatharra	summer 91	E-SE	Lake Mason
20	Meekatharra	summer 92	E-SE	Lake Mason
21	Yeelirrie	summer 91	NE-E-SE	Lake Way
21	Yeelirrie	summer 92	NE-E-SE	Lake Way
24	Giles	winter 92	SE-S	Lake Gillen
25	Giles	winter 92	SE-S	Lake Breaden

The $^{36}Cl/Cl$ ratios and stable Cl concentrations at site 23 (Carnegie) do not suggest that Lake Carnegie, a major salt lake located 100 km to the southwest of site 23, influences the $^{36}Cl/Cl$ ratio. This makes sense when the surface wind directions at Carnegie are considered. The predominant surface wind direction is never from the southwest at Carnegie (Appendix H).

Chivas et al (1994) reported increasing $^{36}Cl/Cl$ ratios, in halite, from modern salt lakes in Western Australia with increasing distance from the coast. This reflects the trend shown by the $^{36}Cl/Cl$ ratios of precipitation and increasing distance from the coast (although at lower levels). The relationship between precipitation and salt lake $^{36}Cl/Cl$ ratios suggests that the main source of stable Cl to the Western Australia landscape is meteoric. Chivas et al (1994) used this to calculate a residence time of ~1 Ma for Cl in the Australian landscape.

High ratios

High ratios of $^{36}Cl/Cl$ are observed at most sites during spring. For coastal sites on the WE array (sites 16 to 18) this is associated with high stable Cl concentrations. At inland sites on the WE array, high $^{36}Cl/Cl$ ratios are observed with low stable Cl concentrations. All sites along the SN array exhibit high $^{36}Cl/Cl$ ratios during spring in association with low stable Cl concentrations. High ratios and/or high fallouts are observed during summer in some instance, in particular along the northern section of the SN array.

The mechanisms for producing high spring and summer ratios have been discussed earlier in terms of the high ^{36}Cl fallouts during these seasons. During spring high

ratios occur because of the enhanced transfer of stratospheric ^{36}Cl that occurs with tropopause rising during this time. High summer ratios in the north of Australia arise from direct entrainment of stratospheric ^{36}Cl during cumulus convective activity associated with the monsoon. The expected, but unobserved widespread occurrence of high ratios during summer suggests that other localised processes, (such as the supply of stable Cl from local salt lakes) can significantly effect the ratios, as has been shown for sites 20 (Barrambie) and 21 (Yeelirrie) on the WE array.

The supposition by Bird et al (1991) that $^{36}Cl/Cl$ ratios in tropical rainfall should be low because of the anticipated high stable Cl fallout due to very high monsoonal rainfall deriving moisture from oceanic areas to the north of Australia, is not true for the northern section of the array. Ratios of approximately 400 x 10^{-15} are measured at sites 30 (Tennant Creek) to 32 (Katherine) for summer 1993. Even for the near-coastal locality 33 (Kapalga) the measured ratio of ~100 x 10^{-15} is significantly greater than ratios observed at a similar distance (50 km) from the southern and western coasts.

The Relationship Between ^{36}Cl and Major-Element Concentrations

The generally accepted process of incorporation of ^{36}Cl into rainfall involves production of ^{36}Cl in the stratosphere, movement into the troposphere, mixing with stable Cl of marine origin within the troposphere and deposition as rain within one week of entry to the troposphere. It has been shown here that an inverse relationship exists between rainfall amount and ^{36}Cl concentration (Figure 6.18). In addition, there is a lack of correlation between ^{36}Cl and stable Cl concentrations (Figure 6.15). For the above process to control the movement of ^{36}Cl from the stratosphere to the troposphere and removal from the troposphere, a correlation should be seen between ^{36}Cl and stable Cl concentrations. Thus a discrepancy appears to be present.

To investigate this discrepancy further, a comparison of the ^{36}Cl concentrations with major-element concentrations was carried out. Table 6.3 shows the correlation coefficients between ^{36}Cl and major elements described in Chapter 5. Of note is that ^{36}Cl does not show a high correlation with Cl, but instead shows a strong affinity with NO_3 and to a lesser extent SO_4 and K. A multivariate analysis of the variations displayed by the major elements, ^{36}Cl and rainfall (Figure 6.21) sees ^{36}Cl grouping with NO_3, SO_4, K and inversely with rainfall amount. The correlation between ^{36}Cl and NO_3 concentration has implications about the phase (gaseous or aerosol) of ^{36}Cl

before its incorporation into rainfall. This is expanded in the Discussion (Section 6.8).

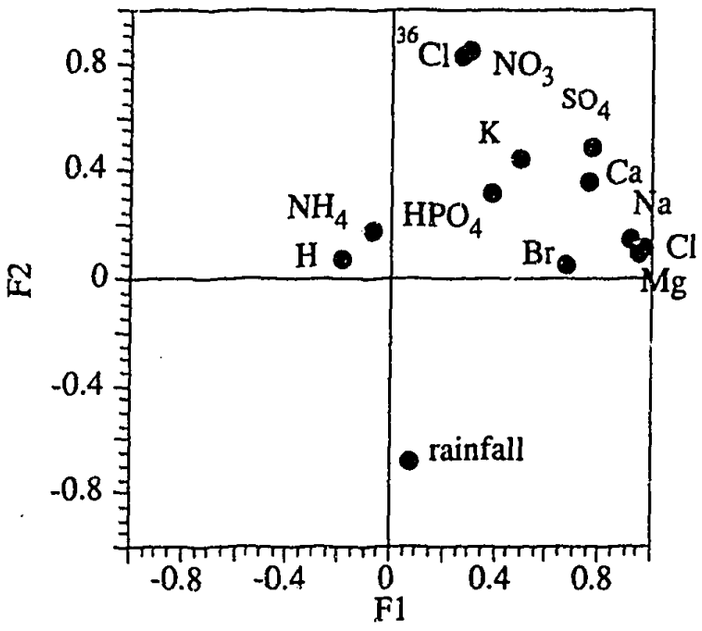

FIGURE 6.21 Factor loading plot for major element and ^{36}Cl concentrations (atoms/L). ^{36}Cl plots close to NO_3, near the F2 axis, not with stable Cl, near the F1 axis.

TABLE 6.3 Correlation coefficients between major element ions, ^{36}Cl fallout and rainfall amount. Bold values highlight coefficients of greater than 0.6. Note that ^{36}Cl has a high correlation with NO_3 and not with Cl or Na.

	H	Cl	SO_4	NO_3	HPO_4	Na	K	NH_4	Ca	Mg	^{36}Cl	rain
H	1.00	.02	-.031	.013	-.12	.08	-.07	-.12	-.06	.03	-.13	-.04
Cl		1.00	**.83**	.14	.55	**.97**	**.73**	.45	**.81**	**.98**	.27	-.06
SO_4			1.00	.57	**.65**	**.90**	**.81**	.58	**.79**	**.86**	**.69**	-.18
NO_3				1.00	.37	.23	.42	.30	.35	.22	**.84**	-.21
HPO_4					1.00	.52	**.88**	**.93**	.58	.59	.50	-.13
BR						.41	.22	.12	.26	.30	.25	-.02
Na						1.00	**.69**	.41	**.81**	**.97**	.31	-.07
K							1.00	**.82**	**.73**	**.78**	**.62**	-.18
NH_4								1.00	.48	.48	.47	-.12
Ca									1.00	**.85**	.45	-.15
Mg										1.00	.34	-.09
^{36}Cl											1.00	-.27
rain												1.00

Dry Deposition

The measurement of $^{36}Cl/Cl$ ratios in samples that showed nil rainfall are an opportunity to investigate the extent of dry deposition of ^{36}Cl to particular sites along each array. Table 6.4 lists the fallout for dry samples compared with the total fallout at the site of dry deposition over the entire sampling period (excluding summer monsoonal fallout, which has been shown to be anomalously high). As the number of measurements differs between sites, the total ^{36}Cl fallout for each site is averaged. Table 6.4 shows that dry deposition contributes less than 50% of the total wet and dry fallout per sample collection period for each of the northern sites of the SN array which typically experience nil rainfall during the winter seasons.

TABLE 6.4 Percentage of ^{36}Cl fallout attributable to dry deposition at sites that experienced nil rainfall during any part of the sampling program.

site	^{36}Cl (atoms/m^2/s) wet + dry	^{36}Cl (atoms/m^2/s) dry	% of ^{36}Cl in dry deposition
30 Tennant Creek	14.77 n=4	0.45 n=2	3±0.5
31 Dunmarra	5.39 n=5	0.84n=3	16±1.9
32 Katherine	4.06 n=4	1.87 n=2	46±10.8
33 Kapalga	5.38 n=3	1.94 n=2	36±6.0

The estimates of dry deposition for the present investigation are comparable with those of Hainsworth (1994) for a site in North America (latitude 38°N). There, dry deposition was seen to range from 19% to 40%. While it is interesting to compare the results of the present study with the results of Hainsworth, the methods used to compare wet and dry deposition in these two studies differ. Hainsworth compared a wet-only with a bulk-deposition collector over three collection periods. In that study uncertainties were introduced by missing wet-only precipitation values arising from equipment malfunction. The present investigation provides an unambiguous assessment of dry deposition, by comparing the ^{36}Cl composition of samples containing precipitation (and therefore representing both wet and dry deposition) with samples of nil rainfall, representing dry deposition only.

It is unfortunate that the only measurements of dry deposition occur along the northern section of the SN array. This section of the SN array experiences different rainfall regimes and climates to the southern section of the SN array and the WE array. Thus, caution should be used when applying the results of dry deposition from the northern section of the SN array to other sample sites. However, assuming

that dry deposition of ^{36}Cl is more important during periods of low precipitation rates, the results from the present investigation may be considered as the maximum amount of dry deposition, since they are associated with nil rainfall.

Table 6.5 compares $^{36}Cl/Cl$ ratios with Ca/Na ratios for the dry samples collected from the northern section of the SN array. Simpson and Herczeg (1994) suggested that Ca/Na ratios of greater than 1 denoted input of resuspended soil material to precipitation. The discussions in Chapter 5 noted that Ca/Na ratios of greater than 1 were only observed in samples from the SN array, during periods of nil precipitation. Sites 32 (Katherine) and 33 (Kapalga) appear to be affected by resuspended soil material during winter seasons. The high Ca/Na and $^{36}Cl/Cl$ ratios observed during winter 1993 at site 33 may suggest a recycled soil source with high $^{36}Cl/Cl$ ratio.

The estimates of dry deposition from Table 6.4 represent upper limits. Thus wet deposition is more significant to the fallout of ^{36}Cl to the northern section of the NS array even when the summer monsoonal periods are not considered. This, and the positive relationship between rainfall amount and ^{36}Cl fallout suggests that wet deposition is the most significant mechanism by which ^{36}Cl is removed from the atmosphere.

TABLE 6.5 $^{36}Cl/Cl$ ratios, stable Cl concentrations and Ca/Na ratios dry deposition samples compared to mean $^{36}Cl/Cl$ ratios and stable Cl concentrations.

site	mean $^{36}Cl/Cl$ $*10^{-15}$	season	$^{36}Cl/Cl$ $x10^{-15}$	Ca/Na
30 Tennant Creek	260±27	winter 92	133	0.30
30		autumn 93	278	0.57
31 Dunmarra	378±25	winter 92	734	0.24
31		winter 93	446	0.16
31		autumn 94	181	0.41
32 Katherine	232±22	winter 92	201	1.58
32		autumn 92	152	0.56
33 Kapalga	179±11	winter 92	155	0.48
33		winter 93	367	1.23

6.6 DISCUSSIONS

Comparison of Measured Fallouts with Predicted Fallouts

As discussed in Section 6.3, the range of latitudes sampled in this project enables us to test the predictions of latitude dependence of ^{36}Cl fallout (Lal and Peters 1967, Andrews and Fontes 1992). The data from this investigation fit the general shape of the predicted curve, but the curve underestimates the amount of fallout. Instead the best fit to the data is obtained by scaling the predicted curve by a factor of 1.4 (the three anomalous points from the northern section of the SN array are removed for this fit) as shown in Figure 6.22. Thus, a revised mean fallout of 15.4 atoms/m^2/s is suggested from this investigation.

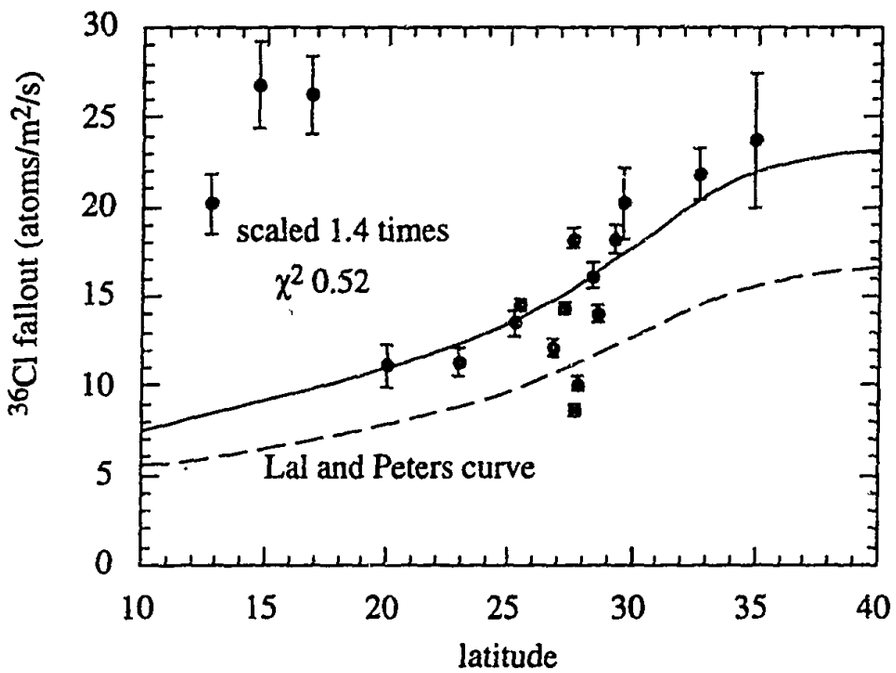

FIGURE 6.22 Mean ^{36}Cl fallout as a function of latitude and the predicted curve of Lal and Peters (1967) scaled by 1.4 times. The scaled curve is the solid line, the unscaled curve is the dashed line. The $\chi 2$ represents the degree of fit each curve shows to the data. The χ^2 for the data to the unscaled Lal and Peters curve is 2.

Solar Activity Effects

Lal and Peters (1967) discussed the dependence of the flux of cosmic rays to the Earth's surface upon solar activity and how the predicted curve needs to be adjusted depending on the 11-year sunspot cycle. At polar regions, cosmic ray fluxes decrease by 30% from a sunspot minimum to maximum. Middle latitudes see a decrease of 25% from sunspot minima to maxima, while the equator sees a decrease of 7%. The curve of Lal and Peters (1967) was calculated for 1948-1949, which represents a sunspot minimum (Figure 6.2). Thus this curve represents maximum

fallout during the 11-year sunspot cycle. The present investigation encompassed a sunspot maximum in 1991 and a reduction in sunspot activity through to 1994. The change in solar activity cannot be used to explain the higher fallouts observed during the present study, since a reduction in fallout is expected with the maxima in sunspot activity.

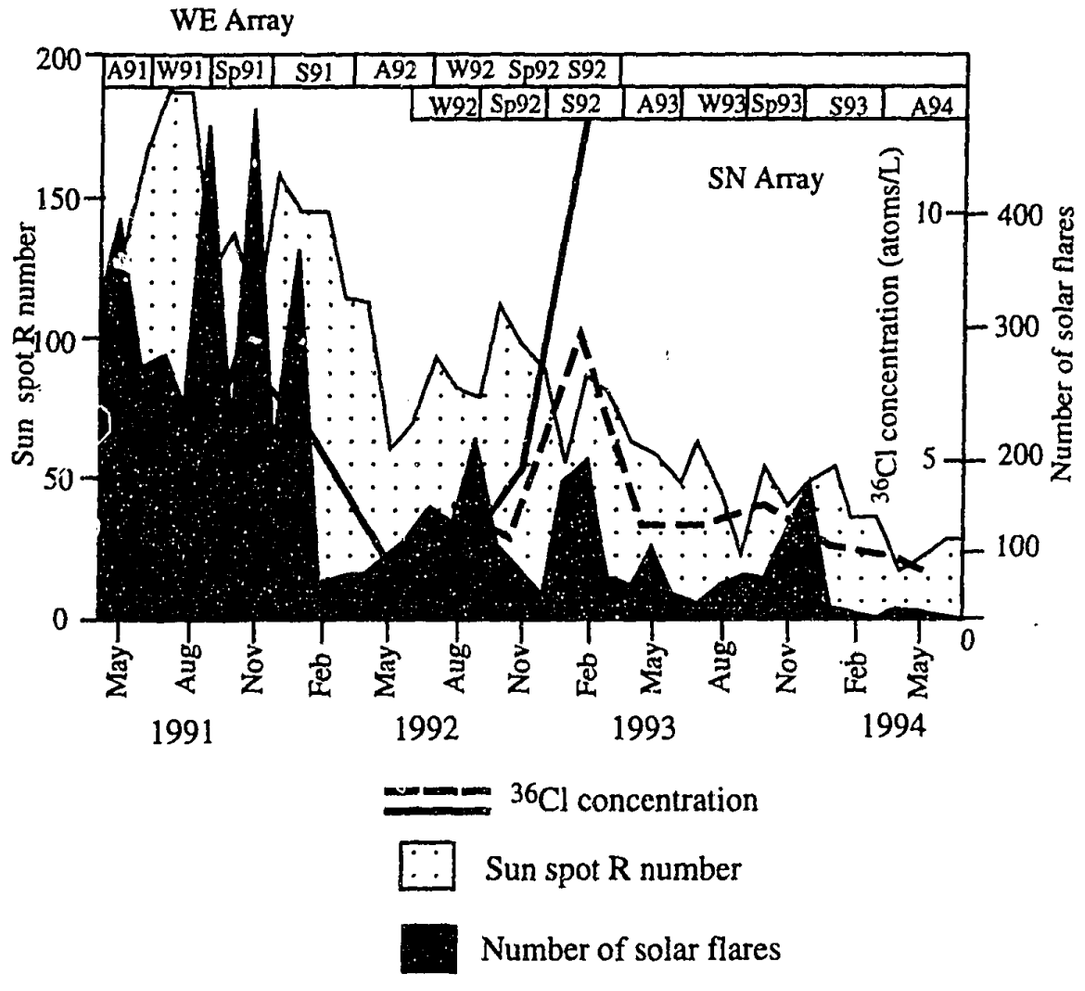

FIGURE 6.23 Sun spot R numbers and the number of solar flares recorded during the sampling program, compared with the ^{36}Cl concentration of precipitation collected at latitude 12.8°S (site 18 of WE array and site 28 of SN array). R numbers = (# of sun spot groups) - # of sun spots) measured by the National Solar Observatory, Sacramento Peak, New Mexico. Solar flare numbers recorded by BATSE (Burst and Transient Source Experiment) from the Gamma Ray Astronomy Group, NASA.

The relationship between solar activity and ^{36}Cl fallout for the present sampling program is shown in Figure 6.23. Sunspot R numbers and the number of solar flares are compared with ^{36}Cl concentration measured in rainfall at latitude 13°S (i.e. site 18 on the WE array and site 28 on the SN array). Sunspot R numbers were measured by the U.S. National Solar Observatory, Sacramento Peak and the number of solar flares was measured by BATSE, NASA. An overall trend of decreasing

sunspot R number and solar flare number is seen as the collection program progresses. However ^{36}Cl concentration of rainfall remains constant (excepting a peak on both arrays during summer 1993). An inverse relationship between solar activity and cosmic ray flux has been demonstrated by ^{10}Be in ice-cores from Greenland and Antarctica (Beer et al 1991). These ice cores have been compared with ^{14}C from tree-ring records to extend the record of solar activity back in time to 2,500 years BP. However it can be seen in Figure 6.23 that the inverse relationship does not appear to be recorded by ^{36}Cl in rainfall from the present investigation. This suggests that transport and depositional processes control the fallout of ^{36}Cl to the Earth's surface on the time scales used in this investigation (i.e. 3 months), rather than changes in solar activity. This is consistent with results from the Camp-Century ice core (Elmore et al 1987) where a correlation between sunspot activity and ^{36}Cl concentration could only be seen after the data had been mathematically smoothed.

Atmospheric Implications

Global Fallouts

The mean fallout of ^{36}Cl to the Earth's surface in the latitudes investigated in this research agree with the general form of the fallout curve predicted by Lal and Peters (1967), but are a factor of 1.4 greater. The mean global fallout calculated from this research is 15.4 atoms/m^2/s. While higher than the predicted mean global fallout of Lal and Peters (11 atoms/m^2/s) this is much lower than the fallouts measured from northern hemisphere investigations, eg. Greenland ice-core data measures a pre-bomb mean global fallout of 30-60 atoms/m^2/s i.e. 3 to 5 times greater than predicted (Suter et al 1987). Hainsworth (1994) and Knies (1994) measured fallouts at 40°N of 40-50 atoms/m^2/s (4 times greater than predicted). However, the fallout measured in this project is similar to that deduced from the only published measurements of ^{36}Cl concentrations in modern precipitation from the southern hemisphere. From Antarctic ice (Table 6.1) a fallout of between 10-14 atoms/m^2/s can be deduced.

This work suggests that the fallout of ^{36}Cl to the Earth's surface in the southern hemisphere is lower (by approximately 3 times) than in the northern hemisphere. Some possible reasons for this are:

a) the production of ^{36}Cl in the northern hemisphere stratosphere is greater than in the southern hemisphere stratosphere.

Such a situation would require a greater flux of cosmic rays to the northern hemisphere and/or a greater concentration of target ^{40}Ar. This is not possible or observed. Cosmic ray fluxes are affected by the Earth's geomagnetic field, but the geomagnetic field is symmetric about the geomagnetic equator. The main components of the atmosphere i.e. N_2, O_2, Ar and CO_2 are mixed in constant proportions up to the mesopause (Warneck 1988).

b) there is an additional supply of ^{36}Cl in the northern hemisphere that does not exist in the southern hemisphere.

This supply may include output from nuclear reactor and processing activities, or recycled ^{36}Cl, remnant from the bomb testing of the 1950s. The density of nuclear installations in North America and Europe is higher than in the southern hemisphere. An investigation of the release of ^{36}Cl to the atmosphere at the Chalk River Laboratories in Ontario (Milton et al 1993), found that only small quantities of ^{36}Cl were released during reactor operations. The dispersion of ^{36}Cl (as measured in rainfall and snow) was dependent on wind direction, with most of the estimated release being deposited locally. Background levels of ^{36}Cl were measured at 140 km from the reactor site. Beasley et al (1992) however, reported that nuclear fuel reprocessing activities at the US Department of Energy's Savannah River Site increased the flux of ^{36}Cl from natural levels of 20-25 atoms/m^2/s by factors of 10 to 20 within 200 km of the site. Measurement of soil cores and groundwaters confirmed the presence of site-derived ^{36}Cl at a similar facility in Idaho (Beasley et al 1990, reported in Beasley et al 1992). The information regarding the atmospheric release of ^{36}Cl from nuclear processing activities appears inconsistent. This inconsistency may simply arise from differences in the magnitude of the operations at the different facilities. A nuclear activity source of ^{36}Cl does not explain the high pre-bomb fallout levels measured in the Greenland ice-cores. The pre-bomb fallouts were measured for 1945 to 1950 (Suter et al 1987), a period before extensive development of nuclear facilities in the northern hemisphere. Thus, while nuclear reactor and processing activities may be important on a local scale, they are not considered to be the main cause of the large difference seen between northern and southern hemisphere fallouts.

Cornett et al (1994) suggest that high fallouts of ^{36}Cl measured in environmental samples from Canada is due to recycling of bomb ^{36}Cl. Phillips et al (1988) compared ^{36}Cl in soil profiles under laboratory and field conditions. They found the movement of ^{36}Cl through the soil profile is dependent upon many conditions

including water content, time, temperature etc. The rate of movement of ^{36}Cl through the soils profile from arid New Mexico was considerably slower than simulated in laboratory experiments. The 1950s bomb spike was retained near the soil surface. Fifield et al (1987) measured the ^{36}Cl in soils from a semi-arid region in South Australia and recorded the bomb spike between 1-1.5 m into the soil.

In order for recycling of bomb-produced ^{36}Cl to influence measurements of ^{36}Cl in precipitation, the ^{36}Cl must reside in the soil surface. While this appears to be the case for New Mexico, experimental studies (Phillips et al 1988) and other investigations (eg. Fifield et al 1987) suggest that the movement of ^{36}Cl through the soil profile is geographically variable. The influence of recycled bomb-produced Cl on the high fallouts of ^{36}Cl measured from the northern hemisphere cannot be discounted. However, a great deal more information regarding the behaviour of ^{36}Cl and soil and the release of ^{36}Cl from soils is required before this possibility can be discussed further.

c) there is greater transfer of ^{36}Cl from the stratosphere to the troposphere in the northern hemisphere.

The review of transfer between atmospheric domains (Section 6.1) showed an asymmetry in the stratosphere-troposphere transfer of ^{90}Sr (Lal 1962), ozone (Fabian and Pruchniewicz 1973) and aerosols (Hitchman et al 1994) between the two hemispheres. Modelling of climate data revealed transfer to be up to 50% greater in the northern hemisphere (Holton 1990). Transfer from the stratosphere to the troposphere occurs at middle-latitudes in association with tropopause gaps (or folding events). Danielsen (1968) suggested baroclinic waves associated with the jet stream enhanced movement of material through the gap region. A global circulation model that incorporates stratospheric-tropospheric transfer (Mote et al 1994) supported this. The asymmetry of transfer between the two hemispheres has been attributed to enhanced lower stratospheric wave driving in the northern hemisphere (particularly during the northern hemisphere winter).

The higher ^{36}Cl fallouts measured in the northern hemisphere are most likely explained in terms of the enhanced transfer of ^{36}Cl from the stratosphere to the troposphere. This occurs in response to the more dynamically active nature of the lower stratosphere in the northern hemisphere, which arises from the difference in orographic and thermal forcing between the two hemispheres.

Revised Estimate of Global Fallout

A mean global ^{36}Cl fallout of 25 to 35 atoms/m^2/s can be calculated. This value incorporates the results from the present investigation (15.4 atoms/m^2/s), estimates from Antarctic ice (10 to 14 atoms/m^2/s, Nishiizumi et al 1979, Finkel et al 1980 and Nishiizumi et al 1983), the higher fallout calculated from measurements of ^{36}Cl in northern hemisphere precipitation (40-50 atoms/m^2/s, Hainsworth 1994 and Knies 1994) and Greenland Ice Core data (30-60 atoms/m^2/s eg. Suter et al 1987). This mean global value is 2-3 times greater than predicted by Lal and Peters (1967). The calculation of production rates is dependent on information pertaining to nuclear reaction cross sections, which for ^{36}Cl production were estimated by Lal and Peters (1967) based upon similar reactions at lower energies than those actually required for the production of ^{36}Cl. It is realised that the estimation of cross-section energies may introduce a variation factor in the production rate calculation of up to two (eg. see Hainsworth 1994).

Phase of ^{36}Cl in the Atmosphere

The behaviour of ^{36}Cl and stable Cl in the atmosphere have been discussed throughout this work. The two species arrive in the atmosphere by very different processes. Chlorine-36 is produced in the stratosphere by cosmic ray spallation of ^{40}Ar, where it exists predominantly as HCl gas. Seawater is the main source of stable Cl to the lower atmosphere. Stable Cl is introduced as an aerosol by breaking waves at the ocean's surface (Erickson and Duce 1988). The bulk of Cl remains associated with large aerosol particles. However, 3-20% is released as gaseous inorganic Cl (Cicerone 1991). The mechanisms of release are not well understood. Numerous workers (including Ericksson 1959, Duce 1969 and Martens et al 1973 to name a few) suggest that Cl release from the aerosol may occur by direct volatilisation of seasalt aerosol that is acidified to low pH by the incorporation of HNO_3 and H_2SO_4. Mechanisms of release of gaseous Cl involving reactions of various N gases with the seasalt aerosol have also been demonstrated (Finlayson-Pitts 1983 and Finlayson-Pitts et al 1989). Keene et al (1990) proposed a photochemical mechanism involving the reaction of O_3 at NaCl surfaces to explain release of Cl in the marine atmosphere. This process produces HCl that can be efficiently rescavenged by the aerosol.

The lack of correlation between ^{36}Cl and seasalt aerosol species such as Na and Cl, and the good correlation between ^{36}Cl and NO_3 concentrations allows us to

speculate about the behaviour of ^{36}Cl from its production in the stratosphere to its deposition at the Earth's surface. In the stratosphere, ^{36}Cl exists predominantly as $H^{36}Cl$ (Wahlen et al 1991). It moves through the tropopause, into the troposphere as a gas. The possible courses of action that may follow are:

a) in the troposphere $H^{36}Cl$ it is scavenged by NaCl aerosol and deposited.

This does not fit our observations as a correlation is not observed between ^{36}Cl, Na and Cl concentrations.

b) in the troposphere, $H^{36}Cl$ remains as a gas and mixes with HCl released by volatilisation of NaCl.

As described above, the volatilisation process only releases less than 30% of Cl contained in NaCl aerosols. The mixed $H^{36}Cl$, HCl and other atmospheric gases such as HNO_3 and H_2SO_4 are then deposited at the Earth's surface. Chapter 2 describes the incorporation of gases and aerosols into cloud drops and raindrops both in and below-clouds. At pH of 4.5 (the typical pH of cloudwater) strong acids (such as HCl and HNO_3) are directly scavenged from the gas phase (Warneck 1988). The correlation observed between ^{36}Cl and NO_3 tends to suggest that ^{36}Cl is directly scavenged from the gas phase before deposition.

Hydrological Implications

The results of this study suggest that on a short timescale (i.e. seasonal), fallout of ^{36}Cl is dependent upon rainfall amount. However, the long-term averages measured in this project are only slightly greater than predicted values. Hydrological investigations generally require estimates of long-term fallouts. Thus this investigation supports the use of scaled predicted ^{36}Cl fallout levels as estimates of inputs of ^{36}Cl to groundwater systems. The Cl concentrations of rainfall from the present investigation display exponential decreases with increasing distance from the coast, as has been shown world-wide. However, it is not possible to characterise the exponential decrease by using regression equations derived from earlier investigations. Thus, this project clearly shows the caution that is required when trying to use a particular regression equation to predict the Cl concentration of rainfall at a given distance from the coast. It is important to recognise that Cl concentration of rainfall is geographically variable. The most effective method of overcoming uncertainties due to Cl concentration of rainfall when estimating $^{36}Cl/Cl$

input to groundwater systems is to undertake a reconnaissance survey of rainfall Cl concentrations.

6.7 SUMMARY

The fallout of ^{36}Cl to the Earth's surface at the latitudes sampled in this project agree with the general form of Lal and Peters (1967) but are 1.4 times greater. The mean fallout of ^{36}Cl calculated for west, north and south Australia is 15.4 atoms/m^2/s, comparable to that calculated for samples of Antarctic ice, but 3 times lower than measured in the northern hemisphere. The lower southern hemisphere fallout rates reflect the lower rates of transfer of stratospheric air to the troposphere in the southern hemisphere. A mean global fallout that incorporates the high fallouts measured in northern hemisphere precipitation of 25-35 atoms/m2/s can be calculated. This value is 2-3 times greater than predicted by Lal and Peters (1967), suggesting that the cross-section for the cosmic-ray production of ^{36}Cl may be underestimated in their paper.

The spatial pattern of stable Cl deposition to the Australian continent is for decreasing deposition from south to north, reflecting the importance of the southern marine airmasses in the supply of Cl. The northern tropical airmasses play a less significant part in this process. The relationship between Cl deposition and distance from the coast can be explained in terms of a double exponential decay, suggesting that two processes control this relationship. These processes may reflect the enhanced mixing of airmasses moving inland and/or differences in the rate of removal of Cl aerosol and Cl gas from marine and continental airmasses.

The $^{36}Cl/Cl$ ratio of precipitation increases exponentially with increasing distance from the coast. The opposite trend displayed by stable Cl concentrations of precipitation reflects the decreasing influence of stable Cl of marine origin on the $^{36}Cl/Cl$ ratios at inland sites.

Low $^{36}Cl/Cl$ ratios are observed at coastal localities and at inland sites when synoptic conditions favour the transport of seawater aerosols great distances inland (eg. during cold frontal activity). Low $^{36}Cl/Cl$ ratios at inland sites on the WE array reflect the diluting effect of stable recycled Cl from local salt lakes which have low ^{36}Cl contents.

Seasonal variations in ^{36}Cl fallouts and $^{36}Cl/Cl$ show high ratios and fallouts during spring, and at some localities, during summer (i.e. the north of the SN array). These

increased spring ^{36}Cl fallouts are attributed to increased transfer of stratospheric ^{36}Cl to the troposphere that occurs as the tropopause height increases during the warmer months. High fallouts during summer in the north of the SN array may be attributed to the direct entrainment of stratospheric air into cumulus clouds during the monsoonal convection.

Wet deposition appears to be the major process of removal of ^{36}Cl from the atmosphere. Chlorine-36 fallout and rainfall amount can be correlated, particularly along the SN array where extremes in rainfall regimes are experienced. Dry deposition accounts for less than 50% of fallout in the north of the SN array.

Chlorine-36 exists in the stratosphere predominantly as HCl gas (Wahlen et al 1991). The correlation between ^{36}Cl and NO_3 and the lack of any relationship between ^{36}Cl, stable Cl and Na concentrations, suggest that ^{36}Cl is scavenged from the atmosphere as a gas rather than aerosol phase.

Long-term average predictions of ^{36}Cl fallout rates used to predict the input ratios of $^{36}Cl/Cl$ in hydrological investigations should be increased by a factor of 1.4 for the southern hemisphere. A simple correlation between stable Cl concentrations and distance from the coast is not the rule however. While stable Cl concentrations in precipitation display a general exponential decrease with distance, the nature of this relationship is geographically variable, and should be investigated for each study by local direct measurements, a process that is simple and inexpensive.

CHAPTER 7 SUMMARY AND CONCLUSIONS

The major-element and ^{36}Cl chemistry of bulk precipitation collected from 18 sites in remote areas of Australia, over two years at three-monthly intervals, has been assessed. Samples were collected from two arrays: the WE array extended in an west-east direction from the coast of Western Australia south of Geraldton, inland to Warburton in Central Australia, and the SN array, extended in a south-north direction from Port Lincoln in South Australia to Kakadu in the Northern Territory. The work can be divided into two related sections: major elements and ^{36}Cl.

7.1 MAJOR ELEMENTS

The aims of investigating the major-element chemistry of precipitation in this project were to assess the sources of ionic constituents to precipitation, assess the seasonal variations in the supply of these sources and to asses the accession rate of ionic constituents to the Australian landmass. This work also adds to the Australian data base of precipitation chemistry, and provides the background on which interpretation of ^{36}Cl data can be based.

A synoptic classification system described in Chapter 2, was used as a simplified proxy for airmass trajectory analysis, to trace the movement of airmasses associated with rainfall during each collection period. In most cases, rainfall events were associated with synoptic processes involving airmasses of marine origin, in particular cold fronts that sourced airmasses travelling from south of the Australian landmass and tropical events that sourced airmasses from north of Australia. Cold fronts were most active during winter with coastal cold front activity occurring all year round. During winter 1991, cold fronts were seen to penetrate as far inland as 2000 km from the west coast of Western Australia. Tropical events mainly affected the northern half of Australia during summer months, and were seen to extend 1000 km southwards from the north coast. Therefore, it was anticipated that precipitation chemistry across Western Australia in winter and northern Australia in summer would exhibit a strong marine signature.

Data quality checks were performed on the WE and SN data sets to remove samples that were not representative of bulk precipitation deposited over the collection area for the collection time. These checks removed 9% of data from the WE array and 16% of data from the SN array. Large ion imbalances in the SN data set were

attributed to the presence of organic acids, which were unmeasured in this analytical program.

All the ionic species displayed an approximately log-normal distribution of depositional rates. The relative magnitude of species in precipitation was Cl > Na > SO_4 >Ca > NO_3 > Mg > H > NH_4 > HPO_4 > Br, with NH_4 showing locally high concentrations at sites from the north of the SN array. An inverse correlation between ionic species concentrations and rainfall amount was attributed to a "washout" effect during the initial stages of a rain event, the initially concentrated rainfall being diluted as the rain event continued.

All ionic species displayed a decrease in deposition with increasing distance from the coast, with generally lower deposition rates at the north coast compared to the south and west. Hingston and Gailitis (1973) found a similar trend for the south and north of Western Australia. Sites along the WE array and southern section of the SN array experienced maximum deposition of all ionic species during winter and minimum deposition during summer. Sites along the northern section of the SN array showed the opposite relationship with maximum deposition occurring during summer. These differences can be correlated with seasonal differences in rainfall amount.

Three main sources/processes were found to control the chemistry of precipitation collected in the sampling vessels: a mixed seawater/continental source represented by simultaneous variances between Cl, Mg, Na, SO_4, Ca and K; acid-base balances in which some or all of H, NO_3, SO_4 and K showed similar variances; and biodegradation. The mixed seawater/continental source was responsible for most variance (usually about 75%) of the WE data set and the southern section of the SN data set. Isolating the two end-members of this source was only possible when the data sets were divided into coastal and non-coastal subsets. Most of the variance in the SN data set was caused by the mixed continental/seawater source and biodegradation. Dividing the data set into wet and dry subsets isolated the seawater source in a factor responsible for only 10% of variance in the wet data set, suggesting that the tropical monsoon activity may provide only a limited supply of ionic species to precipitation in the north of Australia. The components of the acid-base balance factor were suggested to be derived from natural sources such as biogenic emissions, biomass burning and lightning flash production. The nature of the collection program (i.e. sampling vessels were open to the atmosphere for three

months without preservatives) means that biodegradation was also a consequence of sampling procedures.

Seasonal variations of ionic species to Na (acting as a seawater tracer) and Ca (acting as a continental tracer) were used to ascertain periods dominated by a seasalt source. Seasalt was found to dominate precipitation chemistry at southern and western coastal localities throughout the sampling program, and during winter, extend up to 1800 km inland from the west coast. This was associated with cold front activity. A marine signature was also found for the coastal northern site, and was associated with monsoonal activity. However, this marine signature did not extend to 200 km from the northern coast, suggesting that the tropical marine airmass is rapidly modified as it moves southwards over the Australian landmass.

7.2 CHLORINE-36

One of the aims of investigating ^{36}Cl in precipitation was to test the latitudinal-dependent predicted fallout curve of ^{36}Cl to the Earth's surface (Lal and Peters 1967), commonly used to calculate $^{36}Cl/Cl$ ratios in recharge for hydrological investigations. The results of the present investigation agree with the general shape of the predicted curve, but suggest the curve underestimates the true rate of fallout. A revised southern hemisphere fallout of 15.4 ^{36}Cl atoms/m^2/s is suggested. Long-term average predictions of ^{36}Cl fallout rates used to predict the input ratios of $^{36}Cl/Cl$ in hydrological investigations should thus be increased by a factor of 1.4 for the southern hemisphere. The common assumption of a simple correlation between stable Cl concentrations and distance from the coast was not uniformly observed. While stable Cl concentrations in precipitation displayed a general exponential decrease with distance from the coast, the nature of this relationship was shown to be geographically variable, and for theoretical $^{36}Cl/Cl$ estimates, should be investigated for each study by local direct measurements, a process that is simple and inexpensive.

Wet deposition appeared to be the major process of removal of ^{36}Cl from the atmosphere. Chlorine-36 fallout and rainfall could be correlated, particularly along the SN array where extremes in rainfall regimes are experienced. Dry deposition is shown to account for less than 50% of fallout in the north of the SN array.

The spatial pattern of stable Cl deposition to the Australian continent is for decreasing deposition from south to north, reflecting the importance of the southern marine airmasses in the supply of Cl. The northern tropical airmasses play a less

significant part in this process. The relationship between Cl deposition and distance from the coast can be explained in terms of a double exponential decay, suggesting that two processes control this relationship. These processes may reflect the enhanced mixing of airmasses moving inland and/or differences in the rate of removal of Cl aerosol and Cl gas from marine and continental airmasses.

As expected, the $^{36}Cl/Cl$ ratio of precipitation increases exponentially with increasing distance from the coast, due to the opposing trend displayed by stable Cl concentrations in precipitation, reflecting the decreasing influence of stable Cl of marine origin at inland sites. The $^{36}Cl/Cl$ ratio was often perturbed however, by the supply of a source of stable Cl with insignificant or low ^{36}Cl content. For example, low $^{36}Cl/Cl$ ratios were observed at inland sites when synoptic conditions favoured the transport of seawater aerosols great distances inland (eg. during cold frontal activity). Also, low $^{36}Cl/Cl$ ratios at inland sites on the WE array reflect the diluting effect of stable, recycled Cl from local salt lakes with low ^{36}Cl contents.

This work supports the use of ^{36}Cl as a tracer of atmospheric processes. Its production primarily in the stratosphere suggests that it may trace stratosphere-troposphere exchange. Chlorine-36 fallouts and $^{36}Cl/Cl$ ratios were high during spring, and for the north of the SN array, during summer. The increased spring ^{36}Cl fallouts may be attributed to increased transfer of stratospheric ^{36}Cl to the troposphere occurring as the tropopause increases height during the warmer months. High ^{36}Cl fallouts during summer in the north of the SN array may be attributed to the direct entrainment of stratospheric air into cumulus clouds during the monsoonal convection.

The mean fallout calculated from this work, while higher than the theoretical estimate, is three times lower than has been measured for precipitation in the northern hemisphere. Several possible explanations are suggested for this observation: i) an additional supply of ^{36}Cl that is not present in the southern hemisphere. Output from nuclear reactors, which are concentrated in the northern hemisphere is suggested. However, releases of ^{36}Cl to the environment from nuclear reactor operations are too localised and thus cannot be considered to be the cause of the total fallout discrepancy between the northern and southern hemisphere. ii) recycling of bomb-produced ^{36}Cl is also suggested as an explanation, although this does not explain the high fallouts measured in pre-bomb Greenland ice. Further investigations into the behaviour of ^{36}Cl in soil profiles may allow more comment on the role of bomb-produced ^{36}Cl in enhancing fallout of ^{36}Cl in the northern

hemisphere. iii) It is suggested here that enhanced ^{36}Cl fallout in the northern hemisphere actually reflects the lower rates of transfer of stratospheric air to the troposphere in the southern hemisphere, a consequence of the less dynamic nature of the lower southern hemisphere stratosphere as compared to the northern hemisphere.

A mean global ^{36}Cl fallout of 25 to 35 atoms/m^2/s can be calculated. This value incorporates the results from the present investigation, estimates from Antarctic ice and the higher fallout calculated from measurements of ^{36}Cl in northern hemisphere precipitation. This value is 2-3 times greater than predicted by Lal and Peters (1967), suggesting that the cross-section for the cosmic-ray production of ^{36}Cl may be underestimated in their paper.

Another implication from this work for atmospheric investigations arises from the ^{36}Cl relationship to major elements measured in precipitation. A correlation between ^{36}Cl and NO_3 and the lack of any relationship between ^{36}Cl, stable Cl and Na concentrations, suggests that ^{36}Cl is scavenged from the atmosphere as a gas rather than aerosol phase. This is a very preliminary suggestion, and further investigations into the phase of ^{36}Cl through cross-sections of the atmosphere may provide more information required to develop this hypothesis.

REFERENCES

Andreae, M. O. (1984). The emission of sulfur to the remote atmosphere: background paper, in Galloway, J., N.,, Charlson, R. J., Andreae, M. O. and Rodhe, H., eds., *The Biogeochemical Cycling of Sulfur and Nitrogen in the Remote Atmosphere*, NATO ASIO Series, v. Dordrecht, D. Reidel Publishing Company, p. 5-21.

Andrews, D. G. (1989). Some comparisons between the middle atmosphere dynamics of the southern and northern hemispheres: *Pure and Applied Geophysics,* v. 130, p. 213-232.

Andrews, J. N. and Fontes, J. C. (1992). Importance of in-situ production of chorine-36, argon-36 and carbon-14 in Hydrology and hydrochemistry, in IAEA, eds., *Isotope Techniques in Water Resources Development, Vienna*, p. 245-269.

Avery, R. (1984). A preliminary study of rainwater acidity around Newcastle, N.S.W: *Clean Air (Australia)*, v. 18, p. 94-101.

Ayers, G. P. and Gillett, R. W. (1982). Acidity of summer rainfall in Sydney, in Carras, J. N. and Johnson, G. M., eds., *The Urban Atmosphere-Sydney, a case study*, Melbourne, CSIRO, p. 421-432.

Ayers, G. P. and Gillett, R. W. (1988a). Acidification in Australia, in Rodhe, H. and Herrera, R., eds., Acidification in Tropical Countries, SCOPE 36, Chichester, John Wiley and Sons, p. 347-402.

Ayers, G. P. and Gillett, R. W. (1988b). First observations of cloudwater acidity in tropical Australia: *Clean Air (Australia)*, v. 22, p. 53-57.

Ayers, G. P. and Ivey, J. P. (1988). Precipitation composition at Cape Grim, 1977-1985: *Tellus*, v. 40B, p. 297-307.

Ayers, G. P. and Manton, M. J. (1991). Rainwater compositions at two BAPMoN regional stations in SE Australia: *Tellus,* v. 43B, p. 379-389.

Barry, R. G. and Chorley, R. J. (1976). Atmosphere, Weather and Climate. Suffolk, Methuen and Co Ltd, 432.

Beasley, T. M., Elmore, D. E., Kubik, P. W. and Sharma, P. (1992). Chlorine-36 release from the Savannah River site nuclear fuel reprocessing plants: *Groundwater*, v 30 p2539-548.

Beasley, T., Cecil, L., Mann, L., Kubik, P., Sharma, P., Fehn, U. and Gove, H. (1990). Chlorine-36 in the Snake River Plain Aqcuifer. *Fourteenth Annual Radiocarbon Conference*, 20-24 May, 1990., Tucson, Arizona.

Beer, J., Raisbeck, G. M. and Yiou, F. (1991). Time variations of ^{10}Be and solar activity, in Sonett, C. P., Giampapa, M. S. and Matthews, M. P., eds., The Sun in Time, Space Science Series, Arizona, The University of Arizona Press, p. 343-359.

Bentley, H. W., Phillips, F. M. and Davies, S. N. (1986a). Chlorine-36 in the terrestrial environment, in Fritz, P. and Fontes, J. C., eds., Handbook of Environmental Isotope Geochemistry, v. 2. Amsterdam, Elsevier, p. 427-475.

Bentley, H. W., Phillips, F. M., Davis, S. N., Gifford, S., Elmore, D., Tubbs, L. E. and Gove, H. E. (1982). Thermonuclear ^{36}Cl pulse in natural water: *Nature*, v. 300, p. 737-740.

Bentley, H. W., Phillips, F. M., Davis, S. N., Habermehl, M. A., Airey, P. L., Calf, G. E., Elmore, D., Gove, H. E. and Torgersen, T. (1986b). Chlorine-36 dating of very old groundwater 1. The Great Artesian Basin, Australia: *Water Resources Research*, v. 22, p. 1991-2001.

Bird, J. R., Calf, G. E., Davie, R. F., Fifield, L. K., Ophel, T., R., Evans, W. R., Kellett, J. R. and Habermehl, M. A. (1989). The role of ^{36}Cl and ^{14}C measurements in Australian groundwater studies: *Radiocarbon*, v. 31, p. 877-883.

Bird, J. R., Davie, R. F., Chivas, A. R., Fifield, L. K. and Ophel, T. R. (1991). Chlorine-36 production and distribution in Australia: *Palaeogeography, Palaeoclimatology, Palaeoecology*, v. 84, p. 299-307.

Blackburn, G. and McLeod, S. (1983). Salinity of atmospheric precipitationin the Murray-Darling Drainage Division, Australia: *Australian Journal of Soil Research*, v. 21, p. 411-434.

Blanchard, D. C. and Woodcock, A. H. (1957). Bubble formation and modification in the sea and its meteorological significance: Tellus, v. 9, p. 145-158.

Bridgeman, H. A. (1990). Acid rain studies in Australia and New Zealand: *Archives of Environmental Contamination and Toxicology*, v. 18, p. 137-146.

Bridgeman, H. A., Rothwell, R., Pang Way, C., Peng Hing Tio, Carras, J. N. and Smith, M. Y. (1988a). Rainwater acidity and composition in the Hunter Region, New South Wales: *Clean Air (Australia)*, v. 22, p. 45-52.

Bridgeman, H. A., Rothwell, R., Peng-Hing Tio and Pang Way, C. (1988b). The Hunter Region (Australia) acid rain project: *Bulletin of the Meteorological Society of America*, v. 69, p. 266-271.

Brimblecomb, P. (1986). Air Composition and Chemistry. Cambridge Environmental Series, Cambridge, Cambridge University Press, 217.

Brimblecomb, P. and Dawson, G. A. (1984). Wet removal of highly soluble gases: *Journal of Atmospheric Chemistry*, v. 2, p. 95-107.

Browne, E. and Firestone, R. B. (1986). Table of radioactive isotopes. Brisbane, John Wiley and Sons.

Bulletin of Volcanic Eruptions. (1994). Annual report of world volcanic eruptions in 1991: *Bulletin of Volcanic Eruptions, v. 31 for 1991, Supplement to Bulletin of Volcanology 56*, p. 56-58.

Bureau of Meteorology 1991a, Monthly Weather Review, Western Australia (April). Government Printer, Australia.

Bureau of Meteorology 1991b, Monthly Weather Review, Western Australia (December). Government Printer, Australia.

Bureau of Meteorology 1991c, Monthly Weather Review, South Australia (May). Government Printer, Australia.

Bureau of Meteorology 1991d, Monthly Weather Review, Western Australia (July). Government Printer, Australia.

Bureau of Meteorology 1992a, Monthly Weather Review, Western Australia (January to December). Government Printer, Australia.

Bureau of Meteorology 1992b, Monthly Weather Review, South Australia (October). Government Printer, Australia.

Bureau of Meteorology 1993a, Monthly Weather Review, Northern Territory (January to December). Government Printer, Australia.

Bureau of Meteorology 1993b, Monthly Weather Review, South Australia (January to December). Government Printer, Australia.

Cautenet, S. and Lefeivre, B. (1994). Contrasting behaviour of gas and aerosol scavenging in convective rain: a numerical and experimental study in the African equatorial forest: *Journal of Geophysical Research*, v. 99, p. 13013-13024.

Chameides, W. L., Stedman, D. H., Dickenson, R. R., Rusch, D. W. and Cicerone, R. J. (1977). NOx production in lightning: *Journal of Atmospheric Science*, v. 34, p. 143-149.

Chivas, A. R., Kiss, E., Keywood, M. D., Fifield, L. K. and Allan, G. L. (1994). Chlorine-36 in Australian rainfall and playas and the residence time of chlorine in the Australian landscape. *Eight International Conference on Geochronology, Cosmochronology and Isotope Geology* . Berkeley, CA, p. 58.

Cicerone, R. J. (1981). Halogens in the atmosphere: *Reviews in Geophysics and Space Physics*, v. 19, p. 123-139.

Cornett, R., Milton, J., Andrews, H. R., Chant, L. A., Greiner, B. F., Imahori, Y., Kowlosky, V. T., Kramer, S. J. and Milton, J. C. D. (1994). Chlorine-36 deposition: reconciling models and measurements. *Abstract of the Geological Society of Canada Waterloo Meeting*, May 1994.

Crawley, J. and Sievering, H. (1986). Factor analysis of the MAP3S/RAINE Precipitation Chemistry Network: 1976-1980: *Atmospheric Environment*, v. 20, p. 1001-1013.

Danielsen, E. F. (1968). Stratospheric-tropospheric exchange based on radioactivity, ozone and potential vorticity: *Journal of Atmospheric Science*, v. 25, p. 502-518.

Davie, R. F., Kellet, J. R., Fifield, L. K., Evans, W. R., Calf, G. E., Bird, J. R., Topham, S. and Ophel, T. R. (1989). Chlorine-36 measurements in the Murray Basin: preliminary results from the Victorian and South Australian Mallee region: *BMR Journal of Geology and Geophysics*, v. 11, p. 261-272.

Davis, J. C. (1986). Statistics and Data Analysis in Geology. New York, John Wiley and Sons, 646.

Denmead, O. T., Freney, J. R. and Simpson, J. R. (1976). A closed ammonia cycle within a plant canopy: *Soil Biology and Biochemistry*, v. 8, p. 161-164.

Duce, R. A. (1969). On the source of gaseous chlorine in the marine atmosphere: *Journal of Geophysical Research*, v. 74, p. 4597-4599.

Elmore, D., Conrad, N., M., Kubik, P. W., Gove, H. E., Wahlen, M., Beer, J. and Suter, M. (1987). ^{36}Cl and ^{10}Be profiles in Greenland ice: dating and production rate variations: *Nuclear Instruments and Methods in Physics Research*, v. B29, p. 207-210.

Elmore, D., Fulton, B. R., Clover, M. R., Marsden, J. R., Gove, H. E., Naylor, H., Purser, K. H., Kilius, L. R., Beukens, R. P. and Litherland, A. E. (1979). Analysis of ^{36}Cl in environmental water samples using an electrostatic accelerator.: *Nature*, v. 277, p. 22-25.

Elmore, D., Tubbs, L. E., Newman, D., Ma, X. Z., Finkel, R., Nishiizumi, K., Beer, J., Oeschger, H. and Andree, M. (1982). ^{36}Cl bomb pulse measured in a shallow ice core from Dye 3, Greenland.: *Nature*, v. 300, p. 735-740.

Erickson, D. J. and Duce, R. A. (1988). On the global flux of atmospheric seasalt: *Journal of Geophysical Research*, v. 74, p. 14079-14088.

Ericksson, E. (1959). The yearly circulation of chlorine and sulfur in nature: Meteorological, geochemical and pedological implications 1: Tellus, v. 11, p. 375-403.

Erisman, J. W., Beier, C., Draaijers, G. and Lindberg, S. (1994). Review of deposition monitoring methods: Tellus, v. 46B, p. 79-93.

Fabian, P. and Pruchniewicz, P. G. (1977). Meridional distribution of ozone in the troposphere and its seasonal variations: *Journal of Geophysical Research*, v. 82, p. 2063-2073.

Farrington, P. and Bartle, G. A. (1988). Accession of chloride from rainfall on the Gnangara Groundwater Mound, Western Australia, Technical Memorandum, Division of Water Resources, CSIRO, 88/1, 10 pp.

Farrington, P., Salama, R. B., Bartle, G. A. and Watson, G. D. (1993). Accession of major ions in rainfall in the southwestern region of Western Australia, Division of Water Resources, 93/1, 11 pp.

Fifield, L. K., Ophel, T. R., Bird, J. R., Calf, G. E., Allison, G., B., and Chivas, A. R. (1987). The chlorine-36 measurement program at the Australian National University: *Nuclear Instruments and Methods in Physics Research*, v. B29, p. 114-119.

Finkel, R. C., Nishiizumi, K., Elmore, D., Ferraro, R. D. and Gove, H. E. (1980). ^{36}Cl in polar ice, rainwater and seawater: Geophysical Research *Letters*, v. 7, p. 983-986.

Finlayson-Pitts, B. J. (1983). Reaction of NO_2 with NaCl and atmospheric implications of NOCl formation: *Nature*, v. 306, p. 676-677.

Finlayson-Pitts, B. J., Ezell, M. J. and N., P. J. J. (1989). Formation of chemically active chlorine compounds by reaction of atmospheric NaCl particles with gaseous N_2O_5 and $ClONO_2$: *Nature*, v. 337, p. 241-244.

Follows, M. J. (1992). On the cross-tropopause exchange of air: *Journal of Atmospheric Science*, v. 49, p. 879-882.

Galbally, I. E. (1984). The emission of nitrogen to the remote atmosphere: background paper, in Galloway, J. N., Charlson, R. J., Andreae, M. O. and Rodhe, H., eds., Biogeochemical Cycling of Sulfur and Nitrogen in the Remote Atmosphere, NATO ASI Series, v. Dordrecht, D. Reidel Publishing Company, p. 27-54.

Galbally, I. E., Freney, J. R., Denmead, O. T. and Roy, C. R. (1980). Processes controlling the nitrogen cycle in the atmosphere over Australia, in Trudinger, P. A., Walter, M. R. and Ralph, B. J., eds., Biogeochemistry of Ancient and Modern Environments, v. Canberra, Australian Academy of Science, p. 319-326.

Galloway, J. N., Likens, G. E., Keene, W. C. and Miller, J. M. (1982). The composition of precipitation in remote areas of the world: *Journal of Geophysical Research*, v. 87, p. 8771-8786.

Gatz, D. F. and Dingle, A. N. (1971). Trace substances in rainwater: concentration variations during convective rains and their interpretation: Tellus, v. 23, p. 14-27.

Genstat 5 Committee. (1989). Genstat 5 Reference Manual. Oxford, Clarendon Press, 749.

Gentilli, J. (1971). Australian climatic factors: Climates of Australia and New Zealand. World Survey of Climatology, 13, Amsterdam, Elsevier, (J. Gentilli, ed), 35-52.

Gill, A. E. (1982). Atmosphere-Ocean Dynamic. International Geophysics Series, 30, California, Academic Press, 662.

Gillett, R. W. and Ayers, G. P. (1991). The use of thymol as a biocide in rainwater samples: *Atmospheric Environment*, v. 25A, p. 2677-2681.

Gillett, R. W. and Ayers, G. P., Noller, B. N. (1990). Rainwater acidity at Jabiru, Australia, in the wet season of 1983/84: Science of the Total Environment, v. 92, p. 129-144.

Gossard, E. E. and Hooke, W. H. (1975). Waves in the Atmosphere. Developments in Atmospheric Science, 2, Amsterdam, Elsevier, 456.

Hainsworth, L. J. (1994). Spatial and Temporal Variations in Chlorine-36 Deposition in the Northern United States, The University of Maryland, PhD Thesis.

Hainsworth, L. J., Mignerey, A. C., Helz, G. R., Sharma, P. and Kubik, P. W. (1994). Modern chlorine-36 deposition in Southern Maryland, U.S.A. : *Nuclear Instruments and Methods in Physics Research*, v. B29, p. 345-349.

Henry, R. (1987). Current factor analysis receptor models are ill-posed: *Atmospheric Environment*, v. 21, p. 1815-1820.

Herlihy, L. J., Galloway, J. N. and Mills, A. L. (1987). Bacterial utilization of formic and acetic acid in rainwater: *Atmospheric Environment*, v. 21, p. 2397-2402.

Herut, B., Starinsky, A., Katz, A., Paul, M., Boaretto, E. and Berkovits, D. (1992). ^{36}Cl in chloride-rich rainwater, Israel: *Earth and Planetary Science Letters*, v. 109, p. 179-183.

Hingston, F. J. and Gailitis, V. (1976). The geographic variation of salt precipitated over Western Australia: Australian Journal of Soil Research, v. 14, p. 319-335.

Hirsch, R. M. and Gilroy, E. J. (1984). Methods of fitting a straight line to data: Examples in water resources: *Water Resources Bulletin*, v. 20, p. 705-711.

Hitchman, M. H., McKay, M. and Trepte, C. R. (1994). A climatology of stratospheric aerosol: *Journal of Geophysical Research*, v. 99, p. 20689-20700.

Holton, J. R. (1990). On the global exchange of mass between the stratosphere and troposphere: *Journal of Atmospheric Science*, v. 47, p. 392-395.

Hurst, D. F., Griffith, D. W. T. and Cook, G. D. (1994). Trace gas emissions from biomass burning in tropical Australian savannas: *Journal of Geophysical Research*, v. 99, p. 16441-16456.

Hutton, J. T. (1968). The redistribution of the more soluble chemical elements associated with soils as indicated by analysis in rainwater, soils and plants. 9th International Congress of Soil Science, Adelaide, p. 313-328.

Hutton, J. T. (1976). Chloride in rainwater in relation to distance from the ocean: *Search*, v. 7, p. 207-208.

Hutton, J. T. (1983). Soluble ions in rainwater collected near Alice Springs, N.T., and their relation to locally derived atmospheric dust: *Transactions of the Royal Society of South Australia*, v. 107, p. 138.

Hutton, J. T. and Leslie, T. I. (1958). Accession of non-nitrogenous ions dissolved in rainwater to soils in Victoria: *Australian Journal of Agricultural Research*, v. 9, p. 492-507.

Iribarne, J. V. and Cho, H. R. (1980). Atmospheric Physics. Boston, Reidel Publishing Co., 212.

Isbell, R. F., Reeve, R. and Hutton, J. T. (1983). Salt and sodicity in "Soils: an Australian Viewpoint" Division of Soils (CSIRO, pp. 107-118. Melbourne, Academic Press: London .

Janssen, L. H. J. M., Visser, H. and Romer, F. G. (1989). Analysis of large scale sulphate, nitrate, chloride and ammonium concentrations in the Netherlands using an aerosol measuring network: *Atmospheric Environment*, v. 23, p. 2783-2796.

Jiang, S. S., Hemmick, T. K., Kubik, P. K., Elmore, D., Gove, H. E., Tullai-Fitzpatrick, S. and Hossain, T. Z. (1990). Measurement of the $^{36}Ar(n,p)^{36}Cl$ cross section at thermal energies using the AMS technique: *Nuclear Instruments and Methods in Physics Research*, v. B52, p. 608-611.

Junge, C. E. (1963). Air Chemistry and Radioactivity. International Geophysics Series, New York, Academic Press, 382.

Keene, W. C., Pszenny, A. A. P., Jacob, D. J., Duce, R. A., Galloway, J. N., Schultz-Tokos, J. J., Sievering, H. and Boatman, J. (1990). The geochemical cycling of reactive chlorine through the marine troposphere: *Global Biogeochemical Cycles*, v. 4, p. 407-430.

Keene, W. C., Pszenny, A. P., Galloway, J. N. and Hawley, M. E. (1986). Sea-salt corrections and interpretation of constituent ratios in marine precipitation: *Journal of Geophysical Research*, v. 91, p. 6647-6666.

Kessler, C. J., Porter, T. H., Firth, D., Sager, T. W. and Hemphill, M. W. (1992). Factor analysis of trends in Texas acid deposition: *Atmospheric Environment*, v. 26A, p. 1137-1146.

Knies, D. (1994). Cosmogenic Radionuclides in Precipitation, Purdue University, PhD Thesis.

Knies, D. L., Elmore, D., Sharma, P., Vogt, S., Li, R., Lipschutz, M. E., Petty, G., Farrell, J., Monaghan, M. C., Fritz, S. and Agee, E. (1994). ^{7}Be, ^{10}Be and ^{36}Cl in precipitation: *Nuclear Instruments and Methods in Physics Research*, v. B29, p. 350-356.

Lacaux, J. P., Delmas, R., Kouadio, G., Cros, B. and Andreae, M. O. (1992). Precipitation chemistry in the Mayombe forest of Equatorial Africa: *Journal of Geophysical Research*, v. 97, p. 6195-6206.

Lal, D. and Peters B. (1962). Cosmic ray produced isotopes and their application to problems in geophysics: *Progress in Cosmic Ray Physics and Elementary Particle Physics*, v. 6. Amsterdam, North Holland Publishing Co., p. 3-74.

Lal, D. and Peters, B. (1967). Cosmic ray produced radioactivity on the Earth: *Handbuch Der Physik*, v. 46, p. 551-612.

Likens, G. E., Bormann, F. H., Pierce, R. S., Eaton, J. S. and Munn, R. E. (1984). Long-term trends in precipitation at Hubbard Brook, New Hampshire: *Atmospheric Environment*, v. 18, p. 2641.

Likens, G. E., Keene, W. C., Miller, J. M. and Galloway, J. N. (1987). Chemistry of precipitation from a remote, terrestrial site in Australia: *Journal of Geophysical Research*, v. 92, p. 13,299-13,314.

Lilly, D. K., Waco, D. E. and Adelfang, S. I. (1974). Stratospheric mixing estimated from high-altitude turbulence measurements: *Journal of Applied Meteorology*, v. 13, p. 488-493.

Linacre, E. and Hobbs, J. (1982). The Australian Climatic Environment. Brisbane, John Wiley and Sons, 354

Lindberg, S. E. (1982). Factors influencing trace metals, sulfate and hydrogen ion concentrations in rain: *Atmospheric Environment*, v. 16, p. 1707-1709.

Ling Xing and Chameides, W. L. (1990). Model simulations of rainout and washout from a warm stratiform cloud: *Journal of Atmospheric Chemistry*, v. 10, p. 1-26.

Magaritz, M., Kaufman, A., Paul, M. and Boaretto, E. (1990). A new method to determine regional evapotranspiration: *Water Resources Research*, v. 26, p. 1759-1762.

Manabe, S. and Terpstra, T. B. (1974). The effects of mountains on the general circulation of the atmosphere as identified by numerical experiments: *Journal of Atmospheric Science*, v. 27, p. 871-883.

Martens, C. S., Wesolowski, J. J., Harriss, R. C. and Kaifer, R. (1973). Chlorine loss from Puerto Rican and San Francisco Bay area marine aerosols: *Journal of Geophysical Research*, v. 78, p. 8778-8792.

Millero, F. T. (1974). Physical chemistry of seawater: Annual Reviews in *Earth and Planetary Science*, v. 2, p. 101-150.

Milton, G. M., Andrews, H. R., Causey, S. E., Chant, L. A., Cornett, R. J., Davies, W. G., Greiner, B. F., Kowolsky, V. T., Imahori, Y., Kramer, S. J., McKay, J. W. and Milton, J. C. D. (1993). Chlorine-36 dispersion in the Chalk River area: *Nuclear Instruments and Methods in Physics Research*, v. B92, p. 376-379.

Monaghan, M. C., Krishnaswami, S. and Turekian, K. K. (1985/1986). The global-average production of ^{10}Be: *Earth and Planetary Science Letters*, v. 76, p. 279-287.

Moore, A. W., Isbell, R. F. and Northcote, K. H. (1983). Classification and mapping of Australian soils, 'Soils: an Australian Viewpoint', p. 253-266, (Division of Soils, CSIRO). Melbourne, Academic Press, London.

Mote, P. W., Holton, J. R. and Boville, B. A. (1994). Characteristics of stratosphere-troposphere exchange in a general circulation model: *Journal of Geophysical Research*, v. 99, p. 16815-16829.

Neiburger, M., Edinger, J. G. and Bonner, W. D. (1982). Understanding Our *Atmospheric Environment*. San Francisco, W. H. Freeman and Company. 453.

Nishiizumi, K., Arnold, J. R., Elmore, D. E., Ma, X., Newman, D. and Gove, H. E. (1983). 36Cl and 53Mn in Antarctic meteorites and 10Be-36Cl dating of Antarctic ice: *Earth and Planetary Science Letters*, v. 62, p. 407-417.

Nishiizumi, K., Arnold, J. R., Elmore, D., Ferraro, R. D., Gove, H. E., Finkel, R. C., Beukens, R. P., Chang, K. H. and Kilius, L. R. (1979). Measurements of ^{36}Cl in Antarctic meteorites and Antarctic ice using a Van De Graaff Accelerator: *Earth and Planetary Science Letters*, v. 45, p. 285-292.

Noller, B. N., Currey, N. A., Ayers, G. P. and Gillett, R. W. (1986). Naturally acidic rainwater at a site in Northern Australia. *Proceedings of the Seventh World Clean Air Congress, Sydney, Australia*, J. G. Holmes Pty. Ltd., p. 189-190.

Noller, B. N., Currey, N. A., Ayers, G. P. and Gillett, R. W. (1990). Chemical composition and acidity of rainfall in the Alligator Rivers region, Northern Territory, Australia: *Science of the Total Environment*, v 91. p 23-48.

Noller, B. N., Currey, N. A., Cusbert, P. J., Tuor, M., Bradley, P. and Harrison, A. (1985). Temporal variability in atmospheric nutrient flux to the Magela, Nourlangie Creek system, Northern Territory, in Ridpath, M. G. and Corbett, L. K., eds., Ecology of the Wet-Dry Tropics, *Proceedings of the Ecological Society of Australia*, v. 13. Darwin, Darwin Institute of Technology, p. 21-31.

Onufriev, V. G. (1968). Formation of chlorine-36 in nature: *Yad. Geofiz. Geokhim, Izot. Metody. Geol*, v. 1968, p. 364-369.

Peck, A. J., Thomas, J. F. and Williamson, D. R. (1983). Salinity Issues: Effects of Man on Salinity in Australia. *Water 2000: Consultants Report*, No. 8, Canberra, Australian Government Publishing Service, 78.

Phillips, F. M., Mattick, J. L., Duval, T. A., Elmore, D. and Kubik, P. W. (1988). Chlorine-36 and tritium from nuclear weapons fallout as tracers for long-term liquid and vapour movement of desert soils: *Water Resources*, v. 24, p. 1877-1891.

Plumb, R. A. (1989). On the seasonal cycle of stratospheric planetary waves: *Pure and Applied Geophysics*, v. 130, p. 233-242.

Pruchniewicz, P. G. (1973). The average tropospheric ozone content and its variation with season and latitude as a result of global ozone circulation: P*ure and Applied Geophysics*, v. 106-108, p. 1058-1073.

Pruppacher, H. R. and Klett, J. D. (1978). Microphysics of Clouds and Precipitation. Dordrecht, Holland, D. Reidel and Co., 714.

Qin, Y. and Chameides, W. L. (1986). The removal of soluble species by warm stratiform clouds: *Tellus*, v. 35B, p. 285-299.

Raisbeck, G. M., Yiou, F., Fruneau, M., Loiseaux, J. M. and Lieuvin, M. (1978). Measurements of ^{10}Be in 1000- and 5000-year old Antarctic Ice: *Nature*, v. 275, p. 731-732.

Raisbeck, G. M., Yiou, F., Fruneau, M., Loiseaux, J. M., Lieuvin, M. and Ravel, J. C. (1979). Deposition rate and seasonal variations in precipitation of cosmogenic ^{10}Be: *Nature*, v. 282, p. 279-280.

Reiter, E. R. (1975). Stratospheric-tropospheric exchange processes: *Reviews in Geophysics and Space Physics*, v. 13, p. 1-35.

Robinson, E. and Robbins, R. C. (1972). Emission concentrations and the fate of gaseous atmospheric pollutants, in Strauss, W., eds., Air Pollution Control Part 2, v. New York, John Wiley and Sons, p. 1-93.

Robinson, G. D. (1980). The transport of minor atmospheric constituents between the troposphere and stratosphere: *Quarterly Journal of the Royal Meteorology Society*, v. 106, p. 227-253.

Ryaboshapko, A. G. (1983). The atmospheric sulphur cycle, in Ivanov, M. V. and Freney, J. R., eds., The Global Biogeochemical Sulphur Cycle, SCOPE 19, v. Chichester, John Wiley and Sons, p. 203-275.

Saylor, R. D., Butt, K. M. and Peters, L. K. (1992). Chemical characterisation of precipitation from monitoring network in the Lower Ohio River Valley: *Atmospheric Environment*, v. 26A, p. 1147-1156.

Schaeffer, O. A., Thompson, S. O. and Lark, N. L. (1960). Chlorine-36 radioactivity in rain: *Journal of Geophysical Research*, v. 65, p. 4013-4016.

Shaw, G. E. (1991a). Aerosol chemical components in Alaska air masses 1. Aged Pollution: *Journal of Geophysical Research*, v. 96, p. 22357-22368.

Shaw, G. E. (1991b). Aerosol chemical components in Alaska air masses 2. Sea salt and marine product: *Journal of Geophysical Research*, v. 96, p. 22369-22372.

Simpson, H. J. and Herczeg, A. L. (1994). Delivery of marine chloride in precipitation and removal by rivers in the Murray-Darling Basin, Australia: *Journal of Hydrology*, v. 154, p. 323-350.

Smeyers-Verbeke, J., Den-Hartog, J. C., Dekker, W. H., Coomans, D., Buydens, L. and Massart, D. L. (1984). The use of principal component analysis for the investigation of an organic air pollutants data set: *Atmospheric Environment*, v. 18, p. 2471-2478.

Smith, R. B. (1979). The influence of mountains on the atmosphere: *Advances in Geophysics*, v. 21, p. 87-230.

Smith, R. B. and Davies (1977). A note on some numerical experiments with model mountain barriers: *Tellus*, v. 29, p. 97-106.

Smithsonian Institute. (1993). Institute Global Volcanism Network, Summary of recent Volcanic eruptions: *Bulletin of Volcanology*, v. 56, p. 148.

SPSS (1990). Base Systems User's Guide. Chicago, SPSS Inc,

Staley, D. O. (1962). On the mechanism of mass and radioactive transport from stratosphere to troposphere: *Journal of Atmospheric Science*, v. 19, p. 450-467.

Suter, M., Beer, J., Bonani, G., Hoffman, H. J., Michel, D., Oeschger, H., Synal, H. A. and Wolfi, W. (1987). ^{36}Cl studies at the ETH/SIN AMS facility: *Nuclear Instruments and Methods in Physics Research*, v. B29, p. 211-215.

Synal, H. A., Beer, J., Bonani, G., Suter, M. and Wolfi, W. (1990). Atmospheric transport of bomb produced ^{36}Cl: *Nuclear Instruments and Methods in Physics Research*, v. B52, p. 483-488.

Tapper, N., Hurry, L. (1994). Australia's Weather Patterns. Victoria, Dellasta Pty Ltd, 130.

Teakle, L. J. H. (1937). The salt (sodium chloride) content of rainwater: *Journal of Agriculture, Western Australia*, v. 14, p. 115-123.

Turekian, K., Nozaki, Y. and Benninger, L. K. (1977). Geochemistry of atmospheric radon and radon products: *Annual Reviews in Earth and Planetary Science*, v. 5, p. 227-255.

Vesely, J. (1990). Stability of the pH and contents of ammonium and nitrate in precipitation samples: *Atmospheric Environment*, v. 24A, p. 3085-3089.

Vet, R. J. (1991). Wet deposition: Measurement techniques, in Hutzinger, O., eds., Environmental Chemistry: Reactions and Processes, v. 2 part F. Berlin, Springer-Verlag,

Wahlen, M., Deck, B., Weyer, H., Kubik, P. K., Sharma, P. and Gove, H. (1991). ^{36}Cl in the stratosphere: *Radiocarbon*, v. 33, p. 257-258.

Warneck, P. (1988). Chemistry of the Natural Atmosphere. International Geophysics Series, 41, San Diego, Academic Press. 757.

Wedland, W. M. and McDonald, N. S. (1985). Mean airstreams of Australia: *Australian Geographical Studies*, v. 23, p. 28-37.

Wetselaar, R. and Hutton, J. T. (1962). The ionic composition of rainwater at Katherine, N.T., and its part in the cycling of plant nutrients: *Australian Journal of Agricultural Research*, v. 14, p. 319-329.

Willsmore, N. T. M. and Wood, W. (1929). Salinity of rain in Western Australia: *Royal Society of Western Australia*, v. 25, p. xxii-xxx.

Yulaeva, E., Holton, J. R. and Wallace, J. M. (1994). On the cause of the annual cycle in tropical lower stratospheric temperatures: *Journal of Atmospheric Science*, v. 51, p. 169-174.

Zeng, Y. and Hopke, P. K. (1989). A study of the sources of acid precipitation in Ontario, Canada: *Atmospheric Environment*, v. 23, p. 1499-1509.

Danielsen, E. F. (1982). Statistics of cold cumulonimbus anvils based on enhanced infrared photographs: Geophysical Research Letters, v 9, p601-604.

Kley, D., Schmeletkopf, A. L., Kelly, K., Winkler, R. H., Thompson, T. L. and McFarland, M. (1982). Transport of water through the tropical tropopause: Geophysical Research Letters, v9, p617-620.

Newel, R. E. and Gould-Stewart, S. (1981). A stratospheric fountain: Journal of Atmospheric Sciences, v38, p.2789-2796.

APPENDIX A RAIN-PR ODUCING SYNOPTIC CLASSIFICATION

Proportion of rainfall during each collection period at each Met station attributed to synoptic processes as defined in Chapter 2.

A91=Autumn 91, W91=Winter 91, Sp91=Spring 9, S91=Summer 91 etc. CF=cold front, TE=tropical event, WCT=West Coast Trough, T=trough, CoL=cut-off low, MLCB=middle-level cloud band, MLD=middle-level depression, TF=tropical flow, TD=tropical depression, MT=monsoonal trough, GL=gulf lines, TC=tropcial cyclone

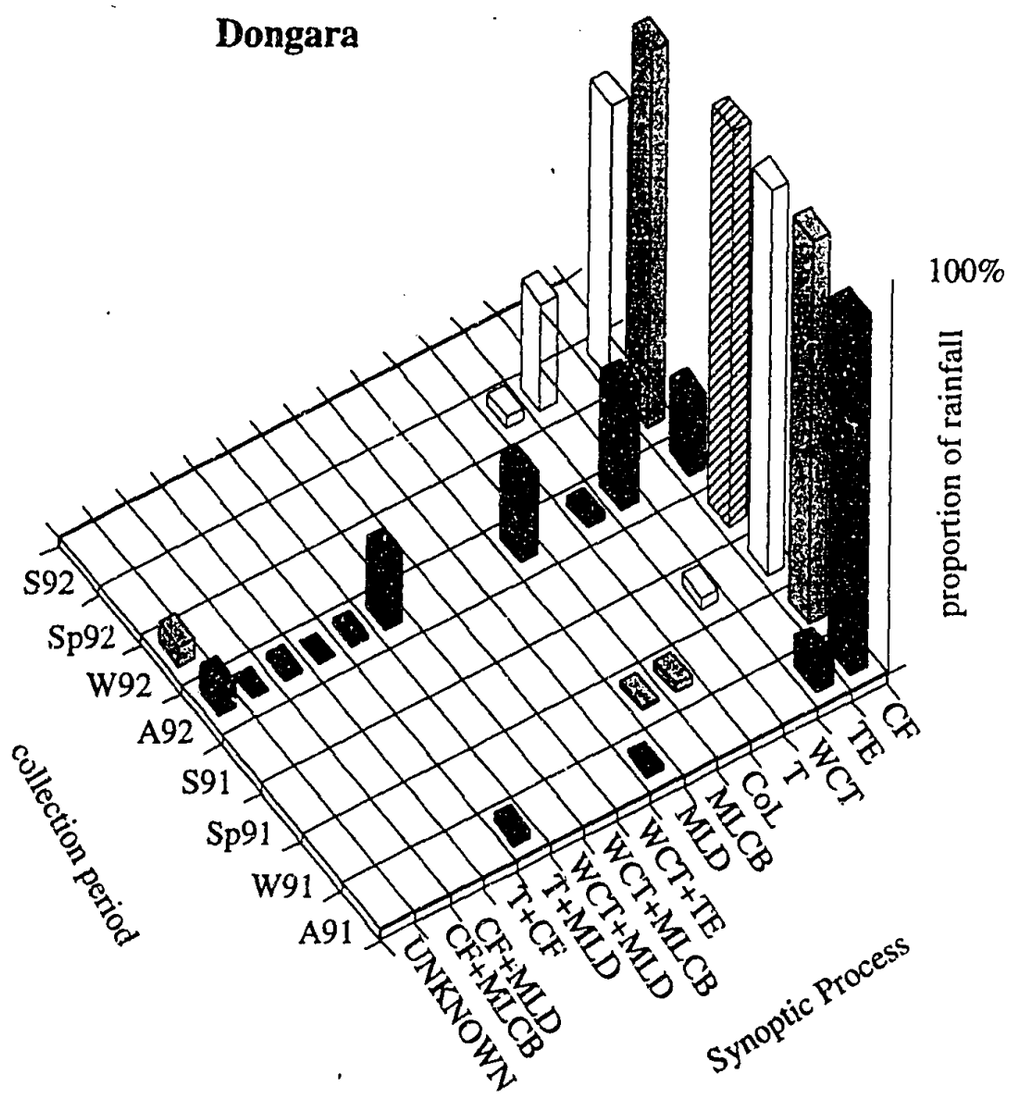

Mount Magnet

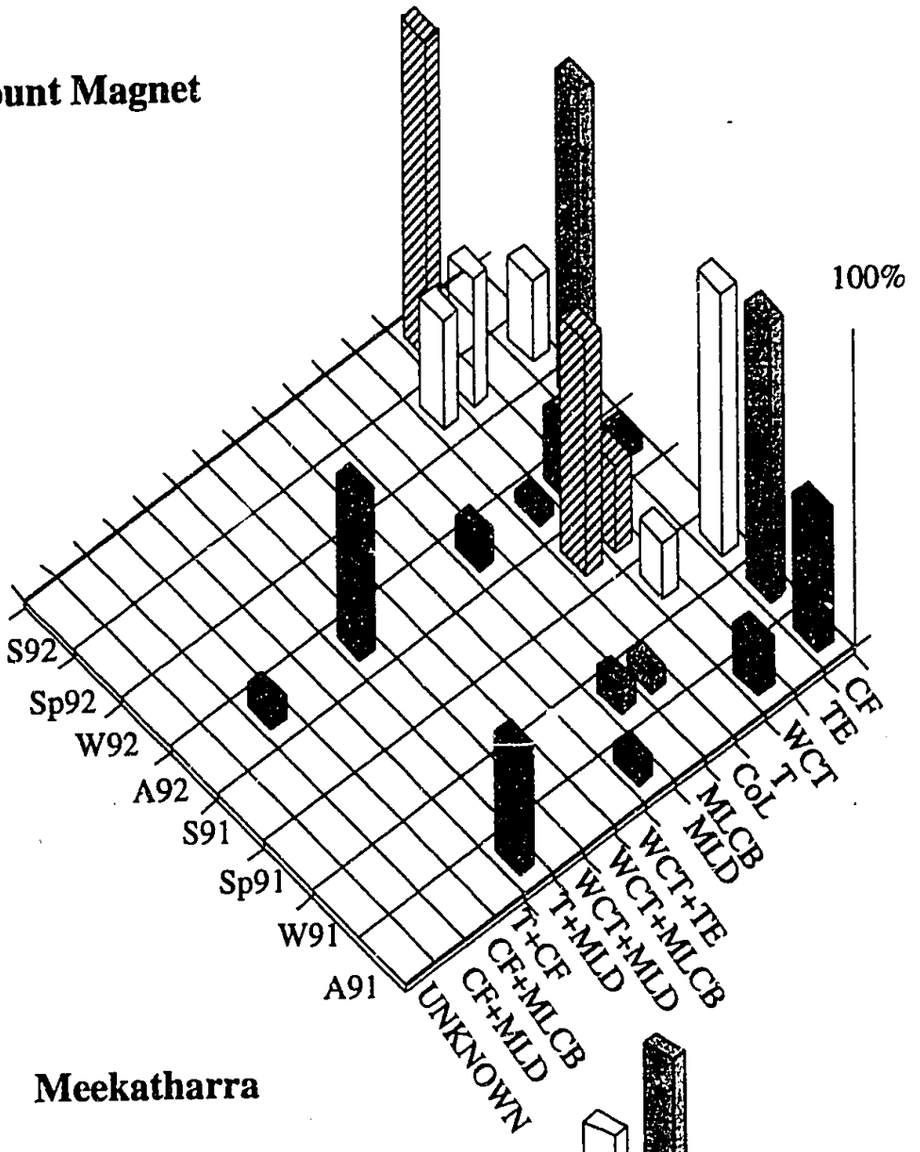

Meekatharra

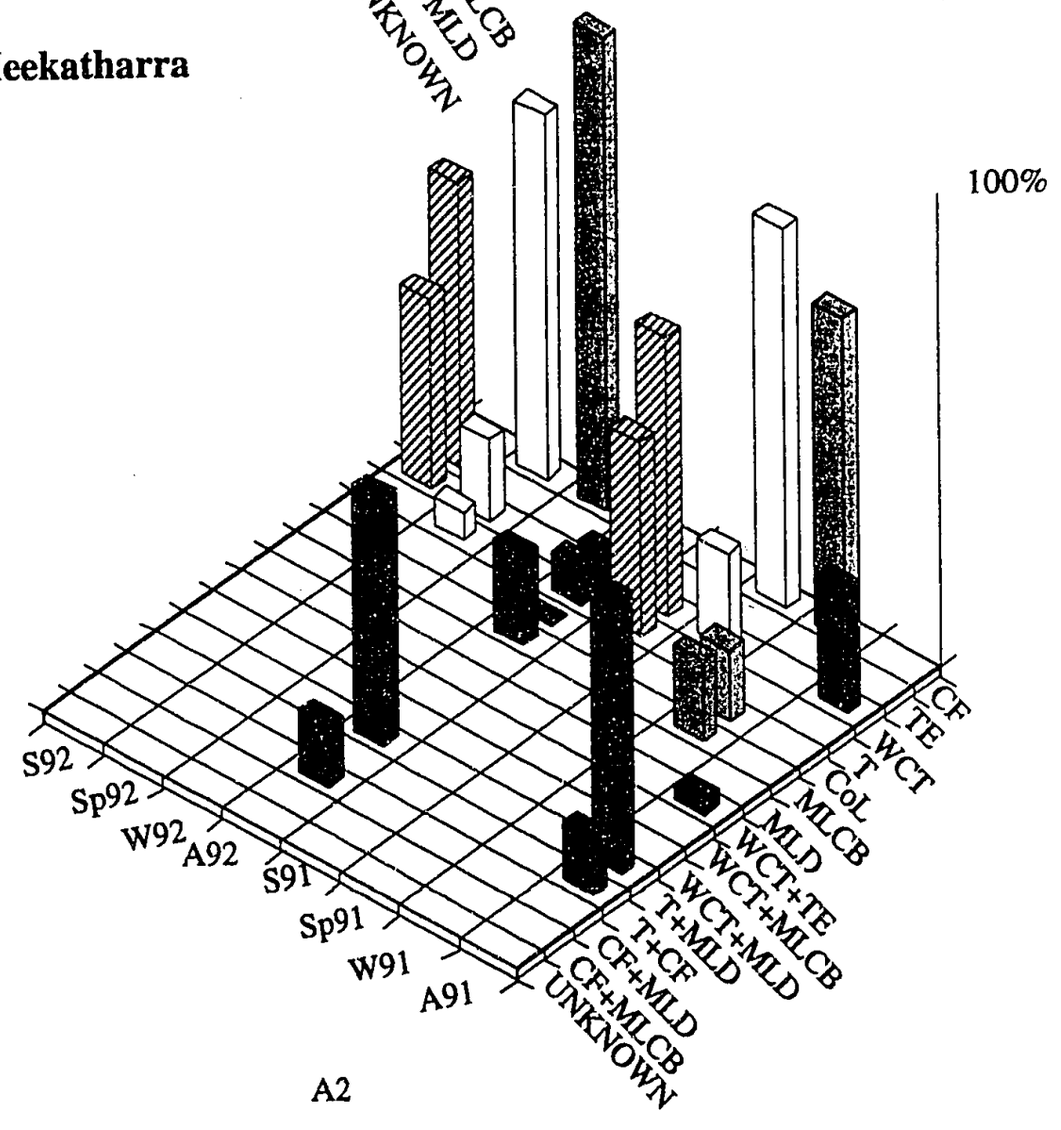

Yeelirrie

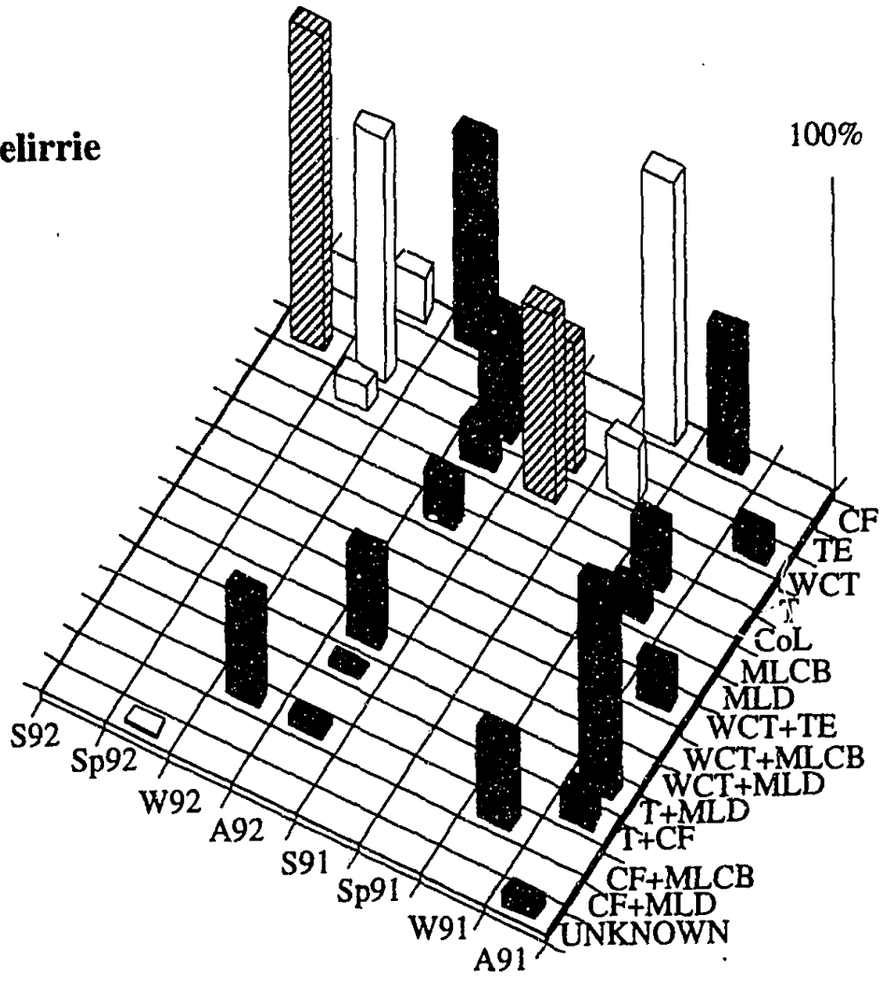

Carnegie

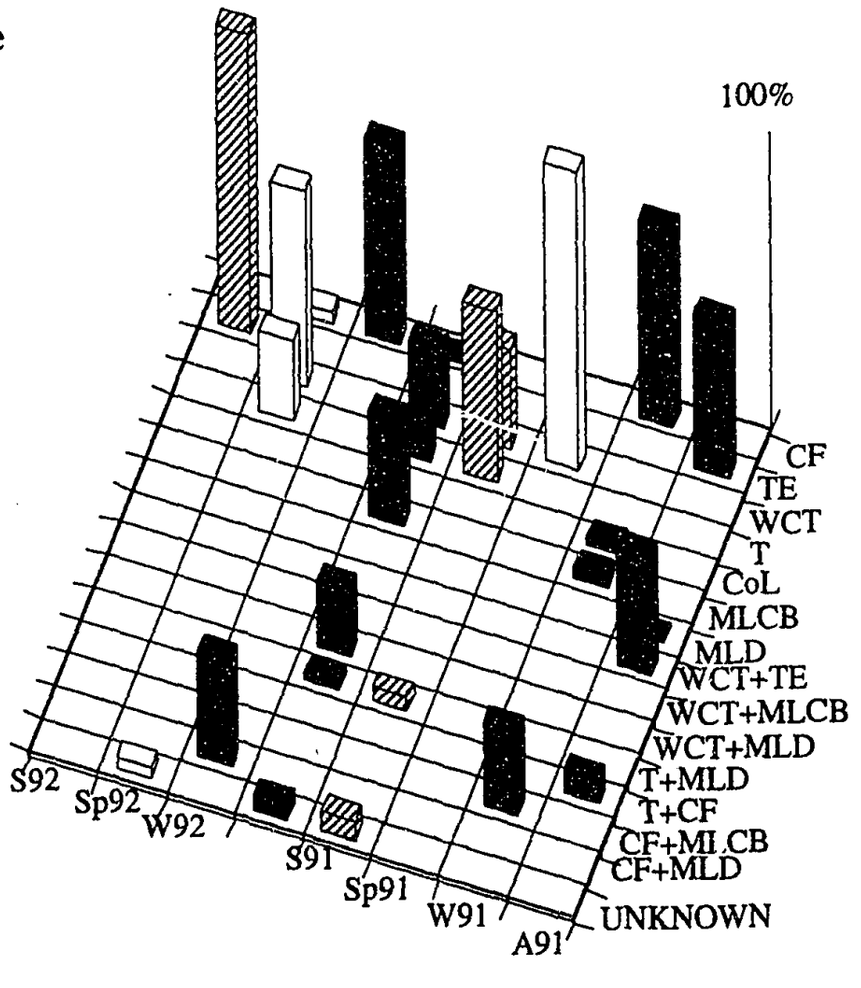

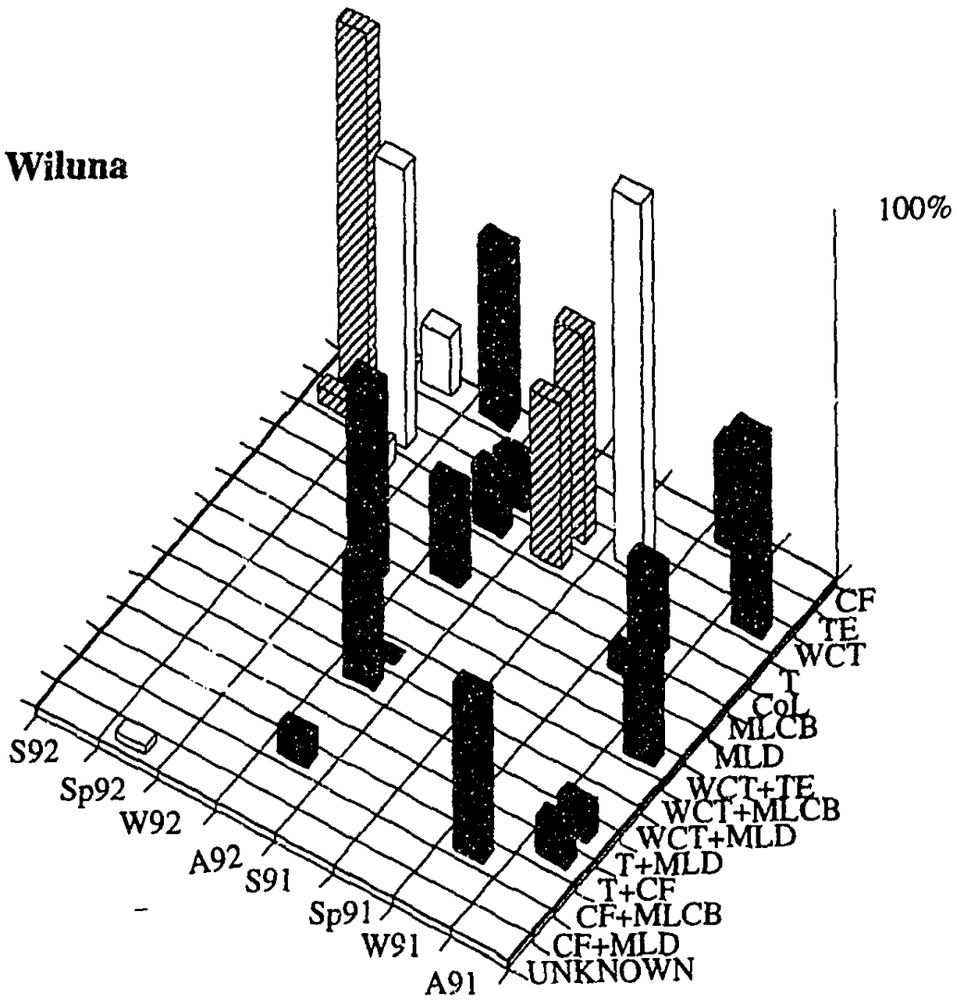
Wiluna
100%
CF
TE
WCT
T
CoL
MLCB
MLD
WCT+TE
WCT+MLCB
WCT+MLD
T+MLD
T+CF
CF+MLCB
CF+MLD
UNKNOWN
S92
Sp92
W92
A92
S91
Sp91
W91
A91

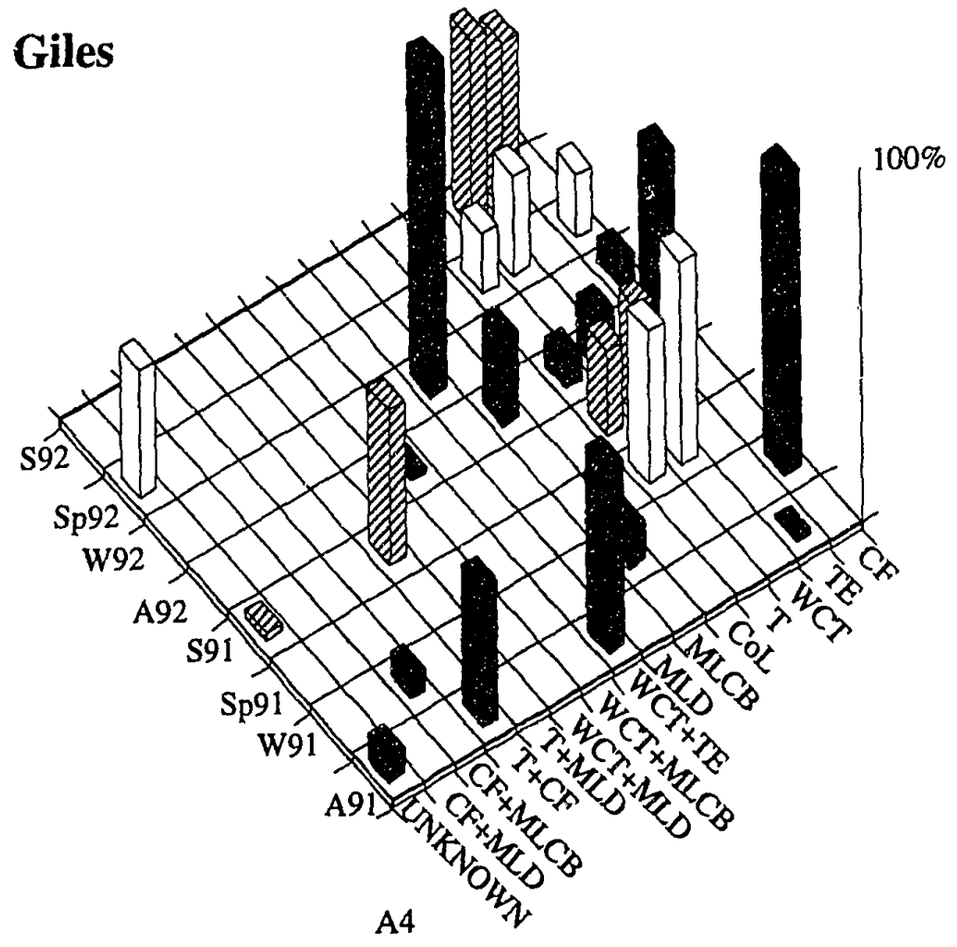
Giles
100%
CF
TE
WCT
T
CoL
MLCB
MLD
WCT+TE
WCT+MLCB
WCT+MLD
T+MLD
T+CF
CF+MLCB
CF+MLD
UNKNOWN
S92
Sp92
W92
A92
S91
Sp91
W91
A91

Port Lincoln

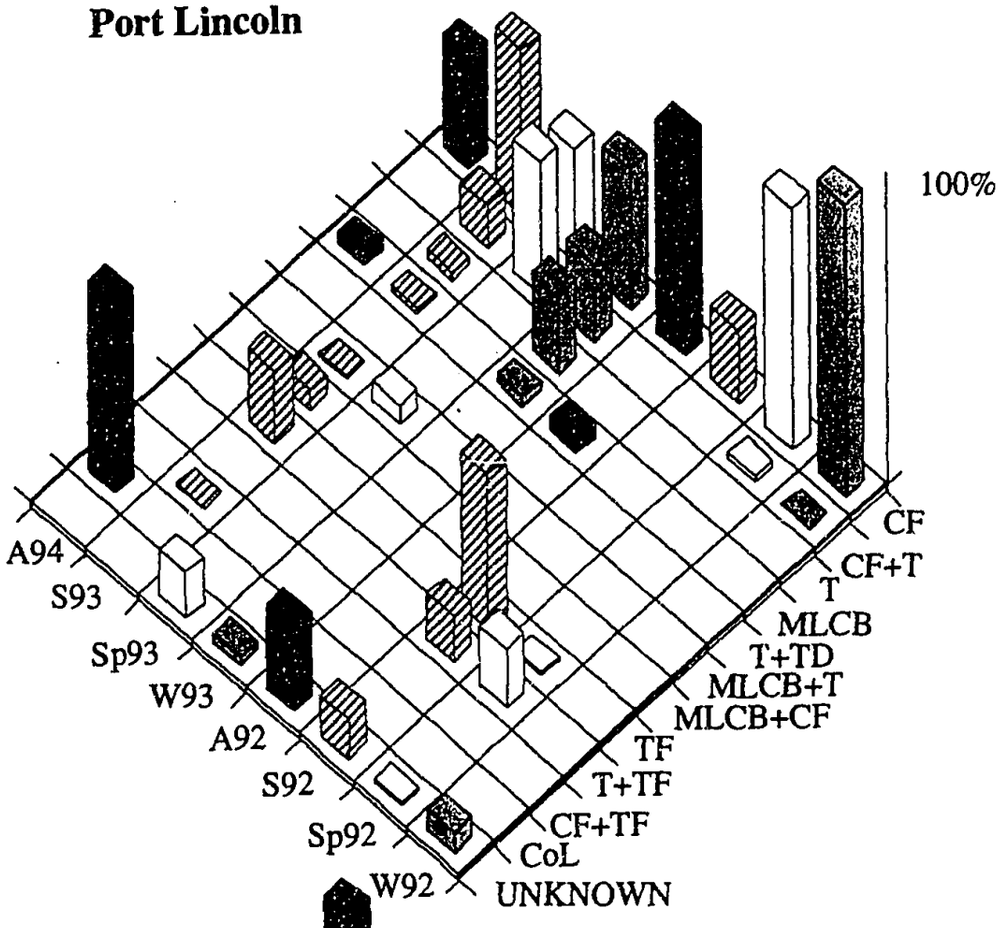

Kyancutta

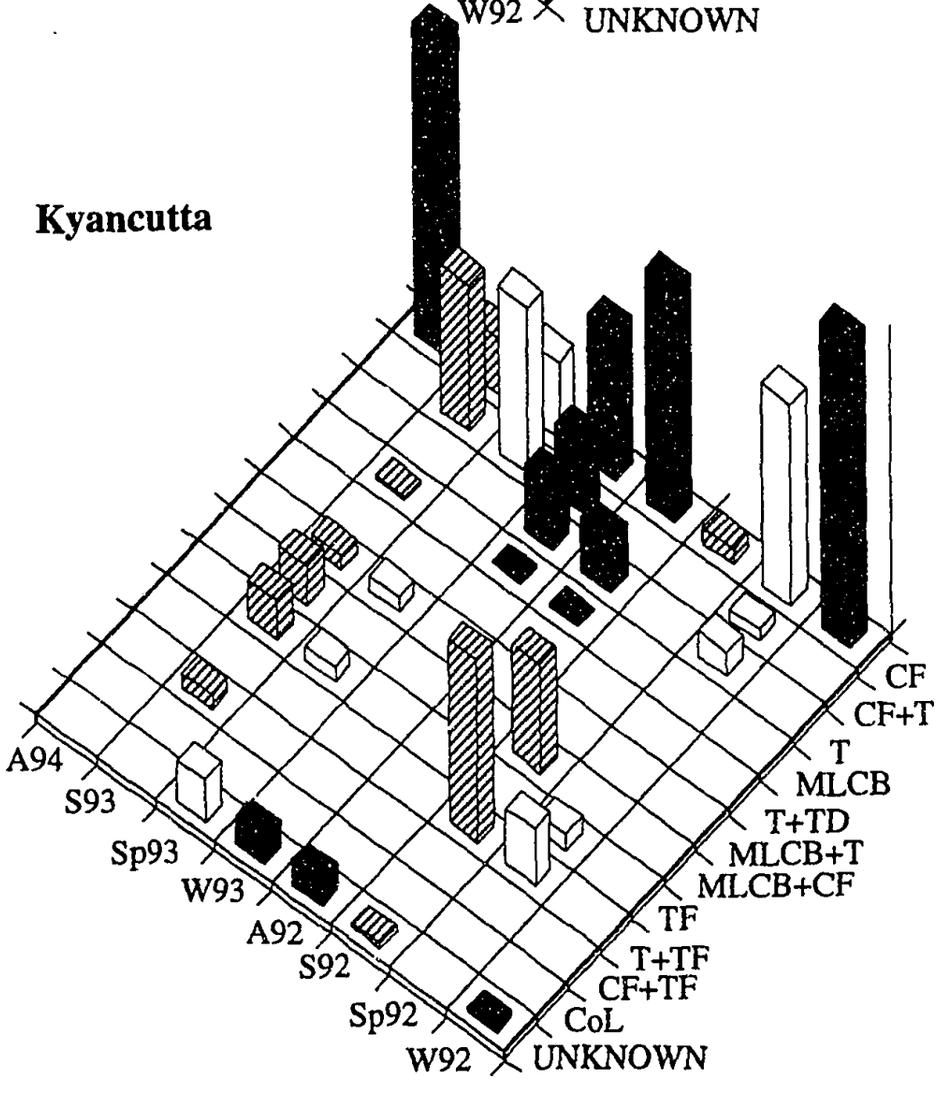

Tarcoola

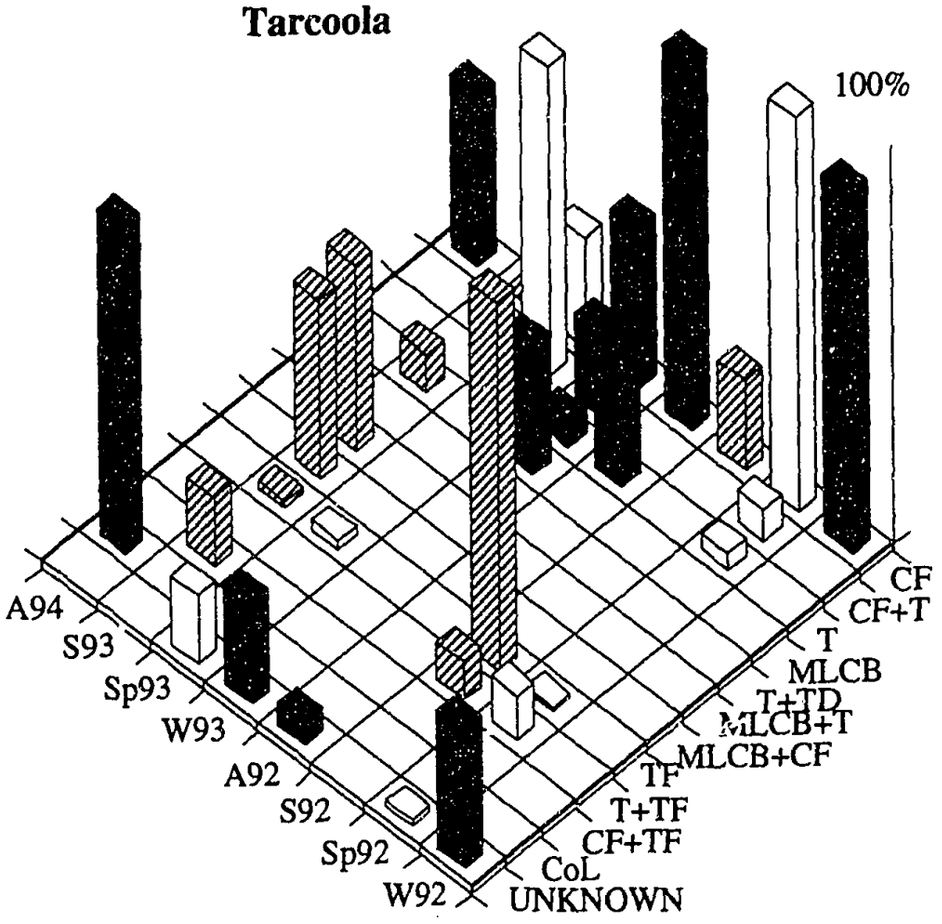

Oonandatta

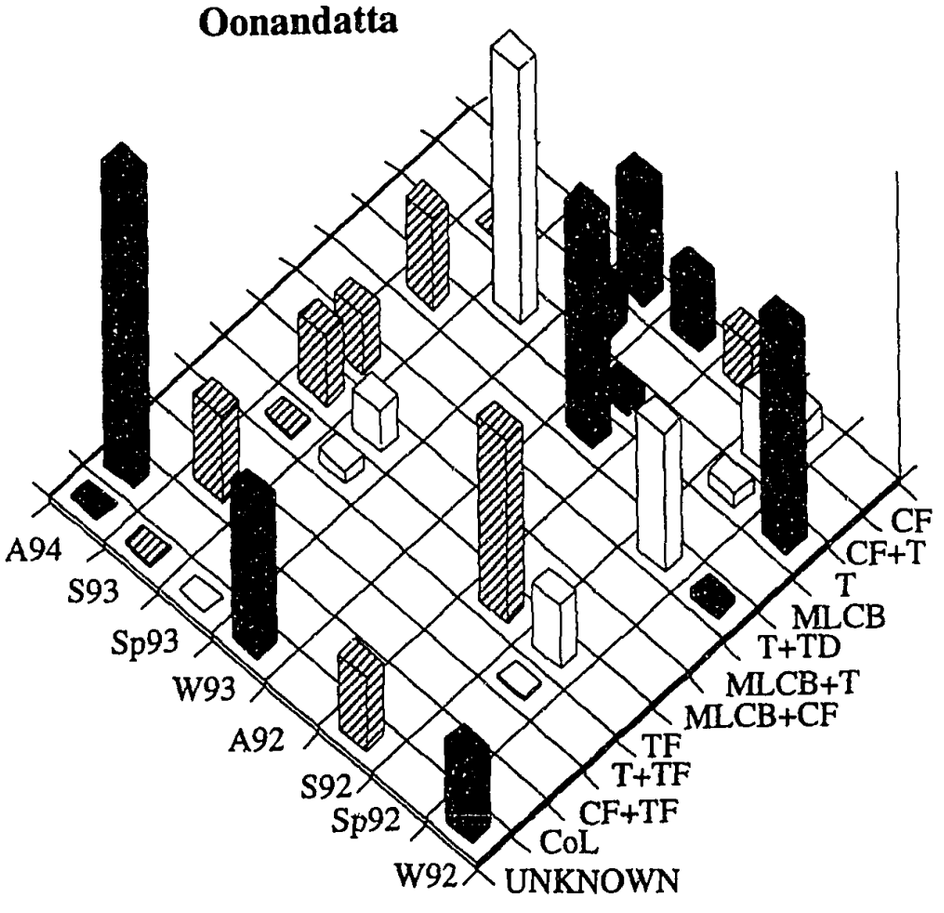

Coober Pedy

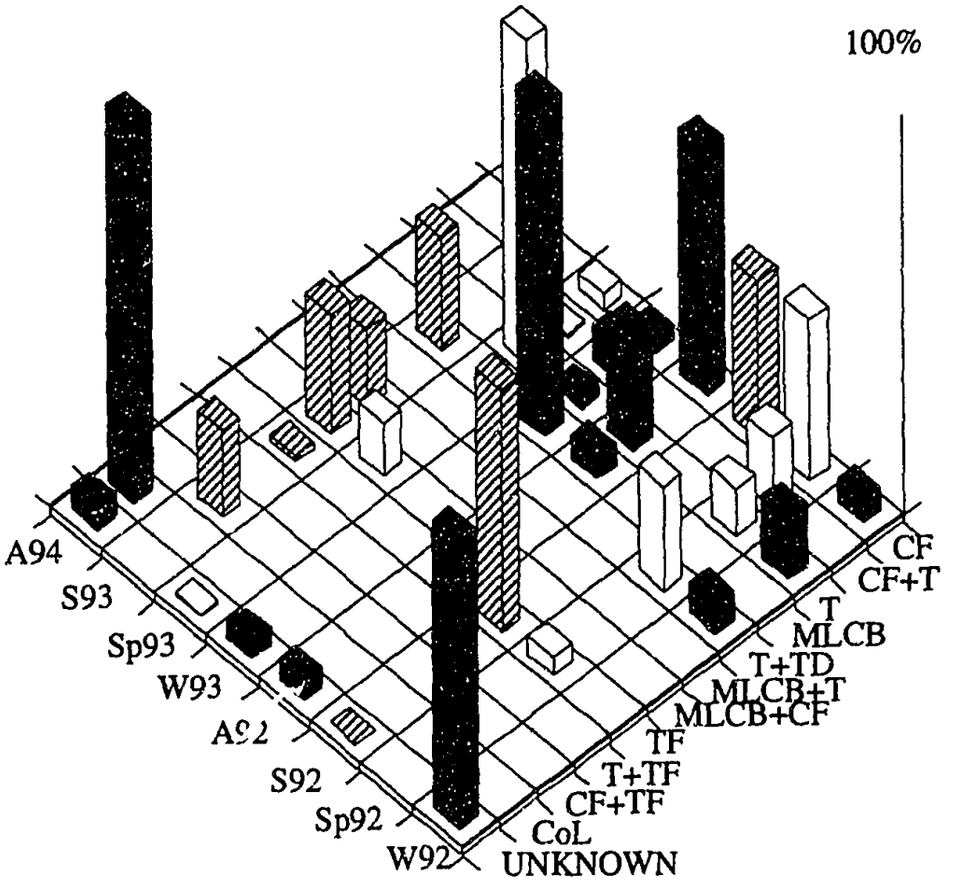

Alice Springs

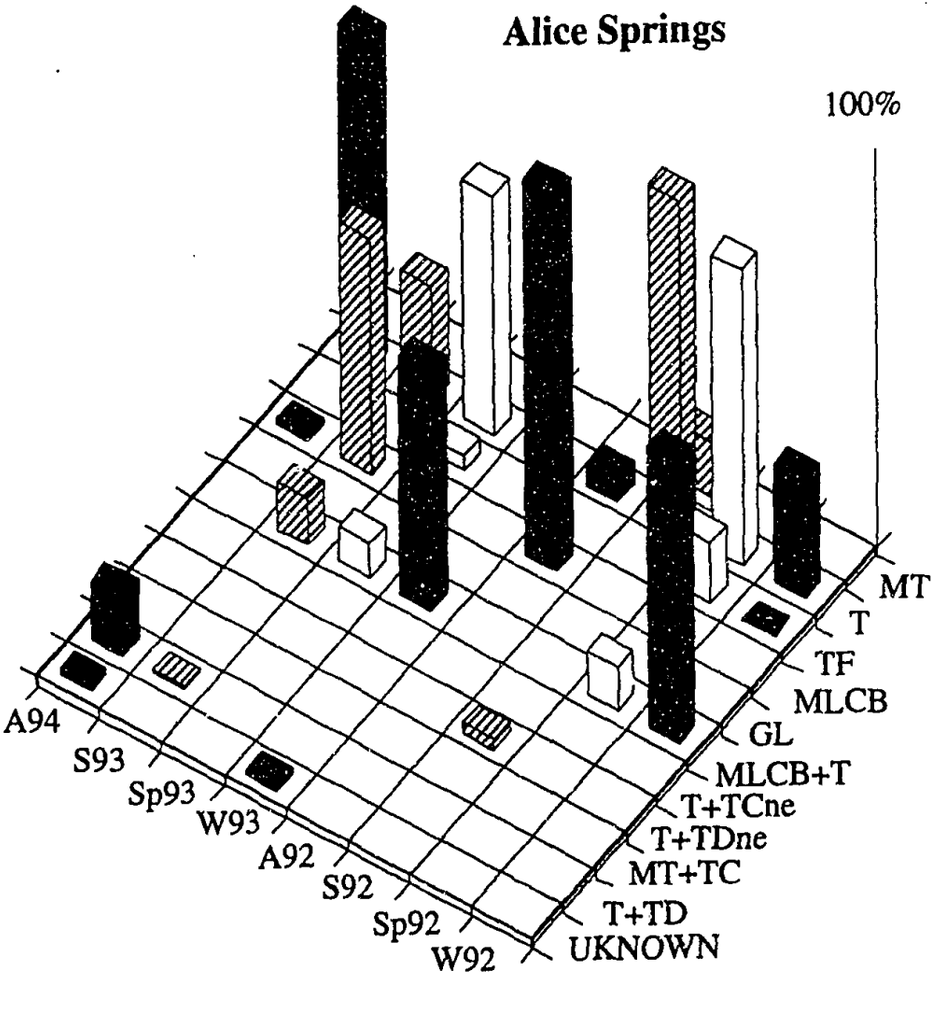

Tennant Creek

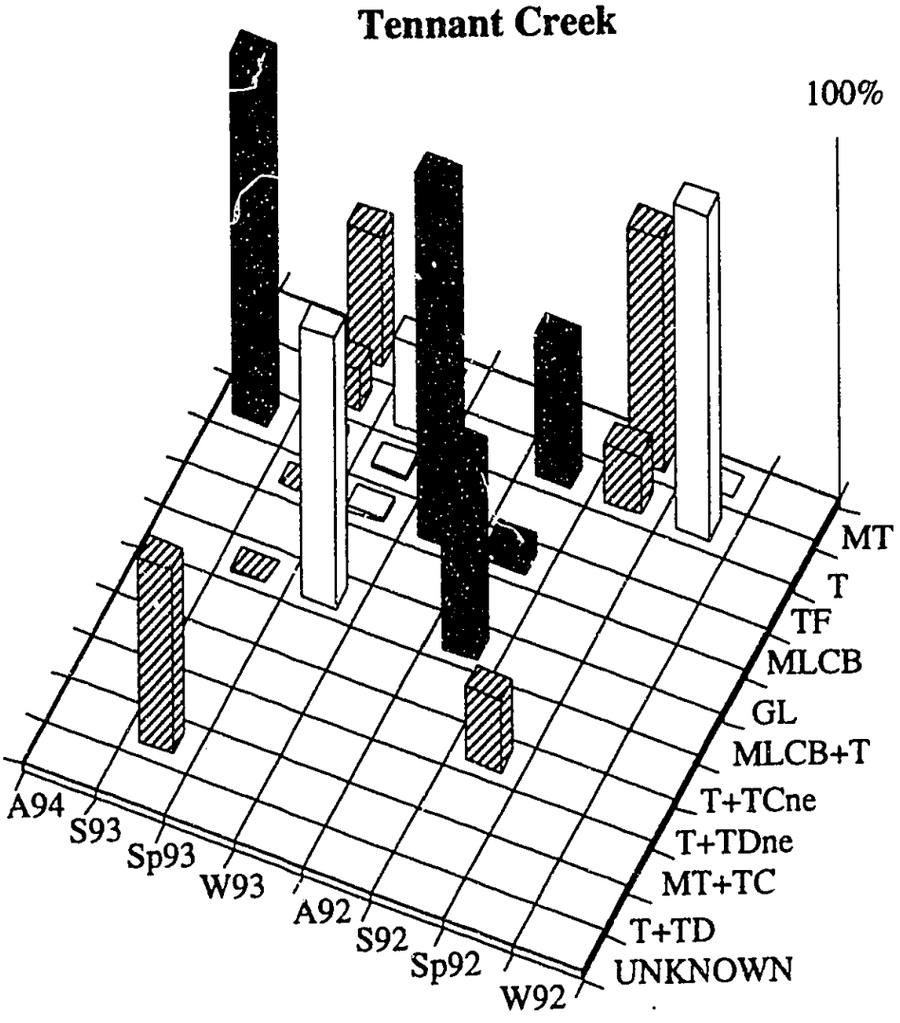

Elliott

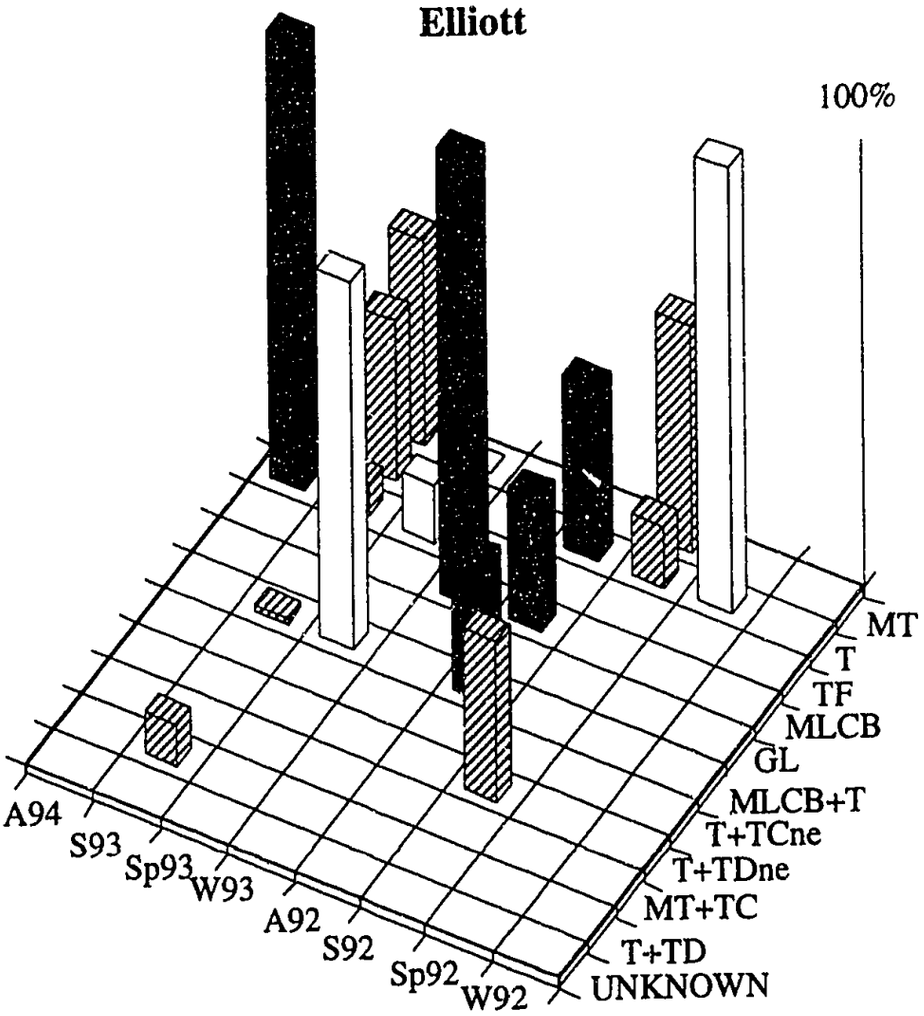

Katherine

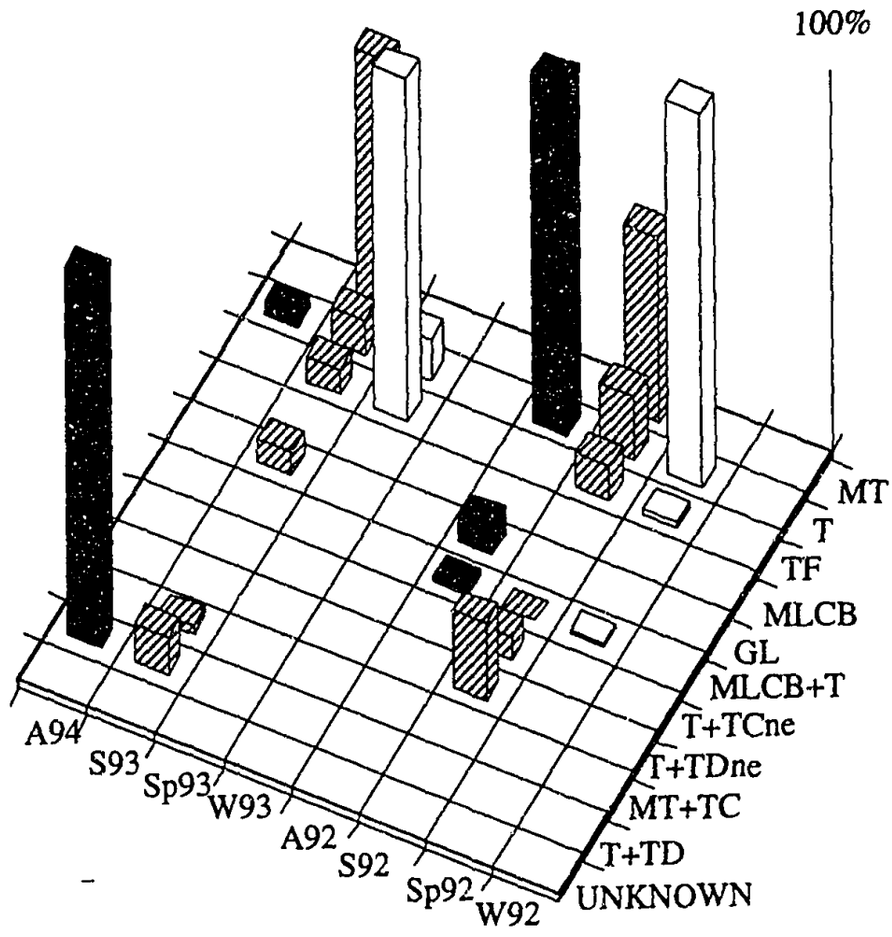

Darwin

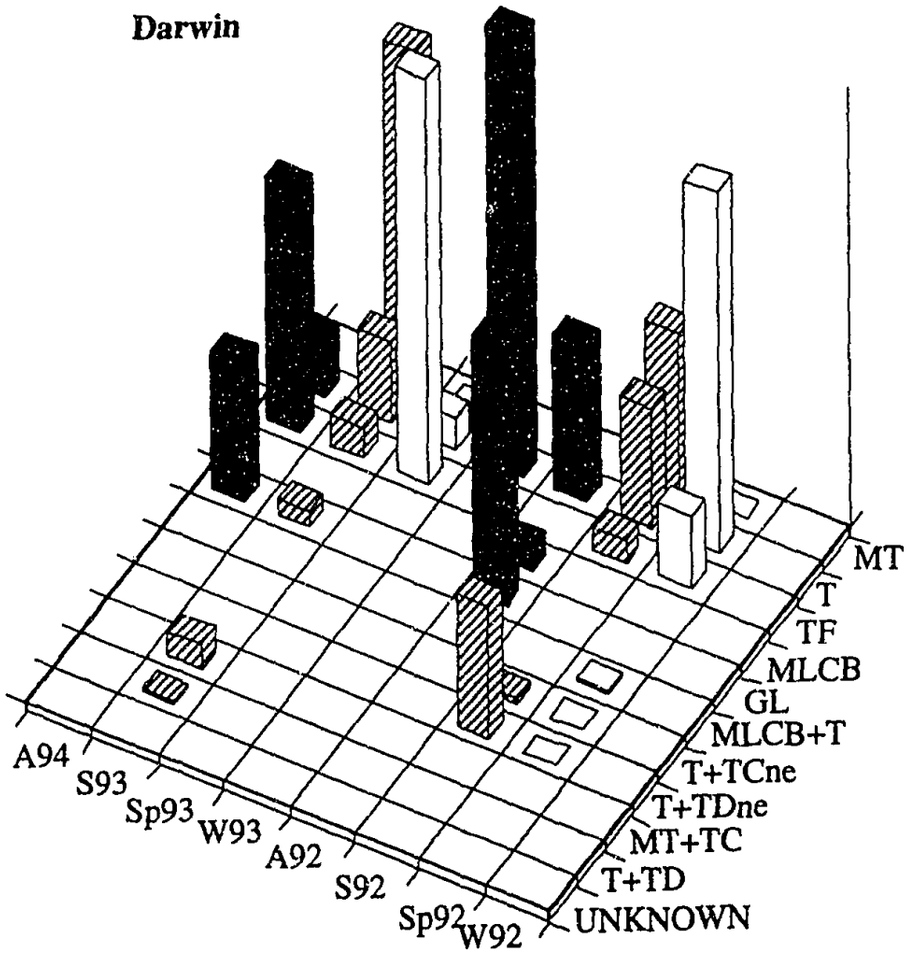

APPENDIX B DESCRIPTION OF RAIN COLLECTOR LOCALITIES

Site: 16
Name: Cliff Head
Location: 29°33'55" S, 114°38'55" E
Elevation: 10m
Physiographic Description: limestone dune ridge covered by aeolian sand; Quaternary
Vegetation: dune type and spinifex
Annual Rainfall: 441 mm (Dongara 2 years of record); 470 mm (Geraldton 48 years of record)
Rainfall Regime: winter rainfall
Climate: temperate coastal, influenced by IsTm
Land Use: recreation

Site: 17
Name: Morawa
Elevation: 409m
Location: 29°12'18" S, 115°50'05" E
Physiographic Description: dissected plateau and hills; minor laterite capping; Archaean granite
Annual Rainfall: 441 mm (Dongara 2 years of record); 470 mm (Geraldton 48 years of record)
Rainfall Regime: winter rainfall
Climate: temperate, may be influenced by IsTm , influenced by sTc all year round.
Vegetation: herbland
Land Use: cattle and sheep grazing

Site: 18
Name: Badja Homestead
Location: 28°34'05" S, 116°43'56" E
Elevation: 350m
Physiographic Description: plains dissected by ridges of the Archaean plateau; Archaean basic volcanics, banded chert and iron formations
Annual Rainfall: 246 mm (Yalgoo 30 years of record)
Rainfall Regime: arid, winter/non season rain
Climate: subtropical to warm temperate, influenced by sTc in both summer and winter months

Vegetation: open shrubland; hummocky grass understorey
Land Use: sheep grazing

Site: 19
Name: Iowna Homestead
Location: 28°30'39" S, 118°04'25" E
Elevation: 300m
Physiographic Description: granitic hills, sandplains, lateritic breakaways, small salt lakes; Archaean granite
Vegetation: open shrubland; spinifex
Annual Rainfall: 234 mm (Mt Magnet 91 years of record)
Rainfall Regime: arid (winter/non season rain)
Climate: subtropical to warm temperate, influenced by sTc both summer and winter months
Land Use: sheep grazing

Site: 20
Name: Barrambie Homestead
Location: 27°32'59" S, 119°13'53" E
Elevation: 550m
Physiographic Description: granitic hills, sandplains, lateritic breakaways, small salt lakes; Archaean granite
Vegetation: open shrubland; hummocky grass understorey
Annual Rainfall: 234 mm (Sandstone 62 years of record)
Rainfall Regime: arid (winter/non season rain)
Climate: subtropical to warm temperate, influenced by sTc in both summer and winter months
Land Use: cattle and sheep grazing

Site: 21
Name: Yeelirrie
Location: 27°11'18" S, 120°03'07" E
Elevation: 500m
Physiographic Description: granitic hills, sandplains, lateritic breakaways, small salt lakes; Archaean granite
Vegetation: open shrubland; hummocky grass understorey
Annual Rainfall: 343 mm (1991-1993)
Rainfall Regime: arid (mainly summer rain)

Climate: subtropical, influenced by sTc in both summer and winter months
Land Use: cattle and sheep grazing

Site: 22
Name: Lake Violet
Location: 26°37'08" S, 121°10'51" E
Elevation: 300m
Physiographic Description: granitic hills, sandplains, lateritic breakaways, small salt lakes; Archaean granite
Vegetation: open shrubland
Annual Rainfall: 234 mm (Wiluna 30 years of record)
Rainfall Regime: arid (mainly summer rain)
Climate: subtropical, influenced by sTc in both summer and winter months
Land Use: cattle and sheep grazing

Site: 23
Name: Carnegie Station
Location: 25°46'55" S, 122°53'38" E
Elevation: 300m
Physiographic Description: sandstone tablelands, stony plains, salt lakes; Permian Officer Basin sediments
Vegetation: open shrubland
Annual Rainfall: 292 mm (Wiluna, 1991-1993)
Rainfall Regime: arid (mainly summer rain)
Climate: subtropical, influenced by sTc in both summer and winter months
Land Use: cattle and sheep grazing

Site: 24
Name: Gunbarrel Highway
Location: 25°25'13" S, 124°00'50" E
Elevation: 300m
Physiographic Description: sandy or lateritic plains of the Gibson Desert; Cretaceous sediments of the Officer Basin
Vegetation: open shrubland
Annual Rainfall: 292 mm (Wiluna, 1991-1993), 256 mm (Giles 34 years of record)
Rainfall Regime: arid (mainly summer rain)
Climate: subtropical, influenced by sTc in both summer and winter months
Land Use: none

Site: 25
Name: Everard Junction
Location: 25°25'13" S, 124°58'26" E
Elevation: 300m
sandy or lateritic plains of the Gibson Desert; Cretaceous sediments of the Officer Basin
Vegetation: open shrubland
Rainfall Regime: arid (mainly summer rain)
Annual Rainfall: 256 mm (Giles 34 years of record)
Climate: subtropical, influenced by sTc in both summer and winter months
Land Use: none

Site: 26
Name: Port Lincoln
Location: 34°52'34" S, 135°41'21" E
Elevation: 50m
Physiographic Description: low rounded hills, partially dune covered; Quaternary
Vegetation: herbland
Annual Rainfall: 491 mm (Port Lincoln 125 years of record)
Rainfall Regime: winter rainfall
Climate: temperate, may be influenced by sPm air masses during winter months, influenced by sTc all year round
Land Use: cattle and sheep grazing

Site: 27
Name: Gawler Ranges
Location: 32°41'22" S, 135°36'53" E
Elevation: 200m
Physiographic Description: rounded hills; Mid to lower Proterozoic acid volcanics of Gawler Block
Vegetation: herbland
Annual Rainfall: 318 mm (Kyancutta 61 years of record)
Rainfall Regime: winter rainfall
Climate: temperate, may be influenced by sPm air masses during winter months, influenced by sTc all year round
Land Use: cattle and sheep grazing

Site: 28
Name: Wintinna Station
Location: 27°47'49" S, 133°57'59" E
Elevation: 300m
Physiographic Description: low tablelands, siliceous and ferruginous duricrust; Cretaceous sediments
Vegetation: shrubland
Annual Rainfall: 172 mm (Tarcoola 84 years of record), 157 mm (Coober Pedy 60 years of record)
Rainfall Regime: arid (winter/non season rain),
Climate: subtropical to warm temperate, influenced by sTc in both summer and winter months
Land Use: cattle grazing

Site: 29
Name: Alice Springs
Location: 22°53'03" S, 134°03'45" E
Elevation: 650m
Physiographic Description: granitic plains with lateritic rises overlain by alluvium, sand silt and gravel; Arunta Block metamorphosed granite and gabbro
Vegetation: shrubland with hummocky grass understorey
Annual Rainfall: 282 mm (Alice Springs 49 years of record)
Rainfall Regime: arid (mainly summer rain)
Climate: subtropical, influenced by sTc in both summer and winter months
Land Use: cattle grazing

Site: 30
Name: Tennant Creek
Location: 19°54'30" S, 134°21'50" E
Elevation: 400m
Physiographic Description: conglomerate, chert, sandstones and dolomites of the Tennant Creek Block
Vegetation: shrubland with hummocky grass and small eucalypt and acacia
Annual Rainfall: 427 mm (Tennant Creek 21 years of record)
Rainfall Regime: arid (mainly summer rain)
Climate: subtropical, influenced by sTc in both summer and winter months
Land Use: ANU Seismic Research Station

Site: 31
Name: Dunmarra
Location: 16°47'38" S, 133°27'20" E
Elevation: 250m
Physiographic Description: black clay plains, sandy rises of laterized sandstone; Cretaceous sediment.
Vegetation: open woodlands
Annual Rainfall: 574 mm (Daly Waters 78 years of record)
Rainfall Regime: summer rainfall,
Climate: tropical monsoon, influenced Tc during winter months and Tm (Pacific) and Tc air masses during summer months
Land Use: cattle grazing

Site: 32
Name: Katherine
Location: 14°37'47" S, 132°27'16" E
Elevation: 200m
Physiographic Description: shallowly dissected plateau of laterized sandstone and alluviated valleys; sediments of Daly River Basin (~500 my)
Annual Rainfall: 973 mm (Katherine 114 years of record)
Rainfall Regime: summer rainfall
Climate: tropical monsoon, influenced Tc during winter months and Tm (north of Australia) and Tc air masses during summer months
Vegetation: tropical savannah with scattered small eucalyptus
Land Use: cropping and pastoral

Site: 33
Name: Kapalga
Location: 12°40'54" S, 132°25'11" E
Elevation: 0-10m
Physiographic Description: dissected lateritic lowlands, coastal estuarine and alluvial plains; sediments in Pine Creek Geosyncline (~500 my)
Vegetation: open tropical forest with eucalyptus
Annual Rainfall: 1480 mm (Jabiru 18 years of record), 1668 (Darwin Airport 50 years of record)
Rainfall Regime: summer rainfall
Climate: tropical monsoon, influenced Tc during winter months and Tm (north of Australia) and Tc air masses during summer months

Land Use: Research Station for Division of Wildlife and Ecology, C.S.I.R.O. The main research activity is an investigation into the effects of fire on the tropical ecosystem at Kapalga. The research station is divided into compartments separated by fire breaks. Each of these compartments is subjected to a particular burning regime, early, progressive, late and natural. The rain collector was located in a compartment of natural burning (i.e. in which no man-made fires were lit). However, the collector was affected by ash fallout associated with burning elsewhere in the research station and Kakadu. Burning of vegetation is a common practise in the northern parts of the Northern Territory. By locating the rain collector in the C.S.I.R.O research station, it was felt that at least this burning was monitored.

Physiographic Description based upon Jennings and Mabbutt, in "Australia: a Geography", D.N. Jeans editor, Sydney University Press, Sydney 1977 and Geological Map of Australia 1976

Vegetation description based upon "Australia: a Geography", D.N. Jeans editor, Sydney University Press, Sydney 1977

Annual Rainfall from Bureau of Meteorology; *Rainfall Regime* from Bureau of Meteorology, "Climate of Australia", AGPS, Canberra 1979

Climate from Gentilli, "World Survey of Climatology, Australia and New Zealand", Eleseiver, Amsterdam 1977; Linarce and Hobbs, The Australian Climatic Environment, John Wiley and Sons, Brisbane 1982; Tapper and Hurry, "Australia's Weather Patterns", Dellasta, Victoria 1994.

APPENDIX C THE CHEMICAL COMPOSITION OF SOIL/DUST AT EACH SITE

The chemical composition of solutions produced after leaching soil/dust collected at each rain collector site in Milli-Q® water for 2 months. Concentration units are µeq/L. b.d is below detection.

site	Cl	error	SO_4	error	NO_3	error	HPO_4	error
Cliff Head 16	2.7	0.2	11.9	0.02	87.3	0.15	2.86	0.01
Morawa 17	0.5	0.017	3.2	0.3	96.3	0.1	b.d	b.d
Badja 18	1.6	0	0.66	0.171	27.9	0.06	b.d	b.d
Iowna 19	0.23	0.02	1.2	0.48	11.7	0.11	b.d	b.d
Barrambie 20	0.28	0.011	2.2	0	4.1	0.03	b.d	b.d
Yeelirrie 21	9.2	0.07	3.5	0.2	38.5	0.2	b.d	b.d
Lake Violet 22	5.6	0.17	43.4	0.91	83.6	0.66	b.d	b.d
Carnegie 23	2.3	0.11	1.5	0.18	22.1	0.07	b.d	b.d
Gunbarrel 24	0.28	0	0.21	0	1.3	0.05	b.d	b.d
Everard Junction 25	0.26	0.037	1	0	4.6	0.09	b.d	b.d
Gawler Ranges 27	0.03	0.002	0.24	0.004	11.5	0.08	b.d	b.d
Wintinna 28	0.28	0	0.42	0.092	13.2	0.14	b.d	b.d
Alice Springs 29	0.28	0	1.3	0.05	19.8	0.3	7.34	0.22
Tennant Creek 30	0.09	0.026	0	0	2.3	0.11	b.d	b.d
Dunmarra 31	0.28	0	0.56	0.057	7.4	0.58	b.d	b.d
Katherine 32	0.28	0	1.2	0.09	1.3	0.01	2.63	0
Kapalga 33	0.28	0	0	0	0.62	0	0	b.d

site	Na	error	K	error	Ca	error	Mg	error
Cliff Head 16	17.4	0.19	6.8	0.01	1396	22	161	2
Morawa 17	6	0.19	7.2	0.01	67	4.55	30.7	2.05
Badja 18	10.1	0.15	20.7	0.04	9.3	1.13	6.9	0.49
Iowna 19	2.9	0.13	2.7	0.01	14.1	1.59	4.5	0.28
Barrambie 20	1.4	0.01	1.2	0.02	3.8	0.64	1.8	0.23
Yeelirrie 21	12.8	0.3	9.1	0.01	12.4	1.14	13.6	0.69
Lake Violet 22	15.1	0.25	12.2	0.04	100	3	29.1	1.27
Carnegie 23	33.9	0.41	46.8	0.09	3.8	0.77	9.2	0.27
Gunbarrel 24	1.5	0.01	3.1	0.02	1.8	0.58	1.4	0.33
Everard Junction 25	1.4	0.02	3.1	0.34	2.7	0.76	2.1	0.22
Gawler Ranges 27	8	0.67	17.9	0.05	26.6	1.49	22	0.36
Wintinna 28	3.9	0.34	15.4	0.66	17.3	1.82	13.6	0.61
Alice Springs 29	1.6	0.19	37.3	0.21	10.4	0.95	20.3	0.74
Tennant Creek 30	1.4	0.11	5.7	0.46	2.4	0.64	2.3	0.37
Dunmarra 31	1.3	0.03	3.7	0.1	3.2	0.68	2.1	0.31
Katherine 32	1.5	0.09	47.1	2.74	24.2	1.96	40.5	3.58
Kapalga 33	1.4	0.02	5.3	0.07	2.6	0.63	4.4	0.53

APPENDIX D WE AND SN MAJOR-ELEMENT DATA SETS

H, Cl, SO_4, NO_3, HPO_4, Br, Na, K, NH_4, Ca and Mg in depositional units $\mu eq/m^2/day$, na is not measured, rainfall volume in brackets is mm of Milli-Q® used to leach dry bottle

WE Data Set

site	season	rainfall mm	error	time days	evaporation %	error	H	error
16	A91	36	2	80	6	5	na	na
16	W91	343	10	107	25	4	na	na
16	Sp91	87	5	69	5	5	na	na
16	S91	57	4	79	0	5	0.19	0.014
16	A92	154	6	136	16	4	0.63	0.025
16	W92	220	7	102	8	4	0.99	0.032
16	Sp92	54	4	56	0	5	0.17	0.013
16	S92	5	3	102	83	2	na	na
17	A91	45	2	80	21	4	na	na
17	W91	168	7	107	19	4	na	na
17	Sp91	63	3	70	4	5	na	na
17	S91	35	2	78	0	5	0.59	0.034
17	A92	236	10	137	42	4	0.83	0.035
17	W92	215	9	101	2	5	9.32	0.393
17	Sp92	71	3	56	4	5	2.85	0.123
17	S92	17	1	102	96	1	na	na
18	A91	36	2	81	27	4	na	na
18	W91	94	4	107	17	4	na	na
18	Sp91	33	1	70	31	4	na	na
18	S91	31	1	79	7	5	10.8	0.36
18	A92	236	10	137	5	4	1.33	0.057
18	W92	124	5	90	4	5	2.89	0.118
18	Sp92	32	1	66	0	5	0.92	0.030
18	S92	2.61	1	102	0	0	na	na
19	A91	31	1	83	14	4	na	na
19	W91	134	5	107	22	4	na	na
19	Sp91	22	1	71	0	4	na	na
19	A92	262	6	142	1	4	3.64	0.086
19	W92	128	5	87	6	4	8.53	0.342
19	Sp92	75	3	65	14	4	11.1	0.47
19	S92	22	1	103	71	2	na	na
20	A91	33	1	83	16	4	na	na
20	W91	70	3	107	9	4	na	na
20	Sp91	4	1	71	44	0	na	na
20	S91	59	2	77	0	5	2.60	0.090
20	W92	120	5	87	34	3	0.46	0.019
20	Sp92	37	1	67	0	5	6.79	0.313
20	S92	40	2	102	7	5	8.75	0.440
21	A91	35	2	82	14	4	na	na
21	W91	63	3	107	45	3	na	na
21	Sp91	1	1	71	0	173	na	na

site	season	rainfall mm	error	time days	evaporation %	error	H	error
21	S91	35	2	77	9	4	0.77	0.044
21	A92	245	10	139	20	4	7.57	0.374
21	W92	38	2	87	8	4	1.46	0.077
21	Sp92	45	2	67	22	3	3.16	0.174
21	S92	44	2	104	26	6	0.12	0.006
22	A91	16	1	81	28	4	na	na
22	W91	60	3	107	0	5	na	na
22	Sp91	2	1	72	54	15	na	na
22	S91	48	2	76	22	4	2.71	0.114
22	A92	255	10	140	20	1	3.50	0.194
22	W92	13	1	87	32	4	0.31	0.024
22	Sp92	55	2	68	37	3	2.74	0.130
22	S92	13	1	106	60	2	0.01	0.001
23	A91	16	1	82	44	3	na	na
23	W91	153	6	107	53	2	na	na
23	Sp91	1.25	1	71	0	0	na	na
23	S91	55	2	77	34	3	2.36	0.089
23	A92	194	4	139	0	5	4.73	0.166
23	W92	31	1	86	1	5	0.68	0.022
23	Sp92	20	0	68	4	4	1.48	0.014
23	S92	33	2	107	0	3	0.29	0.018
24	A91	36	2	83	13	4	na	na
24	W91	118	5	107	60	2	na	na
24	Sp91	14	1	72	6		na	na
24	A92	265	11	141	50	0	6.21	0.368
24	W92	31	1	84	0	0	3.69	0.142
24	S92	79	3	108	25	3	0.31	0.012
25	A91	11	1	83	72	2	na	na
25	W91	118	5	107	45	2	na	na
25	Sp91	50	2	72	11	4	na	na
25	A92	191	8	140	1	1	11.23	0.64
25	W92	22	1	83	0	1	2.84	0.145

SN Data Set

site	season	rainfall mm	error	time days	evaporation %	error	H	error
26	W92	199	8	90	10	4	21	0.880
26	Sp92	334	14	101	23	4	1.53	0.063
26	S92	70	3	104	4	5	0.29	0.012
26	W93	227	9	90	38	3	7.61	0.314
26	Sp93	93	4	72	7	4	6.48	0.271
26	S93	41	2	105	36	3	7.09	0.309
26	A93	103	4	107	7	4	1.21	0.050
27	W92	70	3	90	0	0	0.98	0.041
27	Sp92	299	12	100	18	4	2.97	0.122
27	S92	144	6	104	39	3	0.38	0.016
27	A93	40	2	83	1	5	0.18	0.008

site	season	rainfall mm	error	time days	evaporation %	error	H	error
27	W93	97	4	88	6	4	0.32	0.013
27	W93	97	4	88	6	4	0.29	0.012
27	Sp93	83	3	71	26	4	1.11	0.047
27	Sp93	83	3	71	29	3	0.48	0.020
27	S93	60	3	105	10	4	5.03	0.213
27	S93	60	3	105	10	4	0.73	0.031
27	A93	37	2	106	17	4	0.02	0.001
27	A93	37	2	106	13	4	0.02	0.001
28	W92	27	1	90	0	5	0.93	0.044
28	sp92	134	6	104	45	2	2.54	0.109
28	S92	31	1	105	49	2	0.05	0.002
28	A93	31	1	82	0	0	0.11	0.005
28	W93	49	2	89	6	4	0.18	0.008
28	Sp93	66	3	72	52	2	2.04	0.087
28	S93	74	7	106	37	6	0.26	0.023
28	A94	43	2	104	11	4	0.53	0.023
29	W92	10	1	84	0	0	0.15	0.011
29	Sp92	69	3	105	34	3	2.18	0.095
29	A93	149	6	82	0	0	10.43	0.571
29	W93	14	1	89	13	5	0.12	0.007
29	Sp93	62	3	70	26	3	3.76	0.161
29	S93	85	7	105	60	3	0.56	0.045
29	A94	2	0	106	0	0	0.00	0.000
30	W92	0 (2)	0	85	0	0	0.00	0.000
30	Sp92	57	2	103	35	3	5.98	0.277
30	W93	5	1	90	66	4	0.01	0.001
30	Sp93	59	6	70	13	10	0.97	0.105
30	S93	56	2	105	0	0	0.03	0.001
30	A94	0 (3)	0	106	0	0	0.37	0.012
31	W92	0 (2)	0	86	0	0	0.00	0.000
31	Sp92	57	2	103	13	4	1.89	0.081
31	W93	0 (1)	0	89	0	0	0.00	0.000
31	Sp93	94	4	70	0	0	28.58	2.088
31	S93	768	54	105	0	0	3.19	0.226
31	A94	0 (5)	0	106	0	0	0.13	0.001
32	W92	0 (4)	0	86	0	0	0.00	0.000
32	Sp92	209	9	104	16	4	0.95	0.039
32	A93	0 (3)	0	79	0	0	0.01	0.000
32	W93	0 (3)	0	89	0	0	0.00	0.000
32	S93	854	64	108	0	0	26.81	2.040
32	A94	11	0	106	0	0	0.01	0.000
33	W92	0 (3)	0	80	0	0	0.00	0.000
33	Sp92	290	12	102	0	5	9.84	0.914
33	A93	59	2	80	0	0	1.04	0.044
33	W93	0 (3)	0	89	0	0	0.00	0.000
33	S93	866	40	104	0	0	7.09	0.329

WE Data Set

site	season	Cl	error	SO_4	error	NO_3	error	HPO_4	error	Br	error
16	A91	154	9.7	25.2	1.41	25.4	1.42	1.41	0.267	0.15	0.018
16	W91	1151	41.1	127	3.8	4.65	0.143	0.50	0.015	1.20	0.036
16	Sp91	701	42.9	83.8	4.87	5.99	0.352	0.25	0.014	0.79	0.048
16	S91	122	9.0	26.4	1.89	18.0	1.32	1.65	0.193	0.05	0.003
16	A92	207	8.9	26.5	1.36	5.22	0.266	0.02	0.001	0.06	0.002
16	W92	701	26.0	108	4.3	7.04	0.478	38.0	2.03	0.12	0.004
16	Sp92	477	41.0	69.6	5.82	6.72	0.647	1.81	0.196	0.54	0.064
16	S92	33.4	20.08	6.23	3.746	0.11	0.066	1.01	0.610	0.00	0.001
17	A91	45.9	2.29	12.2	0.55	11.4	0.51	0.83	0.047	0.07	0.017
17	W91	229	10.5	28.8	1.21	3.08	0.153	0.26	0.011	0.24	0.033
17	Sp91	121	6.2	22.5	1.15	7.66	0.376	2.52	0.123	0.12	0.022
17	S91	22.0	1.36	14.3	0.86	12.4	0.76	0.01	0.001	0.03	0.002
17	A92	58.9	3.02	11.9	0.64	7.09	0.435	0.02	0.001	0.06	0.003
17	W92	170	8.0	31.3	1.51	4.37	0.304	0.04	0.002	0.13	0.006
17	Sp92	113	6.8	28.2	1.62	4.55	0.254	1.14	0.075	0.11	0.013
17	S92	4.29	0.32	2.43	0.168	2.57	0.188	0.62	0.047	0.01	0.001
18	A91	12.9	0.74	7.22	0.41	6.70	0.374	0.88	0.073	0.02	0.001
18	W91	68.7	3.27	10.3	0.46	3.18	0.159	0.15	0.007	0.05	0.002
18	Sp91	38.4	1.40	17.9	0.57	11.8	0.37	0.47	0.069	0.08	0.005
18	S91	13.0	0.44	13.4	0.47	13.0	0.50	0.76	0.155	0.02	0.001
18	A92	31.9	1.82	11.2	0.60	7.39	0.497	0.03	0.001	0.10	0.004
18	W92	83.6	4.07	17.1	0.84	2.99	0.296	0.03	0.001	0.08	0.003
18	Sp92	19.8	1.04	11.5	0.57	5.06	0.242	0.54	0.028	0.04	0.004
18	S92	5.41	2.088	5.57	2.143	3.27	1.261	0.00	0.000	0.00	0.001
19	A91	9.06	0.348	6.82	0.224	5.60	0.191	0.33	0.011	0.29	0.010
19	W91	51.5	2.38	10.8	0.44	4.88	0.214	0.20	0.008	0.06	0.002
19	Sp91	29.0	1.51	22.1	1.02	10.6	0.85	0.06	0.003	0.05	0.002
19	A92	29.9	1.29	12.2	0.61	9.43	0.510	0.04	0.001	0.11	0.003
19	W92	44.1	2.56	14.1	0.67	3.57	0.242	0.03	0.001	0.09	0.003
19	Sp92	10.7	0.61	15.7	0.87	6.56	0.353	0.02	0.001	0.06	0.003
19	S92	12.8	0.84	20.1	1.18	10.9	0.69	3.44	0.304	0.04	0.004
20	A91	9.14	0.339	7.72	0.243	6.79	0.210	0.42	0.025	0.02	0.001
20	W91	14.6	0.71	5.08	0.220	2.98	0.130	0.12	0.005	0.04	0.002
20	Sp91	9.5	2.390	13.5	3.37	4.34	1.084	1.45	0.362	0.02	0.005
20	S91	15.3	0.57	14.5	0.53	20.5	0.95	0.02	0.001	0.05	0.002
20	W92	25.2	1.51	11.7	0.57	3.38	0.26	0.02	0.001	0.06	0.002
20	Sp92	5.30	0.345	10.9	0.51	6.46	0.289	0.53	0.048	0.03	0.003
20	S92	8.86	0.612	14.1	0.87	8.04	0.532	0.01	0.000	0.02	0.001
21	A91	8.91	0.552	6.49	0.378	5.15	0.299	0.08	0.004	0.02	0.001
21	W91	6.49	0.323	3.30	0.158	1.98	0.095	0.07	0.003	0.02	0.001
21	Sp91	4.12	4.124	7.77	7.768	3.26	3.265	0.00	0.003	0.00	0.003
21	S91	14.1	0.84	16.0	0.94	13.3	0.81	0.01	0.000	0.05	0.003
21	A92	8.35	0.525	8.80	0.546	9.10	0.555	0.03	0.001	0.09	0.004
21	W92	12.4	0.84	5.60	0.327	2.20	0.172	1.76	0.125	0.03	0.001
21	Sp92	3.38	0.225	8.37	0.491	5.71	0.329	0.37	0.025	0.03	0.001
21	S92	5.03	0.328	6.11	0.361	6.27	0.395	1.55	0.101	0.02	0.001

site	season	Cl	error	SO_4	error	NO_3	error	HPO_4	error	Br	error
22	A91	5.46	0.363	4.80	0.302	5.16	0.324	0.03	0.002	0.01	0.005
22	W91	6.80	0.355	3.73	0.209	4.07	0.208	0.12	0.006	0.04	0.002
22	Sp91	2.79	1.396	3.87	1.937	1.63	0.815	0.00	0.001	0.00	0.002
22	S91	11.1	0.50	12.3	0.54	17.6	0.81	0.51	0.057	0.03	0.001
22	A92	6.17	0.484	6.97	0.467	6.58	0.359	0.03	0.001	0.09	0.004
22	W92	6.82	0.554	4.19	0.337	1.34	0.129	0.00	0.000	0.01	0.000
22	Sp92	3.84	0.206	6.94	0.366	5.04	0.258	1.05	0.137	0.06	0.006
22	S92	4.40	0.395	5.04	0.428	5.19	0.459	1.17	0.106	0.00	0.000
23	A91	4.81	0.316	5.12	0.322	4.04	0.254	0.18	0.011	0.01	0.002
23	W91	5.12	0.277	4.76	0.212	3.36	0.133	0.14	0.006	0.04	0.002
23	Sp91	5.27	4.220	10.3	8.22	3.79	3.031	0.14	0.112	0.01	0.005
23	S91	10.5	0.47	9.81	0.392	16.2	0.68	0.01	0.000	0.03	0.001
23	A92	5.51	0.420	10.5	0.43	9.9	0.427	0.03	0.001	0.09	0.002
23	W92	4.73	0.274	5.57	0.224	2.42	0.160	0.01	0.000	0.02	0.001
23	Sp92	5.73	0.559	10.3	0.39	7.02	0.252	0.71	0.030	0.04	0.004
23	S92	1.10	0.110	1.84	0.130	1.52	0.113	0.33	0.077	0.02	0.001
24	A91	7.24	0.457	7.54	0.422	4.75	0.265	0.08	0.004	0.02	0.001
24	W91	3.36	0.156	2.57	0.191	2.63	0.112	0.09	0.004	0.03	0.001
24	Sp91	5.57	0.413	7.80	0.574	4.92	0.355	0.11	0.011	0.02	0.003
24	A92	3.98	0.313	7.04	0.422	7.73	0.441	0.02	0.001	0.06	0.002
24	W92	6.25	0.395	8.06	0.330	3.45	0.224	0.01	0.000	0.02	0.001
24	S92	2.14	0.189	3.25	0.172	2.75	0.159	1.09	0.065	0.03	0.001
25	A91	4.15	0.395	6.96	0.634	4.28	0.390	0.13	0.012	0.00	0.000
25	W91	2.74	0.207	3.53	0.151	2.35	0.102	0.13	0.005	0.04	0.002
25	Sp91	7.85	0.472	11.4	1.09	8.17	0.336	0.13	0.005	0.02	0.001
25	A92	4.57	0.786	10.7	0.59	11.5	0.69	0.03	0.001	0.08	0.004
25	W92	4.34	0.311	5.74	0.294	2.69	0.194	0.01	0.000	0.02	0.001

NS Data Set

site	season	Cl	error	SO_4	error	NO_3	error	HPO_4	error	Br	error
26	W92	910	58.2	106	5.0	7.09	0.505	0.41	0.017	1.17	0.158
26	Sp92	539	50.6	118	7.9	9.6	0.903	0.53	0.022	0.76	0.121
26	S92	376	22.4	51.9	2.92	10.2	0.61	4.01	0.234	0.33	0.057
26	W93	792	34.1	96.8	5.39	5.06	0.401	0.32	0.013	1.17	0.194
26	Sp93	424	40.4	54.5	6.08	9.5	0.832	9.5	0.853	0.23	0.024
26	S93	271	12.4	48.0	2.21	24.6	1.12	1.52	0.180	0.20	0.018
26	A93	478	21.3	110	7.9	18.4	1	42.7	2.36	0.22	0.016
27	W92	123	7.8	18.4	0.88	3.27	0.215	0.16	0.007	0.10	0.004
27	Sp92	72.8	7.05	34.0	2.35	11.1	1.03	0.51	0.021	0.31	0.013
27	S92	55.4	3.05	15.7	1.16	12.2	0.69	0.18	0.007	0.11	0.004
27	A93	33.4	1.87	11.2	0.58	6.33	0.450	0.10	0.004	0.06	0.003
27	W93	151	6.7	22.9	1.23	4.82	0.322	0.22	0.009	0.13	0.005
27	W93	158	7.8	24.1	1.27	5.26	0.500	0.22	0.009	0.13	0.005
27	Sp93	73.5	7.03	12.7	1.27	4.37	0.307	0.18	0.008	0.11	0.005
27	Sp93	61.3	5.44	14.2	1.32	10.5	0.80	0.17	0.007	0.10	0.004

site	season	Cl	error	SO_4	error	NO_3	error	HPO_4	error	Br	error
27	S93	50.9	2.26	14.3	0.66	29.5	1.28	2.96	0.248	0.41	0.112
27	S93	55.7	2.48	14.1	0.67	24.8	1.13	1.20	0.074	0.40	0.032
27	A93	77.5	4.00	11.8	0.91	2.09	0.150	0.85	0.039	0.04	0.002
27	A93	75.3	3.43	11.9	0.93	2.74	0.214	0.90	0.055	0.04	0.002
28	W92	8.36	0.598	6.11	0.335	4.34	0.300	0.06	0.003	0.04	0.002
28	sp92	6.63	0.693	11.0	0.87	9.9	0.869	0.15	0.006	0.09	0.004
28	S92	9.09	0.526	10.0	0.62	10.6	0.64	0.72	0.053	0.02	0.002
28	A93	4.34	0.244	9.6	0.844	8.18	0.626	1.13	0.075	0.05	0.002
28	W93	10.6	1.18	6.71	0.351	4.25	0.255	0.11	0.005	0.07	0.003
28	Sp93	7.70	0.809	8.15	0.762	8.60	0.637	0.09	0.004	0.06	0.002
28	S93	6.29	0.582	8.15	0.823	9.12	0.850	1.22	0.123	0.05	0.005
28	A94	5.60	0.253	5.39	0.375	1.58	0.109	2.20	0.296	0.05	0.002
29	W92	2.31	0.226	4.37	0.343	2.17	0.178	0.60	0.194	0.01	0.001
29	Sp92	4.59	0.520	10.5	0.760	9.34	0.825	0.09	0.004	0.05	0.002
29	A93	2.22	0.194	11.6	0.673	10.7	1.13	0.38	0.016	0.23	0.009
29	W93	5.34	0.540	5.07	0.338	3.35	0.234	1.06	0.077	0.02	0.001
29	Sp93	11.3	1.05	15.51	1.45	16.4	1.27	2.68	0.320	0.08	0.003
29	S93	3.23	0.288	7.51	0.655	6.64	0.557	0.86	0.194	0.04	0.003
29	A94	1.55	0.021	2.64	0.135	1.75	0.096	0.13	0.013	0.00	0.000
30	W92	0.16	0.009	0.04	0.003	0.10	0.005	0.00	0.000	0.00	0.000
30	Sp92	6.67	0.747	12.2	0.82	10.9	0.94	0.08	0.003	0.05	0.002
30	W93	0.71	0.094	1.48	0.176	0.08	0.016	0.01	0.002	0.00	0.000
30	Sp93	11.4	1.60	18.1	2.47	19.9	2.74	3.00	0.491	0.09	0.010
30	S93	22.7	1.04	32.9	1.50	8.54	0.392	61.7	3.82	0.14	0.110
30	A94	0.40	0.005	0.04	0.004	0.10	0.009	0.01	0.000	0.00	0.000
31	W92	0.10	0.008	0.06	0.005	0.10	0.005	0.00	0.000	0.00	0.000
31	Sp92	8.05	0.757	12.8	0.96	11.6	0.99	0.10	0.004	0.06	0.003
31	W93	0.27	0.01	0.11	0.007	0.12	0.005	0.17	0.005	0.00	0.000
31	Sp93	9.20	3.045	15.6	1.46	26.2	1.71	0.28	0.012	0.17	0.007
31	S93	25.2	1.87	41.1	3.58	23.2	1.74	25.6	2.19	0.92	0.065
31	A94	1.64	0.058	2.57	0.174	0.18	0.018	0.33	0.007	0.01	0.000
32	W92	0.21	0.014	0.01	0.000	0.22	0.011	0.01	0.000	0.01	0.000
32	Sp92	9.69	1.081	14.4	0.95	13.5	1.26	0.35	0.015	0.21	0.009
32	A93	3.25	0.148	1.15	0.036	0.63	0.023	2.09	0.092	0.00	0.000
32	W93	0.37	0.006	0.09	0.005	0.17	0.011	0.30	0.022	0.00	0.000
32	S93	29.5	2.36	22.3	1.78	22	2	1.65	0.123	0.99	0.074
32	A94	11.50	0.65	7.53	0.497	0.93	0.052	11.6	0.23	0.01	0.000
33	W92	1.46	0.000	0.40	0.000	0.14	0.000	0.17	0.000	0.00	0.000
33	Sp92	5.84	0.693	12.8	1.019	9.9	1	0.59	0.024	0.36	0.015
33	A93	19.0	1.09	5.50	0.307	3.87	0.218	0.15	0.007	0.09	0.004
33	W93	0.90	0.000	0.28	0.000	0.14	0.000	0.66	0.000	0.00	0.000
33	S93	64.6	3.51	31.9	1.60	24.7	1.45	1.73	0.081	1.04	0.048

WE Data Set

site	season	Na	error	K	error	NH_4	error	Ca	error	Mg	error
16	A91	122	6.8	5.63	0.31	0.12	0.007	46.8	2.61	32.5	1.82
16	W91	931	27.5	17.5	0.52	0.67	0.020	181	5.4	219	6.5
16	Sp91	614	35.6	8.00	0.463	0.33	0.019	28.9	1.67	130	7.5
16	S91	117	12.4	7.38	1.079	0.20	0.014	52.8	3.72	78.5	5.55
16	A92	184	8.4	5.28	0.225	7.24	0.500	25.0	1.11	53.7	2.13
16	W92	627	25.8	38.0	1.41	191.4	16.8	71.4	4.69	157	6.4
16	Sp92	417	33.8	10.2	1.05	28.1	4.91	66.8	5.01	100	7.6
16	S92	20.9	12.52	2.00	1.198	3.25	1.958	5.52	3.309	8.48	5.087
17	A91	39.2	1.76	1.84	0.083	1.56	0.070	7.00	0.314	9.40	0.422
17	W91	179	7.48	3.68	0.154	0.35	0.015	4.44	0.186	38.7	1.62
17	Sp91	95.9	4.62	2.65	0.128	0.24	0.012	4.57	0.220	22.3	1.07
17	S91	26.7	2.64	2.41	0.339	6.23	0.656	4.32	0.266	11.7	0.69
17	A92	56.4	2.83	3.17	0.303	21.1	1.50	8.07	0.403	17.8	0.76
17	W92	155	7.19	7.11	0.363	13.9	1.46	7.12	0.591	37.7	1.96
17	Sp92	115	6.16	5.17	0.438	11.8	1.94	9.51	0.741	26.1	1.34
17	S92	3.93	0.242	0.97	0.063	1.39	0.111	1.89	0.111	1.68	0.099
18	A91	12.5	0.70	0.80	0.045	6.80	0.380	3.84	0.214	3.08	0.172
18	W91	54.6	2.34	1.38	0.059	0.20	0.009	9.09	0.389	16.8	0.72
18	Sp91	31.7	0.99	1.76	0.055	0.09	0.003	4.59	0.143	9.14	0.285
18	S91	16.8	1.41	2.80	0.373	13.0	1.152	3.38	0.118	5.34	0.181
18	A92	30.8	1.50	2.93	0.136	36.9	2.62	8.12	0.350	13.6	0.586
18	W92	74.9	3.41	3.69	0.273	10.4	0.99	5.90	0.245	19.9	0.816
18	Sp92	22.7	1.09	1.95	0.153	10.5	1.70	3.63	0.221	5.15	0.267
18	S92	8.61	3.303	0.52	0.201	0.97	0.374	3.55	1.360	2.83	1.086
19	A91	7.13	0.234	0.11	0.004	1.27	0.042	3.30	0.108	1.81	0.059
19	W91	38.8	1.46	0.12	0.005	2.06	0.078	9.74	0.366	8.56	0.322
19	Sp91	30.5	1.40	0.04	0.002	0.09	0.004	5.33	0.245	8.96	0.412
19	A92	28.4	0.98	3.55	0.094	19.9	1.22	3.01	0.267	8.91	0.206
19	W92	42.2	1.85	2.23	0.104	4.23	0.455	3.41	0.279	11.7	0.46
19	Sp92	13.3	0.69	1.42	0.128	8.38	1.366	7.44	0.445	3.61	0.169
19	S92	15.3	0.75	4.19	0.205	16.7	1.19	3.03	0.143	2.06	0.095
20	A91	7.38	0.228	0.61	0.019	4.95	0.15	2.75	0.085	2.43	0.075
20	W91	11.3	0.49	0.30	0.013	0.17	0.007	0.59	0.026	2.51	0.108
20	Sp91	14.2	3.56	1.86	0.465	0.01	0.002	3.39	0.848	4.09	1.022
20	S91	15.0	1.27	1.96	0.260	12.3	1.10	3.94	0.146	4.02	0.146
20	W92	19.2	0.89	17.1	0.786	69.0	7.29	5.68	0.239	11.0	0.47
20	Sp92	8.00	0.360	3.22	0.255	12.4	2.02	4.77	0.157	2.48	0.095
20	S92	6.68	0.725	1.20	0.083	3.25	0.535	5.11	0.268	3.06	0.155
21	A91	6.18	0.355	0.23	0.013	1.57	0.090	3.11	0.179	1.64	0.094
21	W91	5.39	0.258	0.27	0.013	0.09	0.004	0.39	0.019	1.07	0.051
21	Sp91	8.50	8.497	0.50	0.498	0.00	0.004	2.38	2.377	2.48	2.479
21	S91	16.2	1.56	1.48	0.215	5.52	0.553	2.37	0.148	1.93	0.114
21	A92	9.32	0.488	1.62	0.069	13.4	1.15	1.93	0.094	3.26	0.212
21	W92	10.4	0.59	1.11	0.067	4.76	0.466	2.11	0.113	3.35	0.184
21	Sp92	5.72	0.323	1.42	0.121	10.4	1.71	3.03	0.190	2.11	0.114
21	S92	6.65	0.348	2.12	0.162	18.3	1.32	6.36	0.329	3.13	0.143

site	season	Na	error	K	error	NH_4	error	Ca	error	Mg	error
22	A91	5.91	0.371	0.49	0.031	1.26	0.079	3.13	0.196	1.65	0.103
22	W91	5.05	0.254	0.43	0.022	0.16	0.008	0.78	0.039	1.16	0.058
22	Sp91	3.64	1.822	0.31	0.157	0.00	0.002	1.27	0.637	1.14	0.572
22	S91	15.0	1.32	2.90	0.396	8.48	0.783	3.54	0.149	2.44	0.103
22	A92	4.56	0.218	1.01	0.046	17.0	1.20	1.02	0.209	1.75	0.109
22	W92	5.09	0.405	3.52	0.279	1.16	0.130	3.85	0.309	1.93	0.154
22	Sp92	4.72	0.233	2.46	0.199	6.91	1.120	3.62	0.207	2.01	0.099
22	S92	5.72	0.452	2.01	0.160	6.00	0.564	4.89	0.382	2.49	0.193
23	A91	4.73	0.297	0.76	0.048	2.31	0.145	2.66	0.167	1.59	0.100
23	W91	3.92	0.155	0.48	0.019	0.19	0.007	0.74	0.029	0.83	0.033
23	Sp91	8.63	6.946	1.81	1.447	0.17	0.139	4.76	3.807	3.09	2.470
23	S91	12.7	1.11	1.57	0.241	6.81	0.627	6.22	0.235	4.75	0.184
23	A92	4.55	0.145	2.18	0.119	18.3	1.106	2.65	0.205	2.94	0.102
23	W92	3.77	0.146	1.36	0.056	7.08	0.625	3.35	0.167	1.92	0.075
23	Sp92	6.87	0.224	1.93	0.139	10.0	1.579	3.94	0.175	2.83	0.023
23	S92	2.40	0.162	0.99	0.096	4.27	0.376	2.07	0.126	1.31	0.082
24	A91	4.27	0.238	0.63	0.035	0.10	0.006	2.58	0.144	1.34	0.075
24	W91	2.00	0.085	0.38	0.016	0.12	0.005	0.42	0.018	0.47	0.020
24	Sp91	5.48	0.393	1.47	0.106	0.05	0.004	2.42	0.174	2.61	0.188
24	A92	3.31	0.188	1.03	0.161	9.08	0.718	1.62	0.075	1.75	0.091
24	W92	4.83	0.194	1.22	0.072	4.22	0.424	3.55	0.119	2.24	0.098
24	S92	3.99	0.205	1.99	0.319	10.6	0.74	3.47	0.154	1.93	0.080
25	A91	5.27	0.480	0.63	0.057	0.01	0.001	2.04	0.185	1.41	0.128
25	W91	2.01	0.085	0.25	0.011	0.17	0.007	0.36	0.015	0.50	0.021
25	Sp91	7.50	0.305	0.95	0.039	0.17	0.007	1.76	0.071	4.14	0.168
25	A92	5.93	0.375	1.76	0.079	12.1	1.17	3.33	0.148	2.46	0.189
25	W92	3.54	0.176	0.81	0.039	0.80	0.069	1.89	0.127	1.62	0.086

NS Data Set

site	season	Na	error	K	error	NH_4	error	Ca	error	Mg	error
26	W92	786	36.0	16.7	0.80	5.97	0.656	50.6	4.65	192	18.8
26	Sp92	831	44.2	19.1	1.12	25.7	1.86	89.0	5.41	247	21.7
26	S92	322	14.8	10.1	0.65	7.65	0.494	38.0	2.28	98.1	8.74
26	W93	699	29.5	14.4	0.82	7.43	0.809	59.2	4.54	208	21.7
26	Sp93	359	18.8	11.3	0.48	45.3	2.75	46.8	2.77	117	9.0
26	S93	316	25.5	8.44	0.556	1.86	0.177	41.6	3.47	82.7	5.71
26	A93	475	45.2	10.5	0.75	0.99	0.041	153	10.2	110	7.5
27	W92	110	5.5	2.72	0.197	6.30	0.546	14.8	1.44	30.9	3.20
27	Sp92	112	6.2	4.80	0.480	29.5	2.36	36.5	2.79	40.8	3.76
27	S92	47.5	2.25	2.04	0.298	12.0	1.014	33.7	2.03	17.6	1.78
27	A93	30.4	1.48	1.58	0.243	3.99	0.450	28.3	2.22	12.5	1.24
27	W93	130	5.6	2.78	0.120	8.33	0.850	50.9	3.54	39.6	3.89
27	W93	137	5.9	2.84	0.132	7.04	0.403	50.8	3.85	41.5	2.06
27	Sp93	58.5	3.36	3.09	0.226	24.9	1.66	17.0	1.29	20.1	1.75
27	Sp93	55.1	2.88	2.88	0.215	18.9	1.08	18.0	1.49	20.0	1.91

site	season	Na	error	K	error	NH_4	error	Ca	error	Mg	error
27	S93	45.4	4.01	4.09	0.239	2.73	0.229	36.9	2.06	14.0	0.96
27	S93	48.2	3.97	3.16	0.272	0.97	0.073	39.8	1.97	14.2	1.15
27	A93	71.3	7.10	3.35	0.496	8.06	0.359	131	9.1	23.0	1.67
27	A93	67.3	6.58	2.43	0.178	6.73	0.570	125	11.1	22.0	1.75
28	W92	7.93	0.413	0.79	0.039	2.93	0.168	2.16	0.182	2.51	0.273
28	sp92	10.2	0.63	1.91	0.121	11.9	0.96	9.72	0.721	5.36	0.574
28	S92	10.5	0.55	1.41	0.135	14.1	0.98	7.24	0.475	3.89	0.350
28	A93	6.05	0.296	1.58	0.223	24.4	1.46	6.98	0.583	3.34	0.476
28	W93	8.97	0.482	0.28	0.084	2.87	0.171	3.35	0.237	3.19	0.415
28	Sp93	7.49	1.529	1.47	0.114	10.8	0.62	7.69	0.442	3.62	0.276
28	S93	8.39	0.986	2.18	0.246	14.3	1.73	8.46	0.819	3.18	0.447
28	A94	5.59	0.704	7.49	0.950	7.13	0.761	6.35	0.511	2.79	0.569
29	W92	2.08	0.158	1.51	0.116	3.14	0.282	2.54	0.287	1.57	0.214
29	Sp92	7.07	0.487	2.09	0.127	10.5	0.84	7.55	0.436	4.60	0.442
29	A93	8.99	0.587	3.71	0.154	4.33	1.152	5.06	0.373	3.97	0.639
29	W93	5.51	0.333	1.80	0.110	4.52	0.364	3.27	0.278	2.50	0.258
29	Sp93	10.7	0.66	3.54	0.177	22.3	1.27	8.93	0.664	5.82	0.608
29	S93	4.08	0.453	1.47	0.169	8.44	1.044	5.99	0.527	2.61	0.339
29	A94	2.10	0.174	0.62	0.038	1.50	0.088	2.55	0.129	1.09	0.077
30	W92	0.07	0.004	0.05	0.003	0.45	0.016	0.04	0.003	0.04	0.004
30	Sp92	10.3	0.70	1.79	0.123	7.45	0.576	6.56	0.398	5.54	0.479
30	W93	0.65	0.076	0.77	0.090	0.50	0.090	0.50	0.071	0.34	0.054
30	Sp93	10.6	1.23	4.93	0.558	32.4	3.89	15.9	1.81	8.15	1.135
30	S93	23.2	1.97	30.8	1.88	224	19.0	23.0	1.15	15.6	1.18
30	A94	0.10	0.008	0.63	0.062	0.17	0.010	0.11	0.011	0.13	0.036
31	W92	0.15	0.007	0.29	0.006	0.34	0.015	0.07	0.005	0.09	0.013
31	Sp92	12.4	0.67	2.59	0.176	11.7	0.94	9.5	0.562	8.36	0.740
31	W93	0.17	0.005	0.50	0.007	0.96	0.039	0.05	0.003	0.08	0.010
31	Sp93	8.20	0.42	4.92	0.207	14.0	0.94	7.83	0.672	11.5	1.01
31	S93	31.5	4.59	24.7	1.98	239	24.8	29.9	2.40	20.6	4.33
31	A94	2.04	0.179	2.24	0.125	1.16	0.042	1.66	0.115	1.26	0.128
32	W92	0.23	0.006	0.17	0.012	0.71	0.020	0.72	0.086	0.30	0.031
32	Sp92	14.9	1.00	15.3	0.99	26.6	2.24	33.4	1.98	29.9	2.83
32	A93	2.28	0.059	3.67	0.104	2.86	0.103	2.56	0.105	2.02	0.155
32	W93	0.35	0.026	0.67	0.015	0.89	0.038	1.40	0.084	0.77	0.077
32	S93	30.3	3.52	7.89	1.251	8.79	0.854	23.7	1.87	18.3	2.10
32	A94	9.8	0.829	15.6	0.93	44.4	0.96	8.43	2.343	7.21	0.786
33	W92	1.29	0.000	1.30	0.000	0.43	0.000	1.25	0.000	1.52	0.000
33	Sp92	9.01	0.660	3.70	0.264	24.7	2.05	5.66	0.308	8.44	1.03
33	A93	17.6	0.85	3.34	0.268	1.19	0.287	4.72	0.262	9.6	0.91
33	W93	1.02	0.000	1.31	0.000	0.69	0.000	2.49	0.000	3.19	0.000
33	S93	63.0	7.01	16.0	1.10	187	16.0	22.8	2.63	29.6	5.14

APPENDIX E MEAN, MINIMUM AND MAXIMUM DEPOSITION OF IONIC SPECIES AND RAINFALL AMOUNT AT EACH SAMPLE SITE ON THE WE AND NS ARRAYS

H, Cl, SO_4, NO_3, HPO_4, Br, Na, K, NH_4, Ca and Mg in units of $\mu eq/m^2/day$

site		rainfall (mm)	error	H	error	Cl	error	SO_4	error
site 16	mean	120	5	0.40	0.007	443	10.1	59.1	1.32
Cliff Head	min	5		0.01		33.4		6.23	
n=7	max	343		0.99		1151		127	
site 17	mean	89	4	2.72	0.055	95.4	2.13	19.0	0.38
Morawa	min	3		0.00		4.29		2.43	
n=8	max	236		10.8		229		31.3	
site 18	mean	87	3	3.19	0.071	34.2	0.95	11.8	0.38
Badja	min	22		0.04		9.14		5.08	
n=8	max	262		11.1		44.1		22.1	
site 19	mean	51	2	5.84	0.090	26.7	0.56	14.6	0.29
Iowna	min	1		0.04		4.12		3.30	
n=7	max	120		8.75		25.2		14.5	
site 20	mean	69	3	4.65	0.091	12.6	0.43	11.1	0.52
Barrambie	min	16		0.12		3.38		3.73	
n=7	max	245		3.16		14.1		16.0	
site 21	mean	43	2	2.62	0.055	7.84	0.546	7.81	0.986
Yeelirrie	min	2		0.01		2.79		3.87	
n=8	max	153		4.16		11.1		12.3	
site 22	mean	61	2	1.85	0.034	5.92	0.225	5.98	0.275
Lake Violet	min	1		0.29		1.10		1.84	
n=8	max	194		5.05		10.5		10.5	
site 23	mean	90	4	1.91	0.036	5.35	0.617	7.27	1.181
Carnegie	min	11		0.31		2.14		3.25	
n=8	max	265		10.4		7.85		11.4	
site 24	mean	30	2	3.40	0.078	4.75	0.128	6.04	0.155
Gunbarrel	min	22		0.05		4.34		4.27	
n=6	max	38		0.84		7.38		7.20	
site 25	mean	92	4	7.04	0.141	4.73	0.114	7.67	0.239
Everard Junction	min	23		0.03		2.30		3.19	
n=5	max	268		0.05		20.6		25.2	
site 26	mean	153	2	6.50	0.128	541	12.4	83.5	1.9
Port Lincoln	min	41		0.29		271		48.0	
n=8	max	334		21.3		910		118	
site 27	mean	92	1	1.04	0.021	82.3	1.55	17.1	0.34
Gawler Ranges	min	37		0.02		33.4		11.2	
n=12	max	299		5.03		158		34.0	
site 28	mean	57	1	0.83	0.019	7.33	0.238	8.15	0.234
Wintinna	min	27		0.05		4.34		5.39	
n=8	max	134		2.54		10.6		11.0	

site		rainfall (mm)	error	H	error	Cl	error	SO_4	error
site 29	mean	56	2	2.46	0.086	4.36	0.194	8.17	0.279
Alice Springs	min	2		0.00		1.55		2.64	
n=7	max	149		10.4		11.3		15.5	
site 30	mean	30	1	1.23	0.049	7.01	0.341	10.8	0.50
Tennant Creek	min	0		0.00		0.00		0.00	
n=6	max	59		5.98		22.7		32.9	
site 31	mean	155	9	5.63	0.350	7.40	0.608	12.0	0.66
Dunmarra	min	0		0.00		0.00		0.00	
n=6	max	768		28.6		25.2		41.1	
site 32	mean	225	29	5.72	0.362	17.3	1.278	10.9	0.63
Katherine	min	0		0.00		0.00		0.00	
n=6	max	854		26.8		66.9		30.5	
site 33	mean	289	11	9.84	0.162	103	1.0	33.6	0.46
Kapalga	min	3		0.00		0.90		0.28	
n=5	max	866		9.84		32.4		14.1	

site		NO_3	error	HPO_4	error	Br	error	Na	error
site 16	mean	9.15	0.269	5.59	0.270	0.37	0.011	379	8.15
Cliff Head	min	0.11		0.02		0.00		20.9	
n=7	max	25.4		38.0		1.20		931	
site 17	mean	6.65	0.147	0.68	0.020	0.09	0.006	83.8	1.70
Morawa	min	2.57		0.00		0.00		3.93	
n=8	max	13.0		2.52		0.29		179	
site 18	mean	6.67	0.227	0.36	0.027	0.05	0.001	31.6	0.84
Badja	min	2.98		0.02		0.02		7.38	
n=8	max	10.9		3.44		0.11		42.2	
site 19	mean	7.37	0.188	0.59	0.044	0.10	0.002	25.1	0.44
Iowna	min	1.98		0.00		0.00		5.39	
n=7	max	20.5		0.53		0.06		19.2	
site 20	mean	7.50	0.229	0.37	0.052	0.03	0.001	11.7	0.57
Barrambie	min	2.20		0.01		0.01		5.05	
n=7	max	13.3		1.76		0.09		16.2	
site 21	mean	5.87	0.433	0.48	0.020	0.03	0.001	8.55	1.087
Yeelirrie	min	1.34		0.00		0.00		3.64	
n=8	max	17.6		1.17		0.06		15.0	
site 22	mean	5.83	0.172	0.37	0.023	0.03	0.001	6.21	0.300
Lake Violet	min	1.52		0.01		0.01		2.00	
n=8	max	16.2		0.71		0.09		12.7	
site 23	mean	6.03	0.452	0.19	0.020	0.03	0.001	5.95	1.007
Carnegie	min	2.35		0.02		0.00		2.01	
n=8	max	8.17		1.09		0.06		7.50	
site 24	mean	4.37	0.115	0.23	0.011	0.03	0.001	3.98	0.096
Gunbarrel	min	0.02		0.01		0.02		3.54	
n=6	max	9.00		7.14		0.02		60.1	

site		NO_3	error	HPO_4	error	Br	error	Na	error
site 25	mean	5.81	0.148	0.08	0.002	0.03	0.001	4.85	0.118
Everard Junction	min	0.03		0.04		0.02		3.41	
n=5	max	11.8		29.7		0.11		21.6	
site 26	mean	12.1	0.28	8.42	0.316	0.58	0.036	541	10.7
Port Lincoln	min	5.06		0.32		0.20		316	
n=8	max	24.6		42.7		1.17		831	
site 27	mean	9.75	0.202	0.64	0.022	0.16	0.010	76.1	1.41
Gawler Ranges	min	2.09		0.10		0.04		30.4	
n=12	max	29.5		2.96		0.41		137	
site 28	mean	7.07	0.211	0.71	0.042	0.05	0.001	8.14	0.279
Wintinna	min	1.58		0.06		0.02		5.59	
n=8	max	10.6		2.20		0.09		10.5	
site 29	mean	7.20	0.285	0.83	0.061	0.06	0.002	5.79	0.169
Alice Springs	min	1.75		0.09		0.00		2.08	
n=7	max	16.4		2.68		0.23		10.7	
site 30	mean	6.60	0.487	10.8	0.64	0.05	0.018	7.48	0.404
Tennant Creek	min	0.00		0.00		0.00		0.00	
n=6	max	19.9		61.7		0.14		23.2	
site 31	mean	10.2	0.438	4.41	0.364	0.19	0.011	9.08	0.776
Dunmarra	min	0.00		0.00		0.00		0.00	
n=6	max	26.2		25.6		0.92		31.5	
site 32	mean	8.34	3.072	2.42	0.043	0.26	0.015	18.5	1.39
Katherine	min	0.00		0.00		0.00		0.00	
n=6	max	22.5		11.6		0.99		71.6	
site 33	mean	24.7	0.336	13.9	0.240	1.04	0.009	103	1.3
Kapalga	min	0.14		0.15		0.00		1.02	
n=5	max	8.72		2.87		0.35		32.6	

site		K	error	NH_4	error	Ca	error	Mg	error
site 16	mean	12	0.31	28.9	2.20	59.8	1.32	97.3	2.02
Cliff Head	min	2.00		0.12		5.52		8.48	
n=7	max	38		191		181		219	
site 17	mean	3.37	0.095	7.08	0.366	5.86	0.144	20.7	0.41
Morawa	min	0.11		0.09		1.89		1.68	
n=8	max	7.11		36.9		9.7		39	
site 18	mean	1.98	0.079	9.9	0.502	5.26	0.217	9.48	0.244
Badja	min	0.04		0.09		0.59		2.06	
n=8	max	4.19		19.9		7.44		11.7	
site 19	mean	1.67	0.040	7.51	0.319	5.04	0.108	51	0.108
Iowna	min	0.23		0.00		0.39		1.07	
n=7	max	17		69.0		5.68		11.0	
site 20	mean	3.75	0.141	14.6	1.095	3.75	0.136	4.22	0.165
Barrambie	min	0.43		0.16		0.78		1.16	
n=7	max	2.12		18.3		6.36		3.35	

site		K	error	NH_4	error	Ca	error	Mg	error
site 21	mean	1.09	0.073	6.75	0.320	2.71	0.303	2.37	0.313
Yeelirrie	min	0.31		0.00		0.74		0.83	
n=8	max	3.52		8.48		4.89		2.49	
site 22	mean	1.64	0.072	5.12	0.239	2.76	0.112	1.82	0.082
Lake Violet	min	0.38		0.10		0.42		0.47	
n=8	max	2.18		18.3		6.22		4.75	
site 23	mean	1.38	0.212	6.14	0.309	3.30	0.548	2.41	0.355
Carnegie	min	0.25		0.01		0.36		0.50	
n=8	max	1.99		10.6		3.47		4.14	
site 24	mean	1.12	0.064	4.03	0.186	2.34	0.051	1.72	0.043
Gunbarrel	min	0.81		0.80		1.19		1.62	
n=6	max	10		74.4		8.14		11.5	
site 25	mean	0.88	0.019	2.65	0.195	1.88	0.046	2.02	0.049
Everard Junction	min	2.37		29.7		3.28		2.49	
n=5	max	37		244		19.4		23.9	
site 26	mean	12.9	0.25	13.6	0.44	68.3	1.77	151	4.9
Port Lincoln	min	8.44		0.99		38.0		82.7	
n=8	max	19.1		45.3		153		247	
site 27	mean	2.98	0.081	10.8	0.29	48.6	1.35	24.7	0.66
Gawler Ranges	min	1.58		0.97		14.8		12.5	
n=12	max	4.80		29.5		131		41.5	
site 28	mean	2.14	0.12	11.0	0.35	6.49	0.190	3.49	0.154
Wintinna	min	0.28		2.87		2.16		2.51	
n=8	max	7.49		24.4		9.72		5.36	
site 29	mean	2.10	0.051	7.82	0.318	5.13	0.158	3.17	0.157
Alice Springs	min	0.62		1.50		2.54		1.09	
n=7	max	3.71		22.3		8.93		5.82	
site 30	mean	6.50	0.329	44.2	3.24	7.69	0.364	4.96	0.284
Tennant Creek	min	0.00		0.00		0.00		0.00	
n=6	max	30.8		224		23.0		15.6	
site 31	mean	5.87	0.333	44.5	4.14	8.18	0.426	6.98	0.751
Dunmarra	min	0.00		0.00		0.00		0.00	
n=6	max	24.7		239		29.9		20.6	
site 32	mean	7.78	0.389	17.4	1.07	20.0	1.48	14.3	1.037
Katherine	min	0.00		0.00		0.00		0.00	
n=6	max	15.6		44.4		70.0		41.5	
site 33	mean	20.9	0.23	187	4.1	29.2	0.54	56.1	1.18
Kapalga	min	1.30		0.43		1.25		1.52	
n=5	max	7.75		66.5		11.0		18.1	

APPENDIX F DETAILS OF FACTOR ANALYSES PERFORMED ON SUBSETS OF THE WE AND SN DATA SETS AS DESCRIBED IN CHAPTER 5

Factor loadings for the coastal subset (n=24) of the WE data set

Loadings	Factor 1	Factor 2	Factor 3
% variance	59.1%	13.3%	10.3%
eigen value	6.4991	1.4606	1.1329
H	.07959	**.86501**	.25986
Cl	**.96785**	.14013	.00819
SO_4	**.93572**	.26229	.06506
NO_3	.07130	**.77087**	-.27935
HPO_4	**.45361**	-.04509	-.05780
Br	**.75746**	**.54200**	-.05442
Na	**.96420**	.18174	.03570
K	**.93029**	.09335	.23900
NH_4	.01785	-.02301	**.96090**
Ca	**.90601**	-.03262	-.08901
Mg	**.97067**	.12202	.01246

Factor loadings for the non-coastal data subset (n=49) of the WE data set

Loadings	Factor 1	Factor 2	Factor 3
% variance	42.1%	16.3%	14.3%
eigen value	4.628	1.790	1.575
H	.04092	.00569	**.92769**
Cl	**.88638**	-.11856	.22293
SO_4	**.84034**	.23231	.20643
NO_3	**.51934**	**.41632**	**.41688**
HPO_4	-.05854	.28065	-.27390
Na	**.95915**	-.00064	.00822
K	.10688	**.80364**	-.18094
NH_4	.16136	**.84883**	.23461
Ca	**.64232**	**.46642**	-.29773
Mg	**.89925**	.19965	-.05541

Factor loadings for the northern data subset, wet data subset and dry data subsets of the NS data set

	all seasons (n=25)		wet samples (n=14)		dry samples (n=11)	
factor	factor 1	factor 2	factor 1	factor 2	factor 1	factor 2
eigen value	8.479	1.168	8.085	1.168	7.69	0.8
percentage var	81.8	11.7	80.8	11.7	77.0	8.0
H	.11701	**.97178**	.04181	**.97366**	-.19498	**-.95129**
Cl	**.93720**	.28184	**.76690**	**.54809**	**.91972**	.29688
SO_4	**.92057**	.25436	**.82524**	**.52829**	**.80597**	.39634
NO_3	**.83001**	**.49515**	**.56149**	**.77499**	**.65938**	**.43028**
HPO_4	**.92071**	-.24488	**.94368**	.03656	**.77643**	**.54426**
Na	**.94048**	.30126	**.75898**	**.58606**	**.95589**	.25826
K	**.97056**	.05432	**.93724**	.26479	**.85558**	.30428
NH_4	**.91924**	.17185	**.91545**	.25690	**.69921**	**.48964**
Ca	**.93380**	.24174	**.78618**	**.55473**	**.90443**	.20231
Mg	**.93950**	.26410	**.74441**	**.62817**	**.92706**	.20525

Factor loadings for southern subset (n=32) of the NS data set

	factor 1	factor 2	factor 3
eigen value	6.709	1.369	1.114
% variation	61.0	12.4	10.1
H	.23014	**.88266**	-.18040
Cl	**.96415**	.13812	.01778
SO_4	**.87664**	**.41408**	.01322
NO_3	.13116	**.82305**	.23283
HPO_4	.32317	.25682	**.66145**
Br	**.68493**	**.64124**	-.07399
Na	**.96575**	.20102	.00446
K	**.77934**	**.40717**	.07778
NH_4	.13875	.13301	**-.75461**
Ca	**.91057**	.03745	.14910
Mg	**.96788**	.21780	-.03139

Factor loadings southern coastal subset (n=19) of the NS data set

	factor 1	factor 2	factor 3
eigen value	6.225	1.805	1.709
% variance	56.6	16.4	15.5
H	**.51802**	**.80141**	-.00244
Cl	**.97211**	.02786	.04578
SO_4	**.95652**	.17055	.13940
NO_3	.01922	**.71708**	**.60728**
HPO_4	.38209	-.04140	**.76950**
Br	**.68349**	**.60452**	.10013
Na	**.98752**	.04423	.04781
K	**.94501**	.19468	.15426
NH_4	.16897	-.07885	**-.79167**
Ca	**.43585**	**-.64148**	**.51731**
Mg	**.99185**	.03989	-.01564

Factor loadings for southern inland subset (n=15) of the NS data set

	factor 1	factor 2	factor 3
eigen value	5.981	1.7807	.9508
% variance	59.8	17.8	9.5
H	.26437	**.90911**	.03321
Cl	**.88141**	-.06643	-.06266
SO_4	**.71186**	**.60889**	.25540
NO_3	**.71936**	**.50814**	.13097
HPO_4	.02604	-.16500	**.91425**
Na	**.84980**	.39032	-.01680
K	-.09850	**.51234**	**.78398**
NH_4	**.66622**	.22248	**.63138**
Ca	**.58344**	.38748	**.56340**
Mg	**.76917**	**.58222**	.19537

APPENDIX G CHLORINE-36 DATA SET

site	season	Volume (Litres)	error	time ±0.5 days	Cl (mg/L)	error	$^{36}Cl/Cl$ ($*10^{-15}$)	error
16	A91	3.02	0.001	80	12.9	0.32	13	2
16	W91	23.12	0.021	107	17.0	0.34	4	1
16	Sp91	7.41	0.006	69	20.7	0.41	5	2
16	S91	5.22	0.001	79	5.99	0.13	21	3
16	A92	11.60	0.012	136	7.72	0.14	4	2
16	W92	18.30	0.018	102	12.5	0.23	8	2
16	Sp92	5.33	0.001	56	17.5	0.75	8	1
16	S92	0.26	0.001	102	142	6.64	6	2
17	A91	3.23	0.001	80	3.66	0.08	35	5
17	W91	12.26	0.013	107	6.37	0.12	6	2
17	Sp91	5.49	0.001	70	4.96	0.09	53	4
17	S91	3.17	0.001	78	1.74	0.04	134	5
17	A92	12.34	0.013	137	2.09	0.06	28	3
17	W92	18.99	0.018	101	2.89	0.06	18	3
17	Sp92	6.06	0.001	56	3.28	0.14	20	2
17	S92	0.22	0.001	102	22.8	1.06	98	8
18	A91	2.30	0.001	81	1.41	0.02	121	8
18	W91	7.04	0.005	107	3.34	0.07	19	3
18	Sp91	2.06	0.001	70	4.18	0.08	81	5
18	S91	2.57	0.001	79	1.26	0.02	198	9
18	A92	20.21	0.019	137	0.69	0.02	64	6
18	W92	10.77	0.011	90	2.24	0.06	31	3
18	Sp92	3.25	0.001	66	1.45	0.06	109	7
18	S92	0.235	0.001	102	7.50	0.35	110	10
19	A91	2.37	0.001	83	1.00	0.02	246	11
19	W91	9.34	0.009	107	1.87	0.05	30	3
19	A92	23.62	0.021	140	0.58	0.02	91	6
19	W92	10.39	0.011	87	1.13	0.06	43	9
19	S92	5.79	0.001	65	0.38	0.02	254	19
19	S92	0.58	0.001	104	7.35	0.34	189	15
20	A91	2.48	0.001	83	0.97	0.02	268	13
20	W91	5.68	0.001	107	0.87	0.02	88	7
20	S91	5.67	0.001	77	0.71	0.01	241	8
20	W92	7.15	0.005	87	0.98	0.04	144	9

site	season	Volume (Litres)	error	time ±0.5 days	Cl (mg/L)	error	$^{36}Cl/Cl$ ($*10^{-15}$)	error
20	Sp92	3.60	0.001	67	0.34	0.02	459	25
20	S92	3.34	0.001	104	0.86	0.04	225	11
21	A91	4.89	0.001	82	0.86	0.02	244	14
21	W91	5.49	0.001	107	0.71	0.01	390	16
21	S91	5.09	0.001	77	1.21	0.02	198	9
21	A92	32.49	0.026	139	0.21	0.01	309	15
21	W92	5.54	0.005	87	1.09	0.05	99	10
21	Sp92	5.60	0.001	67	0.23	0.01	561	22
21	S92	5.15	0.001	105	0.57	0.03	270	11
22	A91	1.86	0.001	81	1.36	0.03	214	11
22	W91	5.42	0.000	107	0.43	0.01	238	12
22	Sp91	0.14	0.001	72	7.74	0.15	151	10
22	A92	26.81	0.023	140	0.15	0.01	119	8
22	W92	1.46	0.001	87	2.38	0.06	375	27
22	Sp92	5.59	0.001	68	0.27	0.01	471	20
22	S92	0.86	0.001	106	3.18	0.15	253	13
23	A91	1.42	0.001	82	1.56	0.03	261	13
23	W91	11.52	0.012	107	0.27	0.01	285	12
23	S91	5.80	0.001	77	0.79	0.02	236	16
23	A92	32.37	0.026	139	0.14	0.01	535	16
23	W92	4.85	0.001	86	0.47	0.02	263	17
23	Sp92	3.06	0.001	68	0.72	0.07	367	16
23	S92	5.20	0.001	107	0.13	0.01	239	17
24	A91	5.01	0.001	83	0.68	0.02	353	14
24	W91	7.62	0.006	107	0.27	0.01	660	25
24	Sp91	2.03	0.001	72	1.08	0.02	483	11
24	A92	32.21	0.026	141	0.15	0.01	621	18
24	W92	5.12	0.001	84	0.60	0.03	298	16
24	S92	5.40	0.001	108	0.14	0.01	406	19
25	A91	0.48	0.001	83	3.96	0.11	277	11
25	W91	10.32	0.010	107	0.16	0.01	527	22
25	Sp91	7.16	0.005	72	0.45	0.02	335	14
25	A92	30.48	0.025	140	0.12	0.02	647	27
25	W92	3.85	0.001	83	0.58	0.03	170	15
26	W92	16.11	0.016	90	16.2	0.79	5	2
26	S92	6.11	0.001	104	20.4	0.86	12	2

site	season	Volume (Litres)	error	time ±0.5 days	Cl (mg/L)	error	$^{36}Cl/Cl$ ($*10^{-15}$)	error
26	W93	12.59	0.013	90	18.1	0.22	5	3
26	Sp93	7.82	0.007	72	12.4	1.07	13	2
26	S93	2.38	0.001	105	38.1	0.54	6	1
26	A94	8.6148	0.01	107	19.0	0.312	4.3	3.2
27	W92	6.36	0.003	90	5.60	0.03	20	2
27	Sp92	22.21	0.020	100	1.05	0.09	86	7
27	S92	7.96	0.007	104	2.31	0.08	79	6
27	A93	3.60	0.001	83	2.46	0.09	56	6
27	S93	4.86	0.001	105	3.50	0.05	52	5
27	S93	4.87	0.001	105	3.83	0.05	49	5
27	A94	5.694	0.001	106	7.59	0.253	11	4
28	W92	4.44	0.001	90	0.99	0.05	149	15
28	Sp92	11.92	0.012	104	0.33	0.03	290	16
28	S92	2.58	0.001	104	2.10	0.08	175	15
28	A93	5.31	0.001	82	0.40	0.01	301	11
28	W93	7.43	0.007	89	0.72	0.07	165	15
28	Sp83	5.13	0.007	72	0.61	0.06	236	12
28	S93	7.42	0.007	106	0.51	0.01	174	13
28	A94	6.0487	0.005	104	0.55	0.007	134	8.4
29	W92	1.50	0.001	86	0.70	0.05	340	42
29	SP92	7.30	0.012	105	0.37	0.04	354	22
29	A92	23.60	0.324	82	0.21	0.02	408	14
29	W93	1.90	0.007	89	1.42	0.12	190	16
29	Sp93	7.31	0.007	70	0.61	0.05	222	11
29	S93	5.41	0.007	105	0.36	0.14	295	11
29	A94	0.323	0.001	106	2.91	0.037	520	48
30	W92	0.2411	0.001	85	0.31	0.017	133	110
30	Sp92	5.94	0.001	103	0.66	0.07	184	9
30	Sp93	8.24	0.007	70	0.55	0.05	625	49
30	S93	0.61	0.001	105	1.51	0.03	84	19
30	A94	0.4213	0.001	106	0.56	0.007	276	56
31	W92	0.3152	0.001	86	0.16	0.013	734	123
31	SP92	8.00	0.007	103	0.59	0.01	129	7
31	W93	0.23	0.001	89	0.58	0.02	446	73
31	SP93	15.46	0.017	70	0.24	0.08	260	16
31	S93	7.68	0.007	105	0.12	0.00	519	26

site	season	Volume (Litres)	error	time ±0.5 days	Cl (mg/L)	error	$^{36}Cl/Cl$ ($*10^{-15}$)	error
31	A94	0.4447	0.001	106	1.25	0.044	181	26
32	W92	0.34	0.001	86	0.17	0.01	201	71.0
32	SP92	15.85	0.016	104	0.20	0.02	140	11
32	A92	0.28	0.001	79	2.90	0.13	152	32
32	S93	8.54	0.007	108	0.13	0.00	459	29
32	A93	0.3197	0.001	106	3.93	0.222	208	21
33	W92	0.24	0.001	80	1.55	0.08	155	22.0
33	A93	5.32	0.247	80	0.92	0.02	92	5
33	W93	0.25	0.001	89	1.04	0.01	367	38
33	S93	8.660	0.007	104	0.28	0.01	103	8

site	season	^{36}Cl (atom/m^2/s)	error	^{36}Cl ($*10^6$ atoms /L)	error
16	A91	14	2.4	2.92	0.49
16	W91	32	8.1	1.15	0.29
16	Sp91	23	8.8	1.66	0.64
16	S9i	19	2.9	2.18	0.34
16	A92	5	3.0	0.47	0.28
16	W92	37	8.4	1.60	0.36
16	Sp92	27	4.6	2.23	0.37
16	S92	5	1.6	14.95	4.87
17	A91	11	1.7	2.18	0.31
17	W91	10	2.4	0.65	0.16
17	Sp91	45	3.7	4.47	0.35
17	S91	21	1.0	3.96	0.17
17	A92	11	1.3	0.98	0.11
17	W92	21	3.6	0.88	0.15
17	Sp92	16	1.7	1.11	0.12
17	S92	10	1.0	38.00	3.57
18	A91	11	0.7	2.89	0.19
18	W91	9	1.3	1.10	0.15
18	Sp91	22	1.5	5.75	0.37
18	S91	18	1.0	4.24	0.20
18	A92	14	1.5	0.74	0.08
18	W92	18	1.9	1.18	0.12
18	Sp92	17	1.4	2.69	0.21
18	S92	4	0.4	14.02	1.43

site	season	^{36}Cl (atom/m^2/s)	error	^{36}Cl (*10^6 atoms /L)	error
19	A91	15	0.9	4.18	0.21
19	W91	11	1.3	0.95	0.11
19	A92	19	1.5	0.90	0.07
19	W92	13	2.8	0.82	0.18
19	S92	19	1.8	1.64	0.15
19	S92	17	1.6	23.60	2.17
20	A91	17	1.0	4.41	0.23
20	W91	9	0.8	1.30	0.11
20	S91	28	1.2	2.91	0.10
20	W92	25	2.0	2.40	0.18
20	Sp92	18	1.5	2.65	0.21
20	S92	14	1.0	3.29	0.22
21	A91	15	1.0	3.57	0.22
21	W91	17	0.9	4.70	0.22
21	S91	19	1.0	4.07	0.20
21	A92	19	1.3	1.10	0.08
21	W92	8	0.9	1.83	0.20
21	Sp92	13	0.8	2.19	0.13
21	S92	9	0.6	2.61	0.16
22	A91	8	1.0	4.95	0.27
22	W91	6	1.0	1.74	0.10
22	Sp91	3	1.0	19.86	1.34
22	A92	4	1.0	0.30	0.02
22	W92	18	1.5	15.16	1.17
22	Sp92	13	0.8	2.16	0.12
22	S92	8	0.6	13.67	0.94
23	A91	9	0.5	6.90	0.37
23	W91	10	0.6	1.31	0.08
23	S91	17	1.3	3.17	0.23
23	A92	21	1.7	1.27	0.10
23	W92	9	0.7	2.10	0.16
23	Sp92	15	1.6	4.49	0.48
23	S92	2	0.2	0.53	0.05
24	A91	18	0.9	4.07	0.18
24	W91	16	0.8	3.03	0.15
24	Sp91	18	0.6	8.86	0.26
24	A92	26	1.2	1.58	0.07

site	season	^{36}Cl (atom/m^2/s)	error	^{36}Cl (*10^6 atoms /L)	error
24	W92	13	1.0	3.03	0.23
24	S92	3	0.3	0.97	0.09
25	A91	8	0.4	18.63	0.88
25	W91	10	0.8	1.43	0.11
25	Sp91	18	1.2	2.56	0.16
25	A92	21	3.9	1.32	0.25
25	W92	6	0.6	1.68	0.17
26	W92	32	13	1.38	0.56
26	S92	32	6	4.24	0.82
26	W93	29	18	1.60	1.01
26	Sp93	38	8	2.68	0.54
26	S93	6	2	3.76	0.91
26	A94	8	6	1.38	1.03
27	W92	17	2	1.90	0.19
27	Sp92	44	5	1.53	0.18
27	S92	31	3	3.10	0.26
27	A93	13	2	2.34	0.26
27	S93	10	1	3.09	0.30
27	S93	11	1	3.19	0.33
27	A94	5	2	1.42	0.52
28	W92	9	1	2.49	0.28
28	Sp92	13	2	1.62	0.18
28	S92	11	1	6.24	0.58
28	A93	10	1	2.05	0.10
28	W93	12	2	2.03	0.28
28	Sp83	13	1	2.46	0.27
28	S93	8	1	1.51	0.12
28	A94	5	0	1.24	0.08
29	W92	5	1	4.06	0.57
29	SP92	11	1	2.25	0.27
29	A92	31	3	1.47	0.13
29	W93	7	1	4.57	0.54
29	SP93	17	2	2.31	0.22
29	S93	7	3	1.78	0.70
29	A94	6	1	25.68	2.39
30	W92	0.15	0	0.71	0.59
30	SP92	9	1	2.05	0.24

site	season	^{36}Cl (atom/m^2/s)	error	^{36}Cl (*10^6 atoms /L)	error
30	SP93	50	6	5.83	0.69
30	S93	14	3	2.16	0.49
30	A94	0.76	0	2.64	0.54
31	W92	0.52	0	1.97	0.37
31	SP92	7	0	1.29	0.07
31	W93	0.83	0.14	4.42	0.73
31	SP93	17	6	1.08	0.36
31	S93	91	8	1.08	0.06
31	A94	1.2	0	3.83	0.57
32	W92	0.29	0	0.57	0.21
32	SP92	9	1	0.48	0.06
32	A92	3	1	7.48	1.61
32	S93	94	9	1.03	0.07
32	A93	3	0	13.89	1.61
33	W92	2	0	4.08	0.62
33	A93	12	1	1.43	0.09
33	W93	2	0	6.50	0.68
33	S93	46	5	0.48	0.04

APPENDIX H MEAN SEASONAL SURFACE WIND DIRECTIONS FOR INLAND SITES ALONG THE WE ARRAY

Mean seasonal wind directions are plotted on wind roses, and the wind roses plotted on a map of salt lakes along the inland section (sites 19 to 25) of the WE array. The wind roses are plotted on Met station sites closest to the sample site (Table 1). The wind roses are drawn from mean daily wind directions during each day of the sampling period. The mean daily wind directions were calculated from three-hourly surface wind direction data purchased from the Bureau of Meteorology. The size of the wedge on the wind rose represents the number of days of a particular wind direction, eg. when the wind direction is predominantly from the southeast, a large wedge will feature in the southeast section of the wind rose.

Table 1 Sample sites and corresponding Met Stations

Sample Site	Met Station
Iowna (19)	Mt Magnet
Barrambie (20)	Meekatharra
Yeelirrie (21)	Yeelirrie
Lake Violet (22)	Wiluna
Carnegie (23)	Carnegie
Gunbarrel (24)	Giles
Everard Junction (25)	

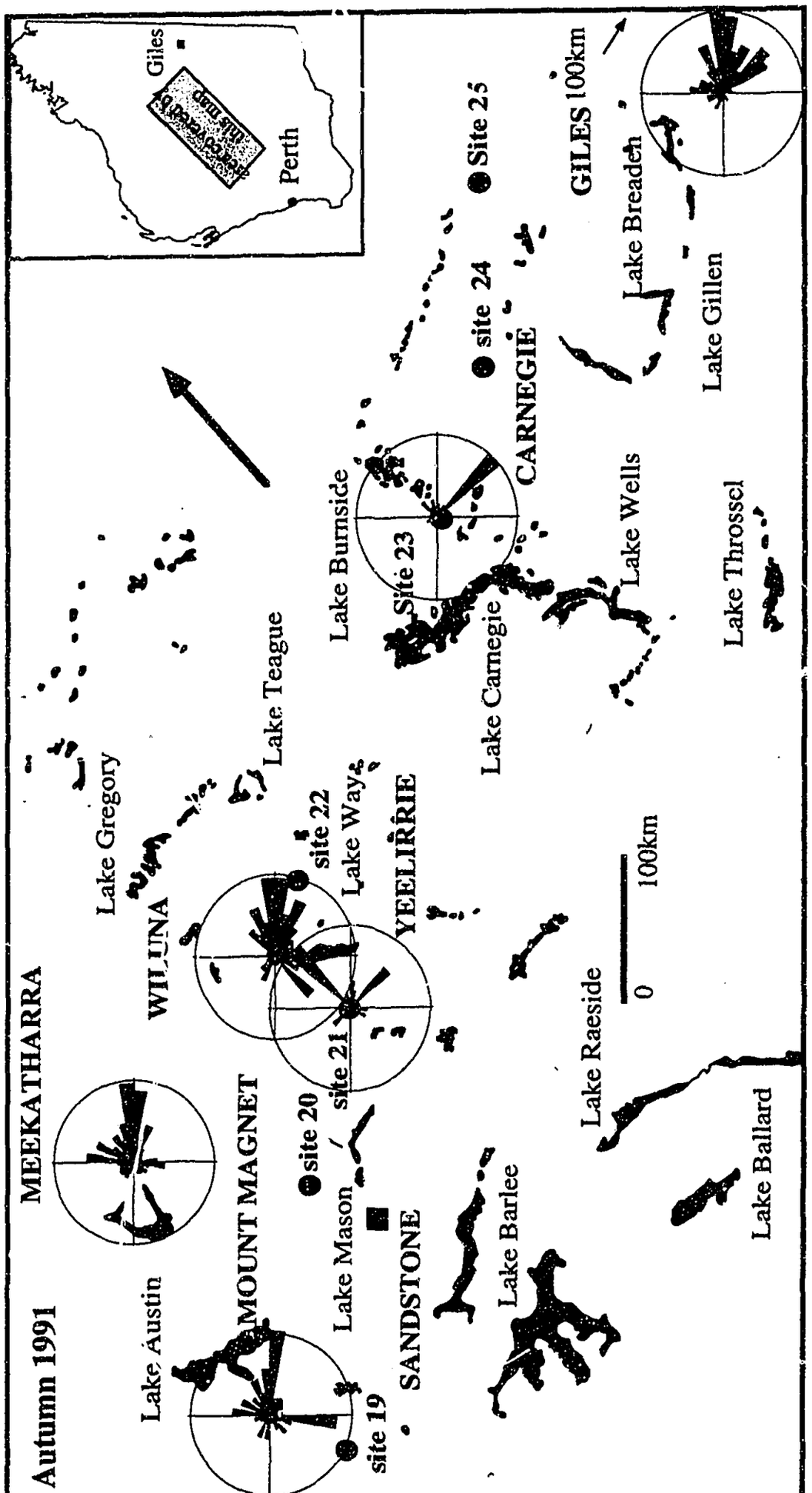
Autumn 1991
MEEKATHARRA
WILUNA
MOUNT MAGNET
SANDSTONE
YEELIRRIE
CARNEGIE
GILES
Lake Austin
Lake Gregory
Lake Teague
Lake Mason
Lake Way
Lake Burnside
Lake Carnegie
Lake Wells
Lake Throssel
Lake Gillen
Lake Breaden
Lake Raeside
Lake Barlee
Lake Ballard
site 19
site 20
site 21
site 22
Site 23
site 24
Site 25
0
100km
100km
Giles
Perth

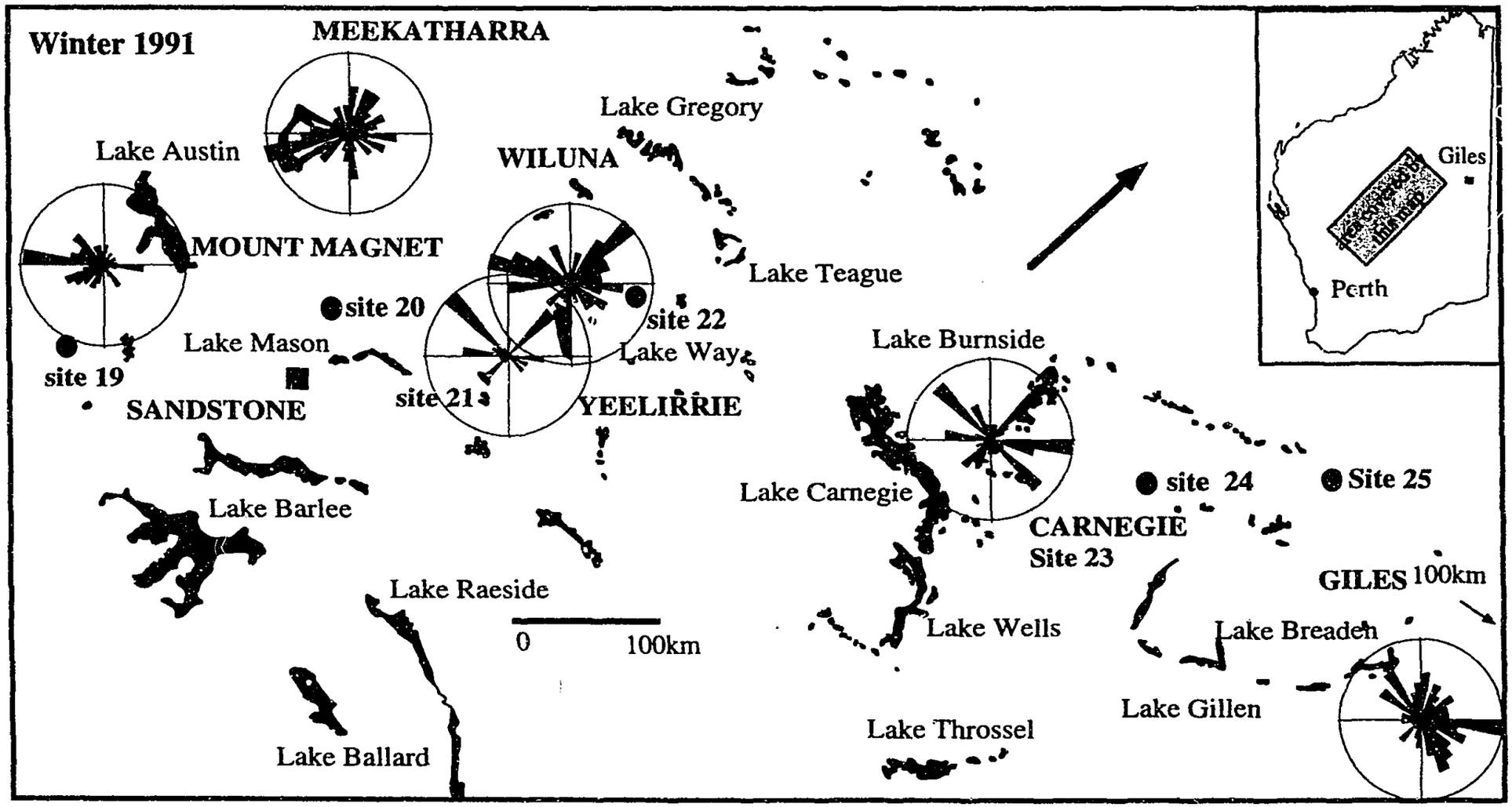
Winter 1991
MEEKATHARRA
Lake Austin
WILUNA
Lake Gregory
MOUNT MAGNET
Lake Teague
site 20
site 22
Lake Mason
Lake Way
site 19
site 21
YEELIRRIE
SANDSTONE
Lake Burnside
Lake Barlee
Lake Carnegie
site 24
Site 25
CARNEGIE
Site 23
GILES
100km
Lake Raeside
0
100km
Lake Wells
Lake Breaden
Lake Gillen
Lake Throssel
Lake Ballard
Giles
Perth

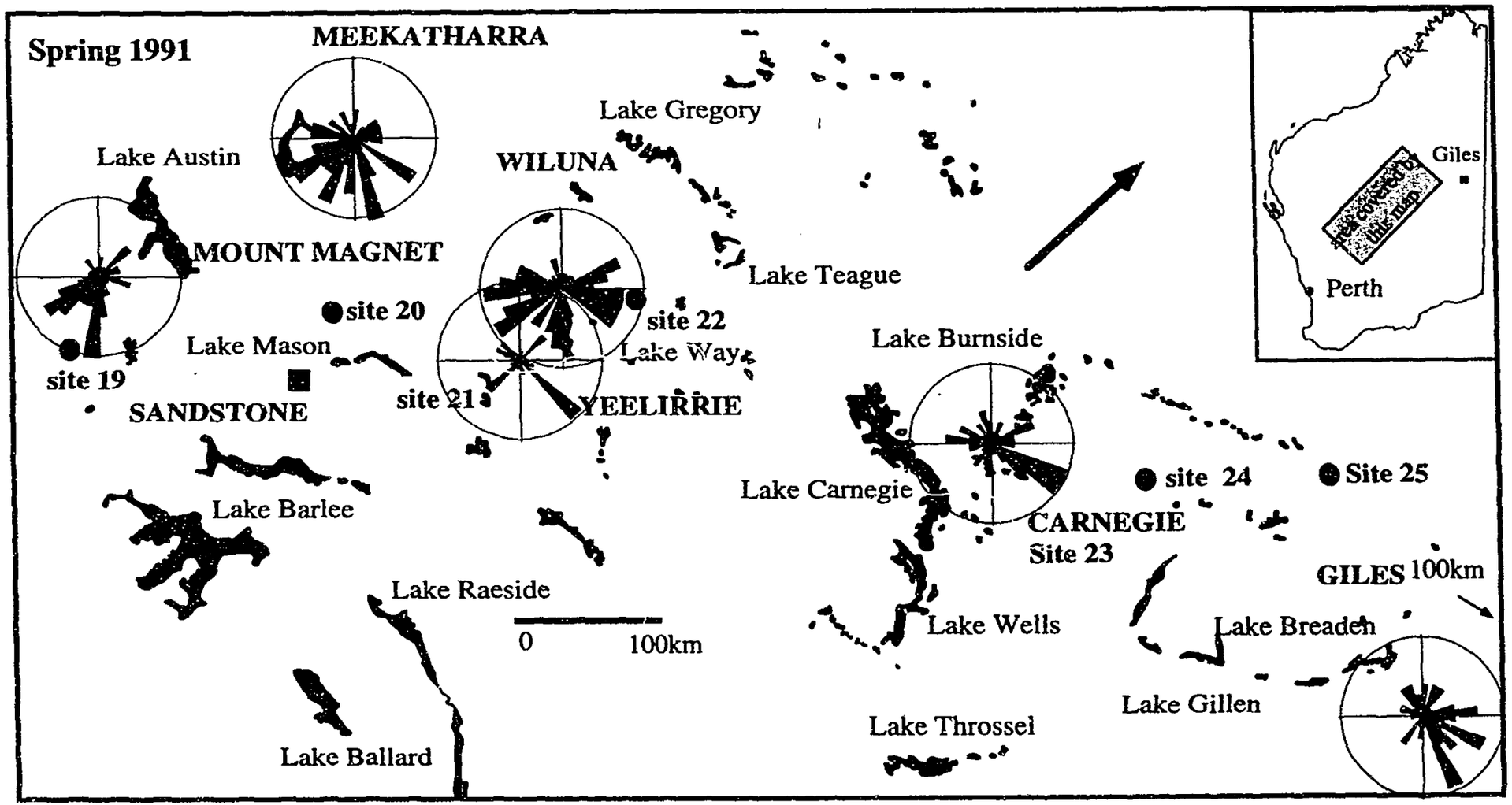

Appendix H Mean Wind Directions During Each Sampling Season for Inland Sites on the WE Array

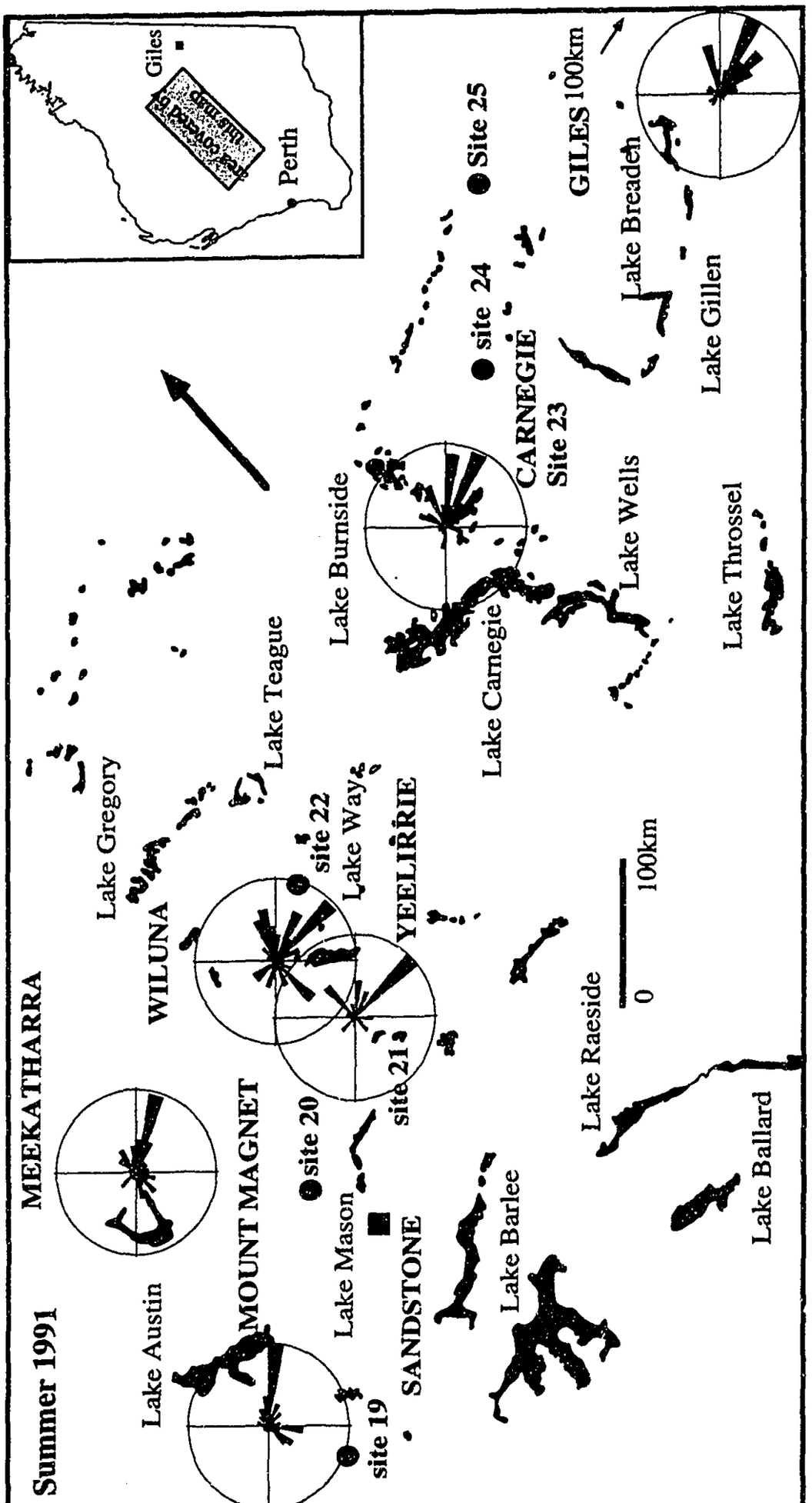
Summer 1991
MEEKATHARRA
MOUNT MAGNET
SANDSTONE
WILUNA
YEELIRRIE
CARNEGIE
GILES
Site 25
site 24
site 23
site 22
site 21
site 20
site 19
Lake Austin
Lake Gregory
Lake Teague
Lake Burnside
Lake Carnegie
Lake Wells
Lake Throssel
Lake Gillen
Lake Breaden
Lake Mason
Lake Way
Lake Barlee
Lake Raeside
Lake Ballard
0
100km
100km
Giles
Perth

Appendix H Mean Wind Directions During Each Sampling Season for Inland Sites on the WE Array

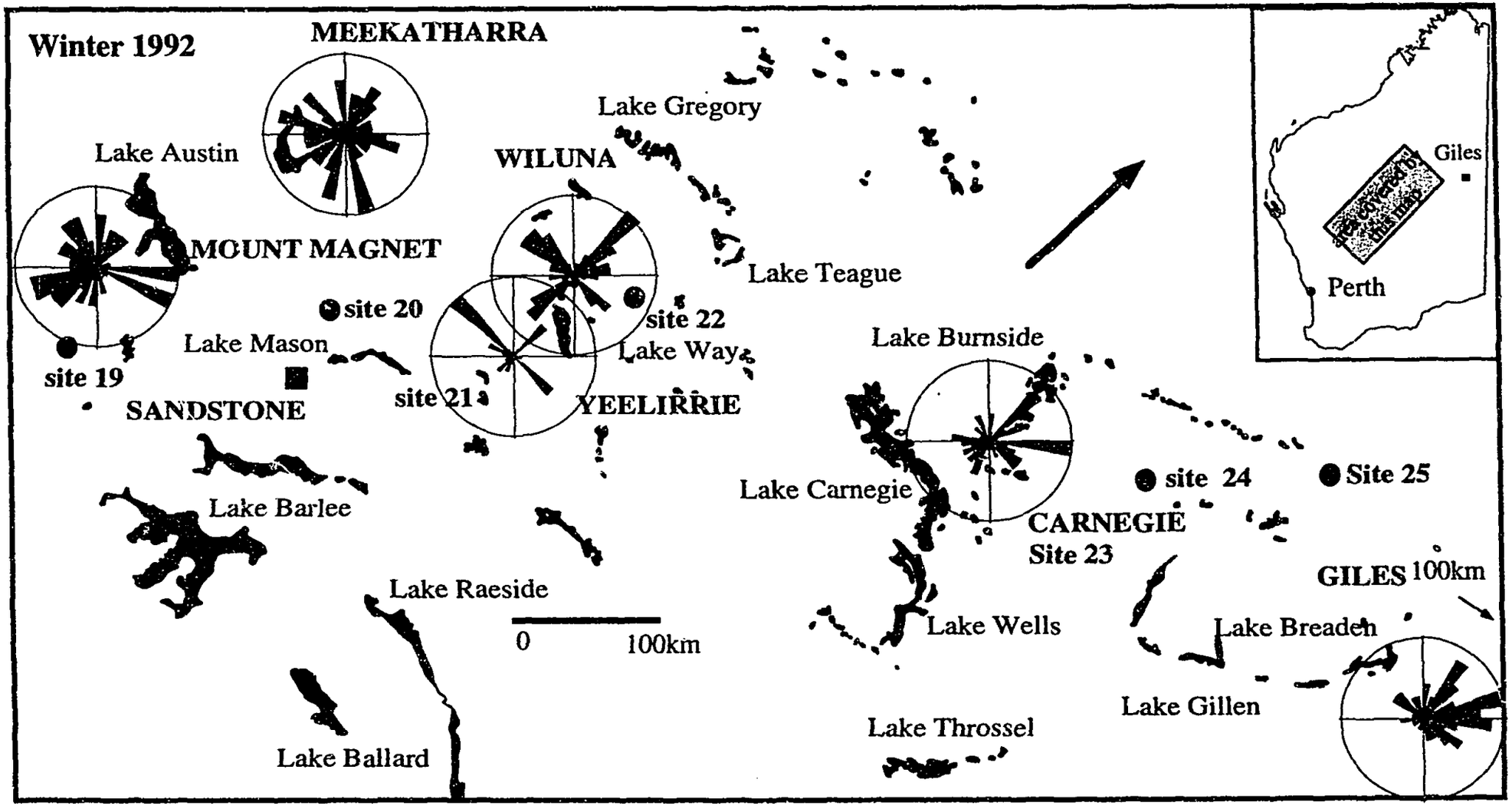

Appendix H Mean Wind Directions During Each Sampling Season for Inland Sites on the WE Array

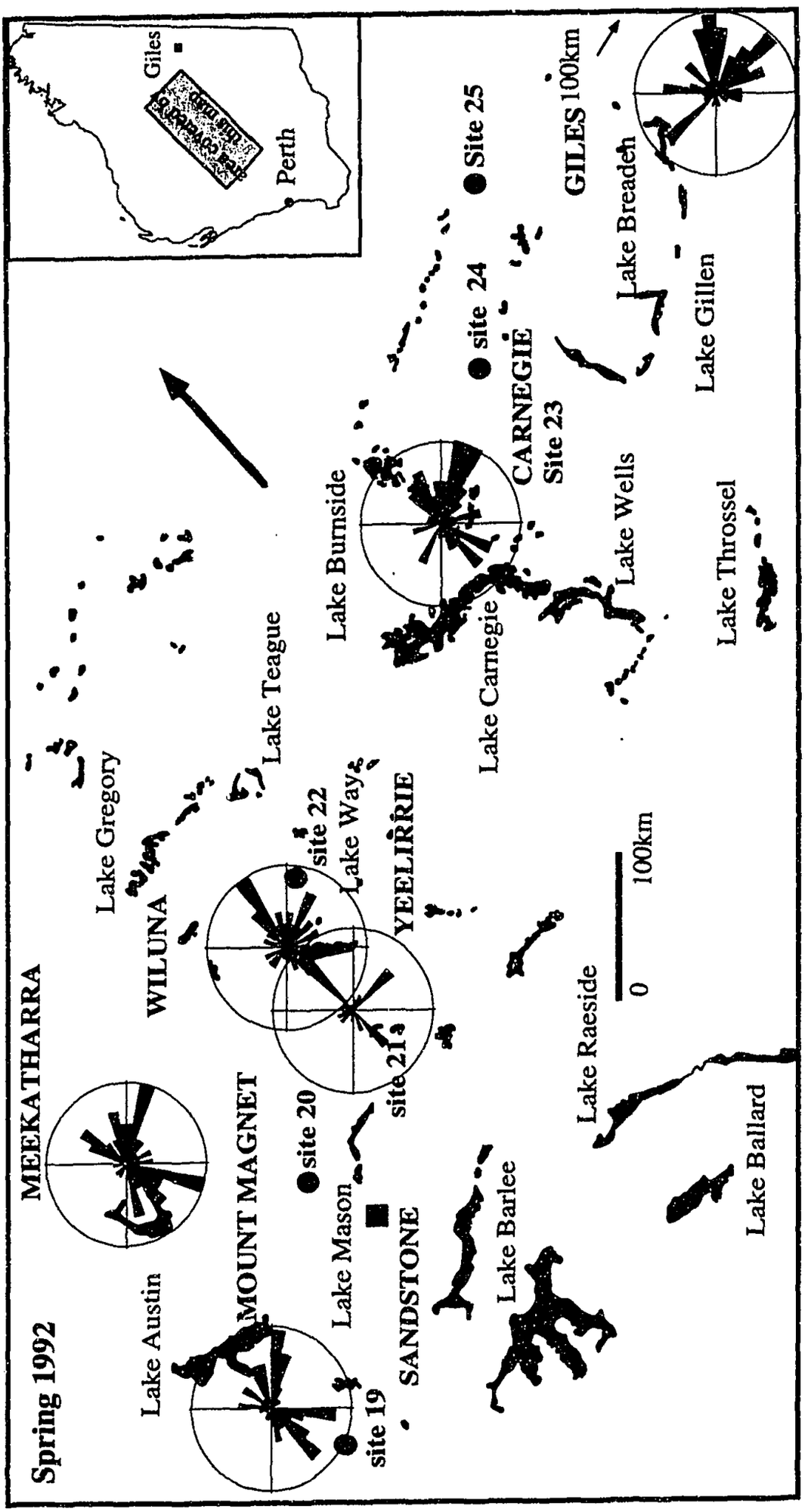
Spring 1992
MEEKATHARRA
Lake Austin
MOUNT MAGNET
site 19
Lake Mason
site 20
SANDSTONE
Lake Barlee
Lake Gregory
WILUNA
Lake Teague
site 22
Lake Way
site 21
YEELIRRIE
Lake Raeside
Lake Ballard
Lake Burnside
Lake Carnegie
site 24
Site 25
CARNEGIE
Site 23
Lake Wells
Lake Throssel
GILES 100km
Lake Breaden
Lake Gillen
0
100km
Giles
Perth

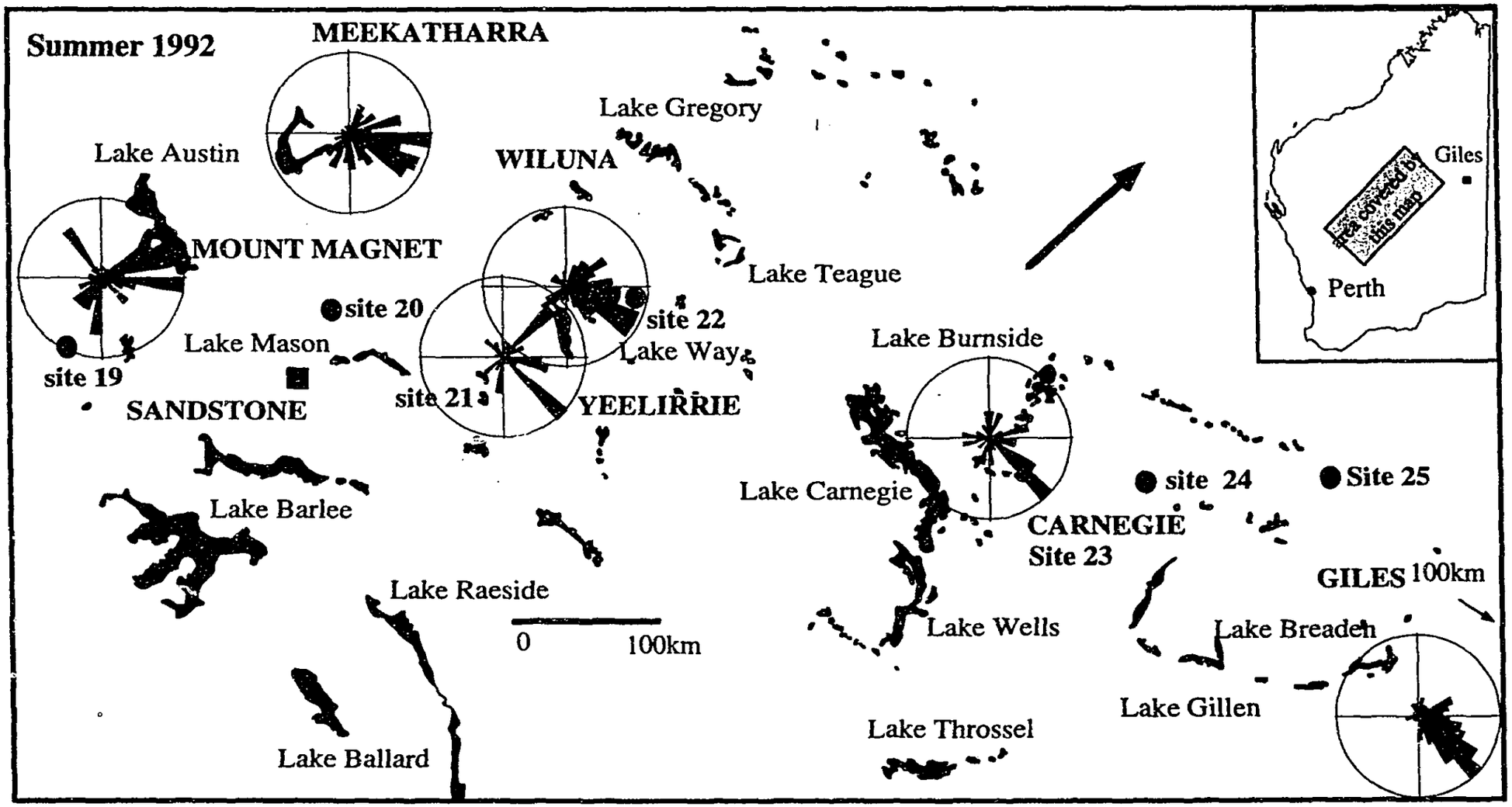

Appendix H Mean Wind Directions During Each Sampling Season for Inland Sites on the WE Array

Examiner 1

The examiner states "p 191, last paragraph- given some variations in ^{36}Cl measurements spatially from different studies, extending the results of this study to represent the entire Southern Hemisphere is questionable. What happens if the seasons in question becomes unusually wet?"

> Response: The fallout values in atoms/m^2/s take into account factors such as rainfall volume etc. I recognise that it is premature to state these fallouts are representative of the southern hemisphere. The main point here is that we cannot take fallouts measured in the northern hemisphere as representative of global fallouts, and as these are the only measurements made for the southern hemisphere, for now, they provide us with an idea of the hemispheric differences in fallout.

The examiner states "...choose an accessible representative site for major-element evaluation on a more detailed temporal scale for one or more seasons. If this was done on an event (or even weekly scale), a much better evaluation of the relationship with meteorology would have been possible, which might have been extended to the rest of the array."

> Response: I agree, and I did consider undertaking a similar activity during the monsoon period at one of the northern sites of the SN array, but time and financial constraints made this impossible.

the examiner states "p98 and elsewhere- if Br is below the detection limit almost all of the time, why not remove it from the data set"

> Response: Br was present in the coastal samples (site 16 and 26) and represents the input of seawater to rainfall at these sites. Thus data from sites 16 and 26 were used in the factor analysis, Br data was kept in the data set in the hope that it would indicate the seawater source.

The examiner states "p 102-103- individual site analysis. Some spatial distributions of the PC variances mapped on the site location maps would have been useful to enhance interpretation. Also the tabular FA results for the individual sites for both arrays should be included in an appendix."

> Response: FA was not performed on data from individual sites because the FA procedure could not be carried out on data sets with few number of cases than variables. This is outlined in Chapter 3.

The examiner states " p126 top paragraph- the speculations regarding sources of acidity are disappointing. The author cannot formally justify biodegradation as a source of acidity from the data (see FA results)."

> Response: I did not mean this discussion to suggest that biodegradation is a source of acidity. Rather that the acidity of the sample is something that has been altered after deposition, rather than a true representation of the atmospheric acidity. Thus biodegradation is used here more as a term to explain the post-depositional degradation.

The examiner states "p2 last two lines- salinisation in the landscape is mainly caused by salt from ancient seas rising to the surface after land clearing and over irrigation. It is not clear whether the author is implying a major role for rainfall chemistry, which is unlikely".

Response: this is not what I am implying. Instead I am stating that in order to remedy salinisation problems we need information such as how much salt is naturally accessed in order make mass balance calculations.

The examiner states "p39 I would have liked a better discussion of the potential problems that the use of glass bottles could have on rainwater chemistry, especially over a three-month exposure period."

Response : Borosilicate glass bottles were chosen for this sampling program to cater for the ^{36}Cl measurements. Fresenius et al (1988) state that "glass bottles are particularly necessary for sampling if a substance to be determined could be secondarily changed by plastics or if changes in concentration of substances contained in water can occur by adsorption onto plastic". Plastic containers use Cl as a binding agent, and although polyethylene bottles have been found to be inert (Fresenius et al 1988), as we were measuring such trace levels of ^{36}Cl in rainwater, we decided it was unnecessary to risk interference from the collection container. Major-elements were sampled from the borosilicate glass bottles so that the Cl concentration used in the ^{36}Cl calculations was analysed from the same sampling vessel.

Disadvantages of glass collection vessels for the collection and measurement of major-elements have been noted. In particular, glass containers are unsuitable for the collection of water with low concentrations of Na and K (Rump and Kirst 1988) since the ion exchange properties of the glass are greater than those of plastic. A review of the properties of collection vessel material (Krajca 1989), however reveals that borosilicate glass is able to withstand heat and weakly acid solutions for long periods of time, making this type of glass particularly suitable in the present investigation where temperatures at central Australian sites can reach over 40oC and where the rainfall is weakly acidic.

As discussed in Chapter 3, the effect of the collection vessel material on the sample chemistry under simulated field sampling conditions was tested and found to be negligible.

Fresenius, W., Quentin, K. E. and Schneider, W. (1988). Water Analysis. Springer Verlag, Berlin 804 pp.

Krajca, J. M. (1989). Water Sampling. Ellis and Horwood Ltd, England 212pp.

Rump, H. H. and Krist, H. (1988). Laboratory Manual for the Examination of Water, Waste Water and Soil. VCH Publishers, Germany 190pp.

Examiner 2
No response required

Examiner 3

The examiner states " Chapter 3- Since no acid is added prior to volume reduction, heating may permit additional biodegradation, and possibly formation of volatiles and/or organic complexes containing Cl which will not be recovered later. I would suggest measurement of stable Cl both before and after volume reduction. Acid is usually added to promote exchange between sample Cl and dead carrier Cl when required."

> Response: The stable Cl concentration of the concentrate was not measured because of low sample amounts. However, the waste material from the concentrating process was analysed for stable Cl on a number of occasions and was found to be below detection. Carrier was added on a very few occasions which is why we did not add acid which may have provided a source of impurities.

The examiner states "Chapter 4- Acid-base balance- little is said about the pH of these samples, but unless this parameter is measured soon after precipitation falls it is unlikely to be accurate. However H appears in all listings of cations. Is this measurement significant in samples that have been sitting for several months?"

> Response: I acknowledge that H concentrations (measured as pH) do not represent the pH of the atmosphere but the processes of sample degradation between deposition and retrieval from the field. This is reflected in the discussions, where H, NO_3, NH_4 and HPO_4 are suggested to indicate biodegradation in the multivariate analysis.